0006558

Report No. FAA-RD-75-123, III

DUE

IDENTIFICATION OF MINIMUM ACCEPTABLE CHARACTERISTICS FOR MANUAL STOL FLIGHT PATH CONTROL

Volume III. Detailed Analyses and Tested Vehicle Characteristics

PROPERTY OF
FAA AERO CENTER
RECEIVED
AUG 3 0 1976
LIBRARY

June 1976

Final Report

Document is available to the public through the
National Technical Information Service,
Springfield, Virginia 22161.

Prepared for

U.S. DEPARTMENT OF TRANSPORTATION
FEDERAL AVIATION ADMINISTRATION
Systems Research & Development Service
Washington, D.C. 20590

NOTICE

This document is disseminated under the sponsorship of the Department of Transportation in the interest of information exchange. The United States Government assumes no liability for its contents or use thereof.

TECHNICAL REPORT STANDARD TITLE PAGE

1. Report No. FAA-RD-75-123, III	2. Government Accession No.	3. Recipient's Catalog No.
4. Title and Subtitle Identification of Minimum Acceptable Characteristics for Manual STOL Flight Path Control, Volume III: Detailed Analyses and Tested Vehicle Characteristics		5. Report Date June 1976 6. Performing Organization Code
7. Author(s) Roger H. Hoh, Samuel J. Craig, and Irving L. Ashkenas		8. Performing Organization Report No. TR-1035-3R-III
9. Performing Organization Name and Address Systems Technology, Inc. 13766 S. Hawthorne Boulevard Hawthorne, California 90250		10. Work Unit No. 11. Contract or Grant No. DOT-FA73WA-3276
12. Sponsoring Agency Name and Address U.S. Department of Transportation Federal Aviation Administration Systems Research and Development Service Washington, D.C. 20590		13. Type of Report and Period Covered Final Report 14. Sponsoring Agency Code

15. Supplementary Notes

16. Abstract

This report presents the detailed results and analysis procedures utilized to identify minimally acceptable flight path control characteristics of powered lift STOL airplanes. Deficiencies in flight path control are identified via closed loop analysis of describing function results obtained during the simulation. Unacceptable characteristics for flare and landing are identified from correlations of pilot rating and commentary with key parameters obtained from closed loop pilot-vehicle analysis. A more concise summary of the overall program and the results is contained in Volume I.

17. Key Words Stability Control STOL Mathematical Model Flight Path	18. Distribution Statement Document is available to the public through the National Technical Information Service, Springfield, Virginia 22161.

19. Security Classif. (of this report) Unclassified	20. Security Classif. (of this page) Unclassified	21. No. of Pages 205	22. Price

Form DOT F 1700.7 (8-69)

METRIC CONVERSION FACTORS

Approximate Conversions to Metric Measures

Symbol	When You Know	Multiply by	To Find	Symbol
		LENGTH		
in	inches	*2.5	centimeters	cm
ft	feet	30	centimeters	cm
yd	yards	0.9	meters	m
mi	miles	1.6	kilometers	km
		AREA		
in^2	square inches	6.5	square centimeters	cm^2
ft^2	square feet	0.09	square meters	m^2
yd^2	square yards	0.8	square meters	m^2
mi^2	square miles	2.6	square kilometers	km^2
	acres	0.4	hectares	ha
		MASS (weight)		
oz	ounces	28	grams	g
lb	pounds	0.45	kilograms	kg
	short tons (2000 lb)	0.9	tonnes	t
		VOLUME		
tsp	teaspoons	5	milliliters	ml
Tbsp	tablespoons	15	milliliters	ml
fl oz	fluid ounces	30	milliliters	ml
c	cups	0.24	liters	l
pt	pints	0.47	liters	l
qt	quarts	0.95	liters	l
gal	gallons	3.8	liters	l
ft^3	cubic feet	0.03	cubic meters	m^3
yd^3	cubic yards	0.76	cubic meters	m^3
		TEMPERATURE (exact)		
°F	Fahrenheit temperature	5/9 (after subtracting 32)	Celsius temperature	°C

*1 in = 2.54 (exactly). For other exact conversions and more detailed tables, see NBS Misc. Publ. 286, Units of Weights and Measures, Price $2.25, SD Catalog No. C13.10:286.

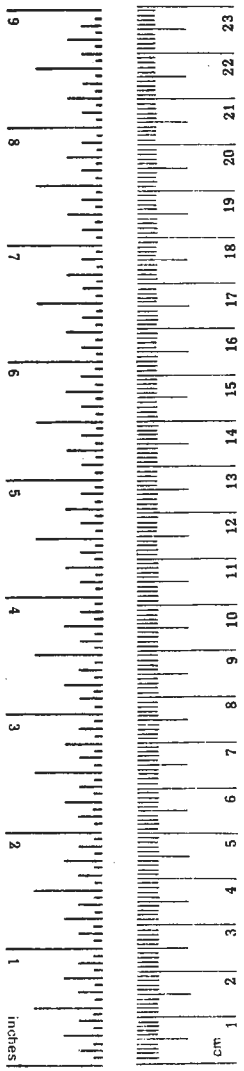

Approximate Conversions from Metric Measures

Symbol	When You Know	Multiply by	To Find	Symbol
		LENGTH		
mm	millimeters	0.04	inches	in
cm	centimeters	0.4	inches	in
m	meters	3.3	feet	ft
m	meters	1.1	yards	yd
km	kilometers	0.6	miles	mi
		AREA		
cm^2	square centimeters	0.16	square inches	in^2
m^2	square meters	1.2	square yards	yd^2
km^2	square kilometers	0.4	square miles	mi^2
ha	hectares (10,000 m^2)	2.5	acres	
		MASS (weight)		
g	grams	0.035	ounces	oz
kg	kilograms	2.2	pounds	lb
t	tonnes (1000 kg)	1.1	short tons	
		VOLUME		
ml	milliliters	0.03	fluid ounces	fl oz
l	liters	2.1	pints	pt
l	liters	1.06	quarts	qt
l	liters	0.26	gallons	gal
m^3	cubic meters	35	cubic feet	ft^3
m^3	cubic meters	1.3	cubic yards	yd^3
		TEMPERATURE (exact)		
°C	Celsius temperature	9/5 (then add 32)	Fahrenheit temperature	°F

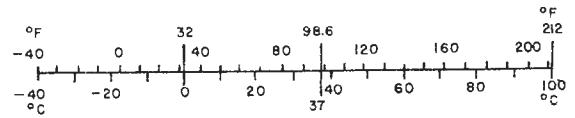

TABLE OF CONTENTS

		Page
I.	INTRODUCTION	1
	A. Background	1
	B. Objectives	1
	C. Description of the Program	2
	D. Guide to the Reader	3
II.	DESCRIPTION OF GENERIC STOL CONFIGURATIONS AND SIMULATION PROGRAM	5
	A. Steady-State Characteristics	7
	B. Dynamic Characteristics	12
	C. Description of the Simulation	17
III.	SIMULATION RESULTS	21
	A. Flight Path Control	21
	B. Path/Speed Coupling	24
	C. Closed Loop Tracking Behavior	27
	D. Flare and Landing	35
	E. Simulator Calibration for Landing	38
	F. Flight Director Results	41
IV.	FLIGHT TEST RESULTS	44
	A. Description of Flight Program	44
	B. Flight Results	44
V.	ANALYSIS OF RESULTS	51
	A. Analysis of Final Approach Tracking	51
	B. Analysis of Flare and Landing	55
	C. Discussion of Key Parameters	78
VI.	CONCLUSIONS	83
	A. Conclusions from Pre-Flight Simulation Phase	83
	B. Conclusions from the Flight Test and Post-Flight Simulation Results	84
	C. Conclusions from Analysis Phase	85
	REFERENCES	86

		Page
APPENDIX A.	PILOT RATINGS, COMMENTARY, AND BACKGROUND	A-1
APPENDIX B.	MANUAL FLARE MODEL DEVELOPMENT	B-1
APPENDIX C.	DFA DESCRIPTION	C-1
APPENDIX D.	PILOT BRIEFING AND QUESTIONNAIRES	D-1
APPENDIX E.	DETAILED SUMMARY OF GENERIC CONFIGURATIONS	E-1

LIST OF FIGURES

		Page
1.	Lift and Drag Characteristics of the Simulated Configurations	6
2.	Stall Characteristics Tested	8
3.	$\gamma - V - \theta$ Plots for the Tested Generic Configurations	9
4.	Pitch SAS Used in Generic STOL Simulation	12
5.	Dynamic Response Characteristics of Beam Rate to Power (Attitude SAS On)	14
6.	Generic Characteristics for Sink Rate Control with Attitude and Throttle	15
7.	Effect of Airspeed on the Dynamic Response	16
8.	Effect of Speed on Path Response to a Unit Step Power Input (AP10)	17
9.	Flight Task Description	19
10.	Pilot Ratings for Tasks 1.01 and 3.1	22
11a.	Example of Typical Airspeed Control on Configuration with Large Speed-Path Coupling and Large L_α (Configuration AP6, Pilot 7) Task 3.1	25
11b.	Example of Pilot Technique for Path Control on Configuration with Very Large Path-Speed Coupling and Low C_{L_α} (Task 1.01 and 2.1 Combined, Pilot 7 Configuration AP10)	26
12.	Effect of 10 Percent Increase in $C_{L_{max}}$ on Stall Characteristics	28
13.	Pilot/Vehicle Loop Structure for Glide Slope Tracking	30
14.	Experimental-Analytical Pilot/Vehicle Model Correlations	32
15.	Comparison of Pilot Ratings for ILS Tracking (IFR) and Final Approach and Landing (VFR)	36
16.	Effect of Turbulence on Pilot Ratings	36
17.	Distribution of Ratings for Soft, Firm, and Hard Landings	39

Page

18. Simulator Landing Correlation Plot 40

19. Effect of Flight Director On Ratings and Performance . . . 43

20. Phase Trajectories for Five Consecutive Flares — No Turbulence — Configuration BSL2, Pilot 7 57

21. Assumed Command Structure for Closed Loop Flare 58

22. Effective Closed Loop System for Flare 61

23. Generic Response Characteristics of Attitude Flare . . . 63

24. Generic Characteristics of Loop Closure for Attitude Flare 66

25. Use of Secondary Control to Stabilize Backside Mode Generic Configuration BSL1 67

26. Effect of Secondary Attitude Closure on Closed Loop Roots for Throttle Flare 72

27. Asymptotes of $|\theta/\dot{H}_F|$ 73

28. Migration of $\ddot{h}/\ddot{H}_F$ Numerator Zeros with Secondary Control (Throttle) Gain, K_{p_2} 74

29. Generic Characteristics of Gust Response in Flare 76

30. Generic Root Locus Characteristics ($\tau = 0$) of $1 + Y_p Y_c = 0$ 80

31. One Possible Way of Using Key Parameters to Correlate Minimum Acceptable Path Control with Aircraft Configuration 81

A-1. Summary of Preflight Simulation Pilot Ratings A-2

B-1. Relationships Between Inertial and Perturbation Coordinates B-3

B-2. Block Diagram of Closed Loop Pilot and Vehicle System for Flare B-5

B-3. Block Diagram of Closed Loop Flare in Perturbation Coordinates and with Step Input Equivalent to Initial Conditions (H_F and $\dot{H}_F$) B-7

C-1. Pilot/Aircraft Model C-2

		Page
D-1.	Pilot Briefing Outline	D-2
D-2a.	Pilot Evaluation — Flight Path Margin	D-3
D-2b.	Pilot Evaluation — Landing	D-4
D-2c.	Pilot Evaluation — Speed Margin	D-5
E-1a.	Untrimmed Drag Polar for BSL1	E-2
E-1b.	Untrimmed Drag Polar for BSL2	E-3
E-1c.	Untrimmed Drag Polar for BSL2 RLD	E-4
E-1d.	Untrimmed Drag Polar for AP1	E-5
E-1e.	Untrimmed Drag Polar for AP2	E-6
E-1f.	Untrimmed Drag Polar for AP3	E-7
E-1g.	Untrimmed Drag Polar for AP5	E-8
E-1h.	Untrimmed Drag Polar for AP6	E-9
E-1i.	Untrimmed Drag Polar for AP6 SR	E-10
E-1j.	Untrimmed Drag Polar for AP6 RLD	E-11
E-1k.	Untrimmed Drag Polar for AP7	E-12
E-1l.	Untrimmed Drag Polar for AP10	E-13
E-1m.	Untrimmed Drag Polar for BSL30 and AP30 (30 deg δ_f)	E-14
E-2.	Trim Drag Polars for Five Test Configurations	E-15
E-3a.	Performance Curve for BSL1	E-18
E-3b.	Performance Curve for BSL2	E-19
E-3c.	Performance Curve for BSL2 RLD	E-20
E-3d.	Performance Curve for AP1	E-21
E-3e.	Performance Curve for AP2	E-22
E-3f.	Performance Curve for AP3	E-23
E-3g.	Performance Curve for AP5	E-24

Page

E-3h. Performance Curve for AP6 . . . . . E-25

E-3i. Performance Curve for AP6 SR E-26

E-3j. Performance Curve for AP6 RLD E-27

E-3k. Performance Curve for AP7 . . . . . E-28

E-3l. Performance Curve for AP10 . . . . . E-29

E-3m. Performance Curve for BSL30 or AP30, 30 deg δ_f E-30

LIST OF TABLES

		Page
1.	Summary of Characteristics of the Simulated Configurations	5
2.	Simulation Task Designation and Description	18
3.	Pilot Commentary Where Flight Path Control Problems on Short Final Were Specifically Noted (Tasks 2.1 and 3.1)	23
4.	Landing "Rating" Scale	39
5.	Summary of Landing Performance	41
6.	Cooper Harper Ratings for Flare and Landing (Flight Program)	46
7.	Cooper Harper Ratings for Final Approach (Flight Program)	46
8.	Cooper Harper Ratings for Flare and Landing Post Flight Simulation-Configuration BSL1	50
9.	Generic Forms of the Effective Controlled Element for Path Control with Throttle	54
10.	Effect of Throttle Step as Secondary Control in Closed Loop Flare Maneuver	75
A-1.	Task Code	A-3
A-2.	Cooper Harper Ratings for Flare and Landing Flight Program	A-4
A-3.	Cooper Harper Ratings for Final Approach Flight Program	A-4
A-4.	Cooper Harper Ratings for Flare and Landing Post Flight Simulation-Configuration BSL1	A-5
E-1a.	Longitudinal Stability Derivatives, Approach Configuration, Aircraft: BSL1	E-31
E-1b.	Longitudinal Stability Derivatives, Approach Configuration, Aircraft: BSL2	E-32
E-1c.	Longitudinal Stability Derivatives, Approach Configuration, Aircraft: BSL2 RLD	E-33

Page

E-1d. Longitudinal Stability Derivatives, Approach Configuration, Aircraft: AP1 . . . . . E-34

E-1e. Longitudinal Stability Derivatives, Approach Configuration, Aircraft: AP2 . . . . . E-35

E-1f. Longitudinal Stability Derivatives, Approach Configuration, Aircraft: AP3 . . . . . E-36

E-1g. Longitudinal Stability Derviatives, Approach Configuration, Aircraft: AP5 . . . . . E-37

E-1h. Longitudinal Stability Derivatives, Approach Configuration, Aircraft: AP6 . . . . . E-38

E-1i. Longitudinal Stability Derviatives, Approach Configuration, Aircraft: AP6 SR E-39

E-1j. Longitudinal Stability Derivatives, Approach Configuration, Aircraft: AP6 RLD E-40

E-1k. Longitudinal Stability Derivatives, Approach Configuration, Aircraft: AP7 . . . . . E-41

E-1l. Longitudinal Stability Derivatives, Approach Configuration, Aircraft: AP10 . . . . . E-42

E-2a. Longitudinal Transfer Functions, (Approach Configuration), Aircraft: BSL1 . . . . . E-43

E-2b. Longitudinal Transfer Functions, (Approach Configuration), Aircraft: BSL2 . . . . . E-44

E-2c. Longitudinal Transfer Functions, (Approach Configuration), Aircraft: BSL2 RLD E-45

E-2d. Longitudinal Transfer Functions, (Approach Configuration), Aircraft: AP1 . . . . . E-46

E-2e. Longitudinal Transfer Functions, (Approach Configuration), Aircraft: AP2 . . . . . E-47

E-2f. Longitudinal Transfer Functions, (Approach Configuration), Aircraft: AP3 . . . . . E-48

E-2g. Longitudinal Transfer Functions, (Approach Configuration), Aircraft: AP5 . . . . . E-49

E-2h. Longitudinal Transfer Functions, (Approach Configuration), Aircraft: AP6 . . . . . E-50

Page

E-2i. Longitudinal Transfer Functions, (Approach Configuration), Aircraft: AP6 SR E-51

E-2j. Longitudinal Transfer Functions, (Approach Configuration), Aircraft: AP6 RLD E-52

E-2k. Longitudinal Transfer Functions, (Approach Configuration), Aircraft: AP7 . . . . . E-53

E-2l. Longitudinal Transfer Functions, (Approach Configuration), Aircraft: AP10 . . . . . E-54

LIST OF ABBREVIATIONS

c.g.	Center of gravity
CTOL	Conventional Takeoff and Landing
DFA	Describing Function Analyzer
EBF	Externally Blown Flap
FSAA	Flight Simulator for Advanced Aircraft
IBF	Internally Blown Flap
IFR	Instrument flight rules
SAS	Stability Augmentation System
STOL	Short Takeoff and Landing
VFR	Visual flight rules
VT/MF	Vectored thrust/mechanical flap

NOMENCLATURE

a_z	Vertical acceleration; ft/sec^2
C_D	Drag coefficient — includes thrust effects
$C_{D_{min}}$	Minimum drag coefficient — includes thrust effects
C_{D_α}	Drag curve slope — includes thrust effects
C_L	Lift coefficient — includes thrust effects
C_{L_α}	Lift curve slope — includes thrust effects
C_{L_o}	Lift coefficient at zero angle of attack — includes thrust effects
$C_{m_{\delta_e}}$	Slope of pitching moment coefficient with elevator
C_μ	Blowing coefficient, T/SQ
d	Deviation from glide slope; ft
d_ϵ	Glide slope error
g	Acceleration due to gravity; ft/sec^2
h	Perturbation altitude (change in altitude from trim); ft
H_F	Flare height; ft
K_D	Flight director display scale or lift/drag relationship in Fig. 1d
K_d	Pilot model parameter in Eq. 6
K_θ	Pitch-attitude-to-elevator feedback gain
$K_{\dot\theta}$	Pitch-rate-to-elevator feedback gain; sec
m	Mass of airplane
M_{δ_e}	Equals $(\rho S U_o c/2I_y)C_{m_{\delta_e}}$
$N^\theta_{\delta_e}$	Numerator of transfer function which describes pitch-attitude-to-elevator response (see Ref. 2); becomes denominator of sink-rate-to-throttle response when attitude is constrained
$N^{\theta\ \dot h}_{\delta_e \delta_T}$	Coupling numerator due to closure of two loops to two different control points; becomes numerator of sink-rate-to-throttle response when attitude is constrained

q_B	Body axis pitch rate; rad/sec
Q	Dynamic pressure; lb/ft^2
R	Range from the aircraft to the glide slope transmitter
S	Wing area; ft^2
t	Time; sec
T	Thrust, percent or lb
T_E	Pitch attitude SAS feedback time constant, $K_{\dot{\theta}}/K_\theta$; sec
T_F	Time constant for exponential flare; sec
T_{h_θ}	Zero of coupling numerator, $N^{\theta}_{\delta_e} \dot{h}_{\delta_T}$; sec
T_{h_1}	Zero of sink-rate-to-elevator numerator, $1/T_{h_1} = -g(\partial\gamma/\partial V)_{\delta_T}$
T_{pilot}	Compensation provided by pilot based on experimental measurements; sec
T_{u_θ}	Zero of coupling numerator, $N^{\theta}_{\delta_e} u_{\delta_T}$; sec
T_{θ_1}	Pitch attitude numerator ($N^{\theta}_{\delta_e}$) zero; speed mode time constant when pitch attitude is constrained (see Eq. 1); sec
T_{θ_2}	Pitch attitude numerator ($N^{\theta}_{\delta_e}$) zero; path mode time constant when pitch attitude is constrained (see Eq. 1); sec
u_g	Horizontal wind gust; ft/sec
U_o	Trim speed; ft/sec
V	Airspeed; ft/sec
V_o	Trim airspeed (same as U_o); ft/sec
V_{trim}	Trim airspeed (same as U_o and V_o); ft/sec
V_{eq}	Equivalent airspeed; ft/sec
w_g	Vertical wind gust; ft/sec
X	Distance from runway threshold; ft
X_u	Equals $-(\rho S U_o/m)(C_D + C_{D_u})$; 1/sec
X_w	Equals $(\rho S U_o/m)(C_L - C_{D_\alpha})$; 1/sec

X_{δ_T}	Equals $-SQC_{D_{\delta_T}}$; $(ft/sec^2)/percent$
Y_p	Transfer function representing pilot control characteristics to a perceived error
Y_c	Transfer function for controlled element (airplane)
Z_u	Equals $-(\rho SU_o/m)(C_L + C_{L_u})$; 1/sec
Z_w	Equals $-(\rho SU_o/2m)(C_D + C_{L_\alpha})$; 1/sec
Z_α	Equals $U_o Z_w$; $(ft/sec^2)/rad$
Z_{δ_T}	Equals $-SQC_{L_{\delta_T}}$
α	Angle of attack; deg or rad
γ	Flight path angle; angle of velocity vector with respect to horizontal
γ_{peak}	Maximum flight path response to a step throttle input
γ_{ss}	Steady-state flight path response after a step throttle input
δ_c	Longitudinal control column position; in.
δ_e	Elevator position; rad
δ_T	Percent power (throttle)
Δ	Characteristic equation
ϵ_{GS}	Glide slope error angle; deg
ζ_θ	See Eq. 8
η_p	Powered-lift efficiency parameter; $-(\partial C_L/\partial C_\mu)(C_\mu/C_L)$
	Pitch attitude; deg or rad
θ_c	Pitch attitude command; deg or rad
θ_T	Effective thrust inclination angle; lumps aerodynamic and thrust effects into an equivalent thrust vector (θ_T = 90 deg) when thrust is perpendicular to flight path); deg
ρ	Air density; slug-ft^2
σ_θ	Closed-loop bandwidth parameter (see Fig. 30)
τ	Pilot model lag (see Eq. 6)
ω_θ	Path mode frequency when pitch attitude is constrained (see Eq. 8)

SECTION I

INTRODUCTION

A. BACKGROUND

This report presents the results of a research effort which included analysis, simulation, and flight test. The goal of this research was to define, in a quantitative way, the factors which result in minimally acceptable path control of physically realizable, 150,000 lb jet STOL configurations. This effort has been conducted on a continuing basis in parallel with a joint FAA/NASA program to develop civil airworthiness criteria for powered-lift aircraft. The purpose of the present program was to allow research of fundamental effects and identify characteristics which strongly influenced manual STOL flight path control. A major benefit of this program has been therefore the ability to concentrate on the more intractable STOL handling problems and to make results immediately available to engineers involved in formulation of airworthiness criteria.

Both the experimental and analytical phases of the program are a direct outgrowth of the notions set forth in Ref. 1 and the experimental results obtained in Ref. 2. Other basic references which set the stage for the present research were Refs. 3 and 4. In many cases the hypotheses and preliminary results set down in the above references were substantiated in this program; whereas in other cases more extensive testing revealed a requirement to modify or change these earlier notions.

B. OBJECTIVES

This experiment was conceived as a detailed study of STOL path mode dynamics independent of conventional short-period attitude control aspects. The overall objective was an identification of conditions for minimum acceptable manual path control in support of future airworthiness requirements. However, the desire to define precise "boundaries for the minimal acceptable condition" in conventional indices was tempered by the knowledge

that the factors limiting manual path control would most likely stem from closed-loop limits which are not easily described by such methods. Thus, the guiding desires of this effort were more precisely to:

1. Identify and quantify critical path control problems and relate these as far as practical to their underlying closed-loop deficiencies.

2. Define configuration variations which may be theoretically and/or empirically related to contemporary (150,000 lb) jet STOL transport aircraft lift augmentation concepts.

3. Verify the importance of task (i.e., glide slope and terminal maneuver), disturbances, and pilot-centered factors on the manual path control. The pilot-centered factors include such effects as adaptability, background, experience, and control technique/strategy during each phase of the approach task.

Item 2, above, was emphasized as a ground rule of the program, i.e., heavy emphasis was placed on consideration of physically realizable STOL transport concepts as opposed to parametric variations of stability derivatives. To establish physically realizable parameters, candidate powered-lift systems were examined to define their crucial lift/drag and power characteristics (see Volume II). These candidates included the five contemporary concepts given below:

- Internally blown jet flaps (IBF)
- Externally blown jet flaps (EBF)
- Augmentor wing (AW)
- Upper surface blowing (USB)
- Vectored thrust with mechanical flaps (VT/MF)

C. DESCRIPTION OF THE PROGRAM

The research effort described in this report spanned a period of approximately two years and involved the several phases of simulation, analysis, and flight test summarized below:

- Definition of the generic properties of various STOL concepts with emphasis on those characteristics expected to result in minimally acceptable path control. This included formulation, programming, and checkout of a digital computer program in which the nonlinear aerodynamic and thrust characteristics of the generic vehicles could easily be modified while maintaining fundamental aerodynamic principles. The computer program equations and relations are given in Volume II of this report. It should be noted that at least three STOL simulations have utilized this computer program (for example, see Ref. 5) since completion of the simulations described herein.

- Conduct of a two-phase simulation program (preflight simulation) with 11 generic STOL configurations and 9 pilots. Both phases of this simulation program were run on the NASA/Ames S-16 Moving Base Simulator.

- Conduct of an abbreviated flight test program on the Princeton University Variable Stability NAVION to allow interpretation of the simulation final approach and landing results in light of a flight environment. The flight test program involved 2 of the 11 configurations tested on the S-16 simulator. There was considerable emphasis on comparing turbulence effects in the simulator with turbulence effects in flight.

- Participation in a NASA-sponsored program involving limited post-flight simulation in the FSAA to resolve questions regarding flight and simulator differences raised by the above flight program.

- Performance of analyses to allow interpretation of simulation results in terms of key parameters and critical flight regimes defining minimum acceptable flight path control for STOL vehicles.

D. GUIDE TO THE READER

The objective of this volume of the report is to document in detail all of the findings obtained during the two year program.

Section II presents a description of the static and dynamic characteristics of the tested configurations. The actual derivatives and transfer functions are deferred to Appendix E. The simulation program is also discussed in Section II.

The results of the simulation program are discussed in Section III.

A short flight test program was conducted to check certain simulator results. This is covered in Section IV. Also discussed in Section IV is a very short (two day) simulation program conducted to answer certain questions relative to discrepancies in flight/simulator comparison.

Sections III and IV present results of simulation and flight test. These results are analyzed, and certain key parameters were identified in Section V.

Finally, the conclusions are summarized in Section VI.

SECTION II

DESCRIPTION OF GENERIC STOL CONFIGURATIONS AND SIMULATION PROGRAM

Eleven generic configurations were derived to characterize the extremes of potential variations in the performance parameters (C_L, C_D, and C_μ). The simulated airplanes are grouped and labeled in terms of their lift, drag, and thrust characteristics in Table 1. More specific descriptions of the variations of the performance parameters with thrust (C_μ) are given in Fig. 1. The configurations were arbitrarily labeled BSL1 and 2 and AP1 through 10. The letters RLD following the configuration label stand for "rounded lift and drag" and are indicative of nonlinear lift characteristics at high angles of attack to be discussed in the following pages.

TABLE 1

SUMMARY OF CHARACTERISTICS OF THE SIMULATED CONFIGURATIONS

GROUP	CONFIGURATIONS	C_{L_o} VS. C_μ	C_{L_α} VS. C_μ	θ_T	REPRESENTATIVE STOL CONCEPT	COMMENTS
I	BSL1, 2, 2RLD	Linear and moderate	Linear and moderate	61 deg	Low efficiency EBJF or VT	BSL1 has 20% lower C_{L_α} than BSL2 and 2RLD. BSL2RLD has modified stall (Fig. 19).
II	AP2, 6, 6RLD	Very non-linear	Nonlinear and moderate	90 deg	High efficiency IBJF	AP6 has improved $\Delta\gamma$ capability (−4 deg). AP6RLD has modified stall (Fig. 19).
III	AP3, 7	Linear and moderately high	Nonlinear and moderate	75 deg	Low efficiency VT/MF or poorly designed EBJF	AP7 has improved $\Delta\gamma$ capability.
IV	AP1, 5	Linear and moderately high	Very low	81 deg	Low efficiency VT/MF	AP5 has improved $\Delta\gamma$ capability.
V	AP10	Very non-linear	Very low	90 deg	High efficiency EBJF	

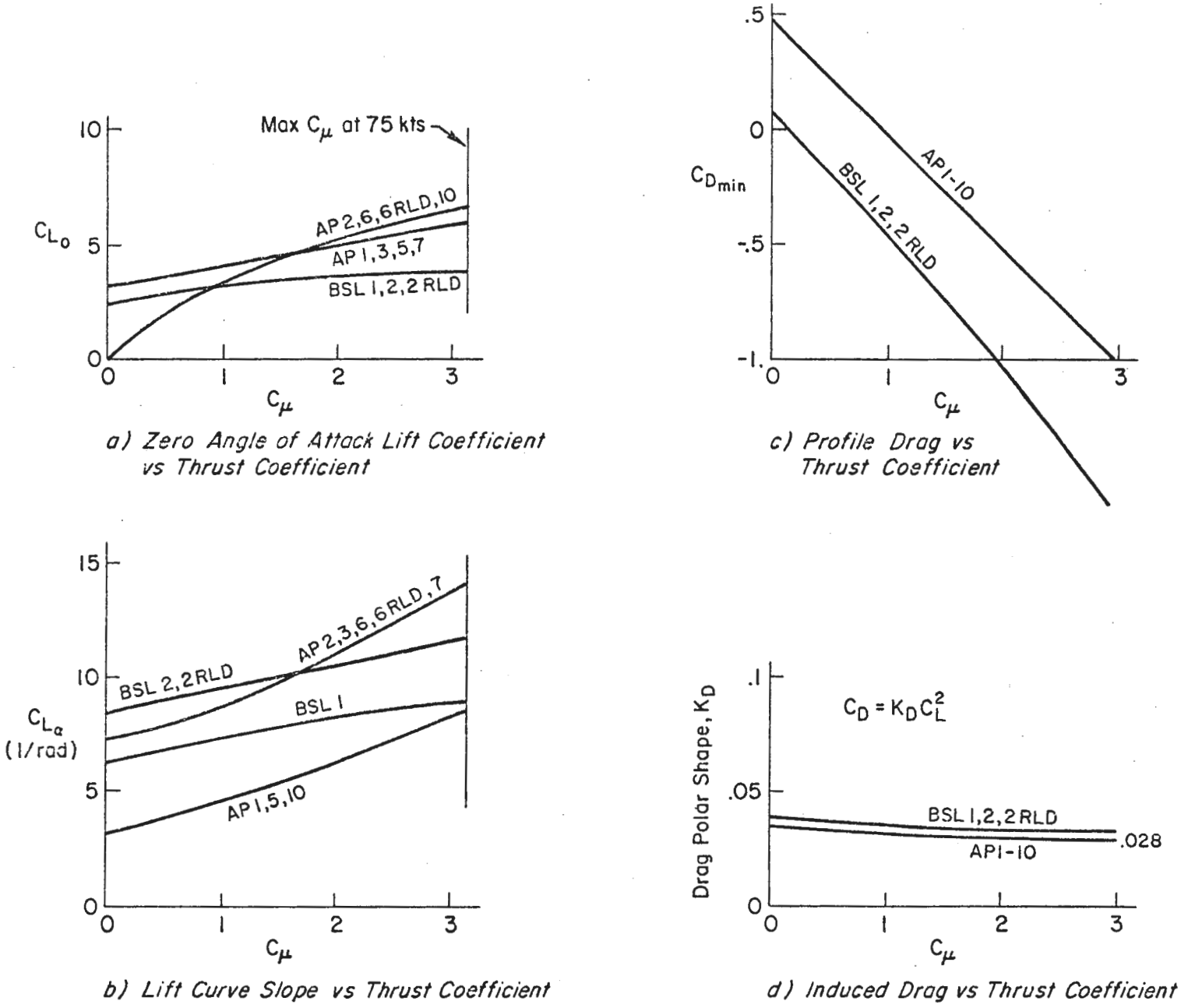

Figure 1. Lift and Drag Characteristics of the Simulated Configurations

The magnitude of the lift and lift curve slope and their linearity with thrust coefficient were the major variables in the study and are classified into five "groups" in Table 1. Group I is representative of low efficiency EBF (externally blown jet flap) configurations with low effective thrust inclination angles, θ_T. The powered-lift effects (C_{L_o} vs. C_μ) are low, and the flight characteristics would be expected to be somewhat conventional. The Group II configurations represent high efficiency powered-lift STOL concepts. Because lift increases rapidly as the power is increased from zero thrust; these configurations have inherently nonlinear C_{L_o} vs. C_μ and C_{L_α} vs. C_μ characteristics as shown in Fig. 1. Group III has the higher C_{L_o} vs. C_μ characteristics of Group II without the nonlinear shape (see Fig. 1a). The C_{L_α} vs. C_μ characteristics of Groups II and III are identical (Fig. 1b). Group IV combines the linear C_{L_o} vs. C_μ characteristics of Group III with a 50 percent reduction in lift curve slope. Finally, Group V combines the nonlinear C_{L_o} vs. C_μ effects of Group II with the very low lift curve slope of Group IV.

Two configurations were picked to investigate the effect of nonlinear lift curve shapes near stall as shown in Fig. 2. The BSL2 RLD configuration represents the effect of a constantly decreasing lift curve slope with increasing angle of attack as compared with the more abrupt change in lift for BSL2. The AP6 RLD stall characteristics were hypothesized to show the effect of stalling at a constant C_L independent of C_μ. This is more typical of CTOL characteristics which show only minor variations in stall speed with power setting.

A. STEADY-STATE CHARACTERISTICS

Of the various methods of presenting steady-state performance characteristics, the most useful is a plot of flight path vs. airspeed ($\gamma - V$) contours for constant power settings and pitch attitudes. Such a map graphically shows how the steady-state values of the important responses vary with trim condition and with off-nominal excursions about trim. The γ, V, θ contours for representative configurations in Groups II through V are given in Fig. 3. Nominal (symbol ✕) and off-nominal (symbols ▽ and △) trim conditions are shown. Key features of these plots are summarized as follows.

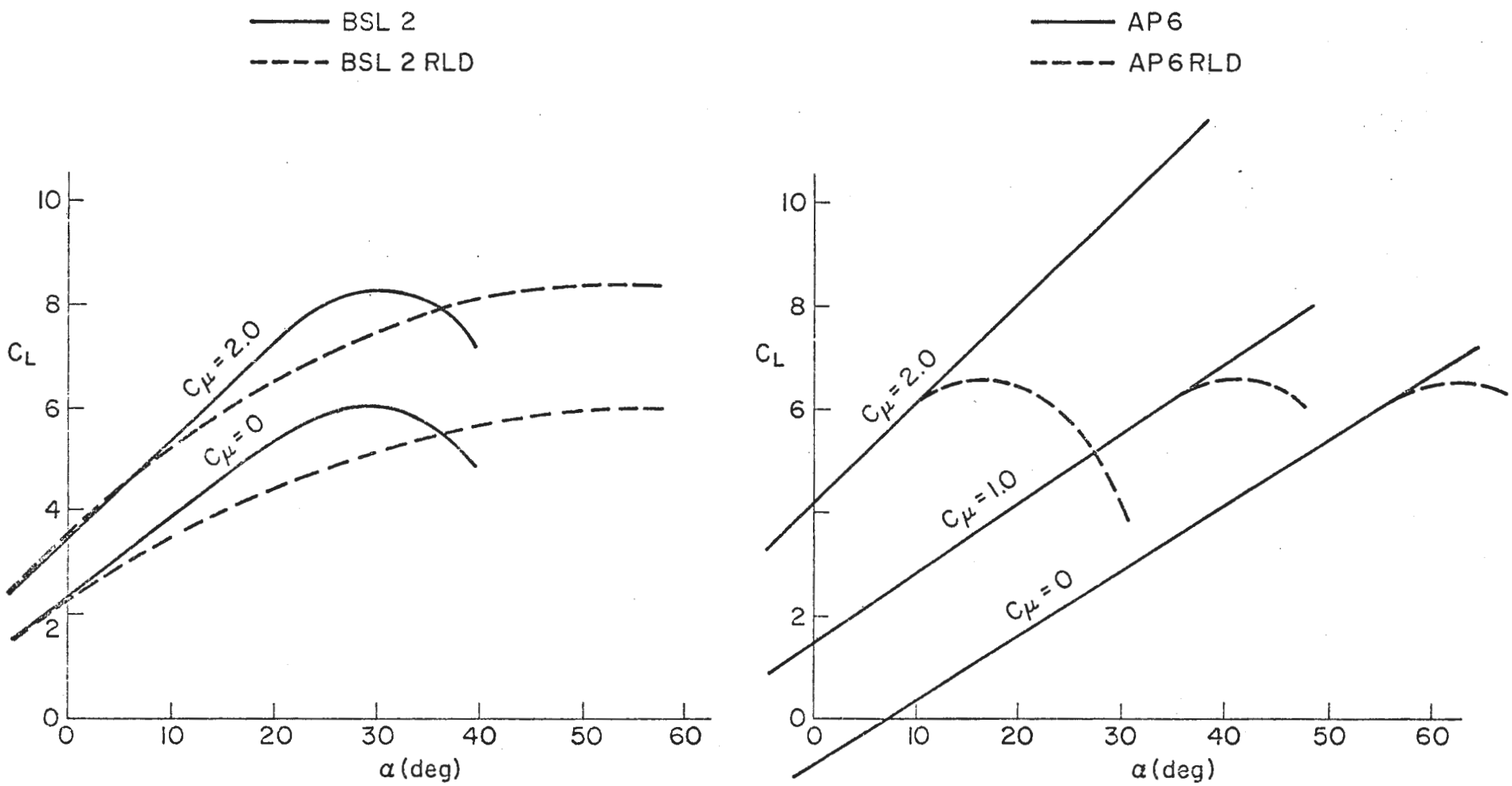

a) BSL 2 and BSL 2 RLD

b) AP6 and AP6 RLD

Figure 2. Stall Characteristics Tested

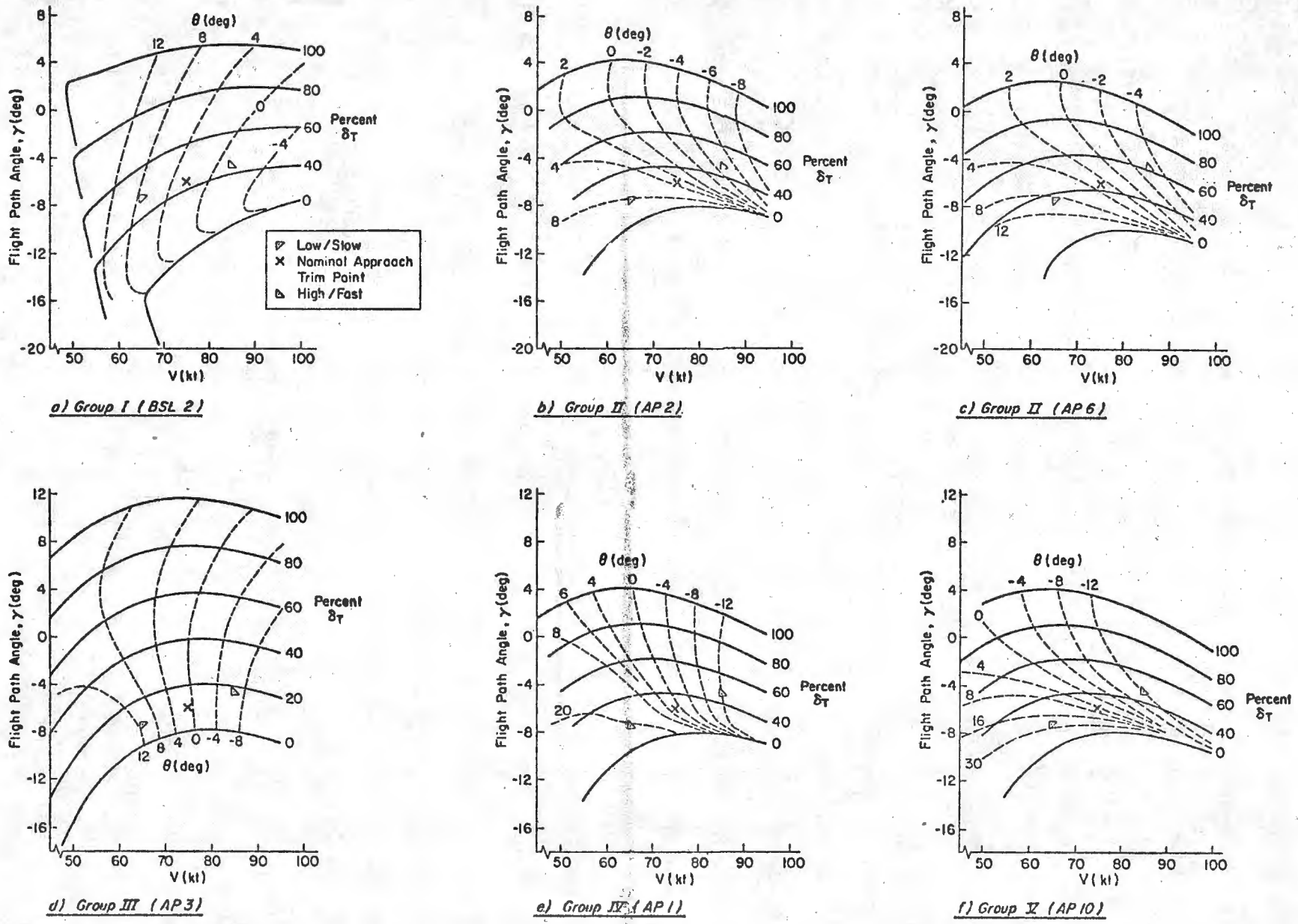

Figure 3. $\gamma - V - \theta$ Plots for the Tested Generic Configurations

1. Constant power lines. Defines the appropriate control technique. If $(\partial\gamma/\partial V)_{\delta T}$ is positive (or negative but small) the STOL technique of using pitch attitude to control speed and power to control sink rate is appropriate. This is the case for all the tested configurations.

2. Constant attitude lines.

   a. The slope of the constant attitude lines $(\partial V/\partial\gamma)_\theta$ defines the magnitude and sign of airspeed/flight path coupling for the steady-state situation. Positive values of $(\partial V/\partial\gamma)_\theta$ are referred to as proverse coupling and are characteristic of the Group I configurations. Physically, this means that for constant attitude flight the trim speed will increase as the flight path angle is increased with power. Proverse coupling is typical of all CTOL aircraft. The constant attitude lines for Group III are nearly vertical $(\partial V/\partial\gamma)_\theta \doteq 0$), indicating neutral airspeed/flight path coupling. Group IV exhibits weak to moderate adverse coupling, $(\partial V/\partial\gamma)_\theta = -1.75$ kt/deg; and Groups II and V show strong adverse coupling, $(\partial V/\partial\gamma)_\theta$ from -4.8 to -5.6 kt/deg).

   b. The spacing of the attitude lines (along lines of constant speed) is indicative of the magnitude of change in trim pitch attitude required to hold airspeed constant while changing flight path angle with power. This gradient, $(\partial\theta/\partial\gamma)_V$, tends to become quite nonlinear at low power settings for the adversely coupled vehicles (Groups II, IV, and V). The resulting large pitch attitude requirements (greater than 30 deg for AP 10) will, in some cases, limit the down γ capability; i.e., if the pilot is unwilling to either let speed vary or use extreme pitch attitude. Increasing the down $(\Delta\gamma)$ capability from -2° to -4° (from the nominal $\gamma = -6^\circ$) tends to increase the attitude gradient. For example, compare AP2 and 6 in Group II (see Fig. 3).

   c. The constant attitude lines may be quite nonlinear at low power settings, resulting in sudden changes in airspeed/flight path coupling. For example, $(\partial\gamma/\partial V)_\theta$ changes abruptly from -1.7 deg/kt to -5 deg/kt as the power is decreased below 20 percent in AP1 (Fig. 3e). Similar effects are seen to occur at very low power settings in Group I.

3. Trim point. The location of the trim point relative to the zero thrust constant power line defines the down capability in terms of degrees of $\Delta\gamma$ from the nominal glide slope angle. Unfavorable constant attitude contours in the region of trim may further restrict the down capability. Additionally, as

the trim point is moved to lower speeds the backside effects are magnified [increased slope of $(\partial\gamma/\partial V)_{\delta_T}$] and the speed/path coupling is increased for adversely coupled configurations (Groups II, IV, and V). In the case of Groups II and V, lower trim speeds will result in flat constant attitude contours [$(\partial\gamma/\partial V)_\theta = 0$], indicating that power has no steady-state effect on flight path. Finally, moving the trim point to higher power settings generally improves the speed coupling characteristics. This implies a lower trim flight path angle or an increase in drag which would move the $\gamma - V$ contours downward.

Simple analytical expressions may be derived from the attitude constrained equations (Appendix B) which relate the basic performance parameters to the slope of the constant attitude linears $(\partial\gamma/\partial V)_\theta$ as follows.

$$\left(\frac{\partial\gamma}{\partial V}\right)_\theta \doteq -\frac{2}{V_{trim}} \frac{(C_D/C_L \tan\theta_T + 1)}{(1 - C_{D_\alpha}/C_L)\tan\theta_T - C_{L_\alpha}/C_L} \tag{1}$$

or in terms of the dimensional derivatives

$$\left(\frac{\partial\gamma}{\partial V}\right)_\theta \doteq \frac{1}{V_{trim}} \frac{\tan\theta_T X_u + Z_u}{\tan\theta_T X_w + Z_w} = -\frac{\tan\theta_T}{V_{trim}} \frac{T_{u_\theta}}{T_{d_\theta}} \tag{2}$$

It follows directly from these equations that adverse airspeed/flight path coupling [$(\partial\gamma/\partial V)_\theta$ negative] occurs when:

$$\boxed{\tan\theta_T > \frac{C_{L_\alpha}}{C_L - C_{D_\alpha}}} \tag{3}$$

or

$$\tan\theta_T > -\frac{Z_w}{X_w} \tag{4}$$

Thus, we have established the underlying relationships which result in adverse airspeed/flight path coupling.

Physically, Eq. 3 shows that the factors responsible for adverse airspeed/flight path coupling are large effective turning angles combined with low lift curve slope and/or large lift coefficients. Note that the more severely coupled configurations (AP10) exhibit combined adverse effects (e.g., large θ_T and C_L, and low C_{L_α}).

B. DYNAMIC CHARACTERISTICS

1. Pitch Attitude SAS

Each of the configurations tested utilized the pitch attitude SAS shown in Fig. 4. The design philosophy of the pitch augmentation was to obtain a minimum acceptable SAS (pilot rating of 3-1/2) that would keep the attitude dynamics from being a dominant factor in the ratings. A relatively low gain closure was utilized (bandwidth of about 0.8 rad/sec).

This augmentation scheme meets the minimum needs of the pilot for attitude stabilization based on the criterion of Ref. 3 and the closed-loop requirements from which the criterion was derived. Furthermore, the attitude closure (i.e., bandwidth) cannot be significantly improved by the pilot's compensation; thus the influence of attitude loop tightness is minimized. The pilots generally did not tighten up on the attitude loop and were basically willing to accept the low gain attitude dynamics during ILS tracking.

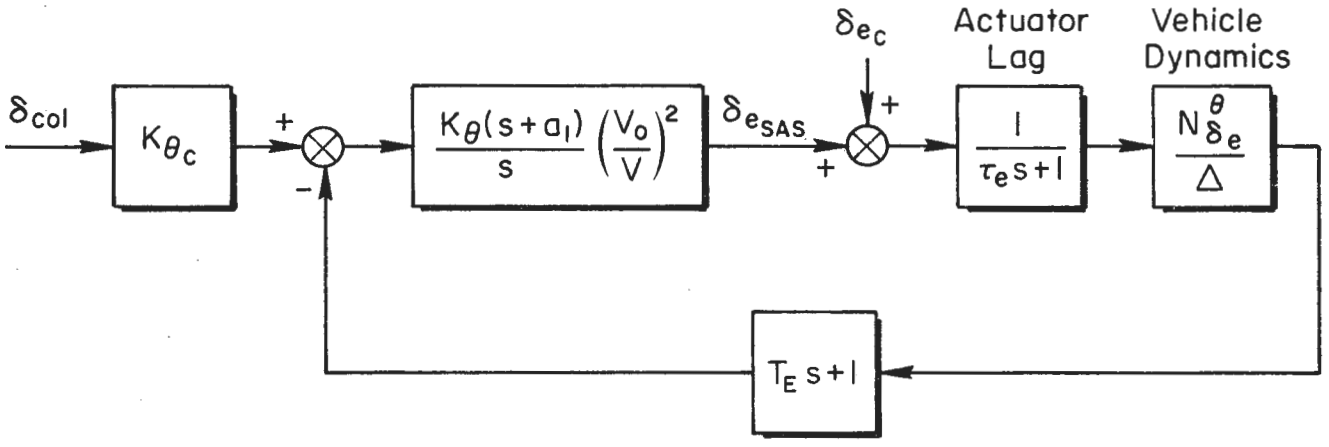

K_{θ_c}	= −4.0 deg/in.	τ_e	= 0.1 sec
K_θ	= −1.0	T_E	= 2.0 sec
a_1	= 0.2 sec^{-1}	V_o	= 75 kt

Figure 4. Pitch SAS Used in Generic STOL Simulation

Thus, the pilots appear to have recognized that they could not improve the attitude loop or the path modes by a tighter inner attitude loop. This is to be expected since the path mode poles drive into the numerator zeros for very low values of K_θ. The result is identical responses of $\dot{h}/\delta_T$ for low and high values of K_θ at path mode frequencies. This explains why the assumption of constrained attitude in Appendix B is also valid for low attitude gain closures when analyzing path mode dynamics.

There was some tendency for the pilots to PIO in pitch attitude during flare and landing when tight attitude control is desired.

2. Flight Path Dynamics

The attitude-constrained beam-rate-to-throttle dynamics for the tested generic configurations are shown in Fig. 5 in terms of time response to a unit step input and frequency response characteristics. The overshoot in the time response for some configurations is seen to be equivalent to a peak in the frequency response. This peak is generally characterized by a first-order zero, $1/T_{h\theta}$, and the roots of the attitude-constrained characteristic equation (Appendix B). Thus, the generic forms of the $\dot{d}/\delta_T$ responses are defined by the coupling numerator zero, $1/T_{h\theta}$, and the two roots of the attitude numerator, $N^{\theta}_{\delta_e}$. The generic forms of the $\dot{h}/\delta_T$ and $\dot{h}/\theta_c$ frequency response asymptotes are shown in Fig. 6. The beam rate to attitude responses either exhibit a sign reversal ($1/T_{h_1}$ negative) or decay to zero ($1/T_{h_1} = 0$). This was discovered very early by the evaluation pilots and path control was accomplished with power in all cases. The $\dot{h}/\delta_T$ overshoot is characterized by low values of the coupling numerator zero, $1/T_{h\theta}$. The definition of $1/T_{h\theta}$ $[1/T_{h\theta} = -X_u - Z_u(X_{\delta_T}/Z_{\delta_T})]$ shows that increasing the effective thrust inclination angle θ_T $[\theta_T = \tan^{-1}(-Z_{\delta_T}/X_{\delta_T})]$ tends to reduce $1/T_{h\theta}$, thereby increasing the overshoot. In fact, it can be shown that the $\dot{h}/\delta_T$ response reverses sign (putting the vehicle on the backside for throttle control) when:

$$\theta_T > 90^\circ + \tan^{-1}(X_u/Z_u) \tag{5}$$

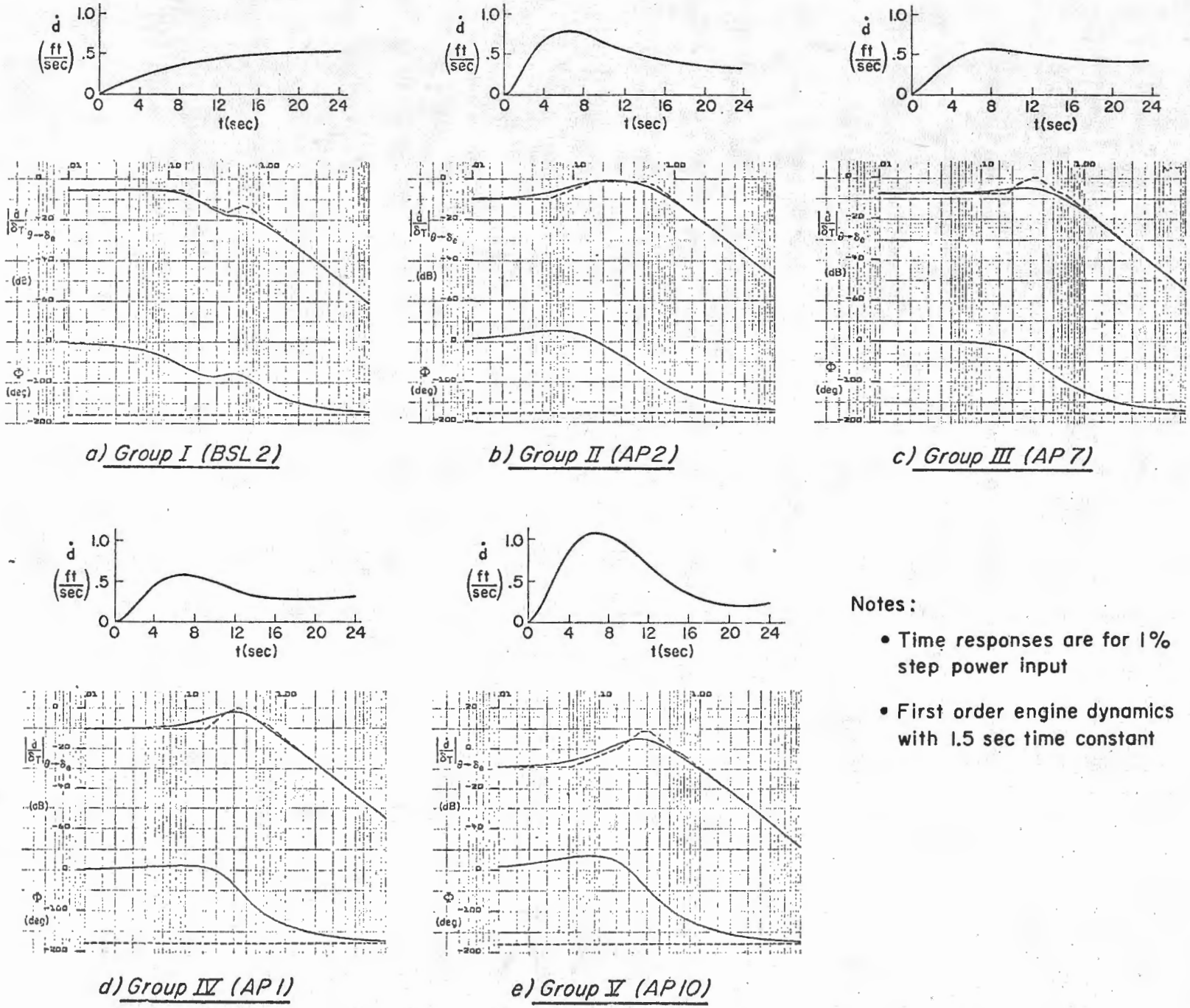

a) Group I (BSL 2)

b) Group II (AP2)

c) Group III (AP 7)

d) Group IV (AP 1)

e) Group V (AP 10)

Notes:

- Time responses are for 1% step power input
- First order engine dynamics with 1.5 sec time constant

Figure 5. Dynamic Response Characteristics of Beam Rate to Power (Attitude SAS On)

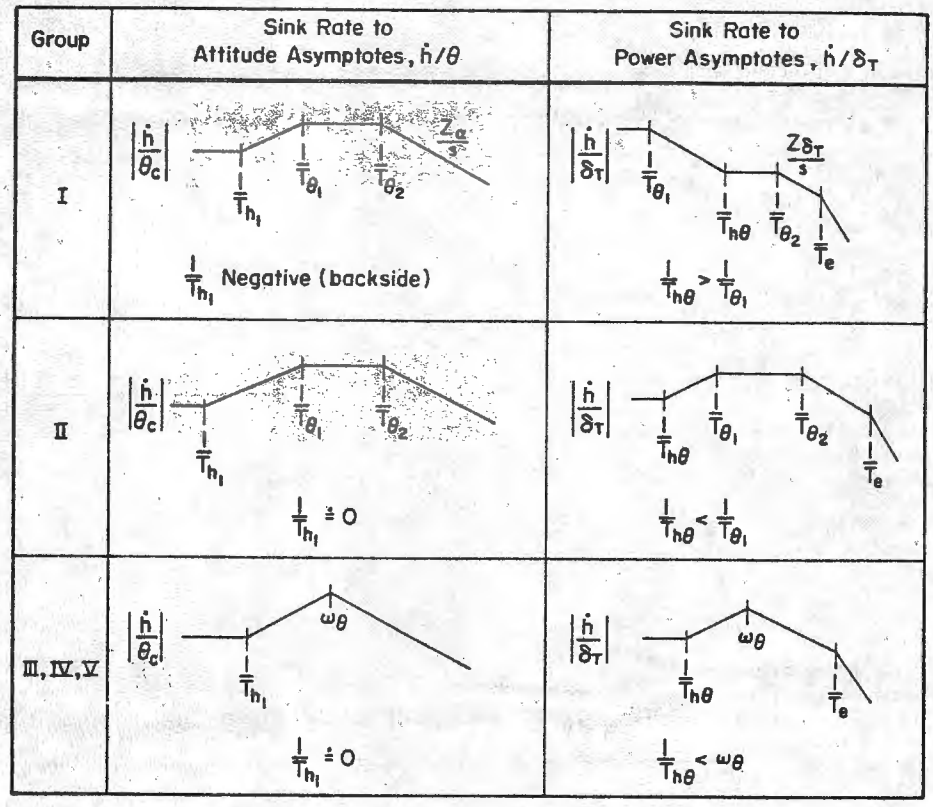

Note: The washout effect is almost negligible in Group III due to high ζ_θ and $1/T_{h\theta}$ close to ω_θ.

Figure 6. Generic Characteristics for Sink Rate Control with Attitude and Throttle

Thus, there is a direct correlation between thrust inclination angle and dynamic path overshoot. Furthermore, the thrust inclination has been shown to be tied to the steady-state coupling (Eq. 1). Hence, there is a direct correspondence between the STOL performance parameters and the dynamic response, and that the dynamic and steady-state characteristics are directly related. Specifically, high effective turning angles and large lift coefficients required for good STOL performance are directly responsible for adverse path/speed coupling and path overshoot. From a practical standpoint numerical solutions to Eqs. 4 and 5 indicate that the condition for low-frequency flight-path-to-throttle sign reversals ($1/T_{h\theta} < 0$) occurs at significantly higher thrust inclination angles than the condition for adverse path/airspeed coupling. For the tested configurations, the value of θ_T required to obtain adverse path/speed coupling ranged from about 85 deg for Group I down to 50 deg on Group V. The critical value of θ_T

which would result in low-frequency $\dot{d}/\delta_T$ sign reversals varied from 100 deg on Group V to 104 deg on Group II. None of the configurations tested had this characteristic at the nominal trim flight condition (75 kt) although three configurations (AP2, 6 RLD, and 10) exhibited a flight-path-to-throttle sign reversal at 65 kt (e.g., add power and end up sinking faster in the steady state).

3. Rate Change of Dynamics

An important aspect of the STOL path control problem is the rate at which the basic vehicle dynamics change with speed or power setting. The piloted simulation results reported in Ref. 5 indicate that large changes in vehicle response characteristics with small changes in speed are very undesirable. In fact, a key issue in the present investigation is the character of speed margins based not only on stall but also on regions of unacceptably poor handling qualities. The variation in the dynamic response with speed for the tested configurations is given in Fig. 7 in terms of the ratio of peak to steady-state values of the Bode asymptotes in Fig. 6. It will be shown later that the shape of the $\dot{h}/\delta_T$ frequency response has a significant effect on closed-loop piloted control during ILS tracking and landing. All of the

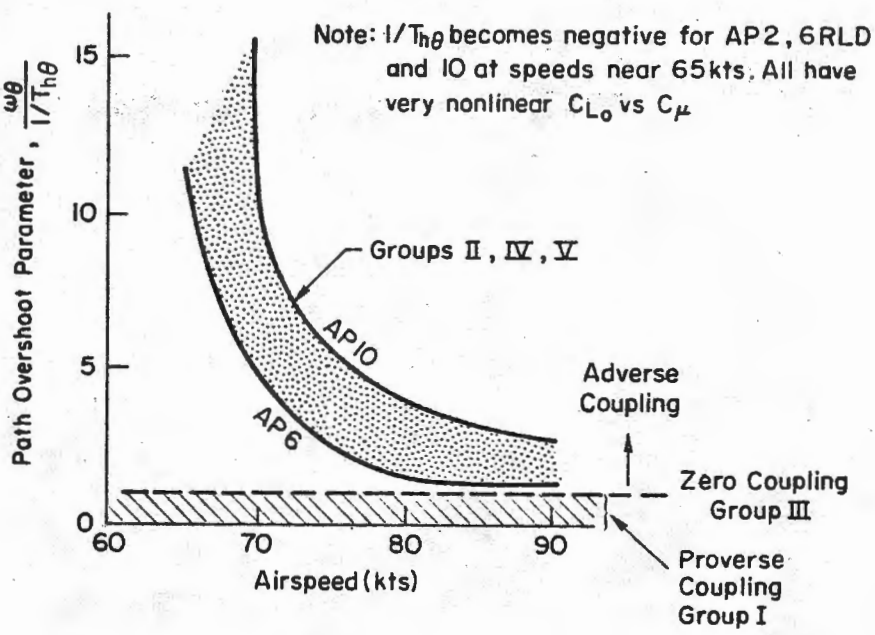

Figure 7. Effect of Airspeed on the Dynamic Response

adversely coupled configurations are seen to exhibit a fairly rapid increase in overshoot with decreasing speed. AP10 has the most rapid degradation and AP2, 6 RLD, and 10 all exhibit a reversal in sign at 65 kt. The time responses for AP10 (see Fig. 8) illustrate the dramatic effect of speed on this configuration.

C. DESCRIPTION OF THE SIMULATION

The equations defining the generic STOL simulator model and a complete description of the cockpit layout, computer facility, and moving base cab are given in Volume II. The instrument display and cockpit controls were typical of a conventional present day CTOL transport.

1. Simulation Scenario

The piloting tasks were broken down into subtasks and a composite task as outlined in Table 2 below. The geometry of the flight task is shown in Fig. 9.

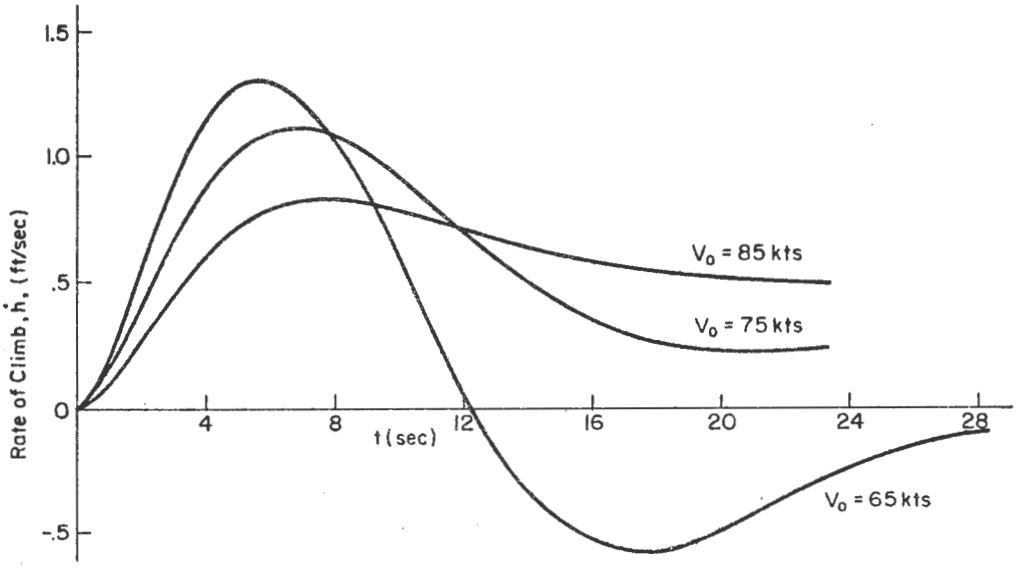

Figure 8. Effect of Speed on Path Response to a Unit Step Power Input (AP10)

TABLE 2

SIMULATION TASK DESIGNATION AND DESCRIPTION

TASK DESIGNATION	TASK DESCRIPTION
Glide slope tracking (Start at 1100 ft and termiminate at 300 ft of altitude — all IFR)	
1.0	Calm air
1.01	Turbulence (σ = 4.5 ft/sec) (IFR only)
1.1	High fast initial condition (IFR only) } See Fig. 9
1.2	Low slow initial condition (IFR only) } See Fig. 9
1.7	Speed change on glide slope (IFR only)
Landing (Initial condition at 300 ft — IFR)	
2.0	Attitude flares and power flares in calm air
2.1	Add turbulence (σ = 4.5 ft/sec)
2.7	Add discrete shear
Composite ILS approach task (Rate glide slope intercept, path control, and flare and landing separately)	
3.0	Calm air (IFR and VFR)
3.1	Turbulence (σ = 4.5 ft/sec) (IFR and VFR)
3.2	Headwind } (IFR and VFR)
3.3	Tailwind } (IFR and VFR)

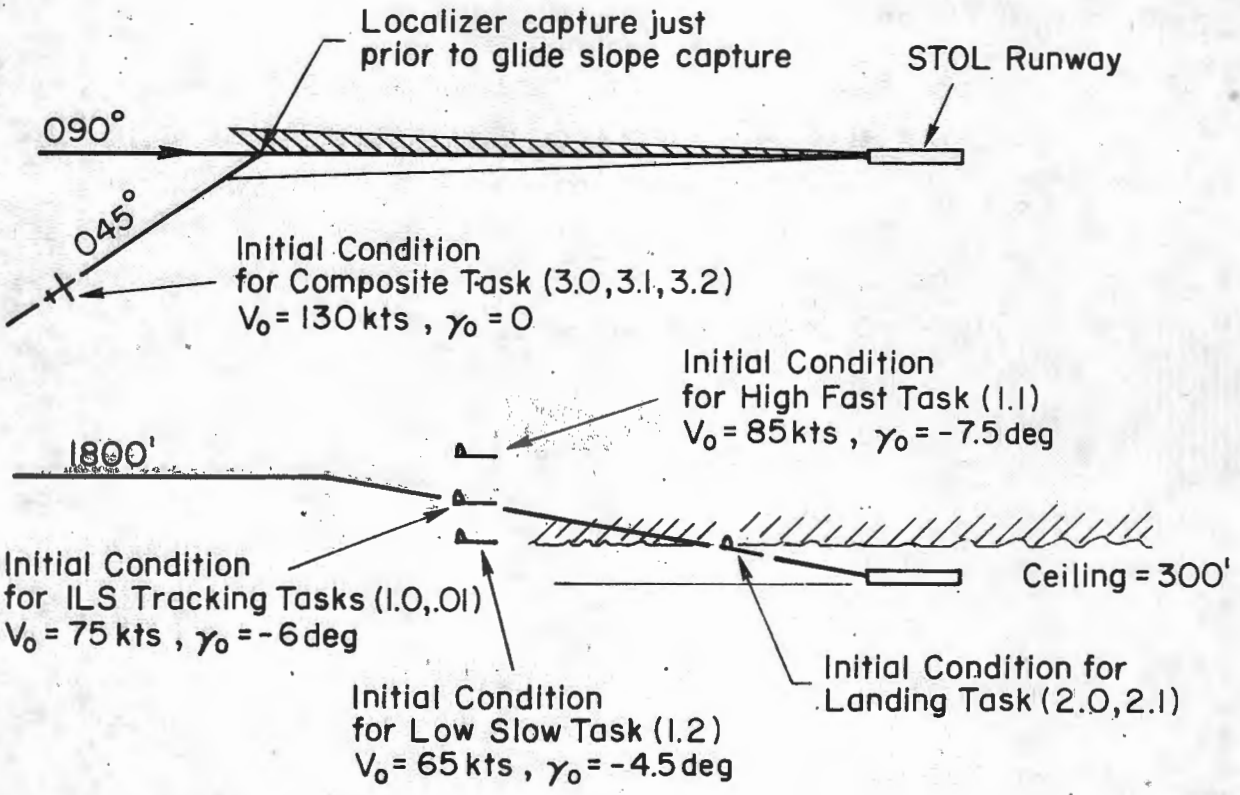

Figure 9. Flight Task Description

Each pilot was given a presimulation briefing which consisted of an oral presentation and a written outline (Appendix D). Several pilot questionnaires were developed (see Appendix D) to obtain pilot opinion of the tested configuration and to help quantify the pilot technique being used. The test engineer (riding in the cockpit with the pilot) utilized these questionnaires to obtain spontaneous pilot responses (and pilot ratings) during and immediately after a series of runs for each piloting task. Particular emphasis was placed on obtaining specific literal interpretations of the Cooper Harper scale. In this regard, the pilots were asked to justify their rating by relating the verbal description on the Cooper Harper scale to specific handling problems they had encountered.

2. Data Gathering

1. The simulation data consist of pilot ratings and commentary, analog strip chart records, pilot performance measures, and describing function data. Pilot ratings were obtained for each of the subtasks listed in the previous section. In addition, pilot ratings were obtained for each segment of the composite ILS approach task; glide slope intercept, glide slope tracking, flare and landing, and an overall rating.

SECTION III

SIMULATION RESULTS

An extensive two-phase simulation program involving eleven generic STOL configurations and nine research pilots was conducted on the NASA Ames S-16 Moving Base Simulator. The first simulation period served to identify the critical flight regions which were then investigated in detail in a second simulation period. The pilot ratings, commentary, and other results presented in the following sections are a direct result of the more detailed investigation (second simulation period).

A. FLIGHT PATH CONTROL

The pilot rating data and commentary for the glide slope tracking, flare and landing, and composite tasks (Tasks 1.01, 2.1, and 3.1) revealed that flight path control deficiencies were most apparent on short final during the visual portion of the approach. It was not possible to obtain a numerical assessment of flight path control on short final (last 300 ft of approach) since this case was not separated out and rated as a separate task during the experiment. However, it was possible to draw certain inferences from comparison of the pilot ratings for the composite approach task (3.1) and the ILS tracking task (1.01). This comparison (shown in Fig. 10) allows us to make the following observations:

- The ratings for the IFR approach tracking task (1.01) showed little difference across the configurations, e.g., none of the configurations were rated worse than a 5.
- The ratings for the composite task, which included both IFR and VFR tracking, indicated that two configurations (AP1 and AP10) were definitely unacceptable (large spread with ratings of 7 or worse) and that two configurations (AP6 and BSL2 RLD) were marginal (large spread with ratings up to 6).
- The only appreciable difference between the glide path tracking portion of Task 3.1 and Task 1.01 was that Task 3.1 included a VFR tracking segment on final approach after breakout (glide slope intercept was rated separately).

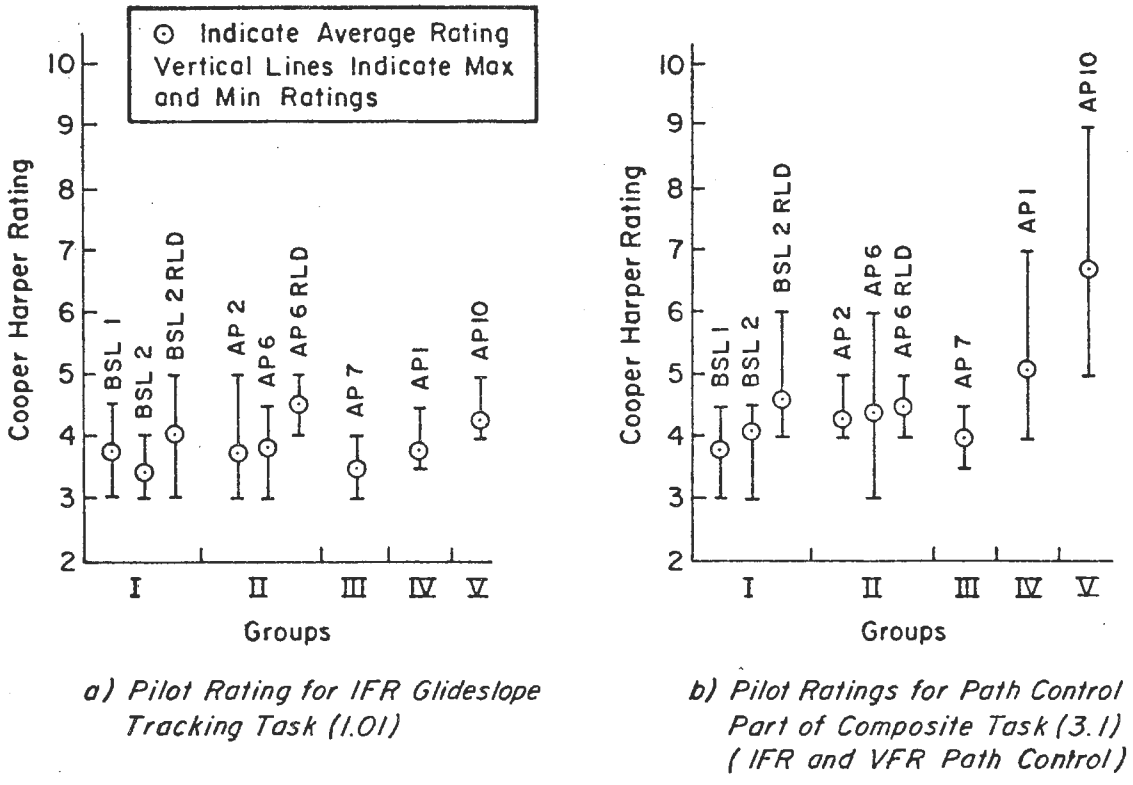

Figure 10. Pilot Ratings for Tasks 1.01 and 3.1

Based on the above observations, it seems reasonable to conclude that the tracking problems that resulted in degraded pilot ratings for Task 3.1 were associated with the final portion of the approach between breakout and initiation of flare. This indirect inference led to a careful review of the pilot comments (see Appendix A) regarding flight path control and any indications of problems in setting up for flare. The results of this review are shown in Table 3 where it can be seen that most of the tested configurations received some adverse commentary regarding flight path control on short final in turbulence. This reflects the experimental design, in that all configurations represent marginal cases of various STOL concepts. (Recall that the basic goal of the study was to find out what features or combinations of features resulted in crossing the boundary from marginal to unacceptable.) The large number of, and intensity of, derogatory comments regarding flight path control on short final for

TABLE 3. PILOT COMMENTARY WHERE FLIGHT PATH CONTROL PROBLEMS ON SHORT FINAL WERE SPECIFICALLY NOTED (TASKS 2.1 AND 3.1)

	PILOT 1	PILOT 2	PILOT 5	PILOT 7	PILOT 8	PILOT 9
BSL1	None	Poor vertical speed response makes it easy to overcontrol Put on too much power to correct for a low condition and then don't get it off in time, etc.		None	None	Am flying glide slope (ILS) to get to window for flare
BSL2	None	None		I am having quite a bit of problems with the turbulence particularly during the final glide slope tracking and the flare	None	None
BSL2RLD	Requires moderate compensation on throttles to set up for flare			None		Poor sink rate to throttle response is responsible for problems in getting set up at flare point Flying IVSI to throttles even in close
AP1	The primary deficiency is a very sluggish sink rate to throttle response. The major problem is the inability to recover from off nominal vertical position in time to set up for landing on this short runway		Pilot rating is a 3 down to breakout and then a 7 on short final	The workload gets too high trying to get the power set for your flare, particularly with these last minute flight path corrections where the power can be going up and down	... real dicey to get a good sink rate and a good aim point on the runway	Primary difficulty was the considerable lag in the throttle and if your effecting a change on glide path the resulting change in sink rate late in the approach will give you real problems
AP2	The primary problem in landing is setting up for the flare with power in the presence of these fairly large gust disturbances	Recovery from turbulence effects coming into the flare was difficult		Turbulence is not a problem and getting set up for flare is also not a problem with this configuration		
AP6	None	None		None		
AP6RLD	Moderate compensation on sink rate control with power is required to set up the flare point			Sink rate response to attitude and power are good		None
AP7	None			None		None
AP10	The sluggish sink rate to throttle makes it difficult to get set up. My primary objection to this configuration lies in the inability to control sink rate during the last several hundred feet of the approach			The main problem with flight path control is that flight path angle washes out after a throttle input. This problem is especially noticeable as you approach the flare point and even during the flare	Got low and slow, a bear to correct	Seems very sensitive to throttle making it difficult to set up for flares. Extremely hard to get into proper flare window

Notes: Blank space means pilot did not fly the configuration.

"None" means that no specific comments relative to flight path control on short final were recorded.

Configurations AP1 and AP10 tended to support the results inferred from the pilot ratings, that is, that these configurations were unacceptable for flight path control and that the primary problem occurred during the visual portion of the approach.

B. PATH/SPEED COUPLING

Based on earlier work (for example, see Refs. 2, 4, and 5), adverse path/speed coupling was expected to be a heavy contributor towards the definition of minimum acceptable boundaries. This was not the case for the configurations tested in this experiment. While the pilots found that adverse speed/path coupling was undesirable, it was not a major factor in the final pilot ratings. The evidence upon which this conclusion is based is summarized below.

- Quantitative measurements of the pilot's closed-loop tracking behavior via describing functions showed no evidence of active (closed-loop) speed control (these measurements are discussed in the next section).
- A review of the pilot commentary (see Appendix A) indicated that speed was monitored rather than controlled for adverse coupled configurations. Additionally, some pilots volunteered that the adverse speed/path coupling represented a rating degradation of only 1/2 to 1 point. (For example, see the commentary for Pilots 2 and 7, Task 1.01, for Configuration AP2 in Appendix A.)
- The strip chart records of the simulation show evidence of changes in trim pitch attitude with long-term speed excursions but no evidence of closed-loop speed control. This result holds true for the IFR glide slope tracking portion of the approach, as well as the visual aim point control after breakout and before the initiation of flare. Two examples of this result are shown in Fig. 11. The example in Fig. 11a illustrates the use of a pitch attitude bias in response to a very large long-term airspeed excursion (see Channels 5 and 6). Note that errors in the flight path (Channel 3) are dealt with by use of the throttle (Channel 7). The lack of concern over airspeed excursions is even more dramatically illustrated in Fig. 11b where the pilot held constant attitude throughout the approach even in the presence of a long-term persistent airspeed error of between 5 and 9 kt. It should be noted that these results are consistent and repeatable across all the pilots for the adversely coupled configurations.

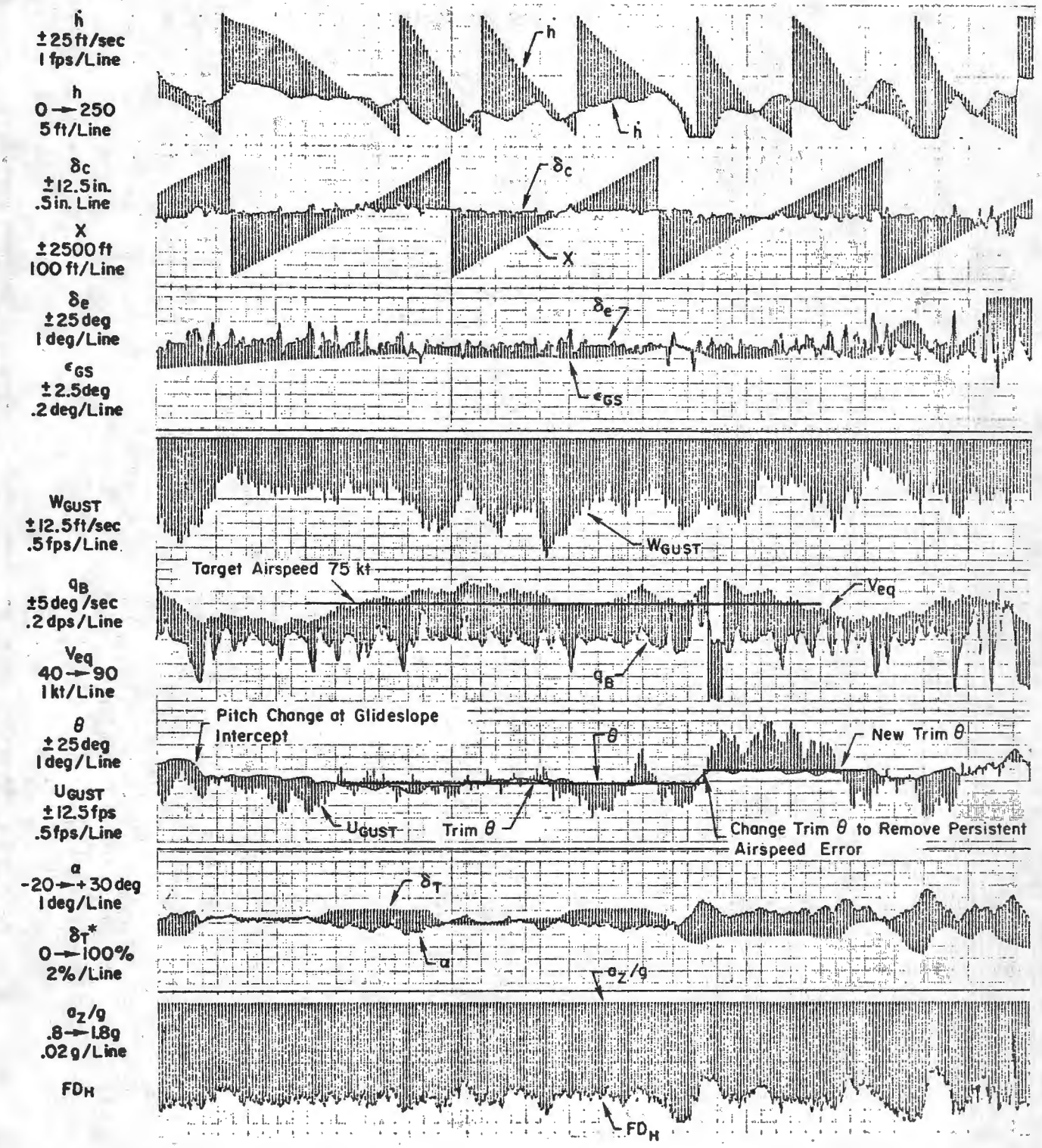

Figure 11a. Example of Typical Airspeed Control on Configuration with Large Speed-Path Coupling and Large L_α (Configuration AP6, Pilot 7) Task 3.1

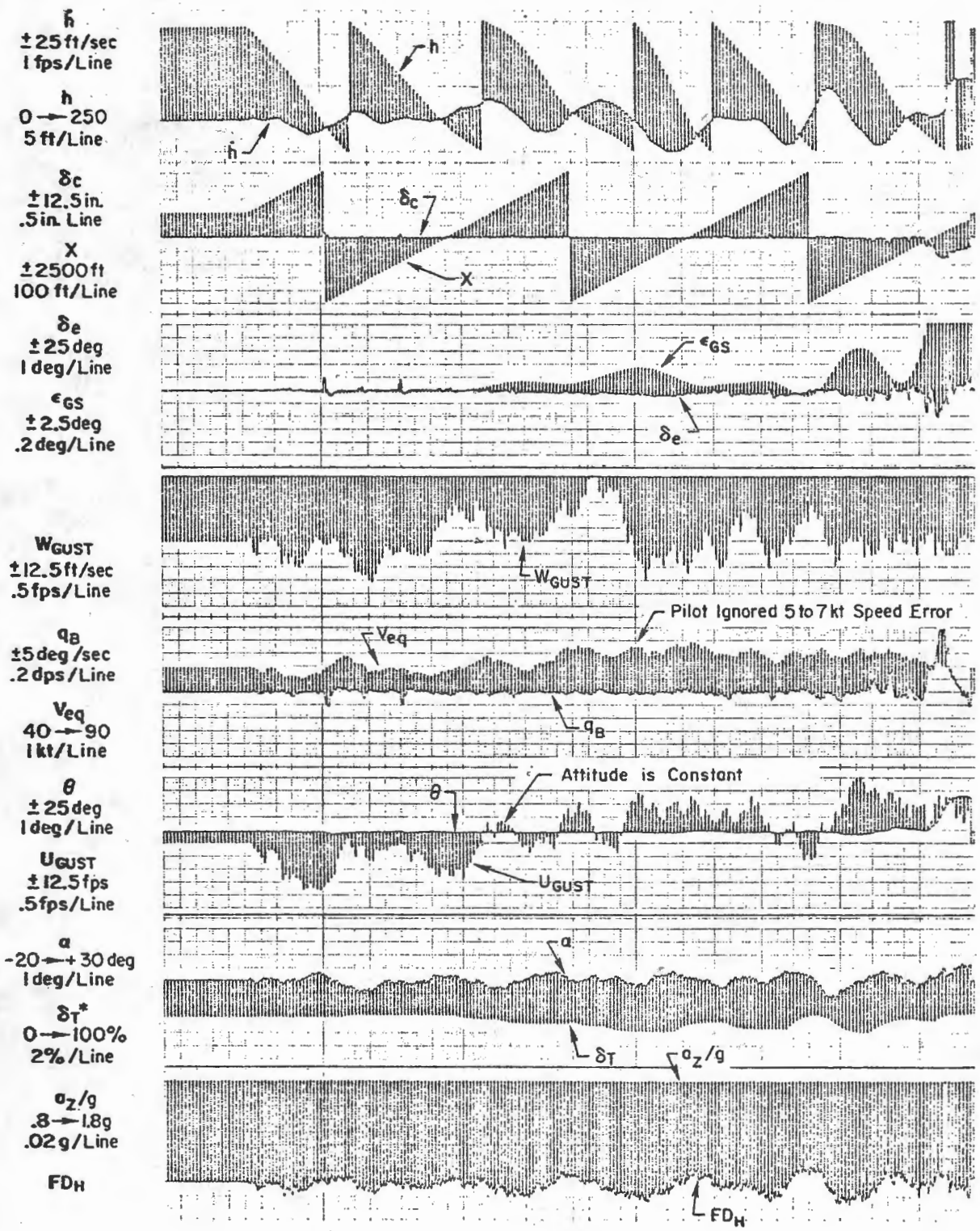

Figure 11b. Example of Pilot Technique for Path Control on Configuration with Very Large Path-Speed Coupling and Low C_{L_α} (Task 1.01 and 2.1 Combined, Pilot 7 Configuration AP10)

- The pilot rating for Configuration AP6 RLD was initially a 9. This rating was given after a run where the pilot got low on short final and added power. Because of the strong adverse coupling on this configuration, the airspeed decreased to below stall and control was lost (too low to recover). The stall speed was decreased slightly (64 kt to 61 kt) so that increasing power at the trim pitch attitude did not result in a stall (increased $C_{L_{max}}$ by 10 percent) as shown in Fig. 12. The pilot rating then improved to a 5.

In summary, the above results indicate that as long as the flight path response or aircraft safety margins were not degraded, the pilots tended to simply monitor speed and fly constant attitude. Adverse speed/path coupling had only a minimal effect on the pilot ratings, which tended to be more directly associated with ability to control the flight path. These results were published in early progress reports and were checked by other investigators running STOL certification simulator programs (Ref. 5). These investigators concurred that the pilots were not controlling airspeed for adversely coupled configurations. There now appears to be a general acceptance of the fact that airspeed control in itself is not the appropriate flight reference for many STOL configurations. For the configurations in this experiment, constant attitude appeared to be a good flight reference. Considerations for formulating a flight reference for various STOL configurations are discussed in Ref. 5.

C. CLOSED LOOP TRACKING BEHAVIOR

1. Pilot Vehicle Loop Structure

All of the pilots indicated that the technique for glide slope tracking was primarily to control the glide slope deviation <u>rate</u> ($\dot{d}$). A summary of pilot commentary and interpretation of the time histories is given below in terms of a set of rules which effectively quantify the technique used for glide slope tracking with <u>power</u>.

a. Keep $\dot{d}$ at a very low level by controlling IVSI with power, e.g., find a target IVSI that keeps the glide slope bug stationary on the display (nominally 800 ft/min)

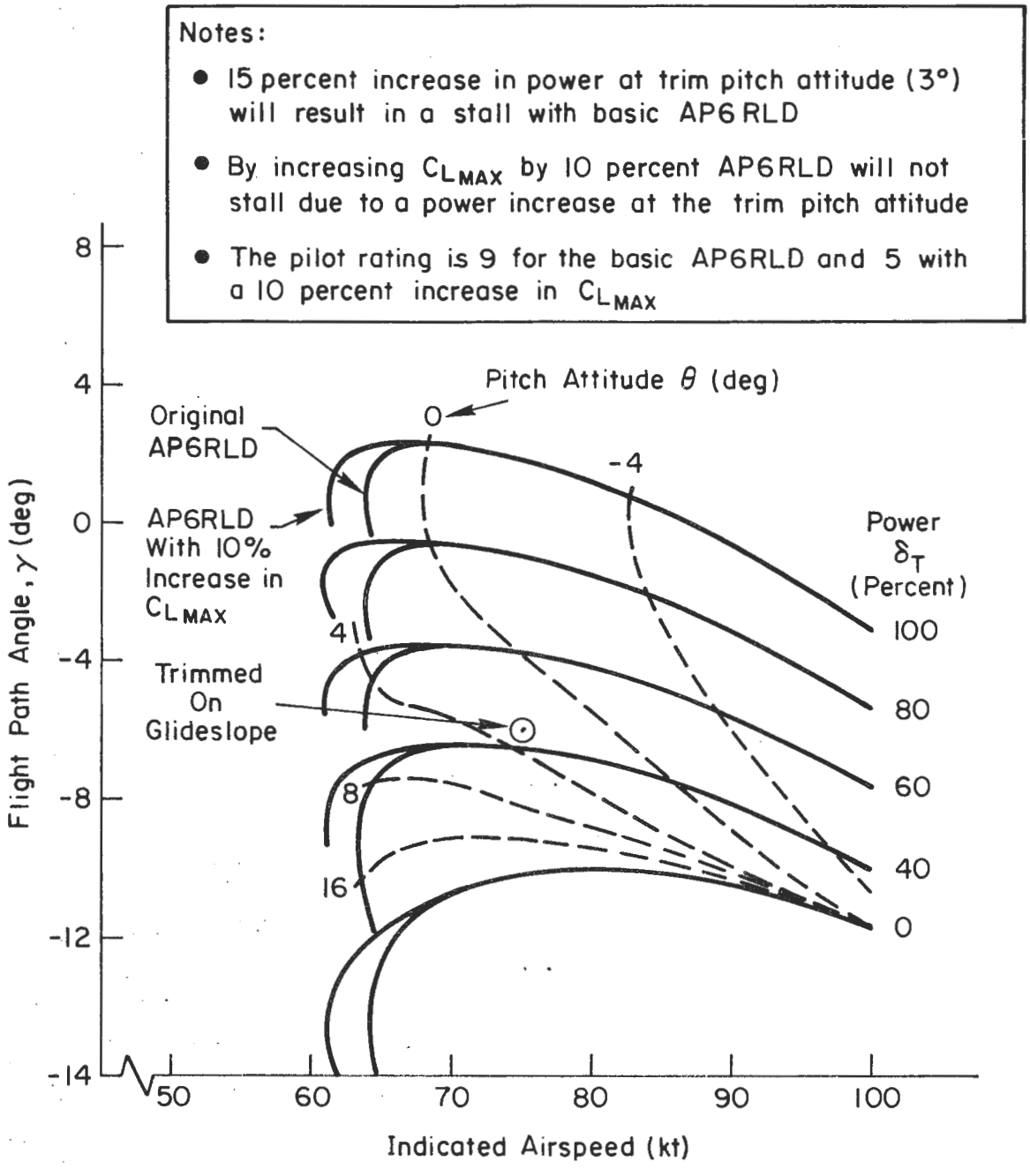

Figure 12. Effect of 10 Percent Increase in $C_{L_{max}}$ on Stall Characteristics

b. If glide slope error (d) is diverging, try to first zero $\dot{d}$, then adjust power so d is slowly converging (i.e., pick a new target sink rate on the IVSI).

c. If the glide slope error is less than one dot, make very small power adjustments (if any).

The attitude control technique suggested by the pilot commentary (Appendix A) and strip chart records (for example, Figs. 11 and 12) may be summarized as:

a. Let the SAS hold attitude and occasionally adjust to correct back to target attitude when required.

b. Bias the target attitude to correct persistent speed errors that are large enough to be outside the indifference threshold.

These rules suggest a basic pilot vehicle system loop structure consisting of beam and beam rate feedback to the throttle with a very low gain attitude to column feedback (assumed to be zero in subsequent analyses). This is shown in block diagram form in Fig. 13. Further quantification of the model was obtained using the results of specifically designed simulation runs where the pilot was given deterministic inputs in beam error, sink rate, and vertical acceleration (sum of six sine waves) which was filtered to give the appearance of random vertical gusts. The method is described in detail in Appendix C. As shown in Appendix C, the describing function representing the pilot plus vehicle system may be experimentally derived from measurements of the system response. Describing function magnitude and phase points were computed at six frequencies thereby giving an experimental frequency response (Bode plot) for the beam to beam error response (the effective controlled element) of the pilot vehicle system which was fitted with pilot model parameters corresponding to the Fig. 13 throttle series loop structure.

The analytical approximation to the effective controlled element used to fit the experimental data was based on the assumption that the pilot flies constant attitude and may be derived from the block diagram in Fig. 13 and approximate factors in Appendix B.

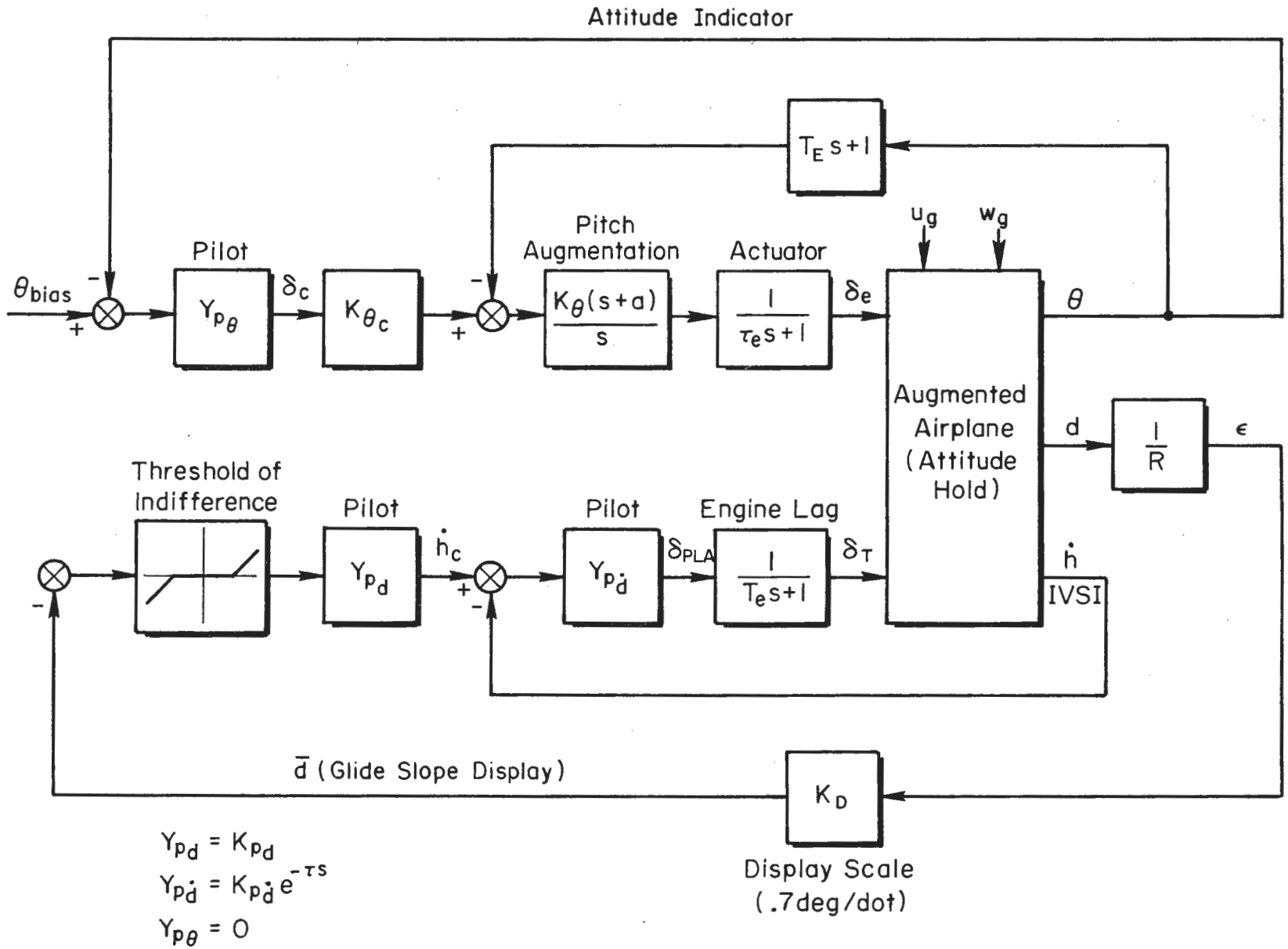

Figure 13. Pilot/Vehicle Loop Structure for Glide Slope Tracking

$$\frac{d}{d_\epsilon} = Y_p Y_c \doteq \frac{Y_p N^\theta_{\delta_e} \delta^d_T}{N^\theta_{\delta_e}}$$

$$\doteq \underbrace{K_d(s + \dot{K}_d)e^{-\tau s}}_{\text{Pilot}} \underbrace{\frac{M_{\delta_e} Z_{\delta_T}(s + \frac{1}{T_{d\theta}})}{sN^\theta_{\delta_e}(T_e s + 1)}}_{\text{Augmented Airframe}} \tag{6}$$

where

$$N^\theta_{\delta_e} = M_{\delta_e}(s + \frac{1}{T_{\theta_1}})(s + \frac{1}{T_{\theta_2}}) \tag{7}$$

or

$$M_{\delta_e}(s^2 + 2\zeta_\theta \omega_\theta s + \omega_\theta^2) \tag{8}$$

K_d represents the pilot's internally derived sink rate command based on a beam error. $\dot{K}_d$ represents the amount of throttle response that was used for a perceived error between the target sink rate and actual sink rate on the IVSI instrument or from the visual display during the final approach segment. τ represents the overall pilot lag that arises from several sources such as neuromuscular and scanning lags. The sink rate command, $\dot{h}_c$, is internally generated by the pilot by observing the IVSI reading that nulls the glide slope deviation rate, $\dot{d}$. As shown in Ref. 6, there is negligible lag associated with internally generated commands, which accounts for the fact that the outer loop pilot transfer function Y_{p_d} is represented as a pure gain ($\tau = 0$).

2. Experimental Results

The pilot model parameters (K_d, $\dot{K}_d$, τ) were varied to obtain the experimental data fits in Fig. 14. Each data point in the figure represents the average experimental value across all the pilots who flew each of the configurations. Two glide slope sensitivities were run for each

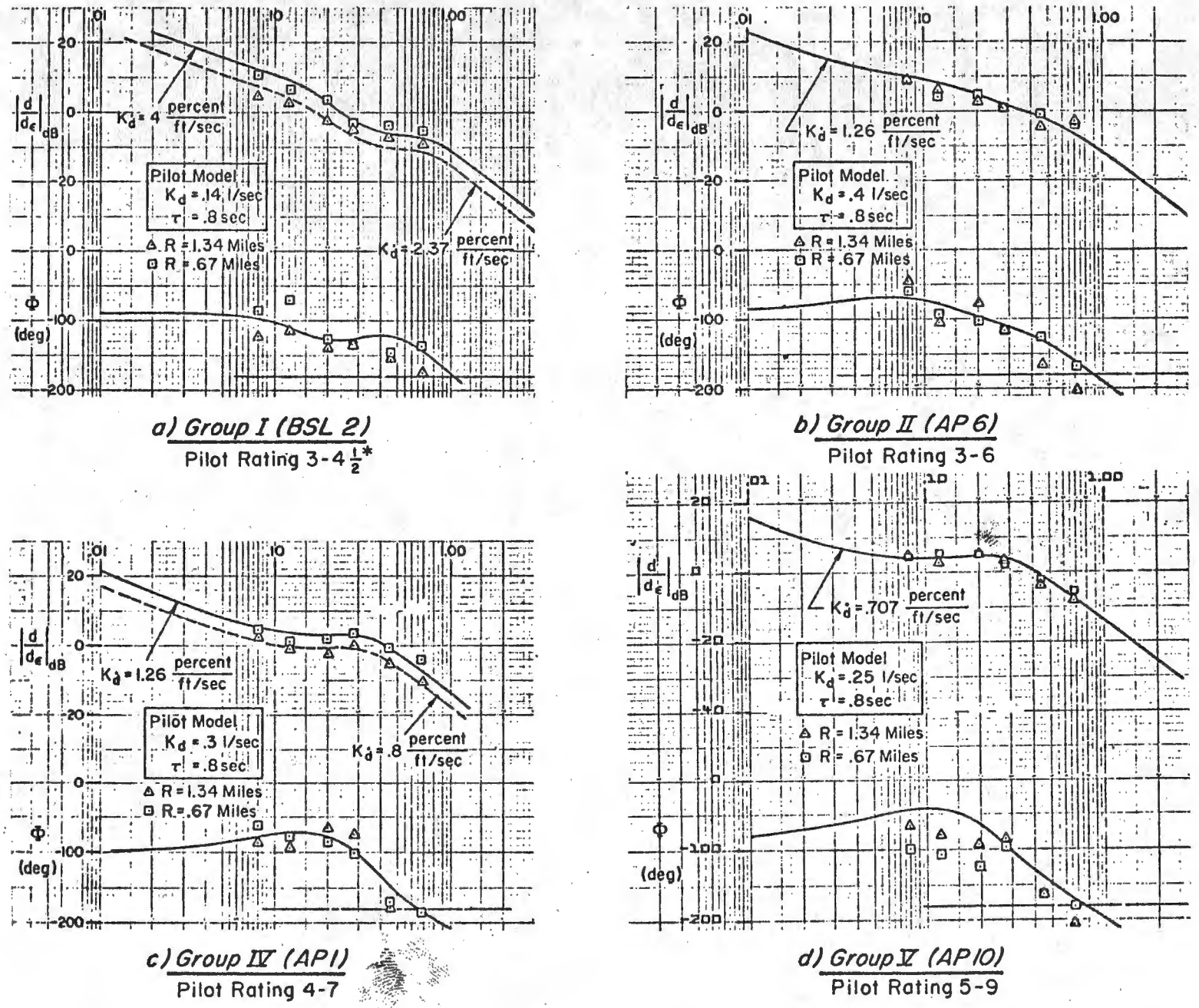

Figure 14. Experimental-Analytical Pilot/Vehicle Model Correlations [Pilot ratings are for the glide path control portion of the composite task (3.1) (IFR and VFR glide path tracking)]

configuration to help quantify the effect of the pilot's "tightening up" as glide slope sensitivity increases near decision height. The high sensitivity (squares) and normal sensitivity (triangles) cases represent a glide slope width of ±50 ft and ±100 ft, respectively. To put this in perspective, these numbers correspond to glide slope tracking at a range of 0.67 miles and 1.34 miles from the 6 deg glide slope transmitter.* Figure 14 shows that the characteristic tightening up near decision height does not occur for some configurations (AP6 and AP10) and appears as an increase in gain for others (BSL2 and AP1). The pilot ratings for path control are shown below the experimental results for each of the configurations shown in Fig. 14. These ratings are seen to be significantly degraded for the cases where the pilots were unable to equalize the effective controlled element to a K/s shape (AP1 and AP10). Other implications of piloting technique to be drawn from these data fits are:

- The pilots are not regulating speed with attitude to any significant degree. This is evidenced by the fact that closure of a speed to attitude loop significantly alters the shape of the analytical fit to the point where it does not match the experimental data. This is especially true on the more highly coupled configurations such as AP10.

- The overriding pilot closed loop operation was beam and beam rate to throttle. Other pilot activity was of such low gain as to have negligible effect.

- The phase margin at crossover was generally about 50 deg for the high sensitivity glide slope resulting in a closed loop bandwidth of about 0.25 rad/sec for BSL1, 2, and 2 RLD, and 0.4 rad/sec for all other configurations.

- The effective pilot lag is considerably higher than indicated on previous single controller experiments (τ is usually about 0.4 sec). This could be due to the higher scanning workload inherent to increased rates of descent and low approach speeds. The latter results in increased lateral workload due to the increase in turn rate for a small bank angle excursion $[r \doteq (g\varphi/V_o)]$ requiring significantly more scanning

*Glide slope width was ±0.7 deg.

activity on the attitude gyro (bank angle) and HSI (localizer). Finally, the high degree of coupling on some configurations probably results in more than usual scanning activity on airspeed. However, a firm explanation cannot be supported from the current results.

3. Conclusions

The results obtained from experimental measurement of the pilot's closed-loop tracking behavior have some very important implications in the definition of minimally acceptable handling qualities. Most importantly, there appears to be very good correlation between the ability of the pilots to equalize the effective controlled element to a K/s (see Fig. 14) and configurations that are less than minimally acceptable (e.g., Configurations AP1 and AP10). Configuration AP1 is an interesting example because it is not especially bad in terms of criteria developed in previous work (see Refs. 5 and 7). For example, Configuration AP2* relative to Configuration AP1 has

a. Thirty percent more flight path overshoot ($\Delta\dot{\gamma}_{peak}/\Delta\gamma_{ss}$)

b. Three times more steady-state coupling ($\partial\delta V/\partial\gamma$).

c. Nearly identical μSTOL characteristics (see Ref. 5).

d. More rapid degradation of dynamics with speed change (see Fig. 7).

e. Identical control power characteristics (both have a -2 deg δ_γ capability).

Based on the above list, we would certainly not expect AP2 to receive better pilot ratings than AP1. However, this was indeed the case for the composite task (3.1), as well as the final approach and landing task (2.1). This

*Configuration AP2 has the same dynamics as Configuration AP6 (which is shown in Fig. 14b, the only difference being that AP2 has -2 deg δ_γ capability compared to -4 deg for AP6.

important result illustrates that limiting flight path control characteristics are more directly identified via analysis of the closed-loop pilot/vehicle system (inability to equalize the effective controlled element to a K/s in the case of AP1) as opposed to considerations of open-loop response characteristics. Unfortunately, closed-loop response measurements are not easy to make. It would therefore be desirable to identify open-loop vehicle characteristics which are a valid measure of, and are sensitive to, changes in the closed-loop pilot/vehicle effective controlled element characteristics.

As earlier stated, deficiencies in flight path control were not apparent to the pilots until the last 300 ft. However, the above describing function analysis results suggest that certain fundamental limitations are apparent in terms of closed-loop tracking behavior on the glide slope long before the pilots recognize the deficiency. Thus, we may conclude that path control deficiencies which are limiting for visual aim point tracking may be identified by taking long term closed loop tracking measurements on the ILS glide slope. (The glide slope sensitivity should be high to induce tight control.) This is an important result in that it is very difficult to quantify the visual aim point tracking problem due to the short amount of time over which this task occurs.

D. FLARE AND LANDING

Comparison of the pilot ratings for the ILS glide slope tracking task (1.01) and the final approach and landing task (2.1) indicate that flight path control deficiencies were far more apparent to the pilots during the final approach and landing task. This comparison is shown in Fig. 15 below where it can be seen that some configurations which received acceptable pilot ratings for ILS tracking were rated as unacceptable for the flare and landing (for example, BSL1, AP1, and AP10). This result probably reflects the increased precision required for the final approach and landing task, especially in the presence of turbulence.

Atmospheric turbulence had a very strong adverse effect on pilot opinion ratings and performance for the final approach and landing. As shown in Fig. 16 below, Configurations BSL1, AP7, and AP1 were particularly sensitive to turbulence. The effect of steady winds was not tested.

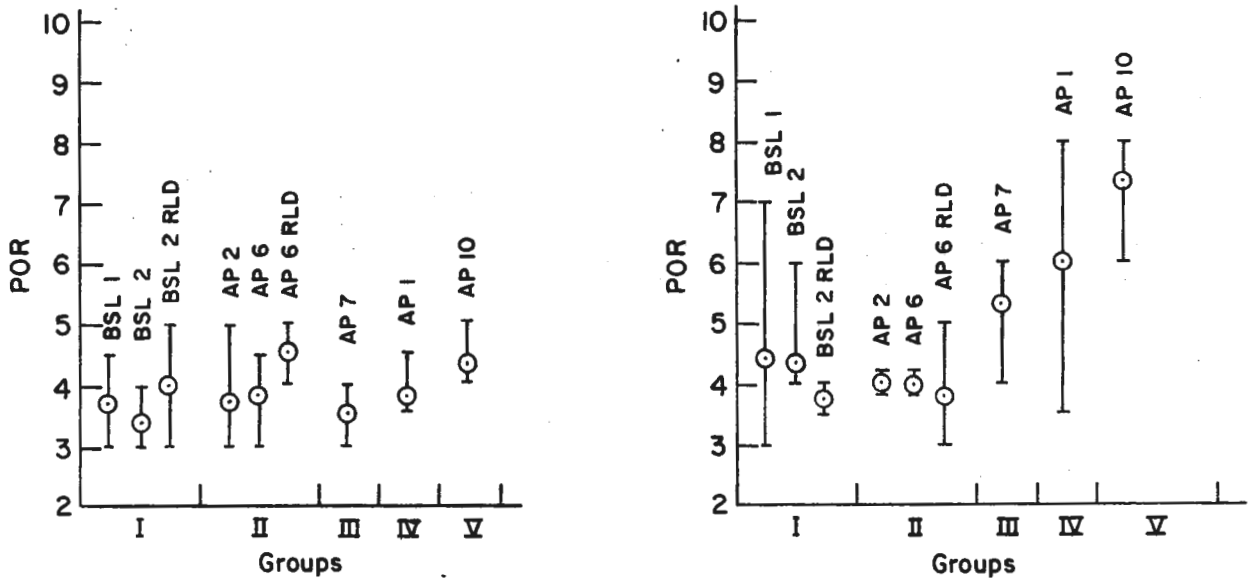

a) ILS Tracking Task (1.01)

b) Final Approach and Landing Task (2.1); σ_{ug} = 4.5 ft/sec

Figure 15. Comparison of Pilot Ratings for ILS Tracking (IFR) and Final Approach and Landing (VFR)

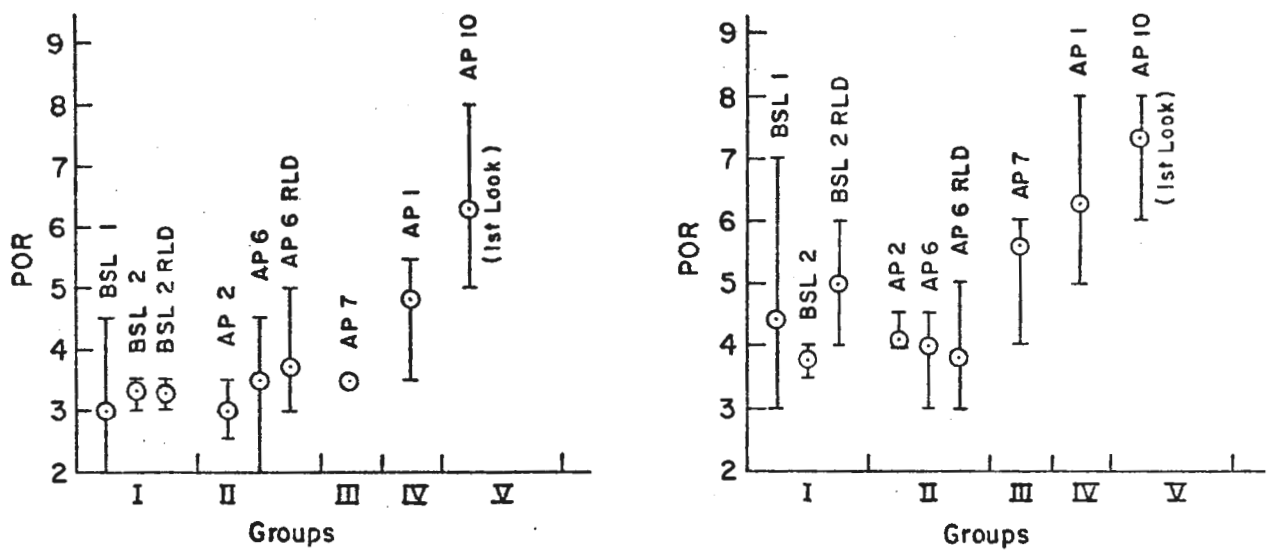

a) Pilot Ratings for Final Approach and Landing Task (2.0); $\sigma_{ug} = 0$

b) Pilot Ratings for Final Approach and Landing Task (2.1); σ_{ug} = 4.5 ft/sec

Figure 16. Effect of Turbulence on Pilot Ratings

There was general agreement among the pilots that the sink rate excursions seemed extremely large near touchdown. This has also been noted on other STOL simulations (Refs. 5, 8, 9) where the pilots have complained of unusually large gusts which seem unrealistic based on CTOL experience. Possible explanations of this are:

- The magnitude of low-frequency shear in the turbulence model was unrealistically high.
- Turbulence effects tend to be magnified in the simulator due to limited peripheral vision, inadequate motion cues in heave, and lack of sink rate perception in the visual display.
- Turbulence has a much more pronounced effect on STOL vehicles than on CTOL airplanes.

A short flight test program using the Princeton University Variable Stability NAVION was conducted as a follow on to this simulation. (Discussed at greater length in Section IV. One of the primary goals of the flight program was to gain a better appreciation of the seemingly unrealistic turbulence effects obtained in the simulator. In order to insure identical turbulence models in the simulator and in flight, a magnetic tape of the simulator turbulence was used to generate artificial turbulence in the variable stability airplane. The following results were obtained

- Qualitatively, the effect of turbulence on the flight path seemed very similar in flight to that experienced in the simulator using the BSL1 configuration in each case.
- The basic NAVION was flown with the turbulence tape and given a pilot rating of 4-1/2 for the landing maneuver. The pilot's comment was that it was like flying with the NAVION in winds of 18 kt with gusts to 25 kt.

These results imply that the simulator results were valid and that the comments and ratings regarding severe effects of turbulence are attributable to STOL deficiencies (which are highly sensitive to turbulence). Only one pilot flew this phase of the experiment. Therefore, more testing is warranted to support this conclusion.

The above experimental results suggest that flight path control deficiencies are more correlated with the VFR task associated with final approach and landing than the IFR tracking task. Those features which appear to contribute most heavily towards this result are

- The effects of path disturbances due to turbulence and shear are very prominent due to near proximity of the ground.

- The terminal control nature of the task requires that errors (in the apparent touchdown aim point) be eliminated immediately. This sense of urgency does not exist in the ILS task.

This has resulted in a switch in emphasis from analysis of the classical glide slope tracking task to the final approach and landing task. It was therefore appropriate to concentrate the analysis for identification of key parameters on the final approach and flare maneuvers. This analysis is presented in Section V of this report.

E. SIMULATOR CALIBRATION FOR LANDING

There was general agreement among the pilots who have flown the NASA Ames simulators that the visual and motion cues do not have one to one correspondence with the real world during landing. Early in the program, it became apparent that what appeared to be a smooth landing was actually firm to hard from the standpoint of computed touchdown sink rate. It therefore appeared desirable to allow the pilots to rate their landing performance based on what they saw on the display. Since all of the pilots had considerable flying experience (greater than 2000 hr) it was reasoned that they should be able to distinguish a good landing from a bad landing. Moreover, the pilot can only operate in a closed loop sense based on his information input, e.g., visual display and simulator motion. Allowing the pilots to rate their performance and using those ratings to calibrate the simulator should compensate in some way for the effect of the missing or erroneous cues from the data. The pilot ratings of touchdown sink rate consisted of "soft, firm, and hard." A numerical scale has been defined which quantifies these ratings in terms of percentage of responses in a given category. The pilot to pilot variation was found to be small enough to group all of the data and define a relationship between actual performance on the simulator and the pilot's subjective opinion across all pilots. This effectively calibrates the simulator.

All the landing data were tabulated according to touchdown sink rate and pilot rating (soft, firm, hard) resulting in the three distributions shown in Fig. 17.

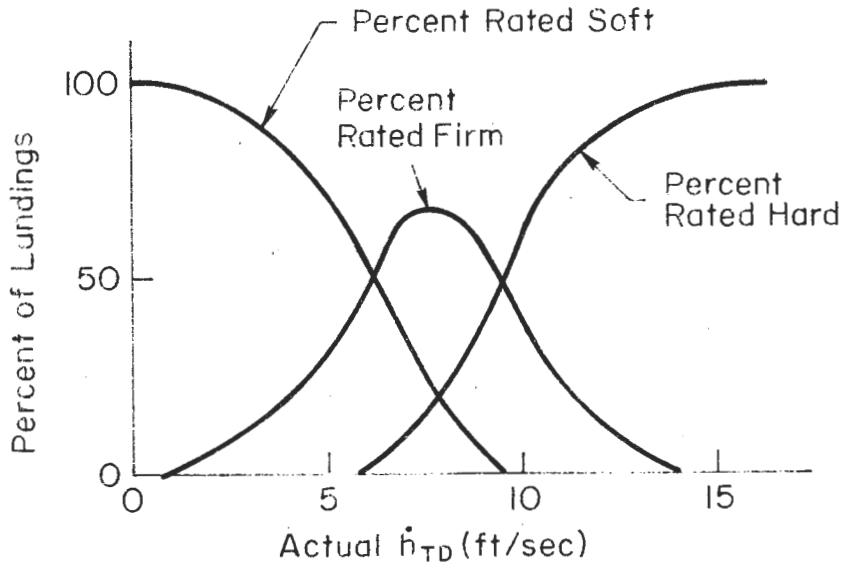

Figure 17. Distribution of Ratings for Soft, Firm, and Hard Landings

Based on these distributions, a numerical scale was developed to quantify the pilot's rating of touchdown sink rate as shown in Table 4. The correlation between simulator and pilot opinion of touchdown sink rate is made by plotting the actual (simulated) touchdown sink rate against the number corresponding to the pilot verbal descriptors in Table 4. The results is shown in Fig. 18.

TABLE 4. LANDING "RATING" SCALE

NUMERICAL SCALE	PERCENTAGE OF LANDINGS RATED AS SOFT, FIRM, OR HARD			VERBAL SCALE
	SOFT	FIRM	HARD	
1	100	0	0	Soft
2	75	25	0	
3	50	50	0	Soft-firm
4	25	65	10	
5	15	70	15	Firm
6	10	65	25	
7	0	50	50	Firm-hard
8	0	25	75	
9	0	0	100	Hard

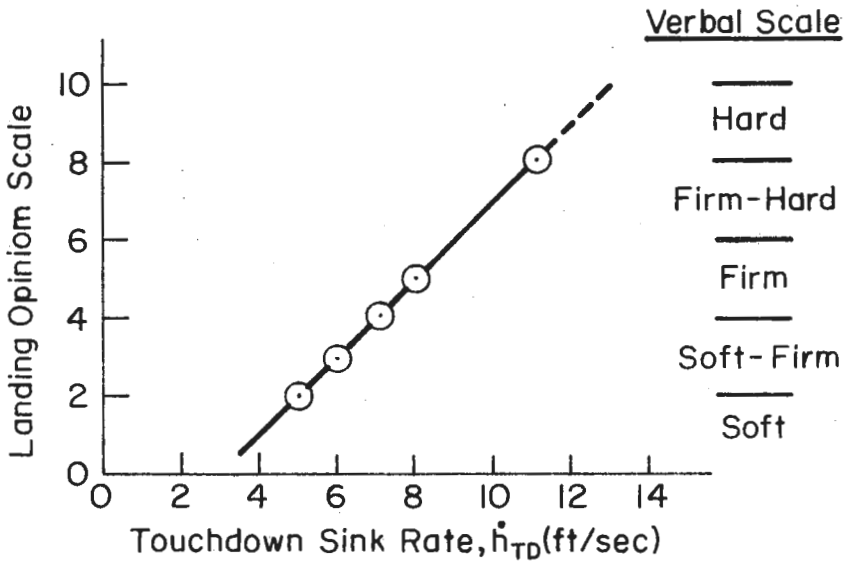

Figure 18. Simulator Landing Correlation Plot

Figure 18 verifies the subjective feeling that what would be a high touchdown sink rate in actual flight (order of 6 ft/sec) looks like a "soft to firm" landing in the simulator. It follows that landing data taken in the simulator ($\dot{h}_{TD}$) should be evaluated based on the landing opinion scale in Fig. 18.

The landing performance data for the tested generic STOL configurations are summarized in Table 5 in terms of the computed and adjusted (Fig. 18) touchdown sink rate and the touchdown position. All landings between 200 and 500 ft were considered as in the touchdown zone. Table 5 reveals that

- None of the configurations could be landed consistently soft and in the touchdown zone.
- The Group II configurations were rated significantly better than the rest.
- The Group II configurations exhibit the lowest touchdown sink rates and also the lowest dispersions from the mean (σ) in X_{TD}.

It should be pointed out that the dispersions of X_{TD} about the mean were not symmetrical, that is, an extremely low number of touchdowns occurred short of the runway. In cases where the possibility of landing short or overshooting existed, the pilots executed a go-around.

TABLE 5

SUMMARY OF LANDING PERFORMANCE
(Turbulence = 4.5 ft/sec rms)

GROUP	CONFIGURATION	TOUCHDOWN PERFORMANCE					AVERAGE PILOT RATING (Task 2.1)
		SINK RATE			POSITION, ft		
		AVG.	σ	AVG. RATING (FIG. 7)	AVG.	σ	
I	BSL1	6.8	3.0	Firm	274	171	3-7
	BSL2	6.1	2.4	Soft-firm	415	200	4-6
	BSL2 RLD	7.3	3.3	Firm	320	304	3.5-4
II	AP2	5.1	2.4	Soft-firm	427	159	4
	AP6	6.0	2.6	Soft-firm	423	161	4
	AP6 RLD	4.3	2.5	Soft	214	82	3-5
III	AP7	7.6	3.0	Firm	444	245	4-6
IV	AP1	6.41	3.18	Soft-firm	361	194	3.5-8
V	AP10	6.7	2.0	Soft-firm	412	206	6-8

F. FLIGHT DIRECTOR RESULTS

Two flight director configurations were designed to provide the pilot with command information for column, throttle, and lateral wheel inputs. The flight directors were designed to be compatible with the Group I and Group II configurations using the STOL flight director design procedures developed in Ref. 10. The primary objectives of the flight directors were to reduce the pilots' workload and to increase glide slope and localizer tracking accuracy. In keeping with these objectives the guidance and control and pilot centered requirements discussed in Ref. 10 were a primary factor in formulating the appropriate feedback signals for the flight directors. A third objective was to investigate the flight director as a means of decoupling the airspeed flight path responses. It was hypothesized that with a good flight director the displayed quantities

can be quite well decoupled with regard to pilot inputs even though the basic airplane responses (airspeed and flight path) are quite highly coupled. The basic loop structures for the column and throttle flight director were taken directly from Ref. 10.

The directors were based on the principle of normal "backside" or STOL operation, i.e., throttle controls path deviations and attitude controls speed. The column flight director was basically an attitude hold with a low gain speed feedback [$\Delta\theta/\Delta V \doteq (0.34$ deg/kt)]. The speed error limiter was set to ±29.6 kt which results in a maximum flight director pitch command of ±10 deg. Attempts to increase the speed feedback gain and/or open up the speed error limiter met with unfavorable pilot commentary. This was primarily due to the increased activity of the pitch command bar. These results are consistent with the concept that the feedbacks to each of the controls must be frequency separated. That is, one control is primary (glide slope to throttle) and the other is a low frequency trim function (airspeed to attitude). We therefore may conclude that the flight director is effective in decoupling the aircraft responses only from the standpoint that one variable (speed in this case) is controlled very loosely. This is entirely consistent with the way the pilots flew the aircraft using "raw data" glide slope information.

The pilot ratings and ILS tracking performance results are summarized in Fig. 19 to show comparisons with and without the flight director in turbulence. These results show that:

- The flight director improves the pilot rating 1 to 1-1/2 points. In terms of Cooper Harper descriptors this implies "moderate to extensive compensation" with raw data to "minimal compensation" with the flight director.
- Averaged rms glide slope tracking performance was improved 25 to 40 percent with the flight director.
- Averaged rms localizer tracking showed the most dramatic improvement in performance (up to 86 percent reduction in rms tracking error).

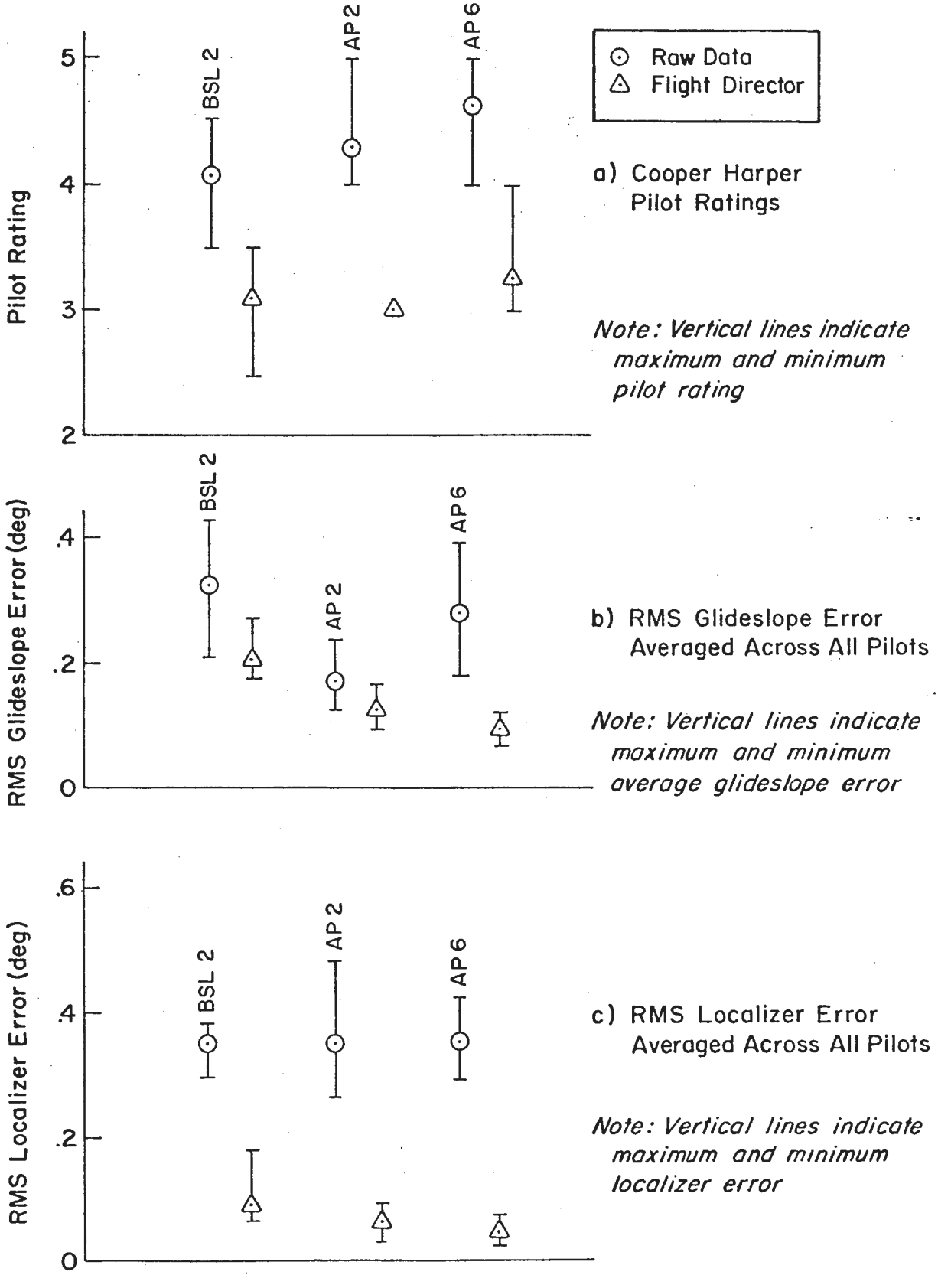

Figure 19. Effect of Flight Director On Ratings and Performance

SECTION IV

FLIGHT TEST RESULTS

A. DESCRIPTION OF FLIGHT PROGRAM

The flight test program which spanned a period of about three months was basically a flight version of the final approach and landing task (Task 2.1 on the simulator). The Princeton University Variable Stability NAVION was programmed and checked out to simulate Configurations BSL1 and AP1. The artificial turbulence was identical to that used on the simulator in that a magnetic tape of one hour of the simulator turbulence was used to generate artificial turbulence in flight.

The flight scenario involved the safety pilot's flying the aircraft around the pattern and setting up for each run, with the evaluation pilot taking over on final approach at about 1000 ft. Approach guidance consisted of a 6 deg microwave landing system glide slope and localizer (TALAR) plus a lighting system which provided visual indication of whether the pilot was above or below the 6 deg approach path. The evaluation pilot flew the airplane to touchdown or to the point at which the safety pilot felt an abort was necessary. Each configuration was tested for three basic levels of turbulence and two levels of attitude SAS bandwidth. The levels of turbulence tested were 0, 2.25 ft/sec rms, and 4.5 ft/sec rms. The attitude SAS bandwidth was tested at a basic level of 0.7 rad/sec and also a level of 1.2 rad/sec.

B. FLIGHT RESULTS

The basic NAVION was mechanized with the turbulence tape and several approaches to touchdown flown to gain an appreciation for the level of simulated turbulence with a known airplane. The pilot rating was 4-1/2, and the pilot commented that the situation appeared to be consistent with tower-reported winds of approximately 15-20 kt with gusts to 25 kt. The evaluation pilot noted that the pilot rating for Task 2.1 (final approach and landing) with the basic NAVION in calm air is about a 2-1/2. This is

an important result, because it associates the unreasonably large disturbances in the simulator with STOL response to turbulence rather than with simulation of unrealistically high gusts. Only one pilot flew this portion of the experiment (Princeton project pilot) and only a few approaches and landings were made. Because of its importance, further experimental validation of this result is warranted.

Two levels of attitude SAS were tested; a high gain SAS and a low gain SAS. The low gain SAS resulted in a very sluggish attitude response to column input (3 sec to 75 percent of steady state) whereas the high gain SAS was quite responsive (1.8 sec to 75 percent). Three levels of turbulence were tested for two configurations (BSL1 and AP1). These configurations were selected because they exhibited marginal characteristics on the simulator and had different limiting effects. That is, BSL1 was very sluggish and AP1 had dynamic coupling problems. The pilot ratings for each of the three levels of turbulence and two levels of SAS response are shown in Table 6 for flare and landing (Task 2.1) and in Table 7 for final approach only.

The following results are indicated from the pilot ratings in Tables 6 and 7.

1. The high gain SAS resulted in consistently better pilot ratings for landing and had no effect on glide path control (on short final).

2. The turbulence level had a dramatic effect on the ratings with both configurations being clearly unacceptable at $\sigma_{u_g} = 4.5$ ft/sec.

3. The ratings for maximum turbulence level ($\sigma_{u_g} = 4.5$ ft/sec) were much worse that obtained in the simulation program. For example, comparison of Fig. 15 with Table 6 shows that BSL1 was rated from 3 to 7 on the simulator and from 7 to 10 in flight.

Result number 2 is consistent with the simulation in that increasing the turbulence level had a degrading effect on the pilot ratings. This effect was more pronounced in flight.

The disparity between simulation and flight (result 3 above) indicated that worse pilot ratings were received in flight where the peripheral and motion cues were better than the simulator. It was not possible to resolve

TABLE 6

COOPER HARPER RATINGS FOR FLARE AND LANDING
(FLIGHT PROGRAM)

TURBULENCE AND SAS	CONFIGURATION BSL1		CONFIGURATION AP1	
	PILOT 1	PILOT 3	PILOT 1	PILOT 3
σ_{u_g} = 0 ft/sec				
High Gain SAS	4-1/2	4	6-1/2	5-1/2
Low Gain SAS	5	5	7	6-1/2
σ_{u_g} = 2.25 ft/sec				
High Gain SAS	5	5	Did not fly enough in turbulence to rate	6-1/2
Low Gain SAS	6-1/2	6		9
σ_{u_g} = 4.5 ft/sec				
High Gain SAS	7	6-1/2 to 10		10
Low Gain SAS	8	7 to 10		10

TABLE 7

COOPER HARPER RATINGS FOR FINAL APPROACH
(FLIGHT PROGRAM)

TURBULENCE LEVEL σ_{u_g} ft/sec	CONFIGURATION BSL1		CONFIGURATION AP1	
	PILOT 1	PILOT 3	PILOT 1	PILOT 3
0	4	4	5-1/2	5
2.25	5	5-1/2	—	6-1/2
4.5	7	8-1/2 to 10	—	9 to 10

Ratings did not vary with high and low gain SAS.

*This rating improves to a 6 with increased throttle control power (throttle was limited to ±20 percent about trim on Navion).

these flight/simulator discrepancies (with any confidence) without considerably more testing (which was beyond the scope of this program). There are two possible hypotheses which help to "explain" the data. These are summarized below.

1. The rating effect of the 4.5 ft/sec turbulence is more pronounced for flight than for simulation. To some extent this may be due to the fact that during the simulation many of the landing problems were attributed to poor simulator cues. The flight tests served to illustrate that the much improved visual and motion cues in flight were of no help in regulating against the large gust inputs near touchdown. In fact, the improved sink rate cues served to increase the pilot's awareness of "how bad things really were." Sink rates of 1200 to 1400 ft/min on short final tend to be far more dramatic in the flight environment than on the simulator with the Redifon display.

2. There were certain discrepancies in the environmental, task, and procedural variables between flight and simulation.

The discrepancies noted in item two above are summarized below.

- Task variables. Task variables comprise all the system inputs and those control system elements which enter directly and explicitly into the pilot's control task. The primary discrepancy here was the limited throttle authority on the Variable Stability NAVION (±20 percent about trim) and lack of any engine noise cues in the airplane (due to variation of thrust with the Beta prop instead of power).

- Environmental variables. These are clearly superior in flight, and flight ratings are usually better than simulator ratings due to improved visual and motion cues and their generally favorable effects on closed-loop performance.

- Procedural variables. These include aspects of the experimental procedure such as instructions, background, indoctrination, training, etc. These variables present a particularly difficult problem for the simulator landing task, especially with regard to definition of "desirable," "adequate," and "inadequate" performance. Clearly, these factors depend on aircraft specifics such as gear strength, gear softness, braking effectiveness, etc. Furthermore, the simulator motion cues at touchdown are frequently inappropriate no matter how the landing gear is modeled (due to hitting the motion

stops or to artificial effects caused by protection circuits to reduce wear on the simulator motion system). The pilots of the simulator program were given rather vague instructions in that they were told to assume that the gear was strong enough "within reason" (touchdown should be at least well below the glide slope sink rate of 13 ft/sec) and that braking effectiveness was such that they could stop the airplane if on the ground and under control at midfield (1000 ft of runway left). The procedural variables in the Variable Stability airplane were quite different. The landing gear has finite strength and is very stiff. It is the safety pilot's responsibility to abort if the sink rate gets into the unsafe region near touchdown. For example, touchdowns of 8 ft/sec were relatively common on the simulator. In the aircraft, a touchdown sink rate of this magnitude was cause for alarm (the tests were interrupted while the gear was checked). There was some attempt during the flight test program to minimize this discrepancy in the procedural variables by having the evaluation pilots try to ignore the aborts and evaluate the landings. It is difficult to impossible to evaluate the ability of a pilot to ignore the fact that he has been aborted for a large percentage of his attempts to land the airplane. It would therefore seem that the safest way to maintain a high level of credibility for flight/simulator comparisons is to mechanize the simulator so that the procedural variables are as close as possible to the flight situation. This was done in the present program during a post-flight simulation and is discussed below.

- Pilot-centered variables. These are the characteristics that the pilots bring to the control task. One of the pilots had extensive experience with the simulation phase of this program, while the other had flown many hours evaluating STOL configurations on the Princeton Variable Stability NAVION. This was felt to be complementary, and the very low variability in ratings between the two pilots indicates that the pilot-centered effects were not responsible for the flight/simulator discrepancies.

In response to these preliminary results and findings, a short-term simulator program sponsored by NASA Ames was undertaken to further investigate the effects of turbulence on STOL landings, especially with regard to simulator/flight comparisons. The same two pilots participated as in the flight test; however, the FSAA simulator was used (the S-16 was the primary simulator in the pre-flight simulations). The BSL1 configuration was used since it received most of the attention in flight. This simulation

period was separated into two phases to evaluate the effects of task, environmental, and procedural variables. The primary differences between these phases were as follows:

- Phase I — Direct Simulator/Flight Comparison

  1. Program the safety pilot as an "abort mode." By scanning the strip chart records from the flight test, it was determined that the safety pilot was reasonably consistent in that he aborted if the sink rate exceeded approximately 6.5 ft/sec below an altitude of about 10 ft. The simulator was programmed to abort (go into reset mode) with this criterion.
  2. Physical stops were clamped on the FSAA simulator throttle quadrant which limited thrust excursions about trim to ±20 percent. (NAVION control power was 20 percent of simulated STOL.)
  3. The pilot position was set to simulate the NAVION (eye height of 8 ft and longitudinal pilot position at the center of gravity).
  4. Engine noise was eliminated (changes in power are not audible in the NAVION since they are accomplished via propeller pitch at constant rpm).

- Phase II — Same scenario as pre-flight simulation (Discussed in Sections III and IV)

  1. Assume gear is "strong as required within reason," e.g., no abort.
  2. The throttle stops were removed.
  3. Engine noise cues were turned back on.
  4. Pilot position was made consistent with a large aircraft (eye height 17 ft and 20 ft forward of the aircraft center of gravity).

The pilots both commented that <u>subjectively</u> the large shears had the same effect in the simulator as in flight, e.g., they appeared extreme. A summary of the pilot ratings for each phase is shown in Table 8. These ratings are closer to the flight values than the original simulation, perhaps lending some credence to hypothesis number 1 above (since both pilots had recent flight experience). Pilot 1 felt that the differences between Phase I and Phase II (effect of experimental variables) was significant (about two rating points) and Pilot 3 did not (ratings about the same). Clearly more data would be required to resolve hypothesis number 2 above.

TABLE 8

COOPER HARPER RATINGS FOR FLARE AND LANDING
POST FLIGHT SIMULATION-CONFIGURATION BSL1

TURBULENCE LEVEL σ_{u_g} ft/sec	PHASE	FLARE AND LANDING		FINAL APPROACH	
		PILOT 1	PILOT 3	PILOT 1	PILOT 3
0	I	4-1/2	4	3	4
2.25	↓	5-1/2	4 to 4-1/2	4	5
4.5	↓	7	5-1/2 to 10	5	7
0	II	3	4	3	4
2.25	↓	3-1/2	4-1/2 to 5	4	5
4.5	↓	5	6 to 10	5	7

While the simulator results did not agree well with flight in terms of absolute value of pilot ratings, the problem areas identified via pilot commentary were identical. Since the objective of this program was to find effects or combination of effects which are limiting, the pilot rating discrepancies do not detract from the simulation results. However, these discrepancies should be resolved before actual numerical boundaries are derived for certification criteria.

One final comment. The majority of simulation was done on the S-16 simulator (very limited motion and marginal redifon) whereas the post-flight simulation was done on the FSAA (better motion and visual). A three day exercise was undertaken during the original simulation where three pilots flew Configurations AP7, and AP10 on the FSAA and S-16 back to back. The FSAA ratings were one to two points better than the S-16, e.g., in the wrong direction to resolve the simulator/flight discrepancy.

SECTION V

ANALYSIS OF RESULTS

Experimental results have shown that flight path control deficiencies were most apparent on short final when the pilot was tracking a visual aim point on the runway and during the flare. The analyses efforts were accordingly concentrated in this area. The approach taken here has been to quantify these tasks in terms of their closed-loop properties and to identify path control problems via the pilot-centered and guidance and control requirements from a well-established theory of closed-loop pilot/vehicle analysis (see Ref. 11, and 12). The structure of the closed-loop pilot/vehicle system is based on a combination of quantitative (describing function) measurements of closed-loop tracking behavior, pilot commentary, and analysis of strip chart records. These data were obtained from the pre-flight and the post-flight (Phases I and II) simulations and the flight test program.

A. ANALYSIS OF FINAL APPROACH TRACKING

The first step in quantification of the pilot's closed-loop structure during the final approach was to find out where the pilots transitioned from tracking the electronic glide slope to looking out the window and tracking the visual aim point on the runway. Most pilots commented that they were "in and out" right down to the point of flare initiation. In most cases the pilots noted that the outside tracking was primarily to get sink rate and lateral line up information. The primary scan inside was the glide slope display and airspeed. This explains the strip chart records which showed that the pilots tended to maintain a glide slope error near zero to very low altitudes. Based on this result, we have assumed that the tracking model close in (visual portion of the approach) is identical to further out (IFR). It follows that the pilot model given by Eq. 6 is valid for analysis of the final approach.

The fundamental hypothesis of this analysis is that minimally acceptable path control is a direct consequence of an inability to satisfy the pilot-centered and guidance and control requirements (see Ref. 11) summarized below:

- Guidance and control requirements
  1. Command following and disturbance regulation
  2. Stability
- Pilot-centered requirements
  1. Minimum equalization to achieve K/s effective controlled element
  2. Wide separation in crossover frequency of the primary and secondary controls
  3. Tolerant of variations in pilot response (desire a broad region of K/s)
  4. Response quality. The closed-loop system should be rapid and well damped, akin to a second-order system with minimum coupling between the modes of motion. The pilot should be able to easily sort out path mode response to a control input.

Assuming that the pilot flies constant attitude (attitude constrained assumption), the generic form of the effective controlled element (pilot plus airplane) for primary path control with throttle is given by Eq. 6. This is repeated below along with a definition of the effective controlled element.

$$\frac{d}{d_\epsilon} = Y_p Y_c \doteq \frac{K_{\dot{d}}\, Z_{\delta_T}(s+K_d)(s+1/T_{d\theta})}{\underbrace{s(T_e s+1)}_{\text{Engine Lag}}\underbrace{(s^2+2\zeta_\theta\omega_\theta s+\omega_\theta^2)}_{\text{Path Mode}}}$$

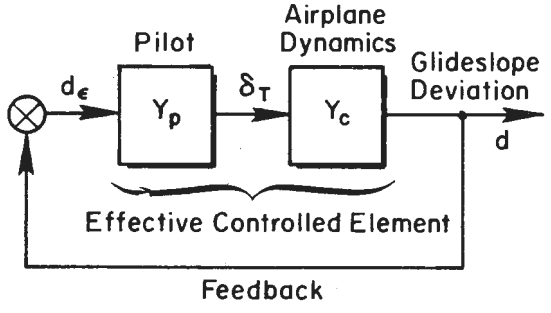

DEFINITION OF EFFECTIVE CONTROLLED ELEMENT (9)

The numerator time constant, $1/T_{d\theta}$, and the path mode frequency and damping are primarily dependent on the STOL aerodynamic characteristics and thrust inclination angle (see Volume II of this report. The engine lag time

constant, τ_e, was 1.5 sec for most of the experimental runs in this study. The primary variables in the experiment which arise from variation of the STOL generic characteristics are the $1/T_{d\theta}$ zero and the path mode frequency and damping, ζ_θ and ω_θ. The extremes of variations in these parameters are well represented by the generic configurations, BSL1 and AP10, where the former is largely characterized by $1/T_{d\theta} \doteq \omega_\theta$ and the latter by $1/T_{d\theta} << \omega_\theta$. The frequency responses for these generic forms and the corresponding limiting factors for closed-loop control are shown in Table 9.

Bandwidth limited configurations ($1/T_{h\theta} \geq \omega_\theta$) were the subject of considerable research in Ref. 9 where two possible criteria for determining the level of acceptability were derived. These criteria were based on the path mode response to throttle and involved correlations between pilot ratings (level of acceptability), the time to achieve one-half peak amplitude, and the phase lag of the path response to throttle transfer function at 0.5 rad/sec. Neither of these two criteria has been finalized; however, present (unpublished) indications are that rise time of greater than 3 sec to one-half peak amplitude result in unacceptable flight path control for the approach.

As can be seen from Table 9, configurations with the generic characteristics involving $1/T_{h\theta} << \omega_\theta$, Groups IV and V, tend to have a larger number of combined effects which are limiting in terms of closed-loop control. We therefore would expect that configurations where the effective controlled element (Y_pY_c) has a region of zero slope are more likely to have deficiencies which are limiting. Experimental evidence to support this conclusion is shown in Fig. 10 where it is seen that Configurations AP1 and AP10 are rated quite poorly (a large spread in the ratings with ratings of 7 or worse), and in Table 3 where the pilot commentary for these configurations regarding flight path control is very unfavorable. Airplanes with nearly vertical thrust inclination angles (small $X_{\delta_T}/Z_{\delta_T}$) tend to have very low values of $1/T_{h\theta}$. Thus, the combination of vertical thrust and a coupled attitude numerator, $(Z_w - X_u)^2 < 4X_wZ_u$, is seen to lead to unacceptably deficient configurations, e.g., $1/T_{h\theta} << \omega_\theta$.

TABLE 9

GENERIC FORMS OF THE EFFECTIVE CONTROLLED ELEMENT FOR PATH CONTROL WITH THROTTLE

GENERIC FORM	LIMITING FACTORS FOR CLOSED LOOP CONTROL
GROUP I, II and III (BSL 2 is example) Closed loop root based on experimentally derived value of K_d (See Fig. 31) 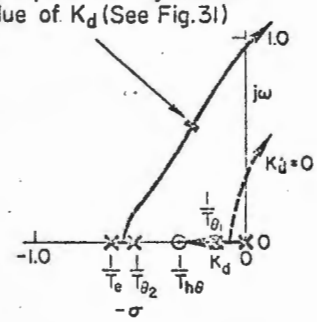 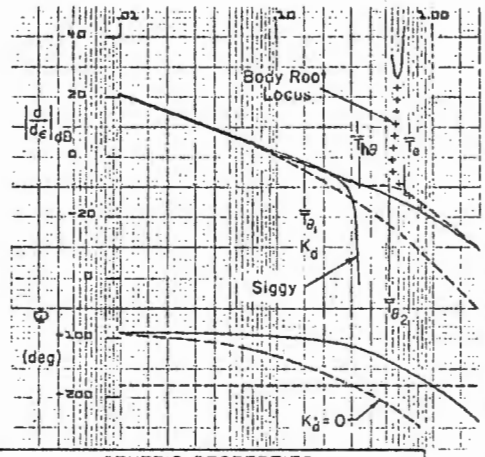 DOMINANT CHARACTERISTICS: • Low Bandwidth • K/s Shape • Δ is Real or Complex With $1/T_{h\theta} \pm 1/T_{\theta_1}$ or $1/T_{h\theta} \pm \omega_\theta$ GENERIC PROPERTIES: • Moderate Lift Curve Slope (C_{L_α}) • Low to Moderate Effective Thrust Inclination (θ_T = 60 deg to 80 deg)	Guidance and Control Requirements • Inability to augment ω_θ to frequencies high enough to regulate against disturbances Pilot Centered Requirements • Lags occur at frequencies too low for practical lead equalization
GROUP IV and V (AP 10 is example) 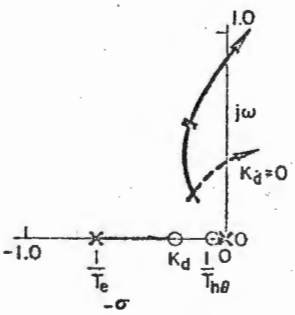 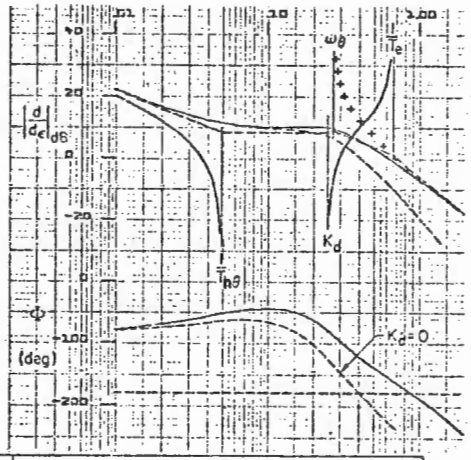 DOMINANT CHARACTERISTICS: • Moderate Bandwidth • Moderate Midfrequency Shelf • Δ is a Complex Pair With $1/T_{h\theta} < \omega_\theta$ GENERIC PROPERTIES: • Low Effective Powered Lift • Low Lift Curve Slope (C_{L_α}) • Moderate Effective Thrust Inclination (θ_T=90 deg).	Guidance and Control Requirements • Poor low frequency response due to inability to close loop at frequencies well above ω_θ, e.g., cannot drive $1/T_{h\theta}'$ into $1/T_{h\theta}$ • Poor response quality due to secondary mode at $1/T_{h\theta}'$. Desire closed loop system that is rapid and well damped. These generic configurations result in primary response at ω_θ and secondary droop response at $1/T_{h\theta}'$ Pilot Centered Requirements • Cannot equalize to a K/s without severely limiting the bandwidth

Conclusions:

- The limiting effects for path control which are due to aerodynamic and thrust inclination effects may be identified via the parameters ω_θ, ζ_θ, and $1/T_{h\theta}$.

- The engine time constant is a direct limitation on the bandwidth of path control with throttles.

- Configurations where the effective controlled element has a mid-frequency zero slope are more prone towards having combined limiting effects. Note that this zero slope can be due to a very large difference between $1/T_{h\theta}$ and ω_θ or can arise from low path mode damping, ζ_θ.

- The data base for bandwidth limited configurations ($1/T_{h\theta} = \omega_\theta$) is fairly complete (for example, see Refs. 5, 8, 9). There are very little data, however, for configurations where $1/T_{h\theta} << \omega_\theta$. Future simulation and flight test experiments should concentrate on this area.

- Adequate piloted path control with throttle is highly dependent on the ability of the pilot to perceive sink rate (see $K_{\dot{d}} = 0$ root loci in Table 9). This result has important implications for development of displays for final approach (head up displays, visual approach slope indicator lights, etc.)

B. ANALYSIS OF FLARE AND LANDING

The flare strategies observed during the simulation included the following:

- Attitude only
- Power only
- Attitude and power with attitude primary
- Attitude and power with power primary

There was little or no objection to the use of two controls in the flare. Upon reflection, this result is not surprising in that it is standard practice to use power in CTOL airplanes as an aid to gust regulation even though attitude is primary during the flare. The guidance and control and pilot-centered requirements for the landing task were therefore based on the use of two controls.

Analysis of the flare and landing was carried out under the assumption that the maneuver was performed by the pilot in a closed-loop regulatory way. The evidence upon which this assumption is based consists of strip chart records showing significant attitude and/or throttle regulation of a nature too complicated to be a precognitive open-loop input. Additionally, there was general agreement among the pilots that attempts to flare these configurations with a fixed open-loop strategy were not satisfactory. It therefore seemed pertinent to proceed with the analysis of the flare as a closed-loop tracking maneuver despite certain difficulties which arose

- There is no external command (such as a glide slope error, visual approach slope indicator lights, etc). The pilot must therefore internally generate the command structure as well as the feedbacks.

- It is not possible to experimentally measure closed-loop behavior (by the use of describing function technique) because of the short duration of the maneuver and the lack of a precise definition of the input.

The development of the command and feedback structure used in the closed-loop pilot/vehicle flare model in this study were based on the following observations, hypotheses, and assumptions:

- The pilot's primary objective in the flare was to reduce the sink rate to some acceptable (target) value at touchdown.

- There should be no abrupt changes in sink rate; that is, if most of the sink rate is eliminated early a "floater" results, and if most of the sink rate is eliminated just before touchdown frequent hard landings result. Thus, we hypothesized that a steady decrease in sink rate with altitude was representative of the pilot's internally generated command structure.

- The trajectories of sink rate vs. altitude for a number of flares in calm air with a reasonably good configuration (where the pilot's performance should have been representative of his command structure) tended to verify the above hypotheses, that is, the effective command for a closed-loop flare maneuver involved an essentially linear decrease in sink rate with altitude. An example of five consecutive calm

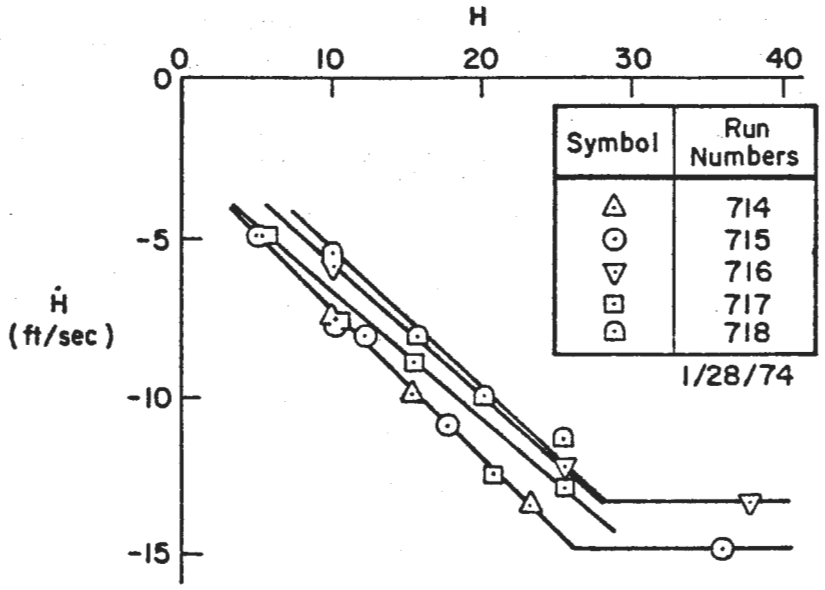

Figure 20. Phase Trajectories for Five Consecutive Flares — No Turbulence — Configuration BSL2, Pilot 7

air flares with Configuration BSL2 (Pilot 7) is shown in Fig. 20. Note that a linear variation of $\dot{h}$ with h is the well known exponential flare which is frequently the basis of autoflare systems.

- Because STOL runways are short, touchdown precision is important. As is well known by experienced pilots, flare strategies that emphasize smooth touchdowns (grease jobs) tend to use up a lot of runway. Therefore, the proper technique for STOL landings most likely involves a reasonably high target sink rate (compared to CTOL) that will minimize the probability of an overflare and resulting float.

The above points may be quantified in terms of an assumed command structure on a phase plane of sink rate vs. altitude in Fig. 21 below. The flare law which derives directly from the phase plane in Fig. 21 is given as:

$$\dot{H}_c = -\frac{1}{T_F} H + \dot{H}_{TD_c} \qquad (10)$$

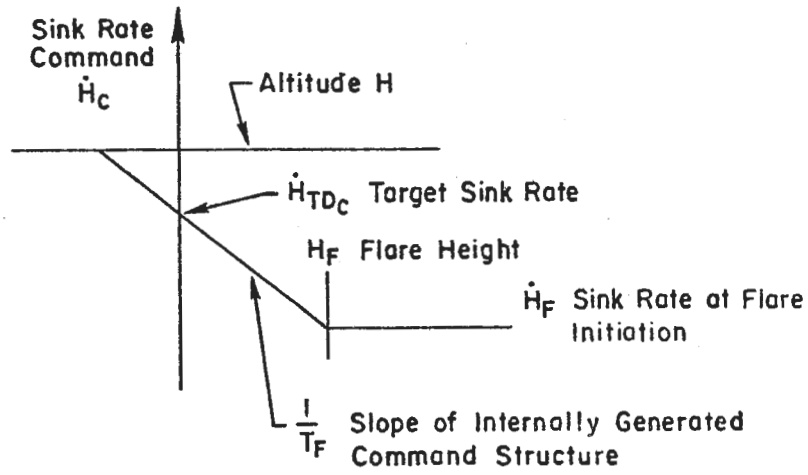

Figure 21. Assumed Command Structure for Closed Loop Flare

The slope of the internally generated command structure ($\dot{H}_C$ vs. H) becomes the flare mode inverse time constant, $1/T_F$. From the geometry in Fig. 21, T_F is seen to be dependent on the sink rate at flare initiation, $\dot{H}_F$, and flare height, H_F.

$$\frac{1}{T_F} = \frac{\dot{H}_{TD_C} - \dot{H}_F}{H_F} \tag{11}$$

Representative values of flare height (between 30 and 50 ft), target touchdown sink rate (3 to 5 ft/sec), and sink rate at flare initiation (13 ft/sec for 6 deg glide path) yields "typical values" of T_F between 2 and 5 sec.

Once the flare is defined in closed-loop tracking terms, the pilot-centered and guidance and control requirements which arise from well developed models of human pilot behavior (see Refs. 9, 13, and 14) may be used to identify those airplane features which are unacceptable. Even if the above formulated model is not exactly correct, it seem intuitive that identification of features which result in poor closed-loop regulation of sink rate as a function of altitude should lead to a good quantification of unacceptable handling in the flare.

1. Guidance and Control Requirements for Flare

- Command following. The assumed command (Eq. 10) may be modeled as a closed loop system. Since $\dot{H}_c$ is a function of the dependent variable altitude, it appears as an outer loop. In block diagram form:

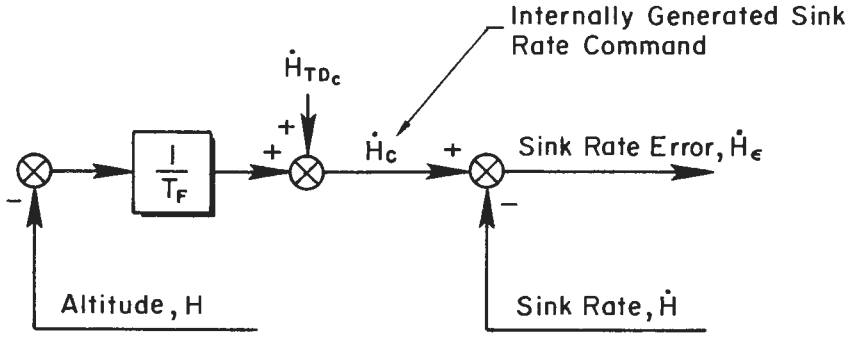

- Disturbance regulation. At low altitude the proximity of the ground precludes large vertical gusts. Therefore, the primary disturbance for the flare maneuver is horizontal wind shear.

- Stability. Repeatable flares require good closed-loop flight path stability to avoid large excursions in sink rate that result in unacceptable flare characteristics such as hard landings and overshoots.

2. Pilot-Centered Requirements for Flare

- Insensitivity to pilot response variations (desire broad region of K/s).

- Minimum pilot compensation. Ability to achieve a K/s effective controlled element with minimum equalization.

- Frequency separation of controls. The primary control should have a high crossover frequency adequate to turn the corner on the flare. The crossover frequency of the secondary control loop must be well separated (occur at a lower frequency) from the primary control loop.

- Response quality. The closed-loop system response should be rapid and well damped with minimum coupling between modes of motion. The pilot should be able to easily sort out the path mode response to a control input.

The primary control for the flare maneuver is usually pitch attitude, and its function is to provide the necessary control over sink rate. This implies a requirement for adequate frequency response to turn the corner on the flare and for adequate control authority to assure that the pitch attitudes required to arrest the sink rate are not excessive. The primary control must also provide the necessary regulation against sink rate excursions due to horizontal wind shear near touchdown. The level of windproofing required of the primary control depends on the quality of the secondary control. In cases where the sink rate response to pitch attitude is not adequate for flare, the primary control must revert to power or a direct-lift-type control device. Both pitch attitude and power are (alternatively) considered as primary controls in the following analyses.

The main requirement on the secondary control is that it complement the primary control, that is, the closure of the secondary control loop should improve the response in the primary loop. A common use of the secondary control in the flare for CTOL, as well as STOL airplanes, is to provide regulation against large gusts or shears that are beyond the capability of the primary control. Another common use of the secondary control is to make up for deficiencies in the low-frequency region of the primary control response. As example would be the elimination of an unstable backside mode (due to negative $1/T_{h_1}$) or excessive speed bleedoff by using the throttle as a secondary control. For purposes of analysis, these strategies were quantified as low gain control of sink rate error with the secondary control. Use of the secondary control to regulate some other flight variable (speed, angle of attack, etc.) was ruled out by the pilots who said they were head up during the flare. It was specifically noted by some pilots that once in the flare airspeed control was no longer a consideration.

Formulation of the analytical pilot model for flare was complicated by the fact that the flare maneuver is actually a response to initial conditions. In order to interpret the flare in terms of transfer functions (which by definition have no initial conditions), the initial conditions had to be reinterpreted in terms of an equivalent input. The details of this calculation and block diagram algebra are given in Appendix B. The resulting block diagrams are given in Fig. 22.

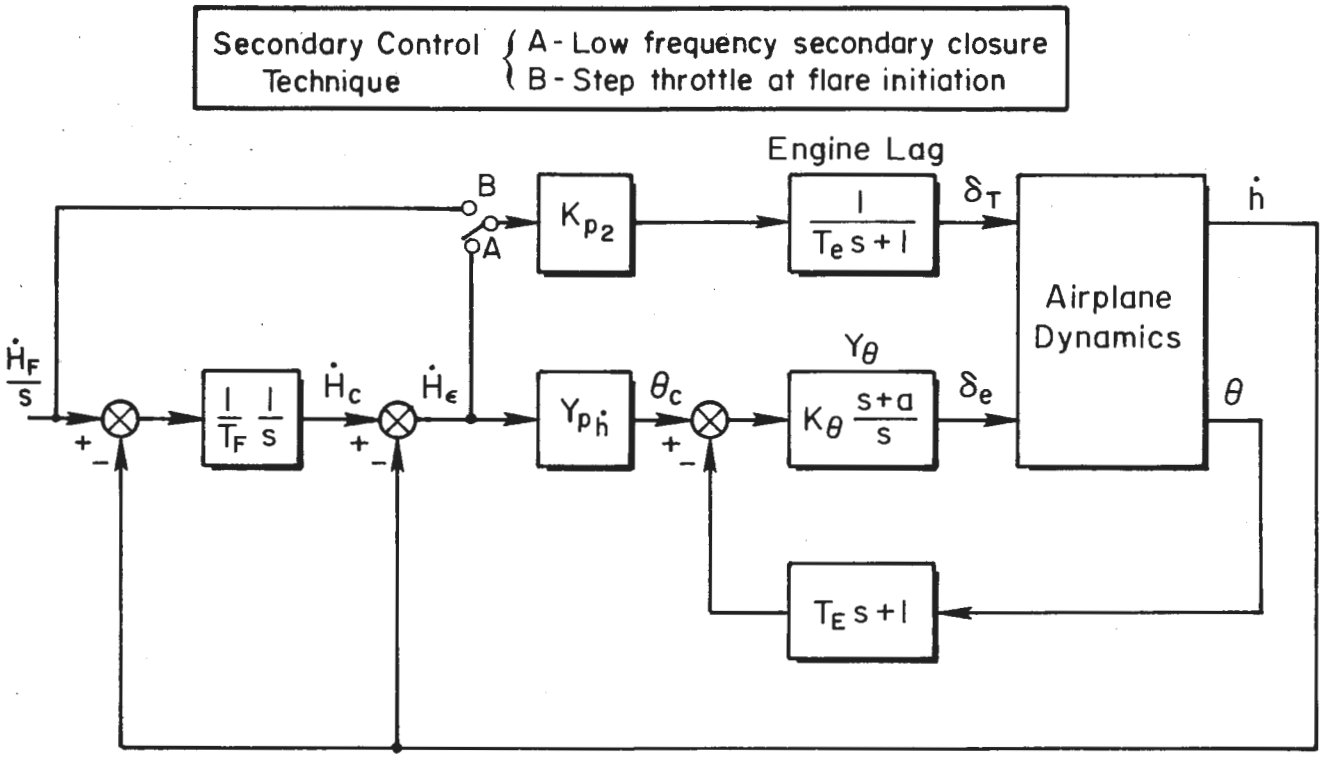

a) Attitude Primary - Throttle Secondary

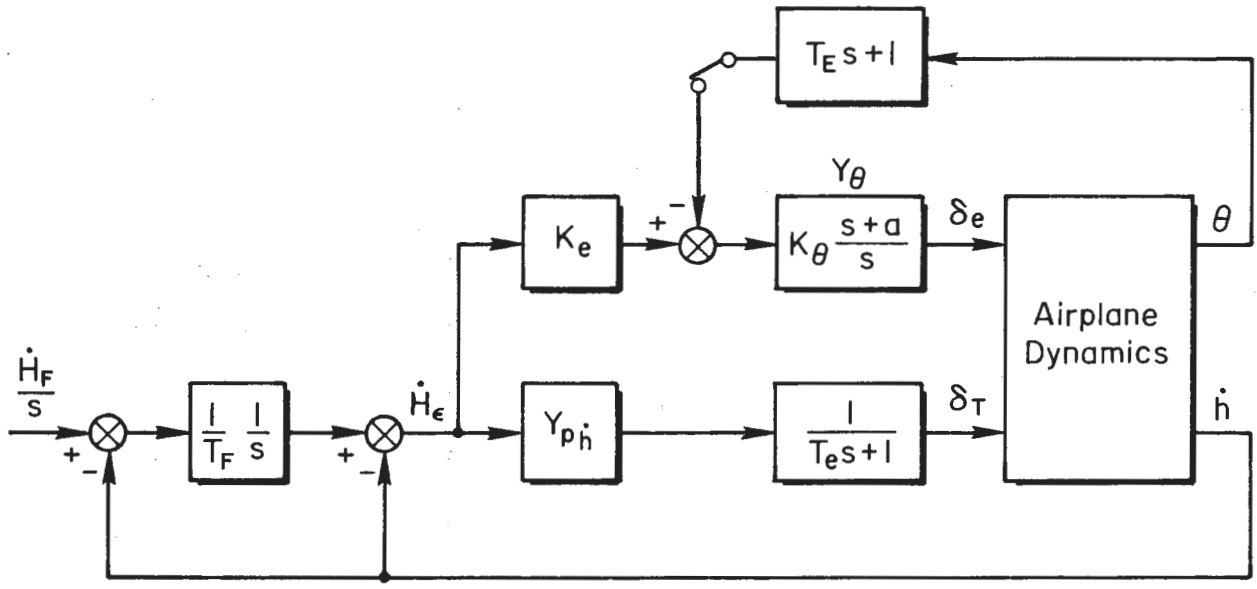

b) Throttle Primary - Attitude Secondary

Figure 22. Effective Closed Loop System for Flare (In terms of perturbation variables and with initial conditions reinterpreted as an input, see Appendix B)

3. Flare with Attitude Only

The approximate solution for the sink rate response of the closed loop pilot plus airplane system for an attitude-only flare (no secondary control) may be derived from Fig. 22a. Ignoring low frequency effects (e.g., assuming $1/T_{h_1} = 0$) the approximate solution for sink rate response in the flare is given as follows:

$$\frac{\dot{h}}{\dot{H}_F} \doteq \frac{1}{\underbrace{s(T_F s + 1)}_{\substack{\text{Effective}\\ \text{Flare}\\ \text{Command}}}\underbrace{\left[\frac{s^2}{\omega_\theta''^2} + 2\,\frac{\zeta_\theta''}{\omega_\theta''}\,s + 1\right]}_{\substack{\text{Path Mode Response —}\\ \text{Defines Departure}\\ \text{From Ideal Response}}}} \tag{12}$$

The details of the piloted loop closure are discussed later in this section as are the effects of nonzero $1/T_{h_1}$. The double prime superscript on ω_θ and ζ_θ indicates that two loops (an inner $\dot{h}$ loop and the outer "command loop") have been closed around the attitude-constrained airplane as shown in Fig. 22a. The first-order response term $(T_F s + 1)$ results from the outer (command) loop closure (should actually be T_F'' but we are assuming $T_F'' \doteq T_F$). It indicates that the assumed linear sink rate vs. altitude command is an exponential function in the time domain. The second-order "path mode response" is due to the fact that the airplane has dynamics which are characterized by the closed-loop frequency and damping (ζ_θ'' and ω_θ''). Thus, the quality of the flare (ability to follow the $\dot{H}$ vs. H command) will depend directly on the pilot's ability to modify the closed-loop path mode frequency and damping to desirable levels.

The generic response characteristics of Eq. 12 (for an initial sink rate of 13 ft/sec) are shown in Fig. 23. The effect of the path mode is seen to cause an initial delay followed by oscillations if the closed-loop damping, ζ_θ'', is low. From Fig. 23a the time history for $\omega_\theta'' = 5/T_F$ sets an approximate lower boundary on path mode frequency in that it returns to the command sink rate in approximately one flare mode time constant.

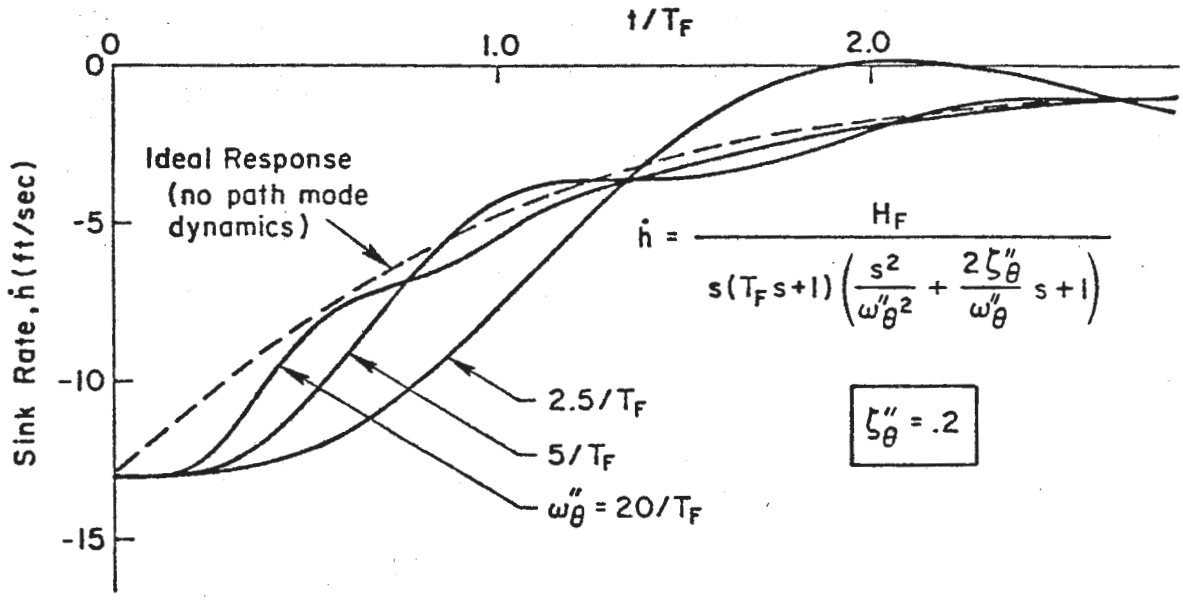

a) Effect of Closed Loop Path Mode Frequency on Flare

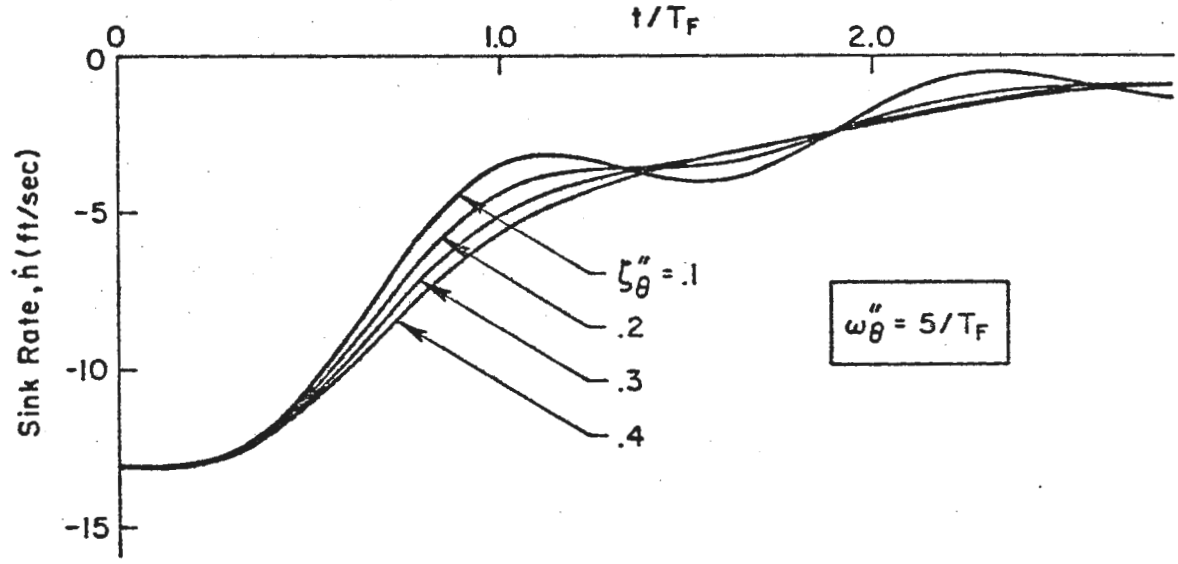

b) Effect of Closed Loop Path Mode Damping Ratio on Flare

Figure 23. Generic Response Characteristics of Attitude Flare (Solution to Eq. 12)

Likewise, from Fig. 23b a logical lower bound in path mode damping, ζ_θ'', (to avoid undue reversals) is seen to be between 0.1 and 0.2, or,

$$\zeta_\theta'' \geq 0.15 \tag{13}$$

Investigation of the detailed loop closure characteristics required to obtain these desired values of closed-loop path mode frequency and damping form the basis for prediction of pilot compensation and workload. From the block diagram in Fig. 22a and the approximate factors contained in Appendix B, an expression for the effective controlled element (pilot plus airplane) may be derived as follows. Assuming a high gain attitude loop closure $[\theta/\theta_c = (1/T_E s + 1)]$, the characteristic equation for the system in Fig. 22a is:

$$1 + \frac{K_{p_{\dot{h}}} e^{-\tau s}(1 + \frac{1}{T_F s}) N_{\delta_e}^{\dot{h}}}{(T_E s + 1) N_{\delta_e}^{\theta}} \tag{14}$$

which is of the form:

$$1 + Y_p Y_c = 0 \tag{15}$$

where $Y_p Y_c$ is defined as the effective controlled element of the system. Using the approximate factors in Appendix B:

$$Y_p Y_c \doteq \frac{K_{p_{\dot{h}}} e^{-\tau s} Z_\alpha (s + \frac{1}{T_{h_1}})(s + \frac{1}{T_F})}{T_E s (s + \frac{1}{T_E})(s^2 + 2\zeta_\theta \omega_\theta s + \omega_\theta^2)} \tag{16}$$

or

$$(s + \frac{1}{T_{\theta_1}})(s + \frac{1}{T_{\theta_2}}) \tag{17}$$

The numerator zero, $1/T_{h_1}$, defines whether the airplane is on the frontside or backside of the power-required curve ($1/T_{h_1} \doteq -1/3\ d\gamma/dv$ in deg/kt). T_F is the flare mode time constant, T_E is the attitude SAS time constant ($T_E = K_{\dot{\theta}}/K_\theta$), and ω_θ is the path mode frequency. The detailed characteristics of the piloted loop closure are given in the system survey shown in Fig. 24. The pilot model used for these closures assumed no lead or lag equalization and a neuromuscular lag, τ, of 0.25 sec, e.g., $Y_p = K_p e^{-\tau s}$. A flare mode time constant of 5 sec was assumed. Note that the attitude SAS mode at $1/T_E$ drives into the zero at $1/T_F$ for low values of pilot gain. Hence, the assumption that $1/T_F'' = 1/T_F$ in the approximation for the closed loop flare response (Eq. 12).

Comparison of the pilot-centered and guidance and control requirements (defined in Subsections V-B-1 and V-B-2) with the pilot/vehicle closure characteristics in Fig. 24 indicates that the ability to increase the closed-loop path mode frequency (ω_θ'') is limited by the SAS, $1/T_E$ (due to the K/s^2 slope of the frequency response at frequencies about $1/T_E$). Pilot equalization (lead in the $\dot{h}$ loop) is impractical since it would require time constants greater than 1 sec to be of any value. (Lead equalization greater than 1 sec is unacceptable; for example, see Ref. 15). Finally, low basic values of path mode damping, ζ_θ, make it impossible to augment the closed-loop path mode frequency, ω_θ'', to the required values necessary to turn the corner on the flare ($\omega_\theta'' > 5/T_F$). This basic deficiency is apparent in Configuration AP1 (see Fig. 24b) where ζ_θ'' is 0.09 (less than the desired 0.15). The pilot rating for approach and landing with AP1 varied from 4 to 7 whereas the pilot ratings for AP2 ($\zeta_\theta'' = 0.15$) were all 4's.

For STOL configurations which operate far on the backside of the power-required curve, $1/T_{h_1}$ will have a relatively large negative value. As shown in Fig. 24a (for Configuration BSL1), this is manifested as a low-frequency flight path instability (the free s at the origin drives into the zero in the right half plane at $1/T_{h_1}$) which is only aggravated by increased pilot gain. Airplanes with this or other deficiencies in the attitude flare characteristics exhibit a requirement for a secondary control (throttles,

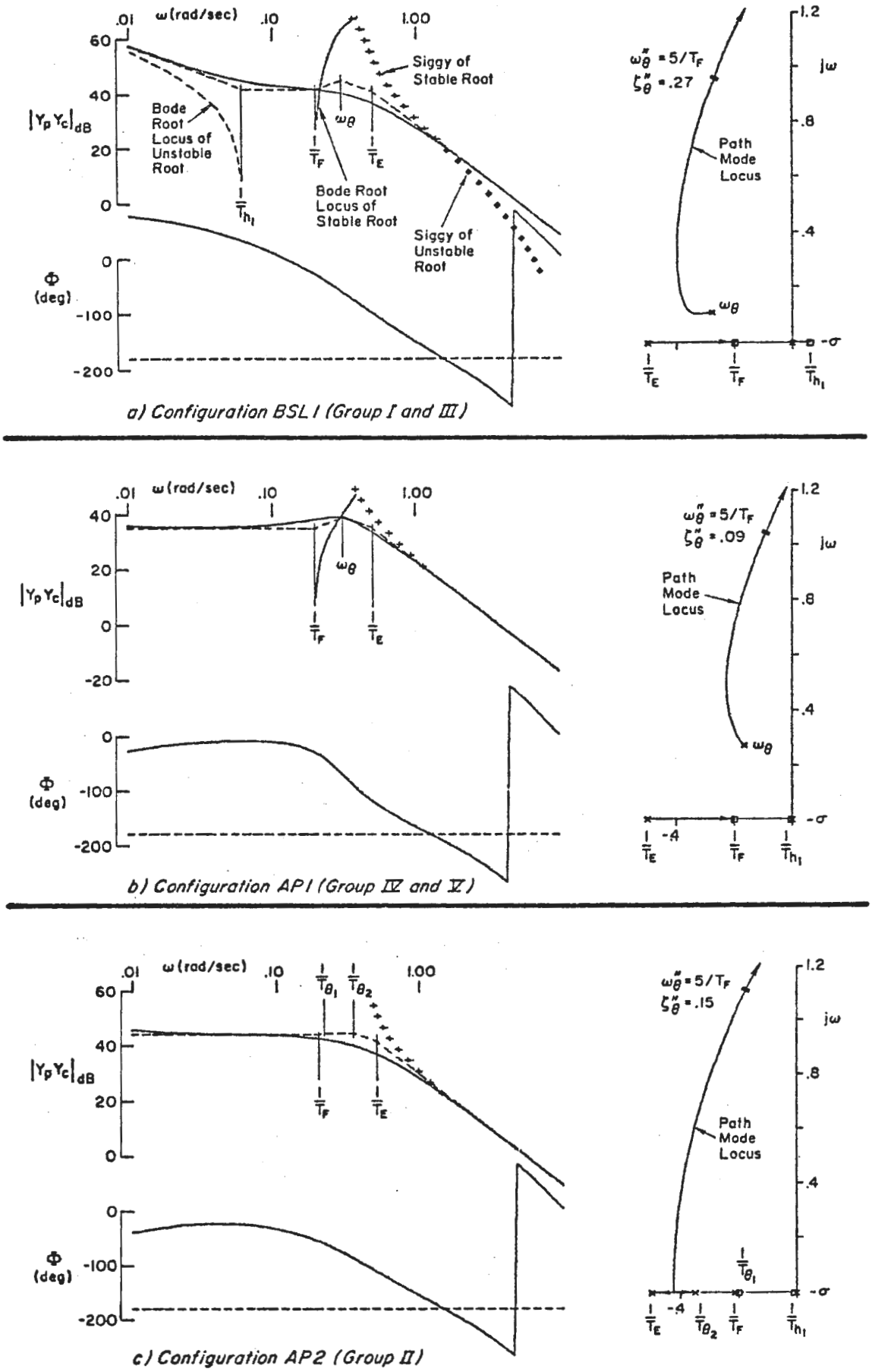

Figure 24. Generic Characteristics of Loop Closure for Attitude Flare

spoilers, etc.). The next subsection covers the effect of throttle as a secondary control; however, these results may also be applied to other types of secondary controls with a reinterpretation of the engine lag, T_e.

4. Flare with Attitude Primary and Throttles Secondary

Consider the feedback of sink rate error to throttle as a low-gain secondary closure (Option A in Fig. 23a). The effect of this secondary closure on the closed-loop characteristic roots is obtained by factoring the characteristic equation as a function of K_{p_2}

$$\Delta''' = \Delta'' + K_{p_2} \frac{\left(s + \frac{1}{T_F}\right)}{\left(s + \frac{1}{T_e}\right)} N^{\dot{h}}_{\delta_T} N^{\theta}_{\delta_e} \tag{18}$$

The migration of the characteristic roots as a function of the pilot's secondary control (throttle) gain is shown in the system survey in Fig. 25 below.

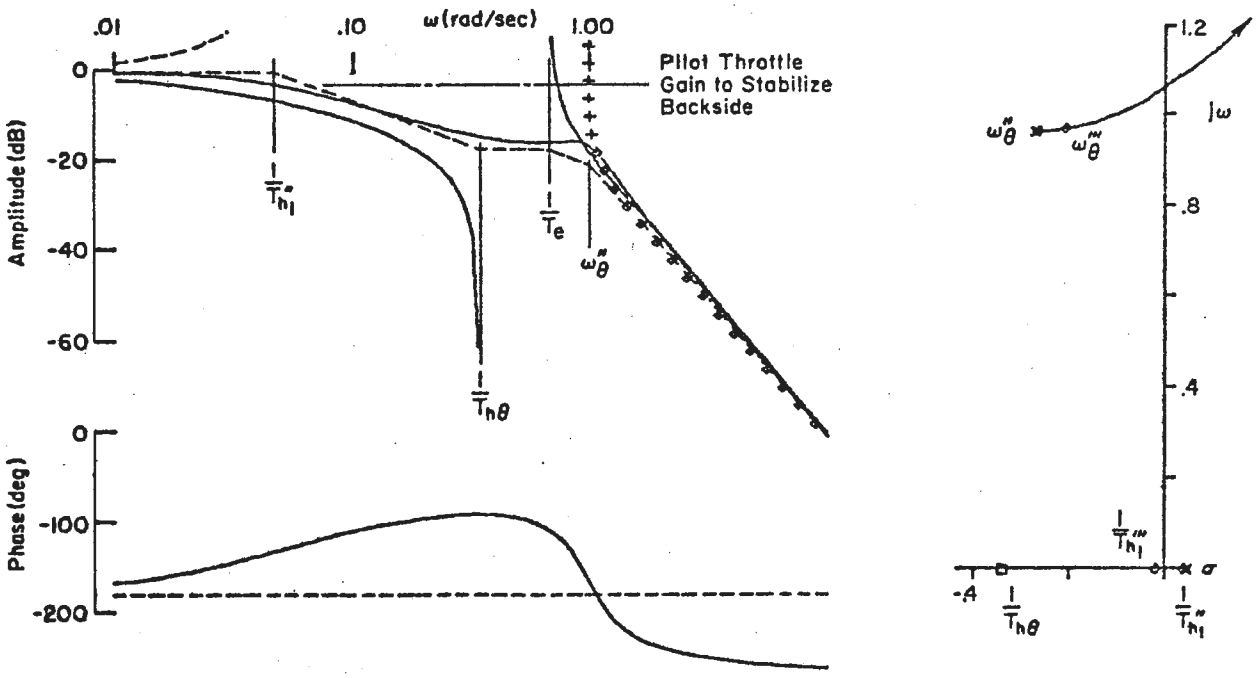

Figure 25. Use of Secondary Control to Stabilize Backside Mode Generic Configuration BSL1

The effect of K_{p_2} on the numerator of $\dot{h}/\dot{H}_F$ is very small for reasonable values of K_{p_2}. Figure 25 allows us to quantify the effects of the secondary closure in terms of satisfying the pilot-centered and guidance and control requirements as summarized below.

- The flight path instability resulting from the pilot's attitude closure (negative $1/T_{h_1}$) can be eliminated by low-gain secondary control activity (throttle). This satisfies the pilot-centered requirement for wide separation in crossover frequency between the primary and secondary control and, at the same time, satisfies the guidance and control requirement for stability.

- The value of the coupling numerator zero, $1/T_{h\theta}$, determines the effectiveness of a secondary loop closure. In terms of basic airplane parameters (see Appendix B):

$$\frac{1}{T_{h\theta}} \equiv -X_u + Z_u\left(\frac{X_{\delta_T}}{Z_{\delta_T}}\right) \tag{19}$$

  Airplanes with large thrust inclination angles (small $X_{\delta_T}/Z_{\delta_T}$) tend to have very low values of $1/T_{h\theta}$. Thus, we would expect that a combination of large thrust inclination angle (low $1/T_{h\theta}$) and operation way on the backside (large negative $1/T_{h_1}$) would receive very poor pilot ratings due to the pilot's inability to improve $1/T_{h_1}$ with the secondary throttle control. That is, the pilot's inability to satisfy the pilot-centered requirements would be expected to result in very poor ratings.

5. Analytical Conclusions for Attitude Flare

The results of the above analysis of the attitude flare with throttle as a secondary control may be summarized as follows:

- The ability to satisfy the guidance and control and pilot-centered requirements for flare (e.g., obtain good pilot ratings) may be quantified in terms of the equalization and pilot effort required to increase the closed-loop path mode frequency, ω''_θ, to values greater than $5/T_F$ (approximately 1 rad/sec) with adequate closed-loop damping ($\zeta''_\theta \geq 0.15$).

- The parameters which affect the ability to improve the closed-loop path mode, ω_θ'', are the flare mode time constant (T_F), the attitude SAS time constant ($T_E = K_{\dot\theta}/K_\theta$), and the attitude constrained path mode damping and frequency (ζ_θ and ω_θ). The flare mode time constant is a function of the flare geometry, depending on the flare height and sink rate at the initiation of flare. Its value for STOL configurations on a 6 deg glide slope is generally on the order of 5 sec.

- Configurations which require a large amount of lead ($T_E = K_{\dot\theta}/K_\theta$) in the attitude stability augmentation system (due to lightly damped or unstable short-period characteristics) are characterized by degraded path mode response characteristics. This effect stems from the fact that the inner-loop lead associated with augmentation of the attitude mode becomes a lag in the outer loop. That is, a closure of the inner, attitude loop in Fig. 22a would result in a numerator zero occuring at $1/T_E$; whereas closure of the outer, path mode loop (shown in Fig. 24) involves $1/T_E$ as a pole or lag in the system. Thus, we see that there is some upper limit to the ratio of pitch rate/attitude feedback that can be used before significant degradation in the path response will occur.

- Low-gain secondary control with the throttle during the flare is very effective in minimizing the effect of large negative values of $1/T_{h1}$. Physically, this tends to minimize the tendency of configurations way on the backside to drop out at the end of the flare.

- The value of the throttle as a secondary control for attitude flares is dependent on the position of the coupling numerator zero, $1/T_{h\theta}$. Low values of $1/T_{h\theta}$ tend to restrict the value of throttle as a secondary control. In fact, for some cases, throttle as a secondary control may actually degrade the response. Experimental evidence to support this conclusion was noted in the pilot commentary for Configuration AP6 (see Appendix A) which had reasonably good flare characteristics with attitude alone. The pilots noted that the use of throttle (as a secondary control) in the flare tended to make things much worse ($1/T_{h\theta}$ on AP6 was 0.05). Other configurations with similar (low) $1/T_{h\theta}$ (AP1 and AP10), but also with marginal attitude flare characteristics (poor ω_θ, ζ_θ location) received very poor ratings. This is attributed to the pilot's inability to improve the response with a secondary control in the presence of a marginal primary control.

On Configuration AP10 the engine lag time constant was reduced from 1.5 sec to 0.5 sec to see if improved bandwidth would help. The resulting pilot commentary was "can see faster response of sink rate to throttle but it doesn't seem to help performance; therefore my pilot rating is unchanged (was a 6)." Thus, the experimental results tend to verify the importance of the effect of low $1/T_{h\theta}$ on setting minimum acceptable boundaries for throttle as a secondary control. These problems arose out of an attempt to compensate for limited control power for flaring with attitude by using a step secondary throttle on Configurations AP1 and AP10. This is further discussed in Section V-B-8.

6. Flare with Throttle as a Primary Control

Using the same technique as for attitude flare, the effective controlled element (pilot plus airplane) may be derived from the block diagram of the closed-loop flare maneuver in Fig. 22b. An approximate expression for the oepn-loop pilot plus airplane (effective controlled element) has been derived from Fig. 22b and the approximate factors in Appendix B and is given as follows:

$$Y_pY_c \doteq \frac{K_{p_h} e^{-\tau s} Z_{\delta_T} \left(s + \frac{1}{T_F}\right)\left(s + \frac{1}{T_{h\theta}}\right)}{s(T_e s + 1)(s^2 + 2\zeta_\theta \omega_\theta s + \omega_\theta^2)} \tag{20}$$

The form of this effective controlled element is identical to the effective controlled element for attitude flares and for glide slope tracking (see Eq. 9 in Section V-A). In fact, recognizing $d \doteq h$, $1/T_{d\theta} = 1/T_{h\theta}$, the terms are identical to the glide slope tracking Y_pY_c except for the zero $(s + 1/T_F)$. It follows that the generic response plots and conclusions stated in Table 9 apply equally well to throttle flares and glide slope tracking, with K_d replaced by $1/T_F$. This is a very important and intuitively satisfying result in that it indicates that problems with flight path control have a one-to-one correlation with flare and landing problems for configurations where power is primary for flare, e.g., serious degradations occur when $1/T_{h\theta} << \omega_\theta$.

7. Flare with Throttle Primary and Attitude Secondary

The ability of the pilot to improve the powered flare characteristics by closing a low-gain attitude loop has been investigated by considering the effect of this closure on the characteristic equation for the closed-loop power flare.

$$\Delta''' = \underbrace{(T_E s + 1)\Delta''}_{\text{Attitude SAS}} + K_{p_2} \underbrace{\frac{s + \frac{1}{T_F}}{s} N_{\dot{\delta}_e}^{\dot{h}}}_{\text{Secondary Control Term}} \tag{21}$$

Charac-teristic Equation with Throttle Loops Closed

Putting this in root locus form for factoring and using the approximate factors in Appendix B

$$1 + \frac{\frac{K_{p_2}}{T_E} Z_\alpha (s + \frac{1}{T_{h1}})\cancel{(s + \frac{1}{T_F})}}{(s + \frac{1}{T_{h\theta}''})(s + \frac{1}{T_E})\cancel{(s + \frac{1}{T_F''})}(s^2 + 2\zeta_\theta''\omega_\theta'' s + \omega_\theta''^2)} = 0 \tag{22}$$

A system survey indicating the effect of the pilot's secondary (attitude) loop closure on the characteristic roots (roots of Δ'') is shown in Fig. 26.

The following conclusions can be drawn from Fig. 26

- No significant changes in any of the characteristic roots occur for "low gain" secondary attitude control.
- The secondary control gain must be increased to crossover frequencies near the closed loop path mode, ω_θ'', before any of the roots are affected ("moderate gain" in Fig. 26).
- Based on the pilot centered requirement for separation of crossover frequencies for primary and secondary controls, attitude is not a good secondary control for flare.

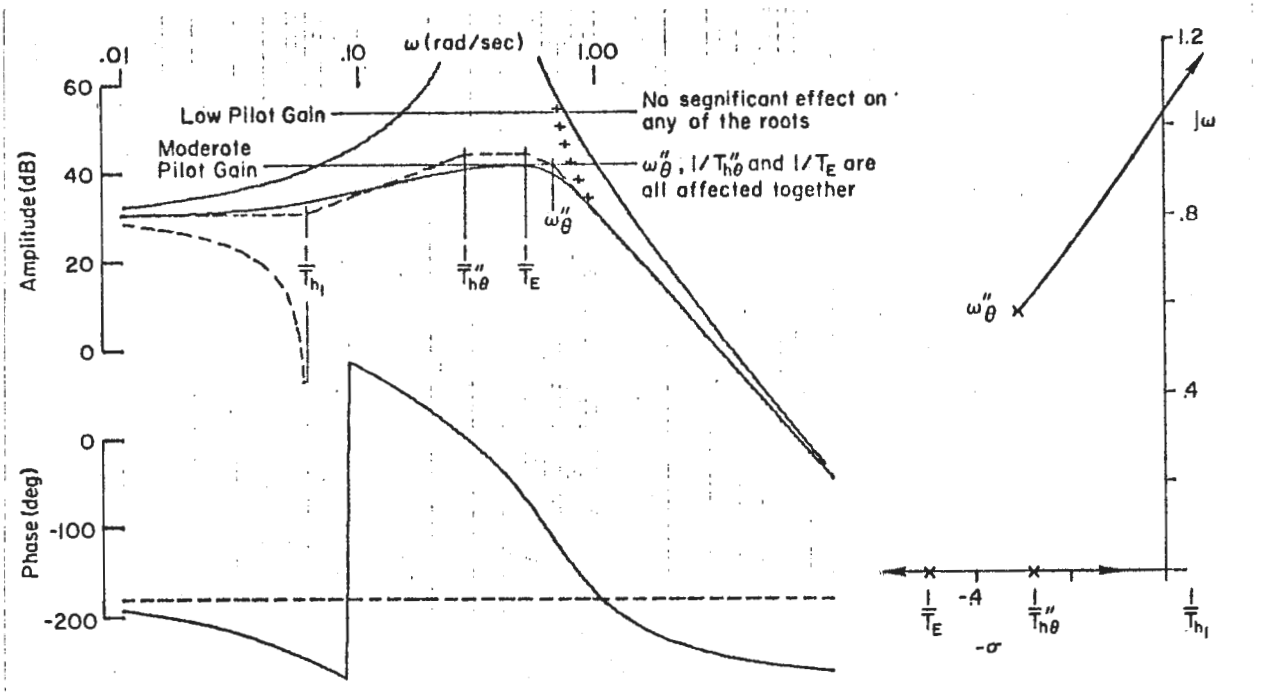

Figure 26. Effect of Secondary Attitude Closure on Closed Loop Roots for Throttle Flare

8. Attitude Effectiveness for Flares

In Subsection V-B-3 attitude only flares were evaluated on the basis of dynamic response characteristics (e.g., closed loop path mode). An important factor that was not considered was the magnitude of pitch attitude required to achieve the flare maneuver. This may be determined from the following expression

$$\frac{\theta}{\dot{H}_F} = \left(\frac{\dot{h}}{\dot{H}_F}\right)\left(\frac{\theta}{\dot{h}}\right) = \frac{N_{\dot{H}_F}^{\dot{h}''}}{\Delta''}\,\frac{N_{\delta_e}^{\theta}}{N_{\delta_e}^{\dot{h}}} \tag{23}$$

Substituting Eq. 12 for $\dot{h}/\dot{H}_F$ and approximate factors in Appendix B for the θ and $\dot{h}$ numerators

$$\frac{\theta}{\dot{H}_F} \doteq \frac{\frac{1}{T_F}\,\frac{\omega_\theta''}{Z_\alpha}}{\left(s + \frac{1}{T_F}\right)\left(s + \frac{1}{T_{h_1}}\right)}\;\frac{s^2 + 2\zeta_\theta\omega_\theta s + \omega_\theta^2}{s^2 + 2\zeta_\theta''\omega_\theta'' s + \omega_\theta''^2} \tag{24}$$

The frequency response asymptotes of Eq. 24 are plotted in Fig. 27.

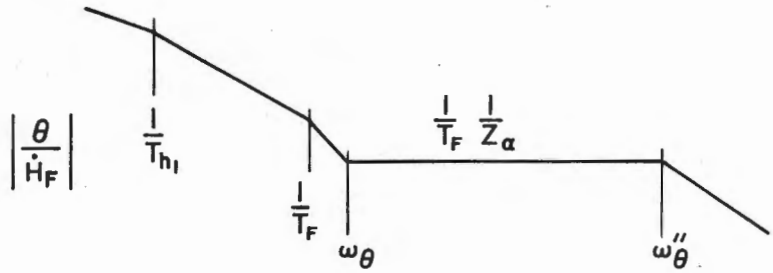

Figure 27. Asymptotes of $|\theta/\dot{H}_F|$

A technique commonly used for configurations with marginal Z_α was to bring in some power (throttle step) at the initiation of the flare. This is shown as Option B for the secondary control in Fig. 22a. The object was to obtain a decrease in the flight path angle and thereby minimize the requirements on pitch attitude in the flare. Since crossfeeds from the command input (feedforward) have no effect on the characteristic equation, the effect of this control stategy is apparent from analysis of the $\dot{h}/\dot{H}_F$ numerator. Making the usual tight attitude control assumption (K_θ large), the numerator is written as:

$$N^{\dot{h}}_{\dot{H}_F} = Y_\theta\left[K_{p_1}e^{-\tau s}\frac{1}{T_F s}N^{\dot{h}}_{\delta_e} + K_{p_2}\frac{1}{T_e s+1}N^{\dot{h}}_{\delta_T}\frac{\theta}{\delta_e}\right]$$

$$\doteq Y_\theta\left[K_{p_1}e^{-\tau s}\frac{1}{T_F s}Z_\alpha\left(s+\frac{1}{T_{h_1}}\right) + K_{p_2}Z_{\delta_T}\frac{s+\frac{1}{T_{h\theta}}}{T_e s+1}\right] \tag{25}$$

$$\doteq Y_\theta K_{p_1}e^{-\tau s}\frac{1}{T_F s}Z_\alpha\left(s+\frac{1}{T_{h_1}}\right)\left[1+T_F\frac{K_{p_2}Z_{\delta_T}s\left(s+\frac{1}{T_{h\theta}}\right)}{K_{p_1}e^{-\tau s}Z_\alpha\left(s+\frac{1}{T_{h_1}}\right)(T_e s+1)}\right]$$

The numerator zeros result from factoring Eq. 25 (with K_{p_2}/K_{p_1} as the root locus gain) which is shown for a generic configuration with very low $1/T_{h\theta}$ (AP10) in Fig. 28.

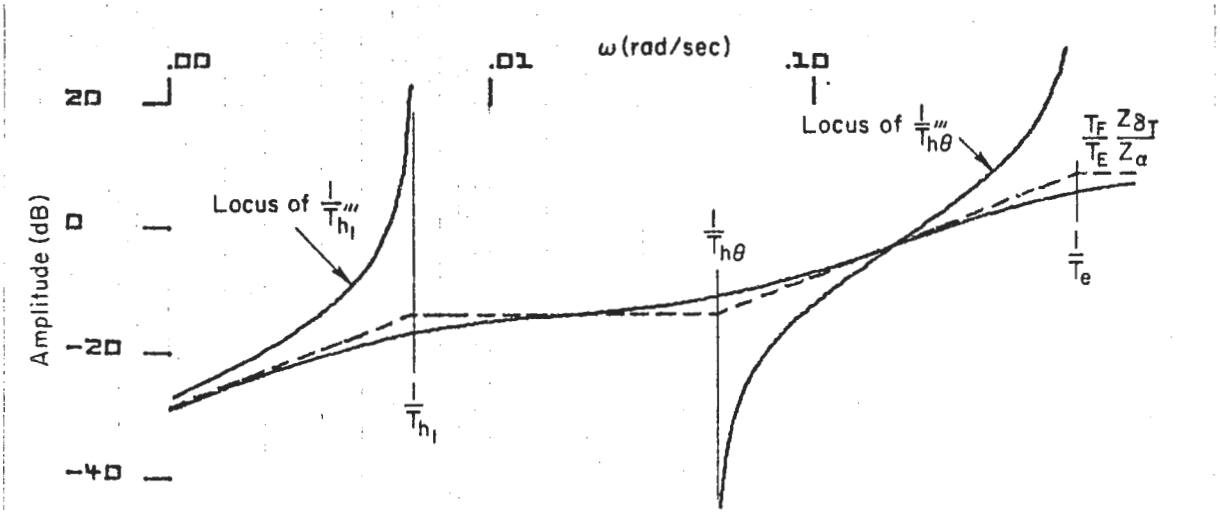

Figure 28. Migration of $\dot{h}/\dot{H}_F$ Numerator Zeros with Secondary Control (Throttle) Gain, K_{p_2}

As would be expected, the magnitude of the pitch attitude required to flare depends on Z_α. The form of the closed loop transfer function for flare is

$$\frac{\dot{h}}{(\dot{H}_F)_{step}} = \frac{\left(K_{p_1}\frac{1}{T_F}Z_\alpha + K_{p_2}Z_{\delta_T}\right)\left(s + \frac{1}{T_{h_1}'''}\right)\left(s + \frac{1}{T_{h\theta}'''}\right)}{(T_e s + 1)\left(s + \frac{1}{T_F}\right)\left(s + \frac{1}{T_{h_1}''}\right)\left(s^2 + 2\zeta_\theta''\omega_\theta'' s + \omega_\theta''^2\right)} \tag{26}$$

Where the triple primed numerator zeros indicate that three loops have been closed (h, $\dot{h} \rightarrow \delta_e$, and $\dot{H}_F \rightarrow \delta_T$), and the double primed denominator indicates that $\dot{H}_F \rightarrow \delta_T$ does not affect the denominator.

Assuming near cancellation of the $1/T_{h_1}$ roots, Table 10 shows some resulting asymptotic Bode sketches. These are to be interpreted <u>not</u> as the equivalent of frequency response measurements but as indicative of the system response to an initial (secondary) throttle step. The primary improvement is seen to be an overall increase in gain (gain is increased by $K_{p_2}Z_{\delta_T}$). If $1/T_{h\theta}''' << \omega_\theta''$, this increase in gain is offset by a mid to

TABLE 10

EFFECT OF THROTTLE STEP AS SECONDARY CONTROL
IN CLOSED LOOP FLARE MANEUVER

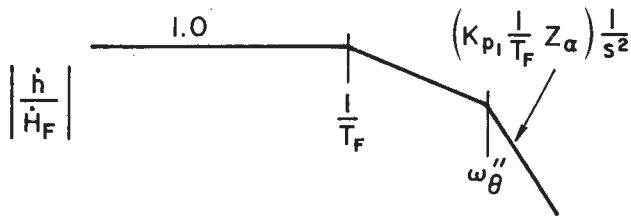

No Secondary Control

- Basic response at $1/T_F$ with "nuisance mode" at ω''_θ
- Tendency to over flare depends on ζ''_θ

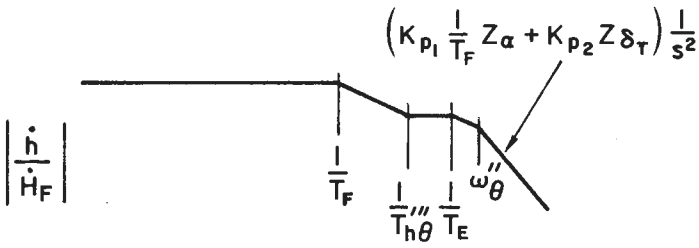

Step Throttle Secondary Control
$1/T_{h\theta} \doteq \omega_\theta$
(Represented by Configurations BSL1, 2, 2RLD in experiment)

- Increased overall response, i.e., effective increase in control power
- Rapid initial response with mid-frequency delay proportional to $1/T'''_{h\theta} - 1/T_F$

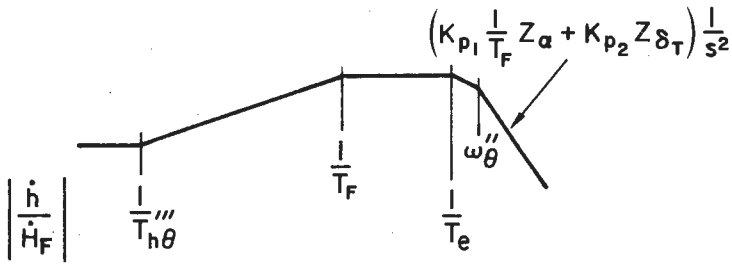

Step Throttle as Secondary Control
$1/T_{h\theta} << \omega_\theta$
(Represented by Configurations AP1, 2, 6, 6 RLD, 10)

- Increased initial response, and decreased final value
- Throttle is highly effective initially followed by droop or falling out at the end of the flare. Highly undesirable.

low "frequency" droop which makes the aircraft appear to fall out at the end of the flare. This characteristic is the same as that which also caused the flight path control problems with power noted earlier (e.g., $1/T''_{h\theta} << \omega''_{\theta}$ for Configurations AP1 and AP10). It is now obvious why the pilots were unable to improve their landing performance by using power as a secondary control on these configurations. Many pilots initially thought the problem was due to the large engine lag, but runs with T_e as low as 0.25 sec did not result in any rating improvement.

9. Gust Regulation

As noted in the pilot-centered requirements, Section V-B-2, one of the functions of the primary control is to provide the necessary regulation against sink rate excursions due to horizontal wind shear near touchdown. The generic characteristics of the sink rate response to horizontal gusts of the closed-loop pilot plus airplane system with attitude or throttle as primary controls are shown in Fig. 29a and 29b, respectively.

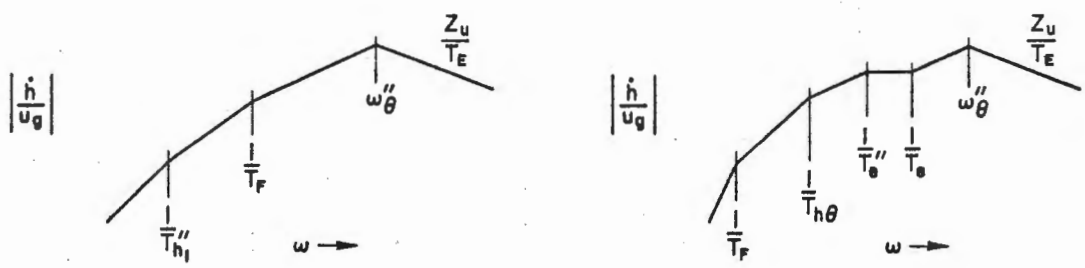

$$\frac{\dot{h}}{u_g} \doteq -\frac{Z_u s^2 (T_E s + 1)}{T_F \left(s + \frac{1}{T''_{h_1}}\right)\left(s + \frac{1}{T_F}\right)(s^2 + 2\zeta''_\theta \omega''_\theta s + \omega''^2_\theta)}$$

a) Attitude Only Flare

$$\frac{\dot{h}}{u_g} = -\frac{Z_u s^3 \left(s + \frac{1}{T_\theta}\right)}{\left(s + \frac{1}{T''_\theta}\right)\left(s + \frac{1}{T''_{h\theta}}\right)\left(s + \frac{1}{T_F}\right)(s^2 + 2\zeta''_\theta \omega''_\theta s + \omega''^2_\theta)}$$

b) Throttle Only Flare

Figure 29. Generic Characteristics of Gust Response in Flare

The following conclusions may be drawn from Fig. 29:

- The sink rate response to a u gust at frequencies above the closed-loop path mode, ω''_θ, is proportional to the stability derivative, Z_u, and is the same for either attitude or throttle flares

- The gust response of the closed-loop system is attenuated at frequencies above and below the closed-loop path mode. The peak response (at ω_θ'') decreases with increasing ω_θ''; this is another reason for wanting to maximize the closed-loop path mode frequency, ω_θ''.

- Maximizing the coupling numerator zero, $1/T_{h\theta}$, will reduce the low frequency gust response (i.e., below ω_θ'')

As was noted in the simulator and flight test results, the pilot ratings for flare and landing were highly sensitive to the gust environment and tended to be especially sensitive to large horizontal shears. It is therefore very desirable to minimize the magnitude of the $\dot{h}$ to u gust response shown generically in Fig. 29. These generic frequency response asymptotes indicate that the stability derivative Z_u sets the magnitude of the $\dot{h}$ to u gust response. For CTOL aircraft Z_u is simply a function of the trim lift, e.g., from Ref. 12

$$Z_u \equiv -\frac{\rho S U_o}{2m}\left(C_L + C_{L_u}\right) \tag{27}$$

For CTOL in subsonic flight, $C_{L_u} = 0$ and

$$Z_u \doteq -\frac{2g}{U_o} \tag{28}$$

However, for STOL configurations, the variation of lift coefficient with speed may be significant ($C_{L_u} \neq 0$), and for vectored thrust configurations a large portion of the vehicle weight may be supported directly or indirectly by the thrust. Z_u for STOL configurations may be written as follows:

$$Z_u = -\frac{2g}{U_o}\left[1 - \frac{\partial C_L}{\partial C_\mu}\frac{C_\mu}{C_L}\right] \tag{29}$$

The efficiency of the powered lift concept is directly proportional to $\partial C_L/\partial C_\mu$. Thus, we would expect that highly efficient STOLs will have lower values of Z_u and therefore decreased gust sensitivity. (A typical number for an EBF is $(\partial C_L/\partial C_\mu)(C_\mu/C_L) = 0.4$.)

C. DISCUSSION OF KEY PARAMETERS

Certain key parameters have been identified as being of primary importance in assessment of minimally acceptable path control. These are summarized as follows:

ω_θ'' and ζ_θ''	Closed loop path mode frequency and damping
$1/T_E$	Attitude SAS mode. Limits ability to obtain desired closed loop path mode for attitude flares
Z_w	Heave damping derivative
$Z_\alpha = U_o Z_w$	Measure of control power for attitude flare
Z_u	Speed coupling derivative. Measure of horizontal gust sensitivity
$T_F = H_F/(\dot{H}_{TD_c} - \dot{H}_F)$	Flare mode time constant. Defines minimum acceptable closed loop path mode frequency, e.g., $\omega_\theta'' \geq 5/T_F$. Usually about 5 sec for STOL
$1/T_{h_1}$	Backside parameter defines tendency to drop out at the end of an attitude flare $1/T_{h_1} = -(1/3)(d\gamma/dV)$ in deg/kt. Sets requirement for secondary throttle control
$1/T_{h\theta}$	Dominant numerator zero for flight path control with throttles. Low values limit usefulness of throttle as a primary or secondary control when attitude numerator is coupled
$1/T_e$	Engine lag. Restricts ability to increase ω_θ'' to its minimum acceptable value

The ability to achieve good flight path control depends on satisfying the pilot centered and guidance and control requirements. The most dominant of the relationships between these requirements and the key parameters are defined below.

1. Guidance and Control Requirements

- Command following. Depends on adequate closed loop path mode frequency ω_θ''. A tentative lower limit (pending more exhaustive testing) of $\omega_\theta'' \geq 5/T_F$ has been set for the flare, but no value

has yet been determined for glide slope tracking. It is suspected that the flare requirements are more stringent and therefore will also set the critical limits for ω_θ'' for final approach.

- Disturbance regulation. The level of sensitivity of a configuration to horizontal gusts (which are the critical input) depends on Z_u. The ability to regulate against these gusts depends on ω_θ''.

- Stability. Satisfying the guidance and control requirements clearly depends on achieving some minimum value of ω_θ'' (tentatively set at $5/T_F$. This, of course, presumes some minimum level of closed loop path mode damping, ζ_θ''. (ζ_θ'' minimum tentatively set at 0.15.)

2. Pilot Centered Requirements

- Minimum pilot compensation. Since closure of the path loop generally occurs at or below 1 rad/sec, pilot lead equalization is generally not possible without degraded ratings. It follows that the effective controlled element must be equalized to a K/s via appropriate selection of feedbacks (usually path error and path error rate). Low values of $1/T_{h\theta}$ ($1/T_{h\theta} << \omega_\theta$) and low values of ζ_θ tend to restrict or make it impossible for the pilots to equalize to a K/s. A large engine lag, T_e, and/or attitude SAS mode lag, T_E, make it impossible to extend the region of K/s to allow the pilot to augment ω_θ'' to its minimum acceptable value.

- Frequency separation of controls. The ability to augment an attitude flare with low frequency throttle control is limited by low values of $1/T_{h\theta}$. Attitude is not a good secondary control because it does not improve the primary loop closure unless closed at path mode frequencies.

- Response quality. Configurations with $1/T_{h\theta} << \omega_\theta$ tend to have very poor response quality for flight path control with throttles.

The pilot's ability to improve the path mode response is central to the issue of defining minimally acceptable path control. It therefore seems logical that pilot opinion should be sensitive to the path mode root locus, e.g., the root locus plot corresponding to $1 + Y_p Y_c = 0$. The generic characteristics of this locus for attitude and throttle as primary controls are shown in Fig. 30. τ has been assumed to be zero to allow a definition of the asymptote of the path mode locus. If the ability to modify ω_θ is indeed

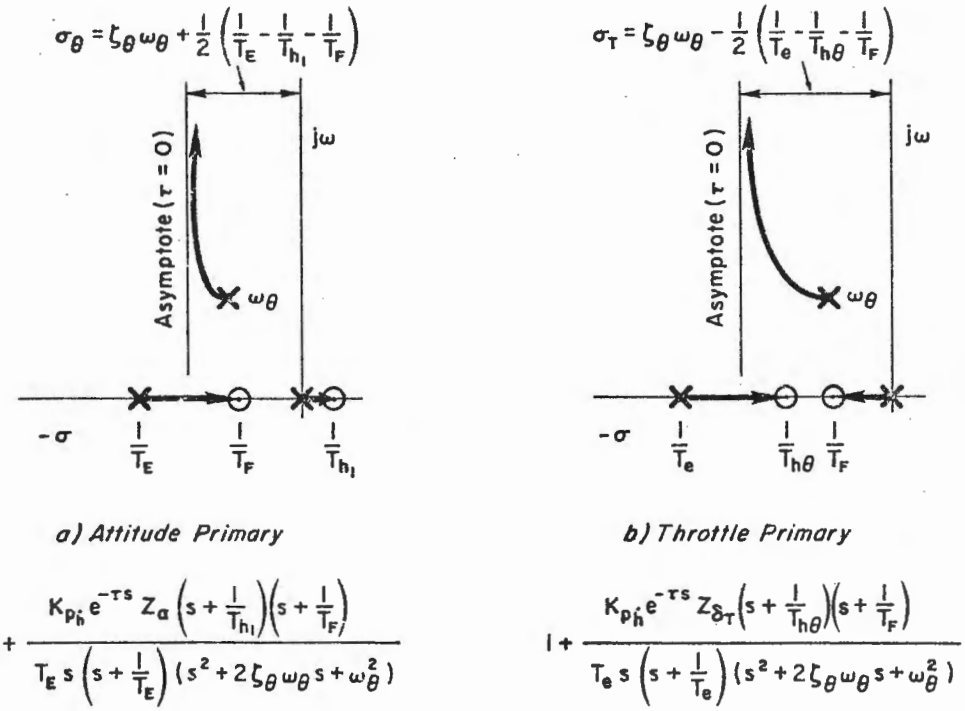

Figure 30. Generic Root Locus Characteristics ($\tau = 0$) of $1 + Y_p Y_c = 0$

a true figure of merit, σ_θ and σ_T would certainly be a logical correlating parameters. They are intuitively desirable because they contain most of the key variables identified in the analysis and summarized at the beginning of this section. The one key variable not accounted for by σ_θ or σ_T is the gust sensitivity Z_u. Clearly, the few generic configurations tested in this experiment do not form a large enough data base to test such hypotheses as these. However, it is not unreasonable to plot up the landing data (Task 2.1) on a grid of σ_θ vs. Z_u. (Z_u is picked as a measure of gust sensitivity on the basis of the $\dot{h}/u_g$ asymptote in Fig. 29 and this is done in Fig. 31.

As was stated in the introduction, the purpose of this study was to identify the key parameters and critical flight regimes and <u>not</u> to define boundaries. It is recommended that based on the results of this study all existing data should be gathered and analyzed to see if appropriate boundaries can be drawn. It is expected that data where $1/T_{h\theta} << \omega_\theta$ will be found to be lacking and will require future simulator experiments with some flight test backup as discussed in Section IV.

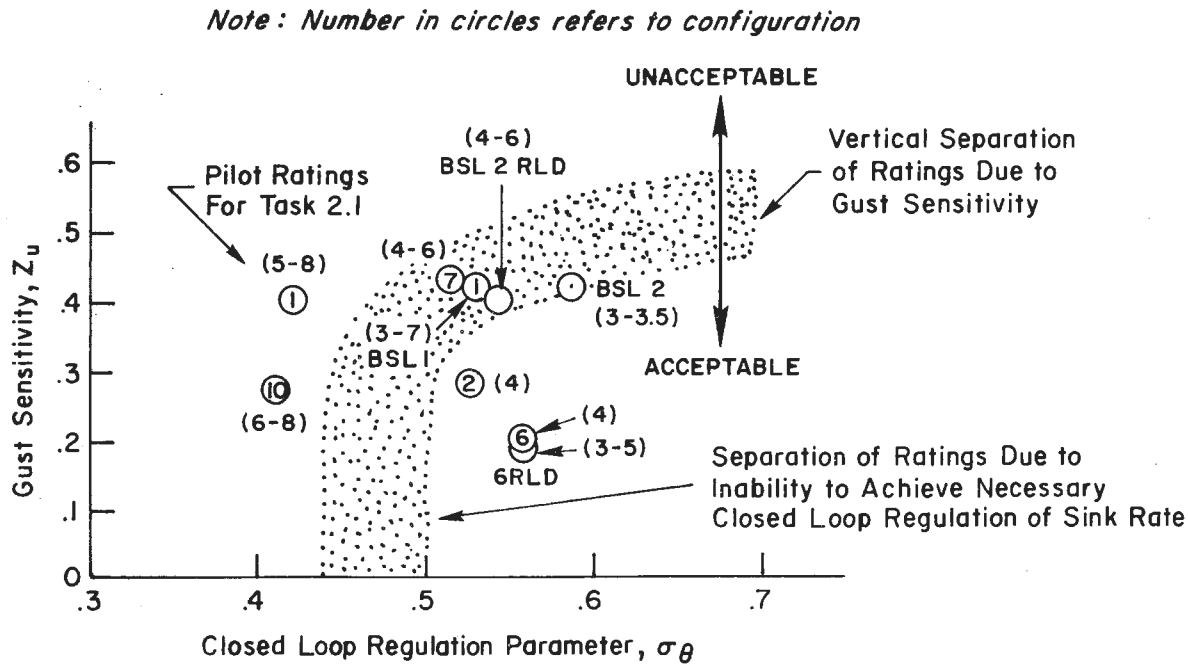

Figure 31. One Possible Way of Using Key Parameters to Correlate Minimum Acceptable Path Control with Aircraft Configuration

Referring to Fig. 31, certain trends in the experimental results (pilot ratings) may be explained by the analysis.

- The low σ_θ for Configurations AP1 and AP10 indicates that the pilot had problems obtaining the necessary closed loop path mode bandwidth making flare with attitude unacceptable. $1/T_{h\theta}$ was very low for both of these configurations ($1/T_{h\theta} << \omega_\theta$) which is indicative of flight path control problems with throttle. Therefore, neither throttle nor attitude was an acceptable primary control, and use of throttle as a secondary control was not a solution (low $1/T_{h\theta}$). Hence, the unacceptable pilot ratings.

- The value of σ_θ for Configurations BSL1, BSL2, AP2, AP6, and AP6 RLD are all about the same (σ_θ = 0.5 to 0.55). From Fig. 31, it is seen that this value of σ_θ is acceptable for configurations with low gust sensitivity (Z_u/T_E). However, as the gust sensitivity is increased to approximately the CTOL value ($Z_u \doteq -2g/U_o$), the pilot ratings begin to degrade into the unacceptable region. (Compare pilot ratings for BSL1 and AP7 in Fig. 16 with and without turbulence.)

Because of the very large engine lag used on the configurations (T_e = 1.5 sec), there is little or no data for correlating throttle as a primary control. Further correlations will require analysis of presently available results from

other experiments and a carefully defined experiment to fill in the gaps in existing data. This will allow definition of quantitative relationships between the key parameters defined in this study and pilot opinion (especially in the region of minimum acceptable flying qualities). The results to date indicate that the pilot ratings tended to become minimally acceptable when:

a. The primary control was in itself marginal, and

b. Use of the secondary control did not improve the response to the primary control

c. The sensitivity to turbulence approached that of an equivalent CTOL ($Z_u \doteq -2g/U_o$) and/or σ_θ was in a marginal region

SECTION VI

CONCLUSIONS

As was discussed in the introduction, this program was carried out in phases — the pre-flight simulation phase, the flight test and post-flight simulation phase, and an analysis of results phase. Each of these phases and the conclusions drawn during each phase are discussed in the body of this report. The conclusions are summarized below.

A. CONCLUSIONS FROM PRE-FLIGHT SIMULATION PHASE

- Major deficiencies in path control were found to be most apparent during short final and flare and landing. IFR glide slope tracking was not found to be critical for any of the configurations.

- Minimum acceptable pilot ratings correlated very well with closed-loop characteristics. Cases where the pilots were not able to equalize the effective controlled element to a K/s shape were rated as unacceptable. These configurations had a coupled attitude numerator and an essentially vertical thrust inclination angle so that $\omega_\theta >> 1/T_{h\theta}$.

- Flight-path/airspeed coupling was found to be undesirable by the pilots but not a dominant factor in the ratings (which were found to be more directly associated with ability to control flight path). Flight-path/airspeed coupling would, of course, be a limiting factor if it led to other problems such as regions of degraded path control or safety limits (such as stall).

- Increased turbulence levels (σ_{u_g} = 4.5 ft/sec) significantly degraded the pilot opinion for the final approach and landing task.

- The addition of a flight director tended to improve the pilot ratings and performance. It did not, however, allow the pilots to decouple the path and speed responses for aircraft with significant path/speed coupling. The most significant effect of the flight director was on the lateral line up at breakout, and this resulted in drastically improved performance. Some pilots noted that while their performance was significantly improved by the flight director, the work-load was also correspondingly increased. This was due to the intense concentration required to keep three needles centered (glide slope, localizer, and throttle directors) while still maintaining some awareness of the status information.

B. CONCLUSIONS FROM THE FLIGHT TEST AND POST-FLIGHT SIMULATION RESULTS

- Agreement between flight and simulator was quite good as long as the environmental, task, and procedural variables were kept nearly identical. The pilot ratings were found to be very sensitive to these effects.

- During the pre-flight simulation it was noted by many pilots that the turbulence model seemed to result in excessive flight path excursions which seemed unrealistically high and inconsistent with past (CTOL) experience. This was checked in flight by flying the Variable Stability NAVION with the simulator turbulence tape but retaining the basic NAVION dynamics. The evaluation pilot (who flies this airplane every day) described the landing task as typical of a day with 15-20 kt gusting to 25 kt wind and rated the basic NAVION a 4.5 in this situation. Hence, there is evidence that: (1) the simulated turbulence was not excessively large and (2) the simulator did not magnify the effect of turbulence.

- Considerable difficulty was encountered in establishing the environmental and procedural variables for the simulator landing because of the credibility problem with the visual display. In many cases the pilots underestimated the validity of the display and rated optimistically with the idea that they could do better with improved visual cues. Once into the flight program, it was found that the improved visual cues were of little value in improving the landing workload or performance and, in fact, served to illustrate how bad things really were. This result points up a requirement to subject the evaluation pilots to some limited flight experience (say, one configuration) to obtain the proper orientation with respect to the environmental variables in each new simulation program.

- Relaxation of constraints on the touchdown sink rate appeared to reduce the pilot workload and improved touchdown precison. This conclusion is based on a comparison of the Phase I and II post-flight simulations where the landing was aborted whenever sink rate exceeded a nominal value in the Phase I part of the simulation. There was some disagreement between the two pilots on this phase of the program as to whether removing the abort criterion resulted in a reduction in workload. Therefore, more extensive testing is required (more pilots) to validate this conclusion. As it stands now, however, it appears that minimum acceptable boundaries are dependent on the touchdown constraints (maximum allowable sink rate and runway length).

C. CONCLUSIONS FROM ANALYSIS PHASE

- Pilot opinion for flight path control on short final was degraded when:

  - The system lags (airframe plus engine) combined to reduce the achievable bandwidth (closed-loop path mode frequency, ω_θ'') to unacceptably low values.

  - The effective controlled element could not be equalized to a K/s response due to $1/T_{h\theta} << \omega_\theta$ and/or low path mode damping, ζ_θ.

- There was experimental evidence that the pilot's effective command structure in the flare was a linear decrease in sink rate with altitude, e.g., $\dot{H}_c = -(1/T_F)H + K$.

- The pilots commonly used two controls during landings, especially in turbulence. This was not deemed undesirable as long as one control could be considered as primary (usually attitude) and the other as a secondary (usually throttle in this experiment). Thus, the analysis of the landing task was based on the premise that to achieve an acceptable landing airplane, the primary control must be adequate in itself or the response to the primary control must be improved by use of a secondary control.

- All of the tested airplanes had a very large engine lag. This made it desirable for the pilots to make attitude primary for landing.

- The pilot ratings for the landing task tended to degrade to unacceptable when:

  - The primary control was in itself marginal, and

  - Use of the secondary control did not improve the response to the primary control, and

  - The sensitivity to turbulence approached that of a CTOL ($Z_u \doteq -2g/U_o$)

REFERENCES

1. Ashkenas, Irving L, and Samuel J. Craig, Multiloop Piloting Aspects of Longitudinal Approach Path Control, ICAS Paper No. 72-46, Sept. 1972.

2. Craig, Samuel J., Irving L. Ashkenas, and Robert K. Heffley, Pilot Background and Vehicle Parameters Governing Control Technique in STOL Approach Situations, FAA-RD-72-69, June 1972.

3. Craig, Samuel J., and Anthony Campbell, Analysis of VTOL Handling Qualities Requirements, Part I: Longitudinal Hover and Transition, AFFDL-TR-67-179, Oct. 1968; Samuel J. Craig, Anthony Campbell, and Richard H. Klein, Part II: Lateral-Directional Hover and Transition, AFFDL-TR-67-179, Part II, Feb. 1970.

4. Franklin, James A., and Robert C. Innis, "Flight-Path and Airspeed Control for the STOL Approach and Landing," STOL Technology, NASA SP-320, Oct. 1972, pp. 181-198.

5. Heffley, Robert K., and Robert L. Stapleford, A STOL Airworthiness Investigation Using a Simulation of an Augmentor Wing Transport, Vol. I: Summary of Results and Airworthiness Implications, NASA TM-X-62,395, FAA-RD-74-179-I, Mar. 1974; Heffley, Robert K., Robert L. Stapleford, Robert C. Rumold, and John M. Lehman, Vol. II: Simulation Data and Analysis, NASA TM-X-62,396, FAA-RD-74-179-II, Oct. 1974.

6. Stapleford, Robert L., Samuel J. Craig, and Jean A. Tennant, Measurement of Pilot Describing Functions in Single-Controller Multiloop Tasks, NASA CR-1238, Jan. 1969.

7. Stapleford, Robert L., Robert K. Heffley, and Robert C. Rumold, A STOL Airworthiness Investigation Using a Simulation of a Deflected Slipstream Transport, Vol. I: Summary of Results and Airworthiness Implications, NASA TM-X-62,392, FAA-RD-74-143-I, Oct. 1974; Stapleford, Robert L., Robert K. Heffley, John M. Lehman, and Wayne F. Jewell, Vol. II: Simulation Data and Analysis, NASA TM-X-62,393, FAA-RD-74-143-II, Oct. 1974; Heffley, Robert K., Wayne F. Jewell, Robert L. Stapleford, and Samuel J. Craig, Vol. III: Breguet 941S Simulation Model, NASA TM-X-62,394, FAA-RD-74-143-III, Oct. 1974.

8. Rumold, Robert C., Robert L. Stapleford, Robert K. Heffley, John M. Lehman, et al., A STOL Airworthiness Investigation Using Simulations of Representative STOL Aircraft, Systems Technology, Inc., TR-1047-2, Dec. 1974.

9. Heffley, Robert K., John M. Lehman, Robert C. Rumold, Robert L. Stapleford, et al., A Simulator Evaluation of Tentative STOL Airworthiness Criteria, Vol. I: Simulation Results and Analysis, Systems Technology, Inc., TR-1047-3-I, June 1975; Heffley, Robert K., John M. Lehman, Robert L. Stapleford, Barry C. Scott, and Charles S. Hynes, Vol. II: Background Information, Systems Technology, Inc., TR-1047-3-II, June 1975.

10. Hoh, Roger H., Richard H. Klein, and Walter A. Johnson, Design of a Flight Director/Configuration Management System for Piloted STOL Approaches, NASA CR-114688, Sept. 1973.

11. McRuer, D. T., and E. S. Krendel, Mathematical Models of Human Pilot Behavior, AGARDograph No. 188, Jan. 1974.

12. McRuer, Duane, Irving Ashkenas, and Dunstan Graham, Aircraft Dynamics and Automatic Control, Princeton Univ. Press, Princeton, N. J., 1973.

13. McRuer, Duane, "The Development of Pilot-in-the-Loop Analysis," J. of Aircraft, Vol. 10, No. 9, Sept. 1973, pp. 515-524."

14. McRuer, Duane, and David H. Weir, "Theory of Manual Vehicular Control," Ergonomics, Vol. 12, No. 4, July 1969, pp. 599-633.

15. McRuer, Duane, Dunstan Graham, Ezra Krendel, and William Reisener, Jr., Human Pilot Dynamics in Compensatory Systems — Theory, Models, and Experiments with Controlled Element and Forcing Function Variations, AFFDL-TR-65-15, July 1965.

APPENDIX A

PILOT RATINGS, COMMENTARY, AND BACKGROUND

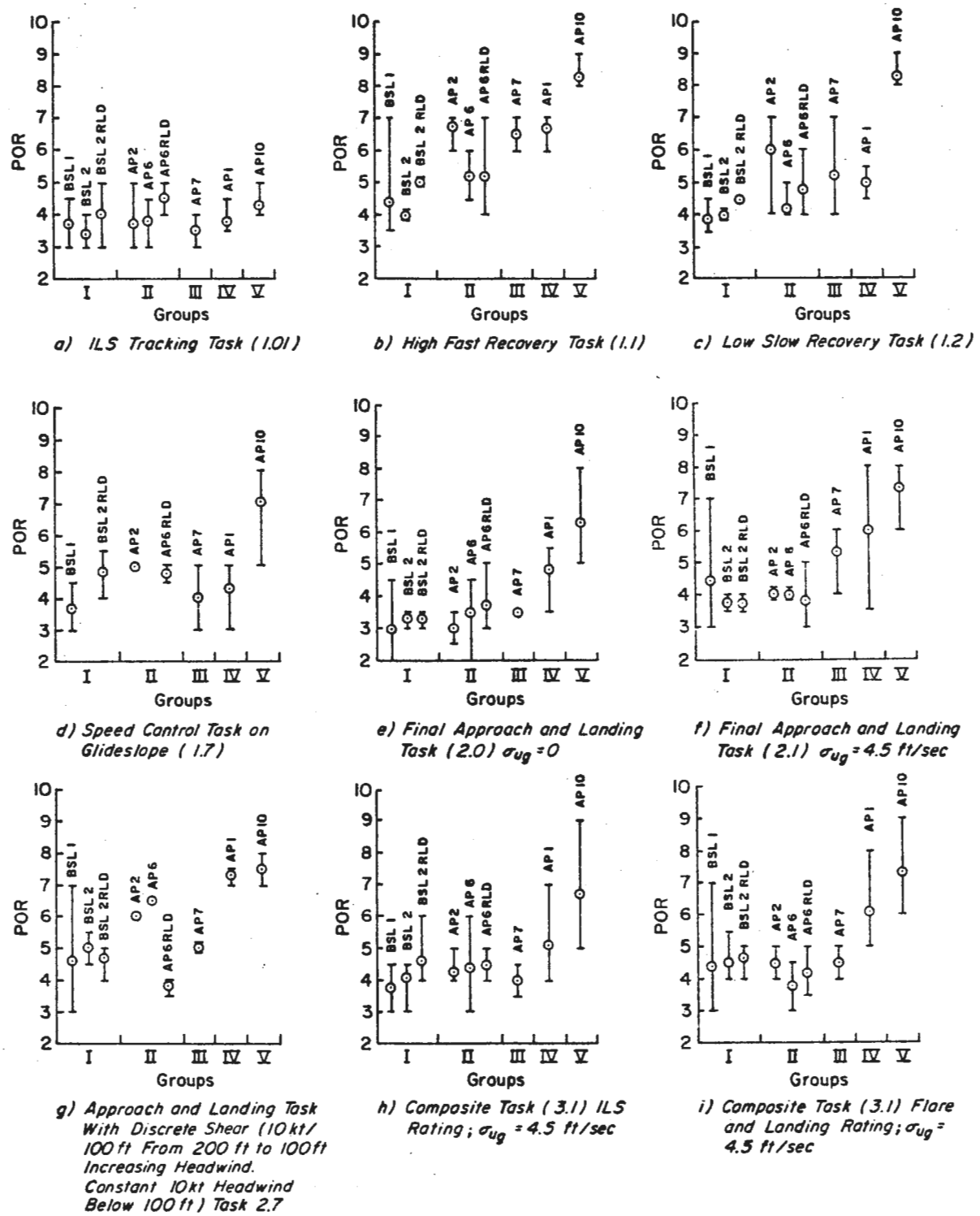

a) ILS Tracking Task (1.01)

b) High Fast Recovery Task (1.1)

c) Low Slow Recovery Task (1.2)

d) Speed Control Task on Glideslope (1.7)

e) Final Approach and Landing Task (2.0) $\sigma_{ug} = 0$

f) Final Approach and Landing Task (2.1) $\sigma_{ug} = 4.5$ ft/sec

g) Approach and Landing Task With Discrete Shear (10 kt/100 ft From 200 ft to 100 ft Increasing Headwind. Constant 10 kt Headwind Below 100 ft) Task 2.7

h) Composite Task (3.1) ILS Rating; $\sigma_{ug} = 4.5$ ft/sec

i) Composite Task (3.1) Flare and Landing Rating; $\sigma_{ug} = 4.5$ ft/sec

Figure A-1. Summary of Preflight Simulation Pilot Ratings

TABLE A-1

TASK CODE

1.01	ILS tracking (IFR) from 1500 ft to breakout at 300 ft — no landing — 4.5 ft/sec rms turbulence
1.1	High fast I.C. — 85 kt IAS and 350 ft above glide slope turbulence off
1.2	Low slow I.C. — 65 kt IAS and 350 ft below glide slope turbulence off
1.7	Turbulence off — change speed on glide slope ±10 kt
2.0	Landing without turbulence; I.C. = 200 ft; all VFR
2.1	Task 2.0 with σ_{u_g} = 4.5 ft/sec
2.4	Task 2.1 with 10 kt crosswind from left
2.7	Task 2.1 with discrete shear — zero wind at 200 ft to a 10 kt headwind at 100 ft (10 kt/100 ft)
3.0	Composite — intercept LOC — intercept glide slope — breakout at 300 ft — land — turbulence off
3.1	Task 3.0 with σ_{u_g} = 4.5 ft/sec
3.2	Task 3.1 with a steady 10 kt headwind
3.3	Task 3.1 with a steady 10 kt tailwind

TABLE A-2

COOPER HARPER RATINGS FOR FLARE AND LANDING FLIGHT PROGRAM

TURBULENCE AND SAS	CONFIGURATION BSL1		CONFIGURATION AP1	
	PILOT 1	PILOT 3	PILOT 1	PILOT 3
σ_{u_g} = 0 ft/sec				
High Gain SAS	4-1/2	4	6-1/2	5-1/2
Low Gain SAS	5	5	7	6-1/2
σ_{u_g} = 2.25 ft/sec				
High Gain SAS	5	5	Did not fly enough in turbulence to rate	6-1/2
Low Gain SAS	6-1/2	6		9
σ_{u_g} = 4.5 ft/sec				
High Gain SAS	7	6-1/2 to 10		10
Low Gain SAS	8	7 to 10		10

TABLE A-3

COOPER HARPER RATINGS FOR FINAL APPROACH FLIGHT PROGRAM

TURBULENCE LEVEL σ_{u_g} ft/sec	CONFIGURATION BSL1		CONFIGURATION AP1	
	PILOT 1	PILOT 3	PILOT 1	PILOT 3
0	4	4	5-1/2	5
2.25	5	5-1/2	—	6-1/2
4.5	7	8-1/2 to 10*	—	9 to 10

Ratings did not vary with high and low gain SAS.

*This rating improves to a 6 with increased throttle control power (throttle was limited to ±20% about trim on Navion).

TABLE A-4

COOPER HARPER RATINGS FOR FLARE AND LANDING
POST FLIGHT SIMULATION-CONFIGURATION BSL1

TURBULENCE LEVEL σ_{u_g} ft/sec	PHASE	FLARE AND LANDING		FINAL APPROACH	
		PILOT 1	PILOT 3	PILOT 1	PILOT 3
0	I	4-1/2	4	3	4
2.25	↓	5-1/2	4 to 4-1/2	4	5
4.5	↓	7	5-1/2 to 10	5	7
0	II	3	4	3	4
2.25	↓	3-1/2	4-1/2 to 5	4	5
4.5	↓	5	6 to 10	5	7

The pilot commentaries obtained from the preflight simulation have been edited to put them in a usable form and are presented on the following pages.

CONFIGURATION BSL1

This configuration was flown by Pilots 1, 2, 6, 7, 8, and 9.

PILOT 1

Task 1.01

Glide slope tracking with this configuration is very straightforward using essentially constant attitude. Didn't notice any coupling effects that would cause any real problem. Speed control is straightforward.

Task 1.1

Considerable amount of juggling between pitch attitude to control airspeed and throttle to control altitude and to try to get nailed down on 75 kt on the glide slope. At this point you are down real close to the runway so the glide slope is highly sensitive.

Task 1.2

Used full power for recovery. The workload is fairly high but it appears to be more of a task problem than an airplane-oriented problem. The high fast and low slow initial conditions are quite large considering the nearness to touchdown.

Task 2.0

Seems like it would be impossible to get a touchdown with zero sink rate in this airplane using pitch attitude only. The sink rate response to an attitude change is quite low. Am using a combination of power and attitude to make landings. On the landings where power is primary, the timing is quite critical. If you get the power in too soon, you tend to float; whereas bringing the power in too late results in a fairly hard touchdown.

Task 2.1

The major pilot compensation appears to be involved in knowing when to use the throttle and how much throttle to add.

Task 3.0

This airplane does not require much compensation for the no turbulence case.

Task 3.1

No difference between this composite task and turbulence and the individual subtasks.

PILOT 2

Task 1.01

Vertical speed response to normal throttle motions is very low with a lot of lag. Basic technique was backside with pitch inputs to get an initial response out of it. Tried frontside with zero results.

Task 1.1

Using either frontside or backside technique, the aircraft has a very limited descent capability. Aircraft performance in this task is not a function of pilot compensation. Overall rating is a 7.

Task 1.2

Response to power was considerably better than I anticipated.

Task 2.0 and 2.1

The poor vertical speed response to thrust aggravates the problem and makes it easy to overcontrol. Put on too much to correct for a low condition and then don't get it off in time, and then you're high and in close. There doesn't seem to be any adequate way to compensate in the flare unless you generate some type of throttle pitch maneuver. Controlling sink rate with power is difficult in turbulence.

Task 3.0

Generally the same commentary as the subtasks.

Task 3.1

Generally the same comment as for the subtasks.

PILOT 6

Task 1.01

No problem tracking glide slope. Turbulence increases the workload a little.

Task 2.0 and 2.1

Flare and landing are quite difficult when using pitch attitude only to flare. Resulted in hard sink rates and considerable touchdown dispersions. Also, high pitch attitude resulted in loss of vision of runway. When using technique of increasing attitude slightly and increasing thrust to arrest sink rate, landing and flare performance was greatly improved. The effect of turbulence was to increase the workload only slightly. Wind shear near touchdown can cause dispersions in sink rate and touchdown distance. I have a tendency to pull off the power when going long which results in the airplane dropping and landing hard.

Task 3.0 and 3.1

Same comments as for individual subtasks.

PILOT 7

Task 2.0

Sink rate to power response is very sluggish but has adequate authority. Require very large attitude to flare. The rating is a 4-1/2 because I have to use power. I should be able to flare with attitude alone.

Task 2.1

Requires power to land in turbulence.

Task 1.01 with engine time constant = 0.5

No noticeable difference in sink rate to throttle response. However, glide slope tracking seems easier for some reason. Back-to-back comparison with engine lag of 0.5 sec and 1.5 sec shows no difference in this task.

Task 2.1 with $T_e = 0.5$

No noticeable effect due to engine lag.

Task 2.7 with $T_e = 0.5$

Feel more comfortable with faster engine. Pilot rating may improve from 5 to 4-1/2. I am using throttle and attitude in the flare. Decreasing the engine time constant to 0.2 still shows no difference.

PILOT 8

Task 1.1

Airspeed response to attitude seems sluggish. Hard to get stabilized on glide slope and airspeed.

Task 1.2

Same comment.

Task 1.7

Same comment.

Task 2.0

Attitude flare is not a problem. Flaring with power is a problem because the power response seems low.

Task 2.1

Tried both power and attitude flares. I like power flares better in turbulence.

Task 3.0

Am using conventional backside control, that is, airspeed to attitude and flight path angle to throttle.

Task 3.1

Hardest job is glide slope tracking because of the lag in flight path angle to throttle. Airspeed to attitude is sluggish.

PILOT 9

Task 1.01

I have the impression of a longer throttle response than on most aircraft. My technique is to command glide slope with IVSI because of long engine lag. I know this will always bring me back to glide slope.

Task 1.1

Speed is not a problem but gross glide slope error is difficult to make with this throttle. Have a tendency to overcorrect. Part of difficulty is tradeoff between speed and altitude initially.

Task 1.2

Easier to handle than Task 1.1. I am not as reluctant to add power as I am to reduce power. I am doing things in the right direction for safety.

Task 2.1

Am flying glide slope to get into window for flare.

Task 2.7

Adequate performance not obtainable with maximum pilot compensation. This is based on my inability to know what to do with power.

CONFIGURATION BSL2

PILOT 1

Task 1.01

Glide slope tracking is straightforward.

Task 1.1 and 1.2

The off-nominal condition seems very severe. Considering this very drastic off-nominal condition, the airplane behaves very well.

Task 2.0

No problem getting into the touchdown zone. The airplane seems to have touchded down naturally at about 250-300 ft with this glide slope location.

Task 2.1

This configuration seems very sensitive to flare height. If I flare just a little too soon, I tend to land down in the 600 ft region; and if I flare at the correct height and flare too quickly, I also get down to the 600 ft region. So it seems to be very sensitive to the correct flare height, and because of the sensitivity of the airplane it degrades to a pilot rating of 4. Of course, the turbulence makes it more difficult to flare in a precise way. Adding a crosswind to the turbulence on BSL2 doesn't really change the task very much. The best technique seems to be to slightly undershoot the glide slope maybe half a dot and let the airplane float down and settle into the touchdown zone. Doing this you can get consistent touchdown sink rates and position on the runway. If you flare too soon or too rapidly and the airplane starts floating, and the touchdown is generally quite hard. Primary control for flaring the airplane is pitch attitude, using throttle only to counteract large gusts.

PILOT 2

Task 1.01

The short-term effect of attitude changes is greater in influencing vertical speed than airspeed. Basic technique was backside, but modified by extensive use of attitude for quick response, using column as a DLC for short-term response. Throttles for long-term vertical speed control. It seems to me to be unreasonable that idle power and a pitch attitude of −10 deg doesn't bring the plane any faster than simulated. Also, airspeed acceleration appears excessive.

PILOT 6

Task 2.0

Preferred flare technique is to start flare at 35 ft and leave power alone.

Task 2.1

Tend to touch down longer in turbulence. Had to use full power to arrest sink rate on one run.

PILOT 7

Task 1.1

I think the main comment is that it is a very extreme offset and to make a comfortable size correction you really don't have time to get back on in, settle down. My basic technique is to get the speed back under control and then worry about flight path. I like to do this because once I get the speed under control then I know what the power-to-flight-path angle relationship is, giving me one less thing to do when I intercept the glide slope. My ratings for high fast and low slow are the same as for straight glide slope tracking in turbulence. The situation is extreme, but the airplane does not change.

Task 1.2

The low slow is no different from the straight glide slope tracking. I feel completely comfortable all the time.

Task 2.0

Initially I had some problems with attitude dynamics — a tendency to PIO a little bit, which went away after three or four touchdowns. Looks like with the geometry situation here it is fairly easy to make soft touchdowns with attitude alone.

Task 2.1

The workload increases quite a bit with turbulence. I am having quite a bit of problems with the turbulence levels, particularly during the final glide slope tracking and the flare. I have an additional comment on this flare and landing with turbulence. I gave it a 6 here, but in real-life situations that would come up a couple pilot ratings.

PILOT 8

Task 2.0

Flares with attitude are touchy to get into the touchdown zone. Flares with power are more precise, allowing me to get consistently soft touchdowns.

Task 2.1

Flares with attitude tend to float. Touchdown is hard after a float. The best technique is to use a little pitch after coming in with power. It is very difficult to recover if I get high and fast in close.

Task 3.0 and 3.1

Comments are generally the same as for the subtasks.

PILOT 9

Task 1.01

...and controlling sink rate with power and airspeed with pitch attitude.

Task 1.1

My primary problem is sink rate to power. I need to get calibrated.

Task 1.2

No real special problem.

Task 2.0

Best flare technique is pitch attitude. Power flares are not consistent. Much better control over touchdown point with pitch attitude.

Task 2.1

It seems like we need a power command. I can't do it precisely by eye.

Task 2.7

Acceptable, but harder in general. Has tendency to float because of last minute power changes. This configuration has good control of sink rate with attitude and is not critical on attitude except perhaps a tendency to float.

Task 3.1

The landing was contaminated by trying to hit the window at 300 ft.

CONFIGURATION BSL2 RLD

This configuration was flown by pilots, 1, 7, and 9.

PILOT 1

Task 1.01

Airspeed response to pitch attitude seems adequate. Sink rate to throttle response is a little sluggish and bearly adequate.

Task 1.1

The task is the major problem in that there is not enough time to get stabilized after capturing glide slope.

Task 1.2

Same comment as on Task 1.1. The aircraft itself is a 3 for both tasks where the ratings apply more to the task than to the airplane itself.

Task 2.0

Requires too much pitch attitude change for pure attitude flare. Best technique is to use power to break initial sink rate and attitude to fine tune it.

Task 2.1

Requires moderate compensation on throttles to set up for flare.

Task 2.7

Tend to land long. Consistently get into a low power, high sink rate condition and overcorrect with attitude and throttle near touchdown.

Task 3.1

Degradation with turbulence is due to higher workload on glide slope. Requires lead on sink rate to power.

PILOT 7

Pilot 7 flew this configuration at 65 kt and therefore quite far on the backside.

Task 1.01

Low initial sink rate to throttle response. Throttles seemed insensitive. Good airspeed control.

Task 1.01 (doubled throttle sensitivity)

This throttle sensitivity is a lot better. Throttle sensitivity was the primary deficiency. Now low I_{α} is a problem. (Pilot noted this later during landing evaluations.)

Task 1.1

Airspeed control easy with favorable flight path to airspeed coupling. Some problem with sink rate to throttle response. Seems very sluggish and has a major effect on my rating.

Task 1.7

This aircraft is really on the backside. Takes a lot of power.

Task 2.0

This configuration has a very low L_α.

Task 2.1

The combination technique works pretty good. That is, I add power and fine tune the touchdown with pitch attitude.

Task 2.7

Use a step and power. There is sufficient L_α to complete the flare.

PILOT 9

Task 1.01

Sluggish sink rate to throttle response. No apparent coupling between airspeed and throttle.

Task 2.0

Flaring with attitude only.

Task 2.1

Good landings if I am set up at flare point. Hard landings if not set up. Poor sink rate to throttle response is responsible for problems in getting set up. No real problems with this configuration.

Task 2.7

Used a technique of watching IVSI as a cue for large shears. Flying IVSI to throttle even in close. Task is very difficult if not in window at flare initiation. Sink rate to throttle lag appears large.

Task 3.1

Using attitude to airspeed and sink rate to throttle exclusively. My glide slope rating is a 6 on the overall task, because of the sluggish throttle respone which is more apparent during glide slope intercept and the ensuing capture. Flare rating is a 4-1/2 to a 5 because of a sensitivity of the outcome to not hitting the window at breakout.

CONFIGURATION AP1

This configuration was flown by Pilots 1, 5, 7, 8, and 9.

PILOT 1

Task 1.01

The turbulence level seems very low and glide slope tracking is not a problem. This configuration has very low C_{L_α}, but this is not a problem because altitude response to power is adequate.

Task 1.1

The coordination required between power and pitch attitude to capture and maintain the glide slope is very difficult.

Task 1.2

The low slow recovery is not as bad as the high fast; however, the pitch attitude and throttle required to recover seem excessively large.

Task 1.7

A very large pitch attitude is required to go from 75 to 85 kt. The speed response is extremely slow in going from 85 to 75 kt, requiring me to overdrive attitude to get the required speed. This results in my going off glide path. The main problem here is maintaining glide slope while using large pitch attitudes to change speed. The IVSI response to throttle seems very sluggish. This is the primary problem in this task.

Task 2.0

This configuration seems to be very unforgiving to initial errors in flare height. This is at least moderately objectionable and perhaps worse.

Task 2.1

The primary deficiency is a very sluggish sink rate to throttle response. The major problem with this configuration is the inability to recover from off-nominal vertical position in time to set up for landing on the short runways. If I get high or low at the initiation of flare, the sink rate at touchdown is usually hard or the landing is long. The sink rate response to pitch attitude for this configuration seems very low. The throttle is not of much help because of the very sluggish sink rate to power response. Unless everything is perfect at the point of flare initiation, the chances of a good touchdown are very low with this configuration.

Task 3.0 and 3.1

Commentary generally the same as for the subtasks.

PILOT 5

Task 2.1

The pilot rating is a 5 up to the threshold and an 8 for the flare and landing.

Task 3.0

Tracking was easy once we were on airspeed and glide slope and localizer.

Task 3.1

Pilot rating is a 3 down to breakout and then a 7 on short final. The control harmony seems good between elevator and ailerons but poor for throttle.

PILOT 7

Task 1.01

My technique is to fly constant attitude and let airspeed vary. If the airspeed variations are not too big and we don't end up getting too close to the margins, then there is no problem. The characteristics of this airplane are similar to the augmentor wing. I really don't think they're quite as bad as on the augmentor wing in the adverse coupling on speed and flight path, and on the augmentor wing we have adopted at least one technique of flying the airplane where you do fly essentially at constant attitude and let airspeed vary back and forth.

Task 1.1

The downside capability of this aircraft is inadequate to do the task. Even with the other configurations, if you recall, I felt that this was an unrealistic task. A guy would go around rather than attempt this kind of correction. The workload is really not all that high. All you do is just pull the power off and sit there and wait for it to come down. I do feel the downside capability of this airplane is adequate. When you pull the power back to idle you can get on the order of 1200 ft/min rate of sink, which I think is adequate. I think on this kind of airplane with adverse flight-path/speed coupling a guy could get more comfortable with it if he flew an airplane that had that characteristic all the time.

Task 1.7

This is definitely a little bit of a tricky task in this airplane, because of the adverse speed and flight path coupling. I seem to have a little more trouble slowing down than I do speeding up. You almost have to know what the nominal attitude for the new speed should be.

Task 2.0

Smooth air flares with attitude rotation only are pretty marginal. You kind of have to use everything you've got just to barely make it. Flares with power and smooth air are an acceptable technique, but not necessarily acceptable for normal operation.

Task 2.1

The workload just gets too high trying to get the power set for your flare, particularly with some of these last minute flight path corrections where the power can be going up and down. You really have to check the power very closely to make sure that as you're going into the flare you have enough power on to flare the airplane. It almost requires a visual check of the rpm indicators, which is at a very inopportune time. Therefore, I would say it is a 7 or worse.

Task 3.1

We just completed a series of runs where you intercept and track and flare and land. I can't see any differences brought up by that task.

PILOT 8

Task 1.01

This machine is very sluggish in response to power for flight path control. It looks like it's quite sensitive to pitch or speed. It's kind of a funny situation where adding power you have to push over the nose to hold your speed up, and vice versa for reducing power. So it can be not too nice an airplane to fly. You have the feeling any displacement would be hard to handle, so I flew the glide slope very tight and it was no problem. Addition of turbulence increased the workload only slightly.

Task 1.1

The biggest task here is this gross attitude change from −11 deg up to 20 deg nose up.

Task 1.2

I just applied maximum power and starting undoing that horrible pitch attitude to where it's nose down and getting speed back. The task required between considerable and extensive compensation.

Task 2.0

The landings in this airplane are bad, bad, bad.

Task 2.1

I did not try power flares until I combined with turbulence, and it seems to me that power flare worked out a little bit better in turbulence than the conventional flare. But, any of them are real dicey to get a good sink rate and a good aim point on the runway. When you consider control of sink rate as part of the controllability, controllability is in question with this. So it's about a 7-1/2 pilot rating.

PILOT 9

Task 1.01

The compensation required for glide slope tracking may be described as moderate to minimal.

Task 1.1

The high fast recovery is very bad. With power off, the aircraft does not sink and I can't get back on glide slope. The attitude goes to extremes.

Task 1.2

Better control. Reasonable performance, but considerable compensation.

Task 1.7

The attitude required to change speed is too large.

Task 2.0

My rating was 5, mainly because of inconsistencies in performance and touchdown sink rate and distance.

Task 2.1

Primary difficulty was the considerable lag in the throttle, and, if you're effecting a change on glide path, the resulting change in sink rate late in the approach will give you real problems. The aircraft's response to pitch seems much reduced here in the flare, so that you've got to be pretty much right on sink rate with the power setting. That is what has caused me the difficulty in the pilot rating. There is a considerable lag between change in throttle and airplane response to that change. I've reconsidered the rating of 7 that I gave on these last runs, and I want to slip those to 8 because considerable pilot compensation is required for control in the sense that sink rate at touchdown is fairly difficult to control.

Task 3.1

Speed control was not too difficult providing you were willing to accept the 3 or 4 kt that turbulence brought into it. You could get to a trim attitude that would fairly well hold a speed. Again, aircraft response to throttle inputs was still the major deficiency. There is a considerable lag between the time you decide to make a flight path change and the time the change actually begins. This tends to make you overshoot the condition you were looking for, and so you're constantly hunting with the throttle all the way through the approach.

CONFIGURATION AP2

Configuration AP2 was flown by Pilots 1, 2, 6, and 7.

PILOT 1

Task 1.01

Sink rate response to throttle seems quite good. This task does not require much compensation. The indicated airspeed stayed at 75 kt with little or no corrections in attitude.

Task 1.1

Could not get adequate performance on indicated airspeed due to large speed/throttle coupling near idle power. Glide slope intercept and tracking was okay.

Task 1.2

Coupling on speed to throttle was not nearly as large at high power settings as it was at low power settings. I was able to get target speed and on glide slope without any real problems. Used a cross-feed of throttle to column for large power changes and used airspeed to attitude and sink rate to throttle for glide slope tracking.

Task 1.7

Airspeed response to attitude seemed sluggish. Adverse coupling precludes precision control of airspeed, and airspeed response to throttle seems to swamp out the airspeed response to attitude. This is especially true if I get high on the glide slope due to the increased coupling at low power settings.

Task 2.0

This configuration seems quite easy to land without turbulence. The sink rate response to attitude is good.

Task 2.1

Am having some problems setting up the proper sink rate with power for flare initiation. The sink rate response to power seems adequate for glide slope tracking, but is too sluggish for the precision control required as I come up to my flare point near touchdown.

Task 3.1

For the IFR portion of the approach, glide slope tracking in itself is not a problem. Control over indicated airspeed is marginal, because of the very sluggish speed to attitude response and the adverse coupling between speed and power. My pilot rating of 4 reflects the fact that the speed variations do not interfere with my ability to do the task. The primary problem in landing is setting up for the flare with power in the presence of these fairly large gust disturbances.

PILOT 2

Task 1.01

Control over glide slope and localizer is not a problem. Pilot rating for this task alone is 2. The unpleasant deficiency for this configuration in turbulence is speed control. My overall rating of glide slope tracking then with speed control is a 3. Turbulence is not a big thing in this task.

Task 1.1

Airspeed control unbelievable for off-nominal conditions. Throttle range required excessive full throttle and idle. My airspeed was too high to land in an 1800 ft strip after recovery from the high fast condition. Glide slope control was okay.

Task 1.2

Airspeed control again was the major problem. Never had the chance to steady out before landing.

Task 2.0

Flare using column only from about 100 ft AGL with nominal power set. I tended to come into the flare on-speed to slightly fast.

Task 2.1

Recovery from turbulence effects coming into the flare was difficult. It is easy to overcontrol with the throttles. I am using sink rate to attitude primarily for the actual flare. Hard landings result when I use throttles to flare.

Task 3.1

The airspeed/flight-path coupling is very bothersome. Working on glide slope control, keeping tabs on indicated airspeed. Since my ability to track the glide slope does not appear to be affected by the poor airspeed control, I can live with it. Technique for glide slope tracking is primarily backside, that is, sink rate to throttle and airspeed to attitude with some attitude to sink rate. Airspeed control is by far the biggest problem. Extreme variations in airspeed combine with high coupling and C_{L_α} response to make it a pretty tricky configuration if departure from nominal conditions is too great.

PILOT 6

Task 1.01

Flight path response to throttle is fine. Cannot get desired airspeed performance.

Task 1.1

Pitch attitude went up to 10 deg and the aircraft never slowed down. My rating of 6 is based on speed problems.

Task 1.2

My pilot rating of 7 is based on a decrease of speed with power addition. The speed went below 60 kt at one point.

Task 2.0

Flaring with pitch attitude only works out just fine.

Task 2.1

I get the best results flaring with attitude alone. Flaring with attitude and power results in a tendency to float and makes the aircraft seem very sensitive to changes in pitch attitude.

Task 2.7

These wind shears require the use of throttles to arrest the sink rate. This results in overcontrolling and floating. Definitely cannot use power in an effective way to help flare this configuration.

Task 3.0

Adverse coupling results in my always having to change pitch attitude.

(Note: This pilot is a Boeing test pilot and required considerable amount of time to adjust his technique to backside control. During his later evaluations of configurations with large airspeed/flight-path coupling, he tended to ignore airspeed variations, holding constant attitude.)

PILOT 7

(Note: Pilot 7 flew this configuration with the engine time constant set to 0.5 sec due to a miss-set constant in the computer program when changing configurations.)

Task 1.01

This configuration looks like AP10. Long as I don't worry about speed it's okay. Initial sink rate response to throttle is good. The long-term sink rate to throttle washes out. The pilot rating is a 4-1/2 and would be a 4 with perfect airspeed control.

Task 1.1

Airspeed excursions are large but I don't care about airspeed in STOL because it is not a measure of lift margin.

Task 1.2

The low slow recovery is not as critical as the high fast recovery.

Task 2.0

This configuration has a lot of L_α.

Task 2.1

Turbulence is not a problem, and getting set up for the flare is also not a problem with this configuration.

Task 2.7

Flare and touchdown are pretty easy. Have to have power set properly at flare initiation.

CONFIGURATION AP6

This configuration was flown by Pilots 1, 2, 6, and 7.

PILOT 1

Task 1.01

Glide slope tracking is not a problem. Precise control of airspeed is very difficult and had problems in attempting to lower the airspeed from 85 kt to 75 kt. Primary task of glide slope tracking is quite straightforward and variations of speed do not seem to affect this task.

Task 1.1

Very high pilot workload. Have to constantly keep in mind that increase in power decreases the speed. I am assuming that the task here is to get both glide slope and airspeed under control.

Task 1.2

This task is easier than 1.1, because it is easier to increase airspeed than to decrease airspeed.

Task 2.0

Sink rate response to attitude is very good. There seems to be a tradeoff between touchdown sink rate and position. Must not flare too late or hit very hard.

Task 2.1

Seem to be getting some very large horizontal wind shears (u gusts got up to 12 ft/sec in 2 sec and stayed at 12 ft/sec for 6 sec just before touchdown). This configuration is a 4 to a 4-1/2 with low to moderate gusts. A severe wind shear such as I got on one run would have to be rated as a 7. However, I do not feel that it is fair to rate this configuration as low as a 7 for a very low probability wind shear case. In actual practice, this would be a go-around. If a go-around was required for several approaches in a row, then the rating on this configuration would have to be lowered to a 7 in this level of turbulence. However, the large shear that I encountered seems to be a low probability case. Therefore, my rating of this airplane in turbulence is a 4-1/2 and a 7 with the large shear.

Task 3.2 (Task 3.1 with headwind)

The higher power required to track the glide slope in this headwind results in low airspeed. It is difficult to hold the glide slope and correct the airspeed to 75 kt. This problem is also true if you get low on the glide slope and need to correct back. My pilot rating, however, is unchanged from pure glide slope tracking, because the airspeed excursions do not seem to affect my capability for tracking the glide slope. My technique is to simply note the airspeed variations but to ignore them in terms of control inputs.

PILOT 6

Task 1.01

Must use backside technique. Throttle controls sink rate and has an adverse affect on airspeed. Airspeed must be controlled by pitch attitude but is very slow to respond. The effect of turbulence on the glide slope tracking is minimal, more perhaps of one Cooper-Harper rating degradation. The throttle is very effective to control sink rate. The only problem with this configuration was to maintain airspeed. Airspeed is very hard to manage and responds very slowly to corrective action. Airspeed control is unacceptable for airline use.

Task 2.0

Landings with this configuration were very conventional. No major problems as long as throttle was not used in the flare.

Task 2.1

Turbulence increased the pilot workload only slightly. My flare technique was conventional. Began pitch increase at 50 ft and held attitude until touchdown. Since throttle controls sink rate, care must be made so as not to add or decrease thrust or aircraft floats or drops, respectively. There were no problems in the flare and landing if thrust was not modulated excessively.

Task 3.1

All subtasks and components of this composite task were primarily downgraded due to lack of airspeed control. The airplane, in general, flies quite well except for airspeed control.

PILOT 7

Task 1.01

My main objection to the airplane is the adverse coupling between speed and flight path. It's not real serious but it's predominant enough to be at least slightly objectionable. The amount of adverse coupling is not enough to be really bothersome; if you just let the airspeed vary, it works out pretty good.

Task 1.1

As with the other configurations, I think the task is a little bit extreme. Not realistic. It would be a go-around situation.

Task 1.2

The increase in workload is negligible due to the low-and-slow, and I really don't feel too uncomfortable with that. It's still a pretty good offset, but at least you don't have to content with the high sink rate and low altitude.

Task 2.1

As far as pilot ratings go and our workload, I think that smooth air is fairly reasonable and then it takes a big jump with turbulence.

Task 2.7

Crosswinds result in no additional workload increase. The shears we looked at are bordering on unacceptable with the situation we have. A couple of times here with turbulence and/or shears I've overflared the airplane to break a high rate of sink. Once you flair too high on this airplane with this nominal pitch attitude, you lose sight of the runway and then you pretty much lose it.

CONFIGURATION AP6 RLD

This task was flown by Pilots 1, 7, and 9.

PILOT 1

Task 1.01 (stall speed = 65 kt)

Adverse speed throttle coupling and low stall margin combines to make a very dangerous situation. Got low on glide slope, added power and stalled. Had to punch out to avert a crash. Pilot rating is 9. Large pitch attitudes are required to keep the indicated airspeed above stall with increased power.

Task 1.01 (stall speed = 65 kt, $C_{L_{max}}$ increased 10%)

A 5 kt reduction in stall speed makes a large difference in this aircraft. It requires a large attitude deviation to get the speed to decrease from 65 kt to 60 kt, and therefore the stall protection is adequate in this aircraft.

Task 1.1

No control over airspeed with attitude and reduced power. Good sink rate to throttle authority but a bit sluggish. Adequate performance not attainable in speed (175, get 100).

Task 1.2

Easier to hold indicated airspeed at 75 kt than it was Task 1.1. Seems like airspeed coupling to throttle is more pronounced at low power than at high power. Major problem was extremely high workload and airspeed to attitude and sink rate to throttle due to the airspeed throttle coupling.

Task 1.7

Very sluggish airspeed to attitude response aggravated by airspeed to throttle effects. Control over indicated airspeed is barely adequate and with moderate compensation.

Task 2.1

Good sink rate response with attitude flares. Lands like a conventional airplane.

Task 2.7

Can get desired performance in the presence of shears. Moderate compensation of sink rate control with power is required to set up the flare point. The sink rate response to attitude is sufficient to account for problems in setting up for the flare with power.

PILOT 7

Task 1.0

Used this task to try stalls in this configuration. Unable to produce a stall with power off due to adverse airspeed power coupling. Impossible to get low speeds with low power settings. Power on stall is a mush.

Task 1.01

Adverse coupling seems large. Pilot rating is a 4-1/2 because glide slope tracking is adequate.

Task 1.1

I don't worry about indicated airspeed.

Task 1.2

Initial response to throttle too high and then washes out.

Task 1.7

Using airspeed to throttle and sink rate to attitude. This aircraft has a better L_α than Airplane 10, and therefore this technique works better.

Task 2.0

Sink rate response to attitude and sink rate response to throttle are good. Poor visual cues keep me from consistently landing in the touchdown zone. Have a tendency to PIO on attitude at touchdown resulting in a high workload.

Task 2.1 and 2.7

Same comments as for Task 2.0.

Task 3.1

Large I_α allows me to control sink rate at glide slope intercept and eliminate ballooning. Still having PIO problems on landing.

PILOT 9

Task 1.0

Do two stalls for familiarization. No problems.

Task 1.01

I don't like reverse speed path coupling. From a certification standpoint, it is unacceptable (a 7). However, it is a four on the Cooper Harper rating scale since the task is to track the glide slope, and the speed excursions do not seem to affect my ability to track.

Task 1.1

Moderate compensation required to recapture glide slope. My technique is to ignore indicated airspeed for this task.

Task 1.2

Basic technique is airspeed to attitude and sink rate to power.

Task 1.7

Quite a juggling act between attitude and power since both affect speed. It takes a long time to find the correct attitude and power.

Task 2.0

All my landings were soft and short. Sink rate response to attitude is good.

Task 2.1

Tending to use combination power and attitude and turbulence. The requirement for power costs one-half of a rating point. As before, the flare technique is to bring in a small amount of power and fine tune with pitch attitude.

Task 2.7

Good sink rate to power response. Easy to cope with wind shears. Use very small power changes.

CONFIGURATION AP7

Configuration AP7 was flown by Pilots 1, 7, and 9. This configuration was flown only during the back to back comparisons between the FSAA simulator and the S-16 simulator. The following comments pertain to the S-16 simulator evaluations.

PILOT 1

Task 1.01

This configuration seems to have reasonably good sink rate to power and airspeed to attitude response.

Task 1.1

Very limited down capability with power. Unable to get back on glide slope and reduce speed before breakout.

Task 1.2

No problem going up, just coming down.

Task 2.0

This configuration seems to have good L_α and is reasonably easy to land with attitude.

Task 2.1

The addition of turbulence affects this configuration considerably. Having considerable problems getting reasonable performance and have evolved a technique of using throttle to flair and fine tuning the touchdown with pitch attitude. Must be very careful not to overcontrol with throttle. Easy to overcontrol with throttle because of the sluggish sink rate to throttle response.

Task 2.7

Easy to overcontrol with throttle with large shear. Tend to float. Can do ok but it requires moderate to considerable compensation. This task would be much easier if the runway was longer.

Task 3.1

Not able to get desired performance consistently on landing. The more I fly this configuration the less I like it. Sink rate to attitude response is poor.

PILOT 9

Task 1.01

This configuration is a little slow on down sink rate to throttle response. Slight adverse speed to throttle coupling.

Task 1.7

Hunt on attitude and speed and flight path. Seems to be slower than normal. Tend to overshoot with power due to lag especially on down.

Task 2.0

Requires just a little too much attitude to flair. Would be a 3 if the sink rate to attitude was better. Power flares okay but I feel some luck is involved here. I rate the attitude flares a 3-1/2 and the power flares at 4-1/2.

Task 2.1

Am using large power changes because of sluggish sink rate to throttle response. My technique to flare is primarily attitude using power when required.

CONFIGURATION AP10

PILOT 1

Task 1.01

Sluggish airspeed to attitude response but this does not seem to effect the glide slope tracking. Sensitive sink rate to throttle but response is slow. Considerable compensation required to handle poor speed control and sensitive throttle. Pilot rating would be much worse if speed control were a dominant part of the task. Pilot rating is a 5 and would be a 4-1/2 for glide slope tracking only. Reducing the engine time constant to 0.5 results in very good sink rate to throttle response. Glide slope control is precise. Pilot rating is 3-1/2 for glide slope control. Decreasing the engine time constant further to 0.2 results in still better sink rate to throttle response. While this further improved response is nice, I'm not able to use it, and therefore the pilot rating for glide slope tracking remains the same at 3-1/2. Engine time constant of 0.5 is good enough.

Task 1.1 (engine time constant back to 1.5)

Very high sensitivity on magnitude of sink rate to throttle. Airspeed to attitude response is terrible. Airspeed to throttle coupling plus poor airspeed to attitude make task nearly impossible. At one point I got to 10 deg of pitch attitude and the airspeed was still 95 kt. I am hesitant to pull more power because the indicated airspeed will increase even further. My pilot rating of 8 reflects a loss of control over airspeed. It should be noted that this task involves control of airspeed and glide slope tracking, and that is reflected in the rating.

Task 1.2

Better than the high-fast recovery but workload still very high. I am able to get adequate performance on capture, but it is difficult to stay on glide slope and speed after capture. Airspeed response to throttle is very slow with high authority. Requires much lead. Again, the pilot rating of 8 reflects a loss of control over airspeed.

Task 1.7

No control over indicated airspeed due to very high speed to throttle coupling and low speed to attitude response.

Task 2.0

Unable to stop sink rate with pitch attitude. Required technique is to break sink rate with power and then tune the final touchdown with pitch attitude. This results in only barely adequate control over sink rate. Tried using attitude first and touchdown with throttle, but the sink rate to throttle response is too slow for this technique.

Task 2.1

Am using throttle first and then pitch attitude to fine tune touchdown. Adequate performance requires extensive lead and sink rate to throttle and sink rate to attitude near touchdown. Control over touchdown position is poor as nearly all of my attention is required to get reasonable sink rates. The sluggish sink rate to throttle makes it difficult to get set up. It's easy to overshoot with throttle and float.

Task 2.1 (with engine time constant of 0.5 sec)

Can see faster response of sink rate to throttle, but it doesn't seem to help performance. Pilot rating is unchanged.

Task 3.0

ILS no sweat until last 500 ft, then same problems as on Task 2.0.

Task 3.1

Same problems as on individual parts. That is, (1) very sensitive but sluggish sink rate to throttle, (2) large adverse speed throttle coupling, (3) low airspeed to attitude response, (4) low sink rate to attitude response. My primary objection to this configuration lies in the inability to control sink rate during the last several hundred feet of the approach. The lack of control over airspeed seems to be a secondary problem in that it does not affect my primary complaint of sink rate control.

PILOT 7

Task 1.01

Any effort to control airspeed is not practical. Technique is to hold pitch attitude and control flight path with throttle. No attempt is made to control airspeed. This does not appear to affect my ability to track the glide slope with power. Compares with the augmentor wing but worse. Am confused by head wind because I can't figure out the power required. Don't like this aircraft period.

Task 1.1

Am having serious problems in completing the tack. The throttles are really supersensitive especially at the low rpm which is very nonlinear.

Task 1.2

I feel like I should rate the high-fast and the low-slow the same as the glide slope tracking and turbulence. Otherwise I'll be rating the task and not the airplane. The high-fast you obviously can take the performance into consideration. It's a 10; as far as the workload goes during the high-fast or the low-slow, there was not too much difference. There's a little bit extra work on the high-fast.

Task 1.7

The airspeed is so affected by power that it's corrupted, and it's very difficult to do. You almost have to know what attitude goes with that condition to get there in a reasonable length of time. I find that the only way that you can do this is to fly attitude, and I didn't know what the attitude was for 85 kt so it took me awhile to find it. I think it's crummy. The more you flew this airplane the better you get at it, because you know what those attitudes were. You'd know if you had a tail wind you'd put a little bit in, so it's not unacceptable by any means but's sure not nice.

Task 2.0

Flaring with attitude is unacceptable. The trick is to add a couple of percent power as you go into the flare and make the final touchdown with pitch attitude. In terms of pilot rating I guess we're saying that adequate performance is hitting on the runway at a reasonable spot not necessarily in the touchdown zone. Considering you have an airplane with 1000 ft ground roll or something, you can float a little bit past the touchdown zone without hurting things.

Task 2.1

The main deficiencies are the requirement to use power and then the overall lack of L_α. The main problem with flight path control is that flight path angle washes out after a throttle input. This problem is especially noticeable as you approach the flare point and even during the flare.

Task 3.1

Have to make small corrections or I get into trouble.

PILOT 8

Task 1.01

Attitude excursions not as extreme as for Configuration AP1, but indicated airspeed response is very slow. Could not get my target airspeed. Pilot rating of 4 is primarily because glide slope tracking is adequate.

Task 1.1

Got to +40 deg of pitch attitude and lost it. Have to be content with high speed until glide slope capture.

Task 1.2

Speed goes the wrong way with power addition.

Task 1.7

Giant pitch attitudes used to attain ±10 kt speeds, wind up at attitude of 30 deg. But would like to revise my statement on Task 1.01; the attitudes for this airplane are more severe than those for Configuration AP1. After several runs, I found I was able to get 75 kt with only +10 max pitch attitude. It was easy to get fooled into using very large attitudes because of very poor airspeed response to pitch attitude. The pilot rating would be a 10 if I got into the large attitude problem.

Task 2.0

Out of control in sink rate with attitude flares. Power flares not much better due to squirrely response of sink rate to power.

Task 2.1

Used power to flare. Tends to skip off. Second landing is a "boomer."

Task 3.1

Got low and slow. A bear to correct. Requires large attitude change. Have to be patient. Power flare only way to land it.

PILOT 9

Task 1.01

Initial control opposite that required for steady state. Very poor.

Task 1.1

No way to hold speed.

Task 1.2

Totally unacceptable. Tends to reduce the minimum control speed, i.e., loss of elevator effectiveness. Pilot rating of 10.

Task 1.7

Large attitude changes with no speed changes. Very confusing.

Task 2.1

Using throttle prior to flare and pitch attitude for final touchdown. Seems very sensitive to throttle making it difficult to set up for flare. Extremely hard to get into proper flare "window."

Task 3.1

Comments the same as for the previous tasks.

PILOT BACKGROUND

A brief description of each of the subject pilot's experience relative to the present program is given below.

PILOT 1 — ROGER HOH (STI)

- Considerable experience as STOL evaluation pilot. Most STOL time has been in simulators with some experience in Variable Stability Navion.
- Extensive light aircraft experience.
- Flew in all phases of present experiment.

PILOT 2 — WILLIAM CASEY (DOUGLAS)

- Primarily involved in checking out customers in DC-9.
- Served as Navy test pilot and was checked out in Harrier.
- Flew in preflight simulation phase of experiment.

PILOT 3 — DAVID ELLIS (PRINCETON UNIVERSITY)

- Project pilot on Variable Stability Navion. Has considerable experience with evaluating STOL configurations on Navion and with high angle approaches in spoiler equipped light aircraft.
- Participated in flight phase and postflight simulation phase of experiment.

PILOT 6 — IRVING DECKER (BOEING)

- Primarily involved in production test flight with CTOL aircraft.
- Has some simulator experience with the Boeing AMST
- Participated in preflight simulation phase.

PILOT 7 — GORDON HARDY (NASA)

- NASA research pilot with considerable experience in a wide variety of aircraft.
- Extensive research simulator experience on STOL programs.
- Limited flight time in NASA Augmentor Wing Jet Research Aircraft and in Variable Stability Navion.
- Extensive light aircraft experience.
- Participated in preflight simulation phase of experiment.

PILOT 8 — RICHARD GOUGH (FAA)

- Involved in various FAA certification programs ranging from the DC-10 to a glider.
- Considerable experience as a STOL evaluation pilot on simulators.
- R and D subject in TIFS (Concorde).
- Participated in preflight simulation phase of experiment.

PILOT 9 — ROBERT KENNEDY (FAA)

- Considerable experience as a STOL evaluation pilot both in flight and in the simulators.
- Served as evaluation pilot for Piasecki and Vertol in ducted fan and helicopters.
- Participated in preflight simulation phase of experiment.

APPENDIX B

MANUAL FLARE MODEL DEVELOPMENT

ATTITUDE CONSTRAINED EQUATIONS

The assumptions and derivations for the governing equations for path control with attitude constrained are given in Volume II of this report. These equations are central to analysis of STOL path control and are repeated below for convenience.

Characteristic Equation

$$\Delta = Y_{p_\theta} N^{\theta}_{\delta_e} = [s^2 + (-Z_w - X_u)s + (Z_w X_u - X_w Z_u)]$$

$$= s^2 + 2\zeta_\theta \omega_\theta s + \omega_\theta^2$$

or (B-1)

$$(s + 1/T_{\theta_1})(s + 1/T_{\theta_2})$$

The latter form results if X_w is small or in general if $(Z_w - X_u)^2 > 4|X_w Z_u|$ then:

$$\Delta \doteq (s - X_u)(s - Z_w) \tag{B-2}$$

with $1/T_{\theta_1} \doteq -X_u$ and $1/T_{\theta_2} = -Z_w$.

Attitude Command Responses, assuming $X_{\delta_e} = Z_{\delta_e} = 0$, are correspondingly given by:

$$\frac{u}{\theta_c} = \frac{1}{\Delta}(X_\alpha - g)\left(s + \frac{gZ_w}{X_\alpha - g}\right)$$

$$= \frac{1}{\Delta}(X_\alpha - g)\left(s + \frac{1}{T_{u_1}}\right) \tag{B-3}$$

where $1/T_{u_1} = gZ_w/(X_\alpha - g)$

$$\frac{\dot{h}}{\theta_c} = \frac{Z_\alpha}{\Delta}\left[s - X_u + \frac{Z_u}{Z_w}\left(X_w - \frac{g}{U_o}\right)\right]$$

$$= \frac{Z_\alpha}{\Delta}\left(s + \frac{1}{T_{h_1}}\right) \qquad \text{(B-4)}$$

where $1/T_{h_1} = [-X_u + (Z_u/Z_w)(X_w - g/U_o)]$ (backside term)

<u>Throttle Responses</u> with $M_{\delta_T} = 0$ become:

$$\frac{u}{\delta_T} = \frac{X_{\delta_T}}{\Delta}\left[s - Z_w + X_w\left(\frac{Z_{\delta_T}}{X_{\delta_T}}\right)\right]$$

$$= \frac{X_{\delta_T}}{\Delta}\left(s + \frac{1}{T_{u\theta}}\right) \qquad \text{(B-5)}$$

where $1/T_{u\theta} = - Z_w + X_w(Z_{\delta_T}/X_{\delta_T})$

$$\frac{\dot{h}}{\delta_T} = -\frac{Z_{\delta_T}}{\Delta}\left[s - X_u + Z_u\left(\frac{X_{\delta_T}}{Z_{\delta_T}}\right)\right] \qquad \text{(B-6)}$$

$$= -\frac{Z_{\delta_T}}{\Delta}\left(s + \frac{1}{T_{h\theta}}\right)$$

where $1/T_{h\theta} = -X_u + Z_u(X_{\delta_T}/Z_{\delta_T})$.

INTERPRETATION OF FLARE AS A CLOSED LOOP TRACKING TASK TO PERTURBATION COORDINATES

The flare is really a response to a given set of initial conditions (e.g., sink rate and flare altitude). Analysis of the flare as a closed loop tracking task is greatly facilitated by reinterpretation of these initial conditions as an input to the pilot plus vehicle system. The following analysis presents the details of how this is done.

Definitions

H	Aircraft altitude above the ground
$\dot{H}$	Aircraft sink rate with respect to the ground
h_p	Perturbation altitude = $u \sin \gamma_o - w \cos \gamma_o + U_o \cos \theta_o \theta$. Has little physical significance for $\gamma \neq 0$. (Note that h_p can be finite even if aircraft stays on original glide slope but changes speed)
$\dot{h}_p$	Perturbation sink rate. Difference in sink rate from the initial sink rate at flare initiation
h	Difference in altitude from flare height (initial condition, H_F) and present altitude, H. Is <u>not</u> the same as h_p
$\dot{h}$	Aircraft sink rate with respect to ground $\dot{h} = \dot{H}$

The equations relating perturbation and inertial coordinates are:

$$H = H_F + h \tag{B-7}$$

$$\dot{h}_p = \dot{H} - \dot{H}_F \tag{B-8}$$

$$h = \int_o^t \dot{H}\, dt \tag{B-9}$$

$$\dot{h} = \dot{H} \tag{B-10}$$

These relationships are further illustrated in the following figure.

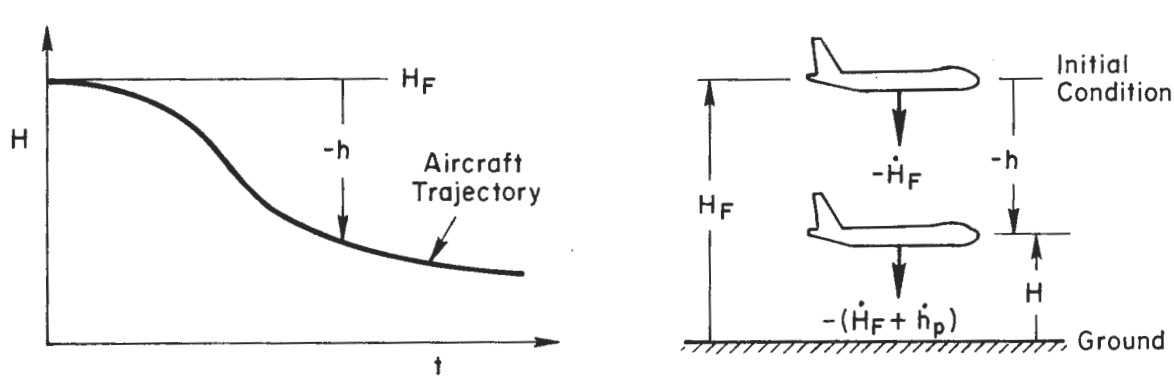

Figure B-1. Relationships Between Inertial and Perturbation Coordinates

The assumed flare law for the closed loop task (see text for justification) is given as

$$\dot{H} + \frac{1}{T_F} H = \dot{H}_{TD_C} \tag{B-11}$$

This flare law is satisfied by developing a sink rate command signal

$$\dot{H}_C = \dot{H}_{TD_C} - \frac{1}{T_F} H \tag{B12}$$

The corresponding block diagram which represents the pilot-vehicle feedback structure to satisfy the flare law is shown in Fig. B-2.

The error signal is defined as

$$\begin{aligned} \dot{H}_\epsilon &= \dot{H}_C - \dot{H} \\ &= \dot{H}_{TD_C} - \frac{1}{T_F}(H_F + h) - \dot{H} \end{aligned} \tag{B-13}$$

The block diagram may be rewritten with the output of the airplane equations of motion in terms of perturbation variables as follows.

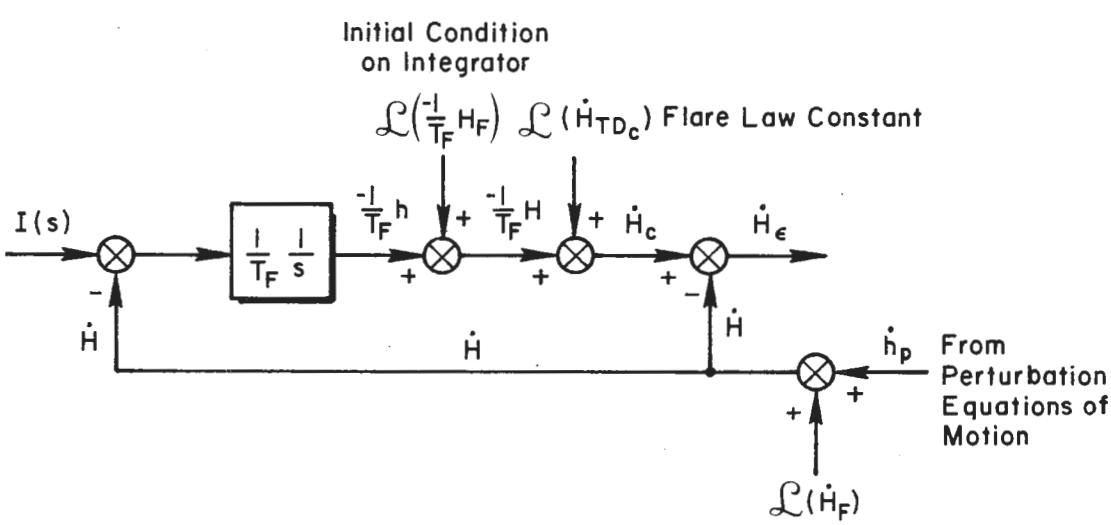

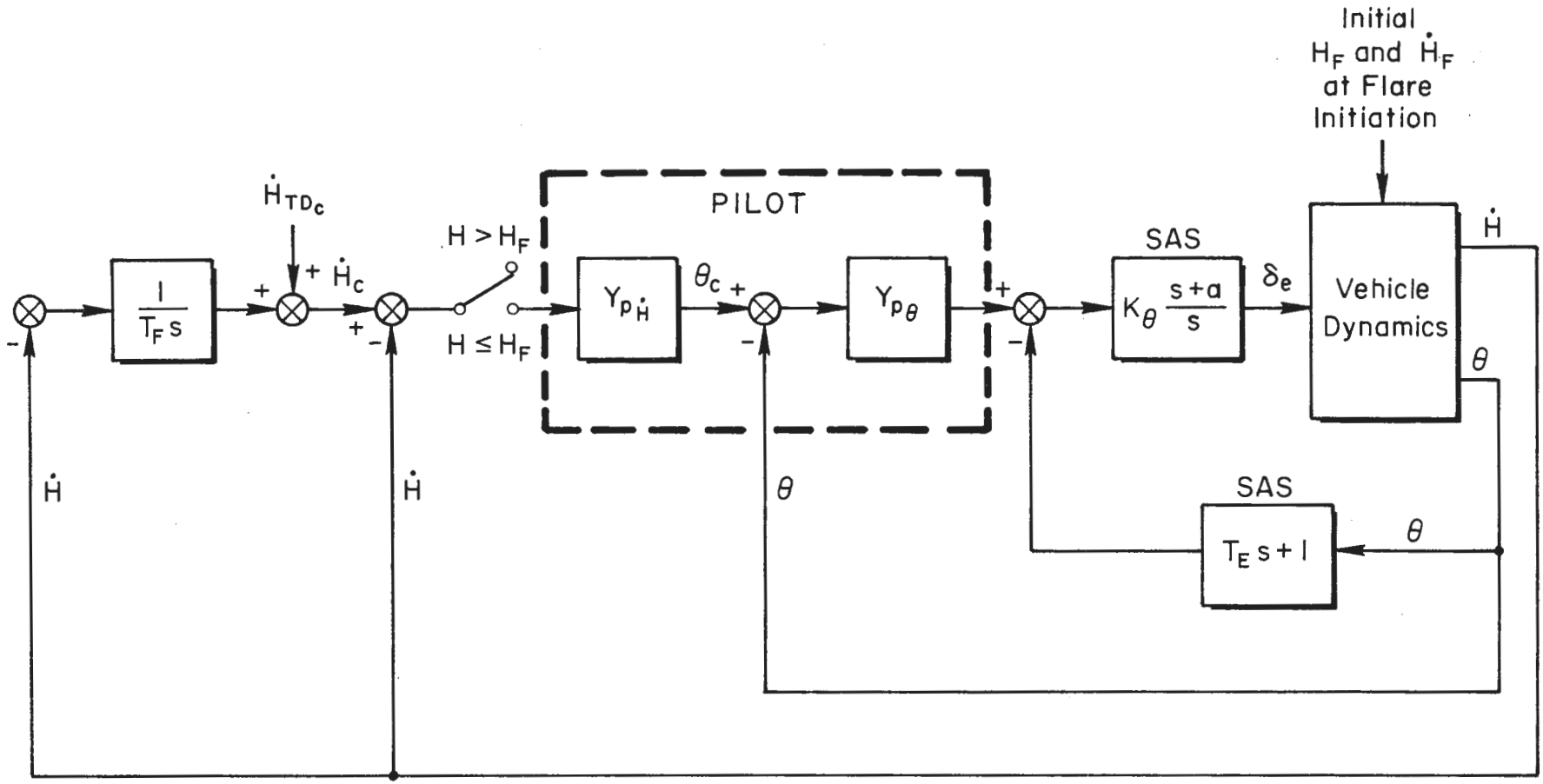

Figure B-2. Block Diagram of Closed Loop Pilot and Vehicle System for Flare

Using block diagram algebra (for example, see Ref. 12), the input summing points involving the initial condition quantities (in fixed coordinates) can be moved to the I(s) summer to form an effective single system command.

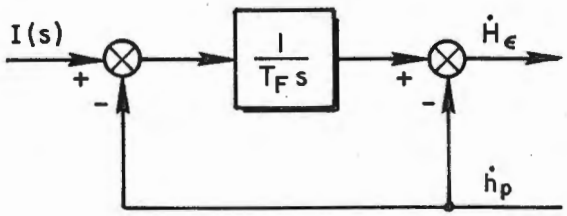

$$I(s) = s\,\mathcal{L}[(-H_F + T_F\dot{H}_{TD_C})] - \mathcal{L}(\dot{H}_F) - T_F s\,\mathcal{L}(\dot{H}_F)$$

$$= -T_F(\dot{H}_F + \frac{1}{T_F}H_F - \dot{H}_{TD_C}) - \frac{\dot{H}_F}{s} \qquad \text{(B-14)}$$

If T_F is set to satisfy basic flare law (Eq. B-11) at t = 0, e.g.,

$$\frac{1}{T_F} = \frac{\dot{H}_{TD_C} - \dot{H}_F}{H_F} \qquad \text{(B-15)}$$

then the first term in Eq. B-14 is zero and

$$I(s) = -\frac{\dot{H}_F}{s} \qquad \text{(B-16)}$$

The physical interpretation of Eqs. B-15 and B-16 are

- $1/T_F$ is equivalent to flare height and is internally generated by the pilot. If the pilot's judgment is correct, he will select a T_F according to Eq. B-15.
- The dynamics of the response of perturbation sink rate ($\dot{h}_p$) to a step input of magnitude $-\dot{H}_F$ in the block diagram of Fig. B-3 is equivalent to the sink rate response (H) to the initial conditions $\dot{H}_F$ and H_F in in the block diagram in Fig. B-2

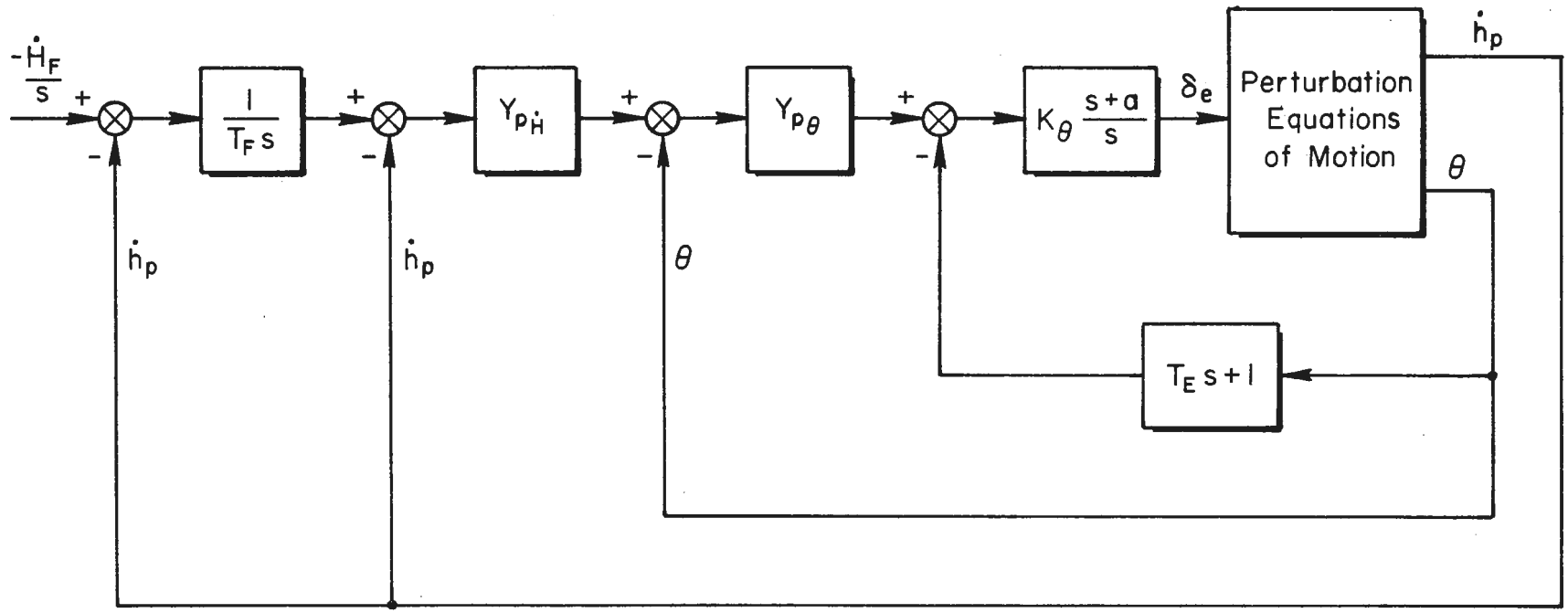

Figure B-3. Block Diagram of Closed Loop Flare in Perturbation Coordinates and with Step Input Equivalent to Initial Conditions (H_F and $\dot{H}_F$)

- The perturbation sink rate actually differs from the inertial sink rate by a bias equal to $\dot{H}_F$. The time response to Fig. B-3 and from an analog computer solution to the complete equations mechanized based on Fig. B-2 for the same flare would take the following form

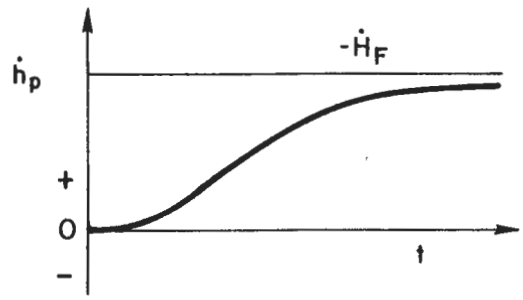

Perturbation Solution to Step Input, $\dot{H}_F$

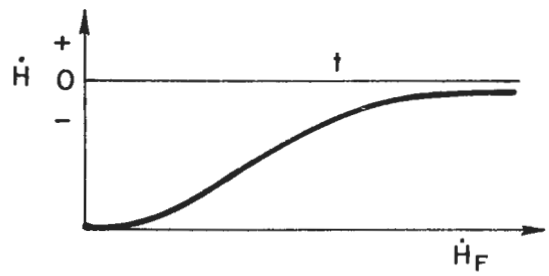

Computer Solution With Initial Conditions

Thus, the perturbation solution should be interpreted such that the final value is zero, e.g., $\dot{H} = \dot{H}_F + \dot{h}_p$

APPENDIX C

DFA DESCRIPTION

OBJECTIVE

The basic objective of the DFA tests was to determine how the pilots were performing the flight path control function. To define the describing function which we wished to measure, let us consider the pilot/aircraft model shown in Fig. C-1. For the moment we will ignore the inputs shown there (d_c and w_g).

In this model the pilot uses data from the glide slope and IVSI indicators to regulate flight path by means of the throttle, δ_T. When he perceives a glide slope error, he mentally generates a rate of climb bias ($\dot{h}_c$) and then tries to control to that rate.

The characteristic equation for the system shown in Fig. C-1 can be written as:

$$1 + \frac{Y_{\dot{h}} N^{\dot{h}}_{\delta_T} + Y_d Y_{\dot{h}} N^{d}_{\delta_T}}{\Delta} = 0 \qquad \text{(C-1)}$$

$$1 + G_{FP} = 0 \qquad \text{(C-2)}$$

It should be noted that the transfer functions used throughout this discussion do <u>not</u> refer to open-loop (bare airframe) transfer functions even though that notation is used for convenience. Rather the transfer functions are those with the SAS and any other manual (e.g., speed control) loops closed.

To study flight path control, we should measure the describing function, G_{FP}, which is given by:

$$G_{FP} = \frac{Y_{\dot{h}}\left(N^{\dot{h}}_{\delta_T} + Y_d N^{d}_{\delta_T}\right)}{\Delta} \qquad \text{(C-3)}$$

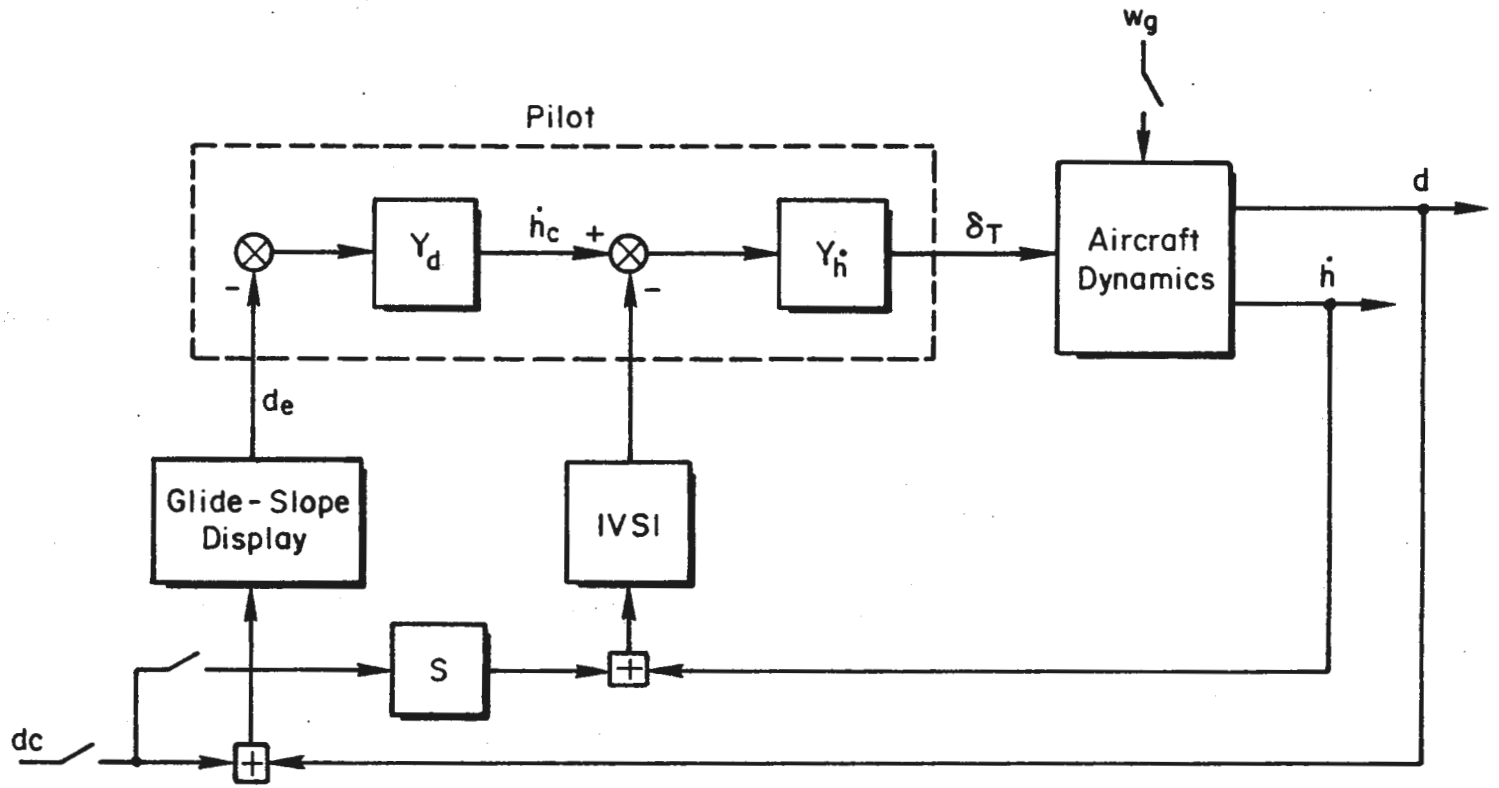

Figure C-1. Pilot/Aircraft Model

Furthermore, since $\dot{h}$ and $\dot{d}$ are approximately equal (h is measured vertically and d is perpendicular to the trim flight path), G_{FP} can be approximated by:

$$G_{FP} \doteq Y_{\dot{h}}(s + Y_d) \frac{N^d_{\delta_T}}{\Delta} \tag{C-4}$$

INPUT SELECTION

A number of possible inputs could be used to excite the pilot/aircraft system. Three specific ones will be considered here.

- Beam noise — d_c in Fig. C-1 but without the input to the IVSI.
- Vertical gust — w_g in Fig. C-1.
- Pseudo gust — d_c in Fig. C-1 with $\dot{d}_c$ fed to the IVSI.

For beam noise, the closed-loop aircraft responses are:

$$\frac{d}{d_c} = \frac{-Y_d Y_{\dot{h}} N^d_{\delta_T}}{\Delta + Y_{\dot{h}} N^{\dot{h}}_{\delta_T} + Y_{\dot{h}} Y_d N^d_{\delta_T}} \tag{C-5}$$

$$\frac{d_e}{d_c} = 1 + \frac{d}{d_c} = \frac{\Delta + Y_{\dot{h}} N^{\dot{h}}_{\delta_T}}{\Delta + Y_{\dot{h}} N^{\dot{h}}_{\delta_T} + Y_{\dot{h}} Y_d N^d_{\delta_T}} \tag{C-5}$$

From these expressions we see that the desired describing function, G_{FP}, can not be measured with this input.

For a vertical gust, the closed-loop response is:

$$\frac{d}{w_g} = \frac{N^d_{w_g} + Y_{\dot{h}} N^d_{w_g} \dot{h}_{\delta_T}}{\Delta + Y_{\dot{h}} N^{\dot{h}}_{\delta_T} + Y_{\dot{h}} Y_d N^d_{\delta_T}} \tag{C-6}$$

Since $\dot{d} \doteq \dot{h}$, the coupling numerator term will be small and the response can be approximated by

$$\frac{d}{w_g} \doteq \frac{N^d_{w_g}}{\Delta + Y_{\dot{h}} N^{\dot{h}}_{\delta_T} + Y_{\dot{h}} Y_d N^d_{\delta_T}} = \frac{N^d_{w_g}/\Delta}{1 + G_{FP}} \tag{C-7}$$

or

$$G_{FP} \doteq \frac{w_g}{d} \frac{N^d_{w_g}}{\Delta} - 1 \tag{C-8}$$

Therefore if a gust input is used, the data reduction routine must include the gust transfer function, $N^d_{w_g}/\Delta$, for that particular configuration. While we could calculate the gust transfer function for the airplane + SAS, there is no way to account for the effects of additional manual feedbacks, such as airspeed to pitch.

The third possibility, pseudo gust, is the one that was actually used. A vertical gust is approximated by adding d_c to the glide slope display, $\dot{d}_c$ to the IVSI, and $\ddot{d}_c$ to the cab vertical motion. In this case the closed-loop responses are given by:

$$\frac{d}{d_c} = \frac{-Y_{\dot{h}}(s + Y_d) N^d_{\delta_T}}{\Delta + Y_{\dot{h}} N^{\dot{h}}_{\delta_T} + Y_d Y_{\dot{h}} N^d_{\delta_T}} \tag{C-9}$$

$$\doteq \frac{-Y_{\dot{d}}(s + Y_d)\, N^d_{\delta_T}}{\Delta + Y_{\dot{d}} N^d_{\delta_T}(s + Y_d)}$$

$$\frac{d_e}{d_c} = 1 + \frac{d}{d_c} = \frac{\Delta + Y_{\dot{h}}\left(N^{\dot{h}}_{\delta_T} - N^{\dot{d}}_{\delta_T}\right)}{\Delta + Y_{\dot{h}} N^{\dot{h}}_{\delta_T} + Y_d Y_{\dot{h}} N^d_{\delta_T}} \tag{C-10}$$

$$= \frac{1 + Y_{\dot{h}} \dfrac{\left(N^{\dot{h}}_{\delta_T} - N^{\dot{d}}_{\delta_T}\right)}{\Delta}}{1 + G_{FP}}$$

or

$$G_{FP} = \frac{d_c}{d_e}\left[1 + Y_{\dot{h}} \frac{\left(N^{\dot{h}}_{\delta_T} - N^{\dot{d}}_{\delta_T}\right)}{\Delta}\right] - 1 \qquad \text{(C-11)}$$

Since $\dot{h} \doteq \dot{d}$, the numerator difference is small and can be neglected. This gives:

$$G_{FP} \doteq \frac{d_c}{d_e} - 1 \qquad \text{(C-12)}$$

This is a convenient expression as it is independent of the aircraft dynamics and it is the one used in the data reduction routine.

INPUT SCALING AND SHAPING

The amplitudes of the input sine waves were selected to approximate vertical turbulence. Comparison of the closed-loop transfer functions given above shows this can be accomplished if,

$$d_c = \frac{N^{d}_{w_g}}{\Delta} w_g \qquad \text{(C-13)}$$

or

$$\dot{d}_c = \frac{N^{\dot{d}}_{w_g}}{\Delta} w_g \qquad \text{(C-14)}$$

To scale the input, it was assumed that

$$\frac{N^{\dot{d}}_{w_g}}{\Delta} = \frac{.5}{s + .5} \qquad \text{(C-15)}$$

and that w_g has an rms level of 4 ft/sec and a power spectral shape of

$$\Phi_{w_g} = \frac{k_1}{\omega^2 + .25} \qquad \text{(C-16)}$$

This gave an rms $\dot{d}_c$ of 2.8 ft/sec. To match this amplitude, the input components must satisfy the constraint:

$$(2.8)^2 = \frac{1}{2} \sum_i (\omega_i A_i)^2 \qquad \text{(C-17)}$$

To provide reasonable frequency shaping of the input, the $\dot{d}_c$ component amplitudes were varied with frequency as $(N^{\dot{d}}_{w_g}/\Delta)w_g$ varies or

$$\omega_i A_i = \frac{k_2}{\omega_i^2 + .25} \qquad \text{(C-18)}$$

where k_2 is an arbitrary constant which was selected to match the rms $\dot{d}_c$ of 2.8 ft/sec.

The pilots considered the input a reasonable approximation of turbulence.

APPENDIX D

PILOT BRIEFING AND QUESTIONNAIRES

The briefing outline used to familiarize the pilots with the simulation scenario is given in Fig. D-1. Three questionnaires used as prompting notes for the test engineer are shown in Fig. D-2. Attempts to have the pilots fill out these questionnaires after the simulation period were abandoned early in the program. This was primarily because the pilots tended to confuse configurations and to forget key points that occurred during the runs.

Figure D-1. Pilot Briefing Outline

A. General

1. Jet STOL transport aircraft
2. Weight = 150,000 lbs
3. Approximately 150 passengers
4. Representative of the worst case configurations of five STOL-type vehicles; Internally Blown Flap (IBF), Externally Blown Flap (EBF), Vectored Thrust, Augmentor Wing, and Upper Surface Blowing (USB)

B. Series of tasks representing a precision instrument approach on a 6 deg glide slope

1. ILS tracking - consideration for evaluations

   a. Glide path control
   b. Airspeed control
   c. Pilots indicate acceptable limits on glide slope and speed excursions. Consider normal ATC speed requests for separator and maximum allowable speed and glide path errors at decision height to achieve acceptable touchdown conditions on a STOL runway

C. Flare and Landing

1. Idealized situation - problem initialized with aircraft at target speed and on glide slope at 300 ft (decision height)
2. Fly aircraft to a VFR touchdown
3. Considerations for evaluations

   a. Touchdown sink rate
   b. Precision of Touchdown point -- ability to stop -- probability of landing short
   c. Acceptable values for sink rate and touchdown position to be evaluated by pilot considering available runway to stop, passenger comfort, and landing gear strength
   d. Tradeoffs between the above (a and b)
   e. Would an increased runway length have a significant bearing on your rating?

D. Composite task

1. Intercept final approach course and fly ILS to touchdown with winds and turbulence
2. Consider individual tasks (B and C) in light of the overall approach task
3. Rate the overall task and emphasize key issues that affect your rating (make comments)

E. Pilot ratings and commentary

1. Verbal to experimenter in simulator during runs
2. Summary into tape recorder after each series of runs
3. Written summary of each configuration using attached sheet.

Figure D-2a. Pilot Evaluation — Flight Path Margin

PILOT: _____ DATE: _____ RUN: _____

CONFIGURATION: _____

APPROACH

Pilot Ratings: Calm Air _____ ; In Turbulence _____

1. Evaluate the $\Delta\gamma$ capabilities of this configuration. Would it cause any operational problems?

2. How often did you hit the throttle stops?

3. Did the $\Delta\gamma$ limits affect the piloting technique for large corrections? If yes, describe.

FLARE AND LANDING

Pilot Ratings: Calm Air _____ ; In Turbulence _____

4. What flare technique was used?

   Did you add power?

5. Was there a problem in landing within the touchdown zone or arresting sink rate? Was there a tendency to land short? Long? Hard?

6. Was visibility over the nose a factor?

7. What were the major factors which influenced the above ratings?

Figure D-2b. Pilot Evaluation — Landing

PILOT: _____ DATE: _____ RUN: _____

CONFIGURATION: _____

PILOT RATINGS: Calm Air _____

In Turbulence _____

1. Which of the following flare techniques did you try?
   a. Pitch only, no thrust inputs.
   b. Pitch primary, open loop thrust input.
   c. Thrust only, no pitch change.
   d. Thrust primary, open loop pitch change.
   e. Other (describe) _____

   _____

2. Which technique did you finally select? Why?

3. Describe the technique used in as much detail as possible (e.g., altitude at which flare was initiated, magnitude of pitch and thrust changes, and primary cue for flare initiation).

4. Was there a problem in landing within the touchdown zone or arresting sink rate? Was there a tendency to land short? Long? Hard?

5. Was visibility over the nose a problem?

6. Did a tailwind significantly affect the task? If yes, describe how and rate task with and without tailwind.

7. What were the major factors which influenced the above ratings?

Figure D-2c. Pilot Evaluation — Speed Margin

PILOT: _____ DATE: _____ RUN: _____

CONFIGURATION: _____

APPROACH

Pilot Ratings: Calm Air _____ ; In Turbulence _____

1. Evaluate the safety margins in calm air and in turbulence.

2. What piloting technique was used in general?

   Did it involve any control crossfeed, e.g., power to elevator?

3. What piloting technique was used to avoid exceeding the speed or angle of attack limits?

4. Was it difficult to avoid the limits? Would it be difficult under operational conditions?

5. What were the major factors which influenced the above ratings?

FLARE AND LANDING

Pilot Ratings: Calm Air _____ ; In Turbulence _____

6. What flare technique was used?

   Did you add power?

7. Was there a problem in landing within the touchdown zone or arresting sink rate? Was there a tendency to land short? Long? Hard?

8. Was visibility over the nose a factor?

9. What were the major factors which influenced the above ratings?

APPENDIX E

DETAILED SUMMARY OF GENERIC CONFIGURATIONS

A digital computer program was developed to aid in the designing of the various test configurations. This program trims the aircraft (based on power and velocity inputs) and calculates the derivatives necessary to factor the longitudinal and lateral-directional small perturbation equations of motion (e.g., $\partial C_L/\partial\alpha$, $\partial C_L/\partial C_\mu$, etc.).

Construction of trim drag polars, aircraft performance curves (γ vs V), and evaluation of various handling quality parameters are made relatively simple via this computer program. The following sections present this type of information for all the test configurations (aircraft) evaluated. All results are based on numeric values presented in various sections of this report.

Subjective descriptions of the origin and differences in the test configurations are also included. These are intended to give a brief insight into the rationale used to arrive at these configurations.

A. DRAG POLARS

1. Untrimmed

Untrimmed drag polars for all aircraft are shown in Figure E-1a through m. These figures depict the blowing effects, C_μ, on the static lift and drag (that is, tail off and no ram drag included) for each test configuration.

2. Trimmed

Trimmed drag polars for five aircraft are shown in Figure E-1a through e. Note that in addition to lines of constant blowing, lines of constant angle of attack are drawn on each drag polar. Three approach trim points are also shown. These are three typical approach flight conditions used throughout the simulation.

K+E 10 X 10 TO THE CENTIMETER 46 1512
18 X 25 CM. MADE IN U.S.A.
KEUFFEL & ESSER CO.

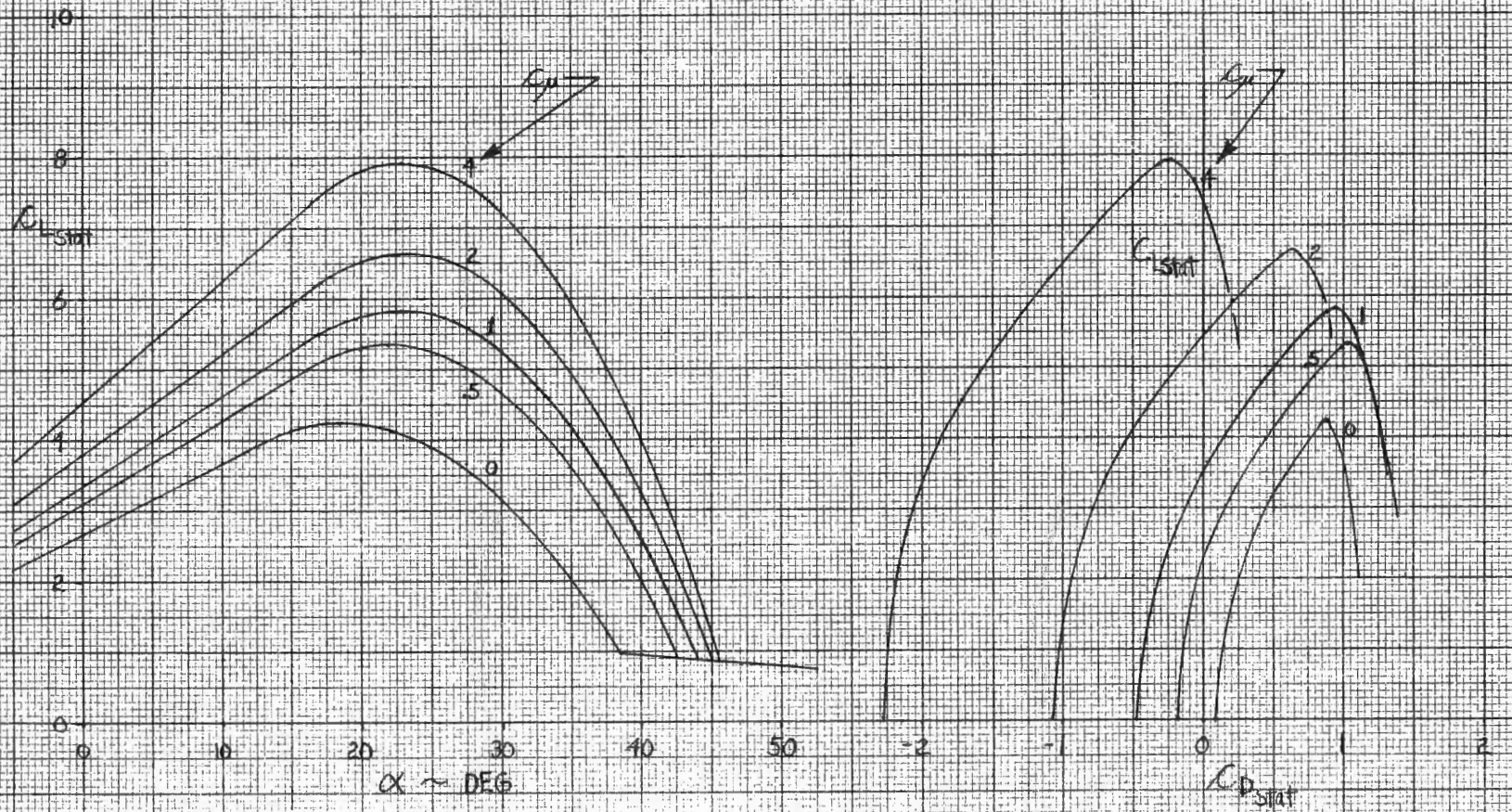

Figure E-1a. Untrimmed Drag Polar for BSL1

K+E 10 X 10 TO THE CENTIMETER 46 1512
18 X 25 CM. MADE IN U.S.A.
KEUFFEL & ESSER CO.

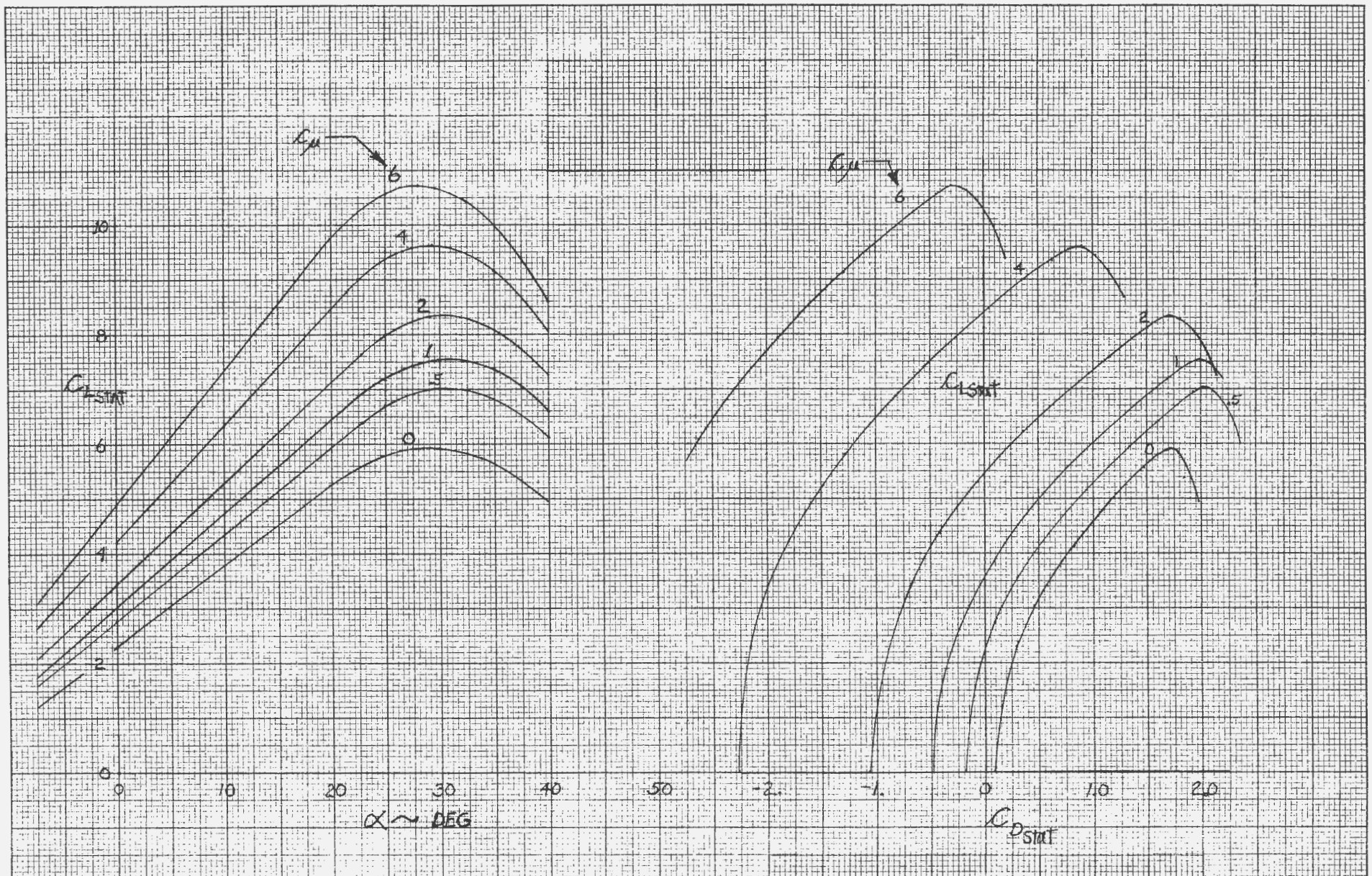

Figure E-1b. Untrimmed Drag Polar for BSL2

K+E 10 X 10 TO THE CENTIMETER 46 1512
18 X 25 CM. MADE IN U.S.A.
KEUFFEL & ESSER CO.

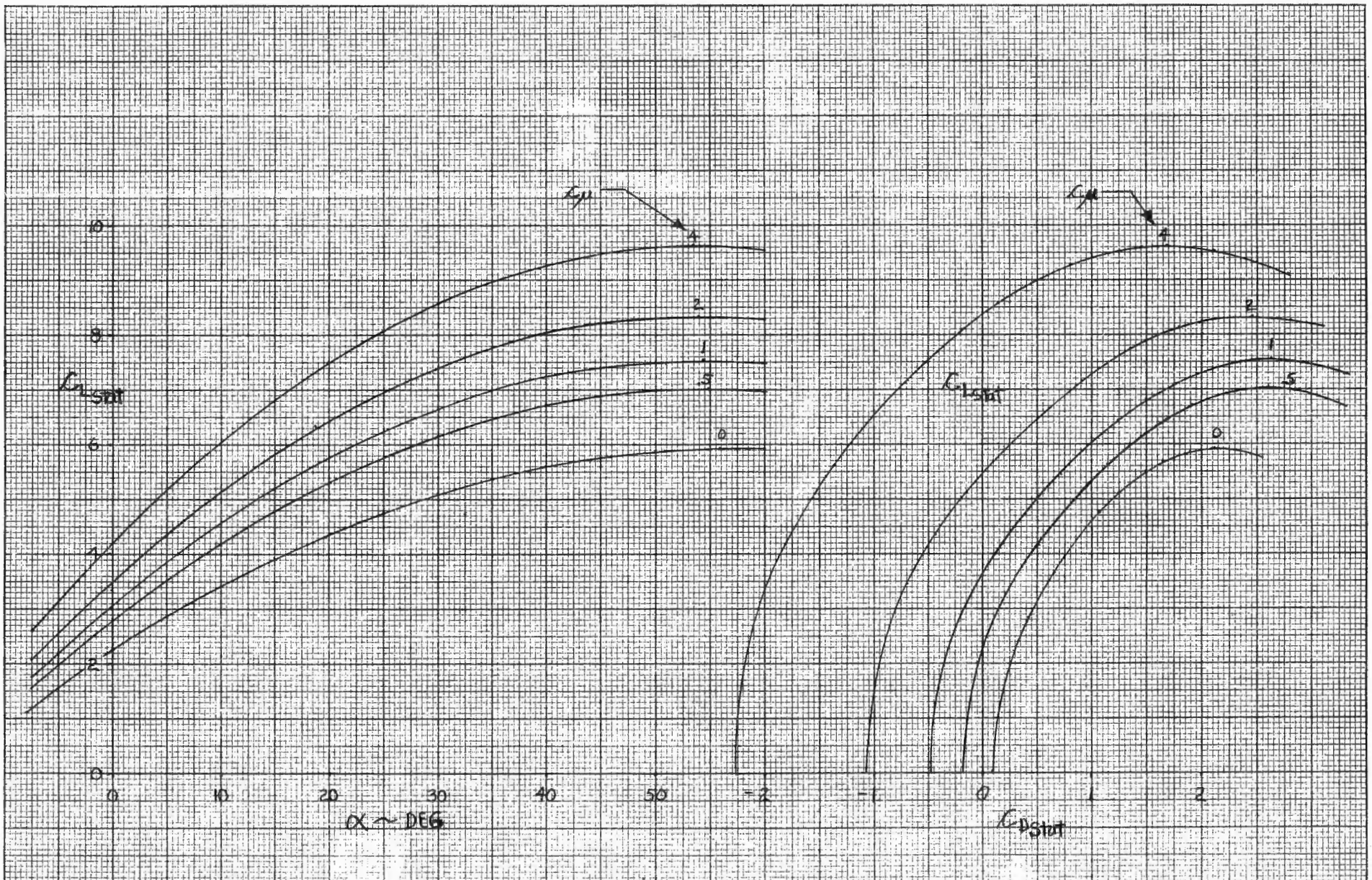

Figure E-1c. Untrimmed Drag Polar for BSL2 RLD

K+E 10 X 10 TO THE CENTIMETER 46 1512
18 X 25 CM. MADE IN U.S.A.
KEUFFEL & ESSER CO.

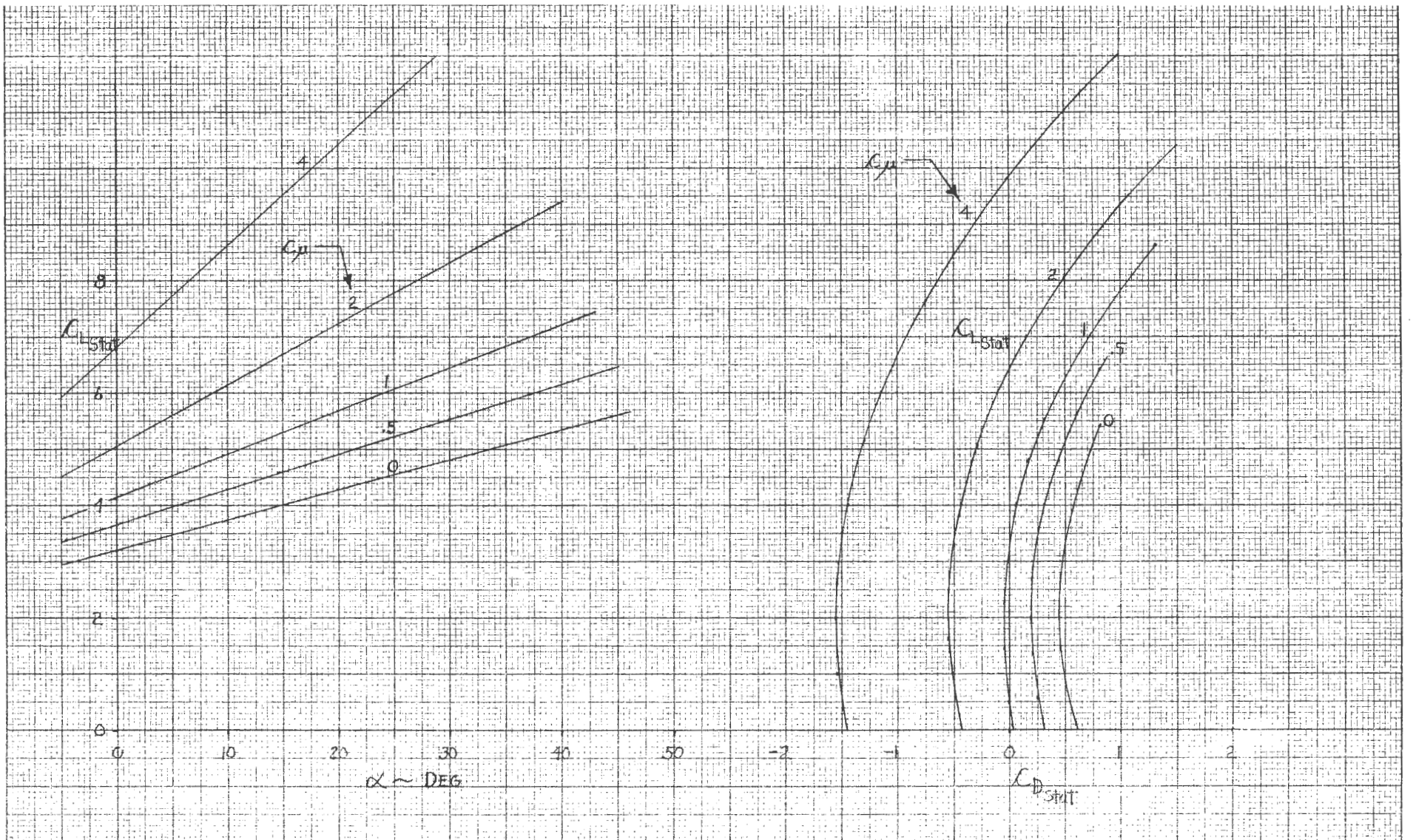

Figure E-1d. Untrimmed Drag Polar for AP1

K+E 10 X 10 TO THE CENTIMETER 46 1512
18 X 25 CM. MADE IN U.S.A.
KEUFFEL & ESSER CO.

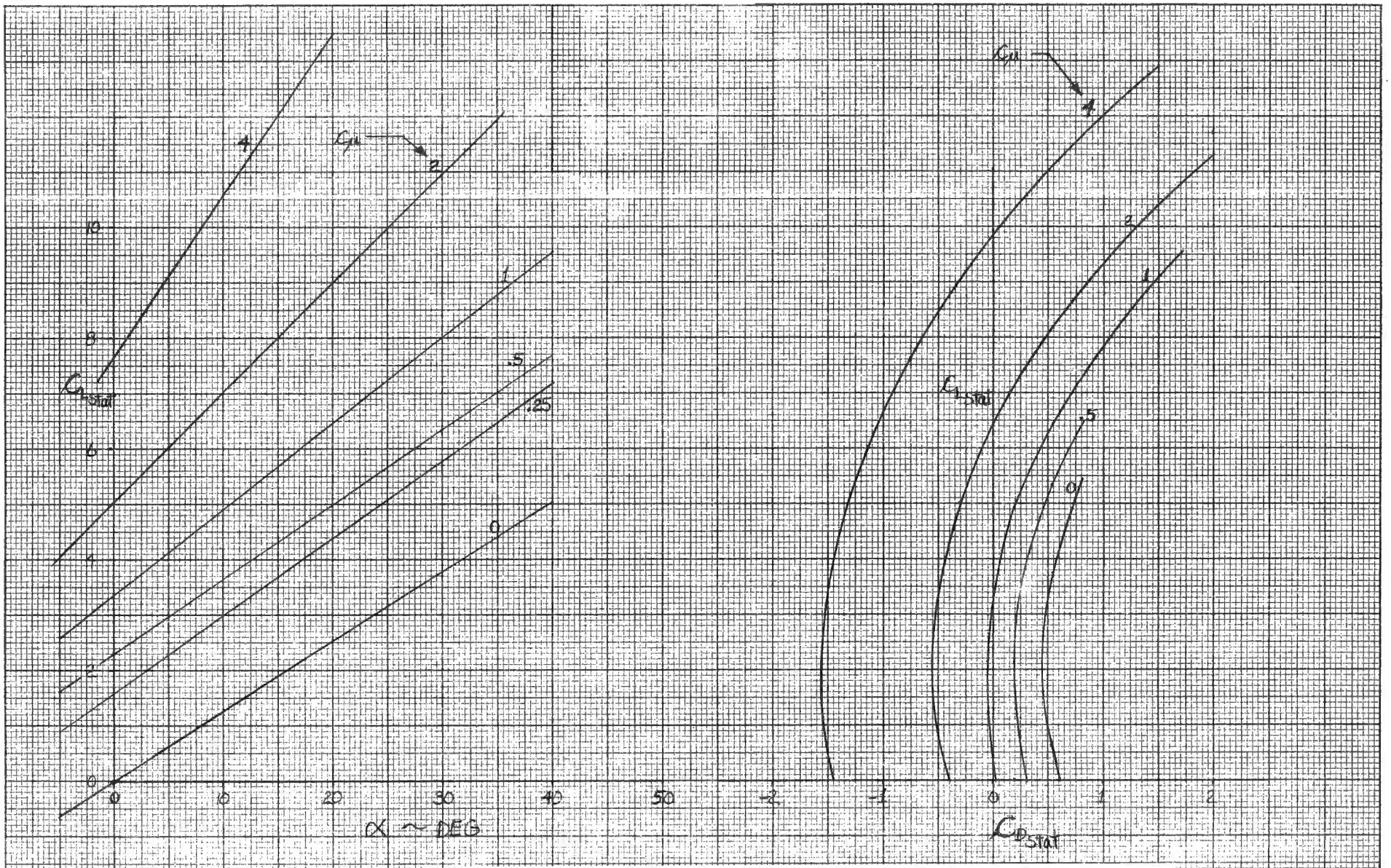

Figure E-1e. Untrimmed Drag Polar for AP2

K+E 10 X 10 TO THE CENTIMETER 46 1512
18 X 25 CM. MADE IN U.S.A.
KEUFFEL & ESSER CO.

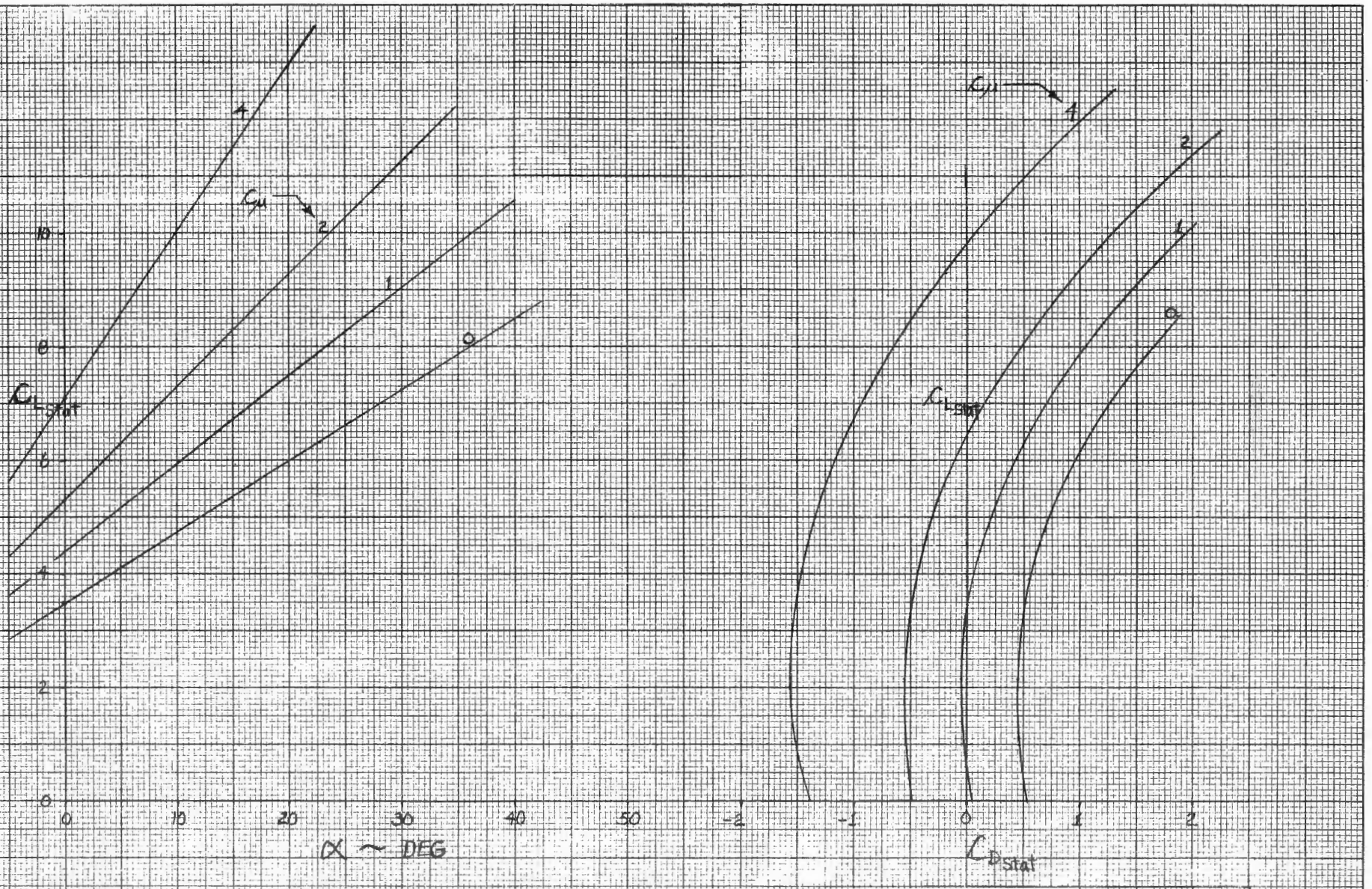

Figure E-1f. Untrimmed Drag Polar for AP3

K+E 10 X 10 TO THE CENTIMETER 46 1512
18 X 25 CM. MADE IN U.S.A.
KEUFFEL & ESSER CO.

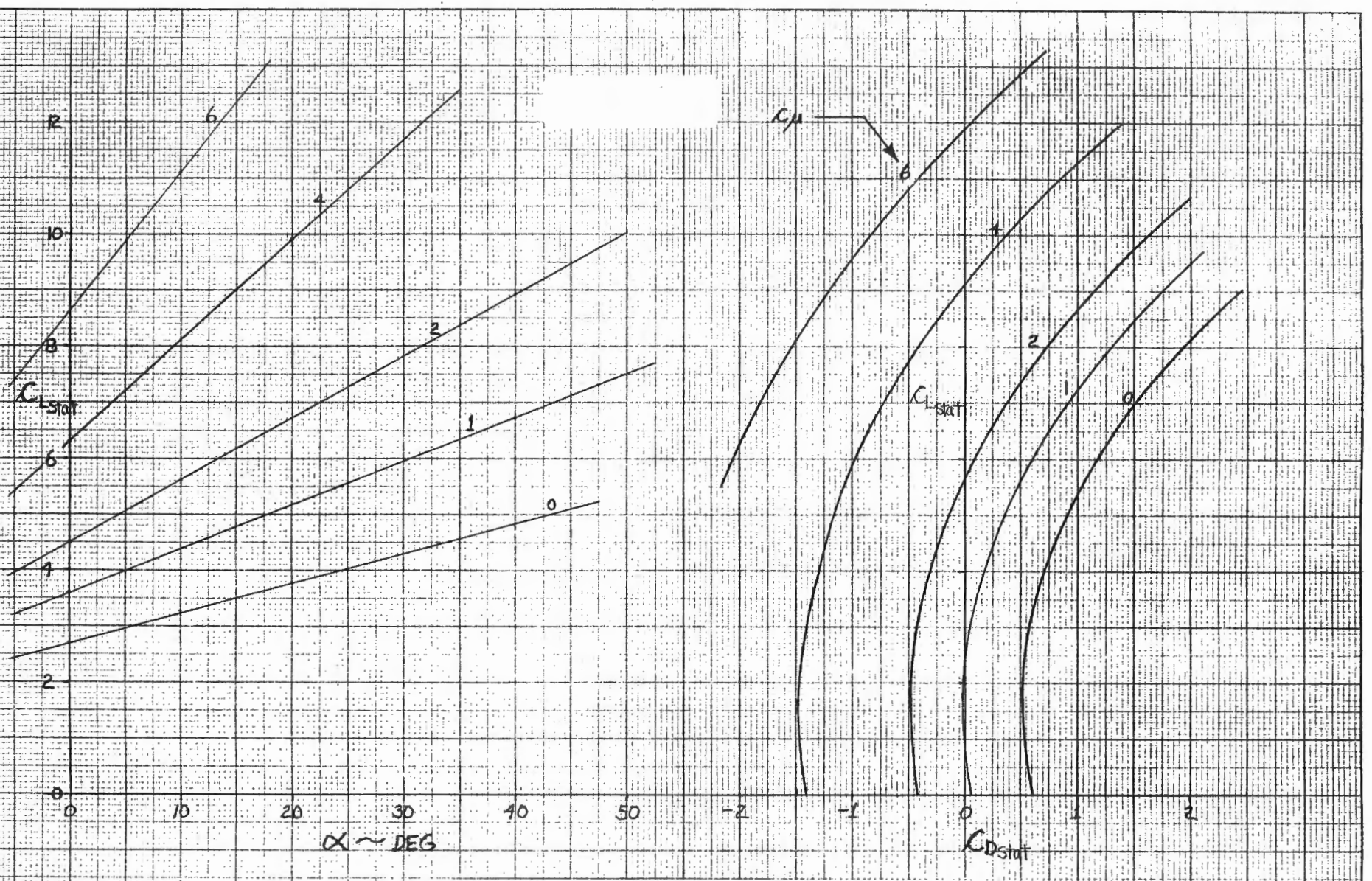

Figure E-1g. Untrimmed Drag Polar for AP5

K+E 10 X 10 TO THE CENTIMETER 46 1512
18 X 25 CM. MADE IN U.S.A.
KEUFFEL & ESSER CO.

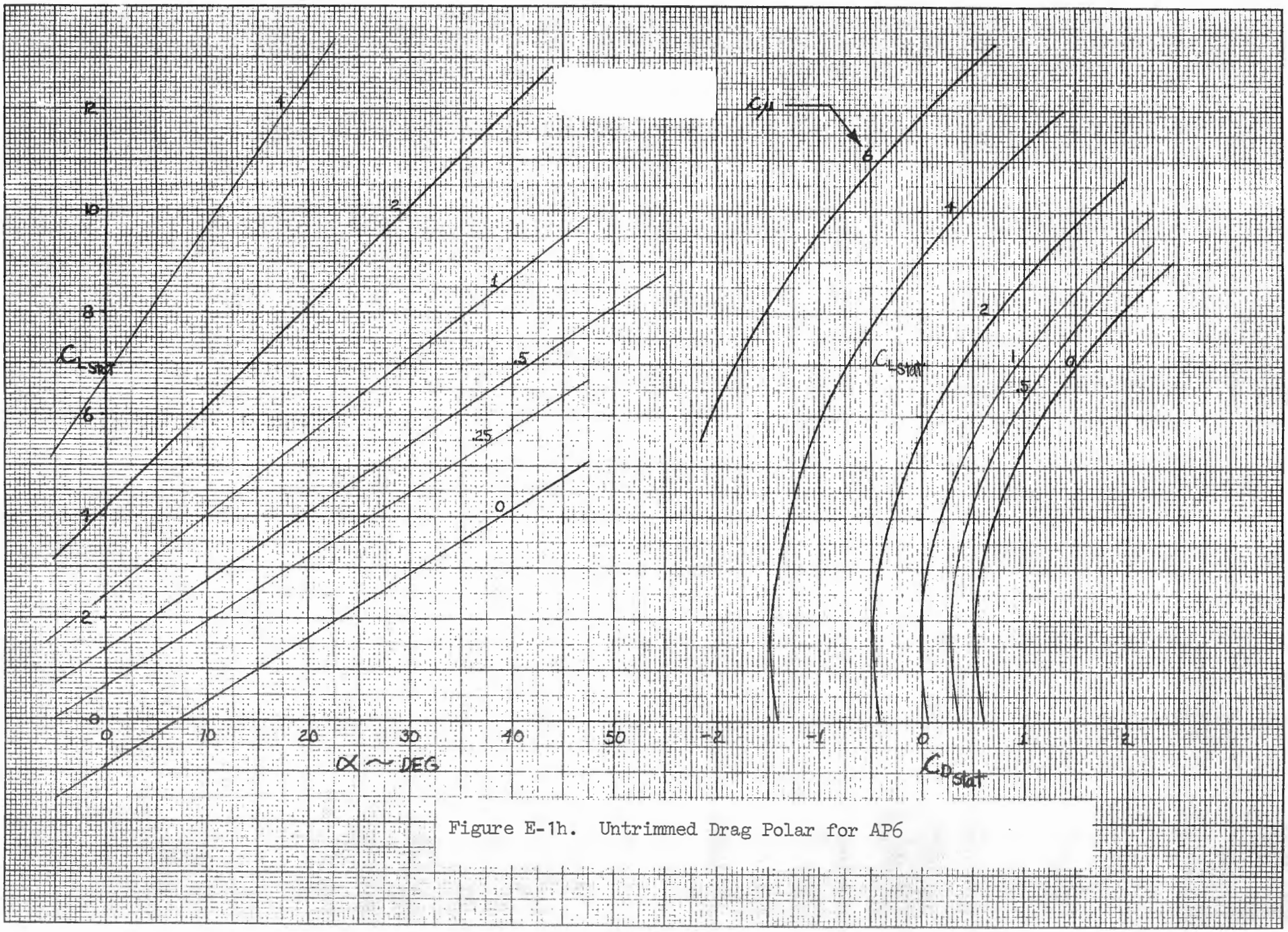

Figure E-1h. Untrimmed Drag Polar for AP6

K+E 10 X 10 TO THE CENTIMETER 46 1512
18 X 25 CM. MADE IN U.S.A.
KEUFFEL & ESSER CO.

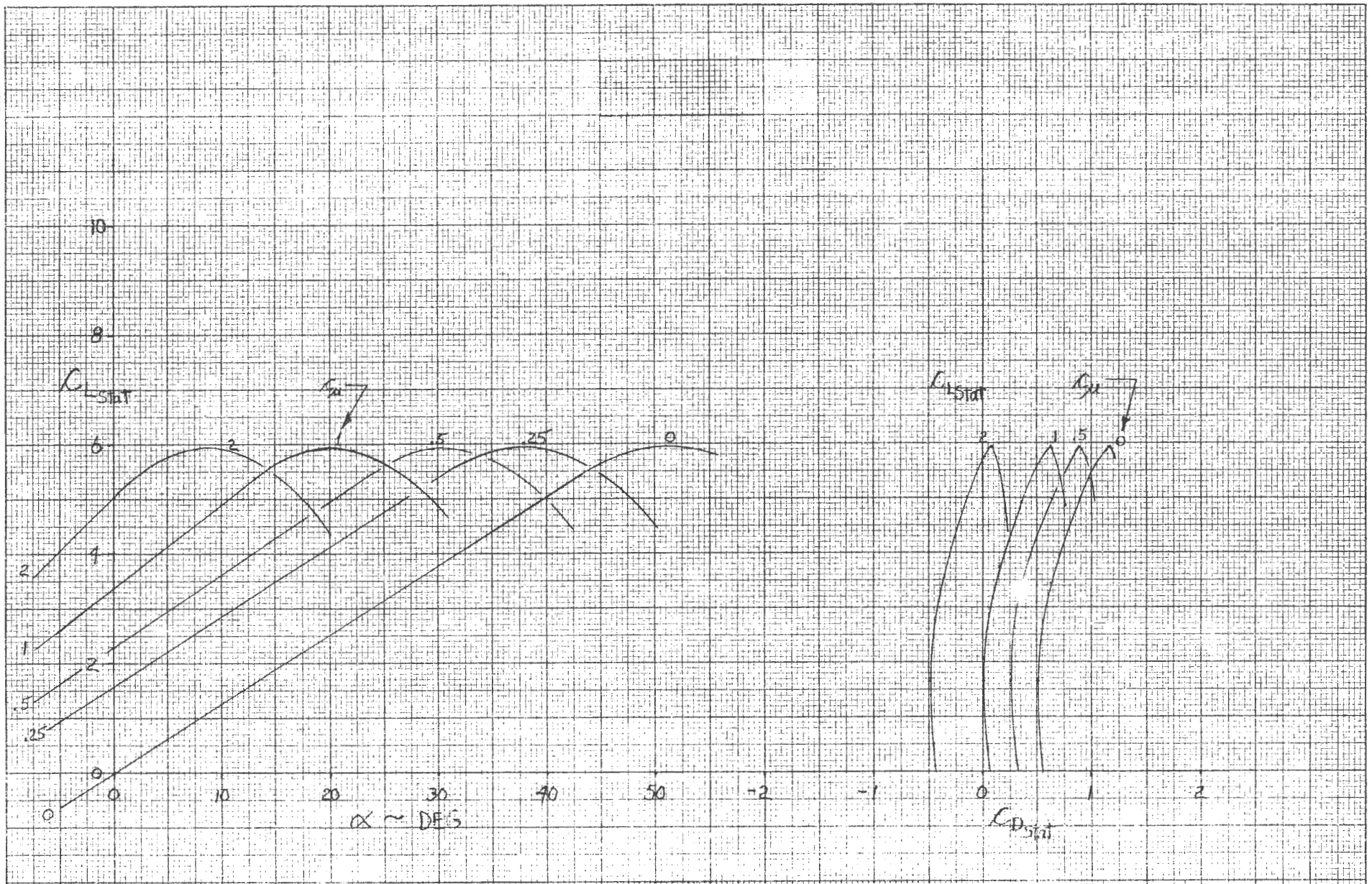

Figure E-1i. Untrimmed Drag Polar for AP6 SR

K+E 10 X 10 TO THE CENTIMETER 46 1512
18 X 25 CM. MADE IN U.S.A.
KEUFFEL & ESSER CO.

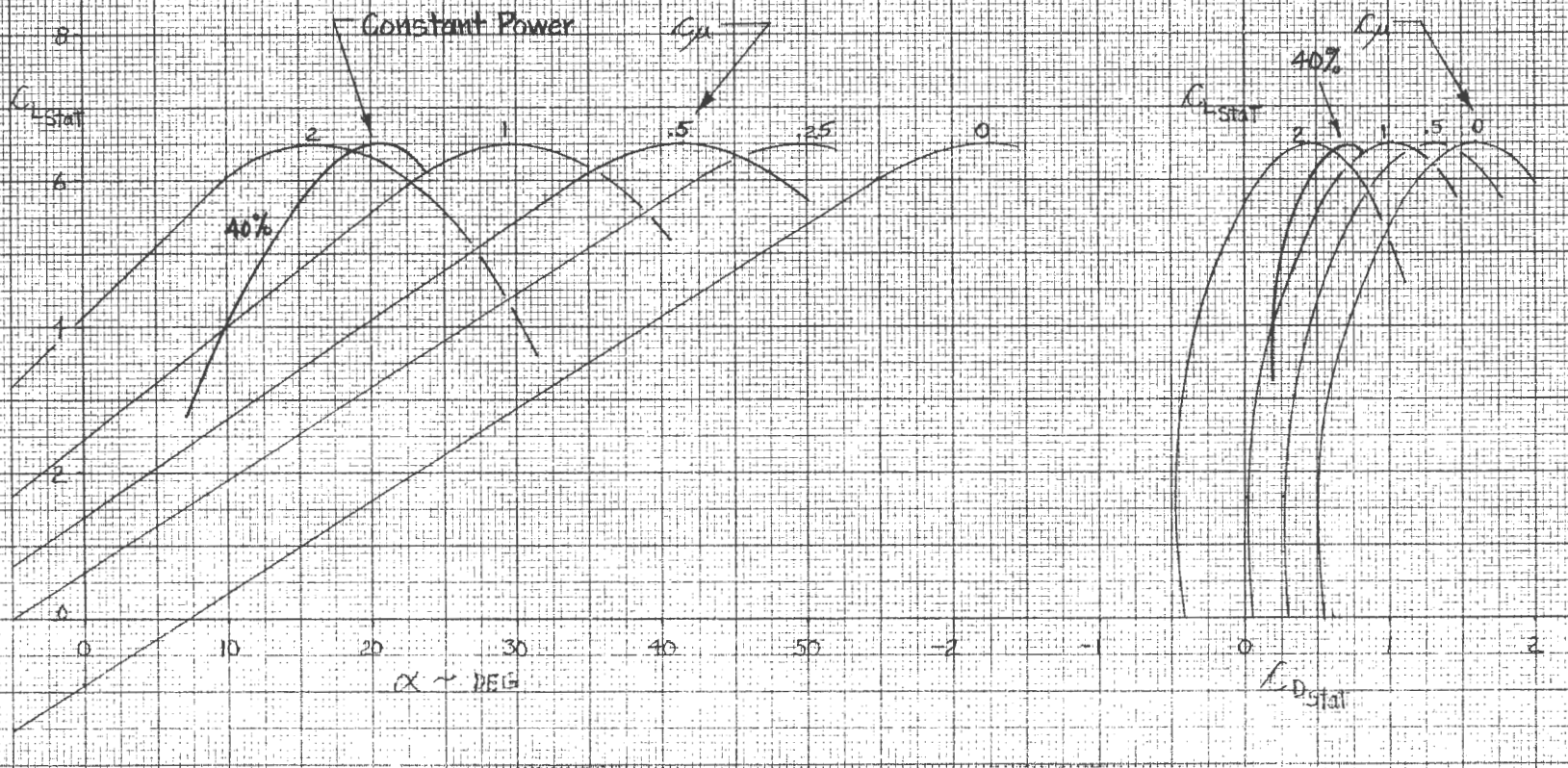

Figure E-1j. Untrimmed Drag Polar for AP6 RLD

K+E 10 X 10 TO THE CENTIMETER 46 1512
18 X 25 CM. MADE IN U.S.A.
KEUFFEL & ESSER CO.

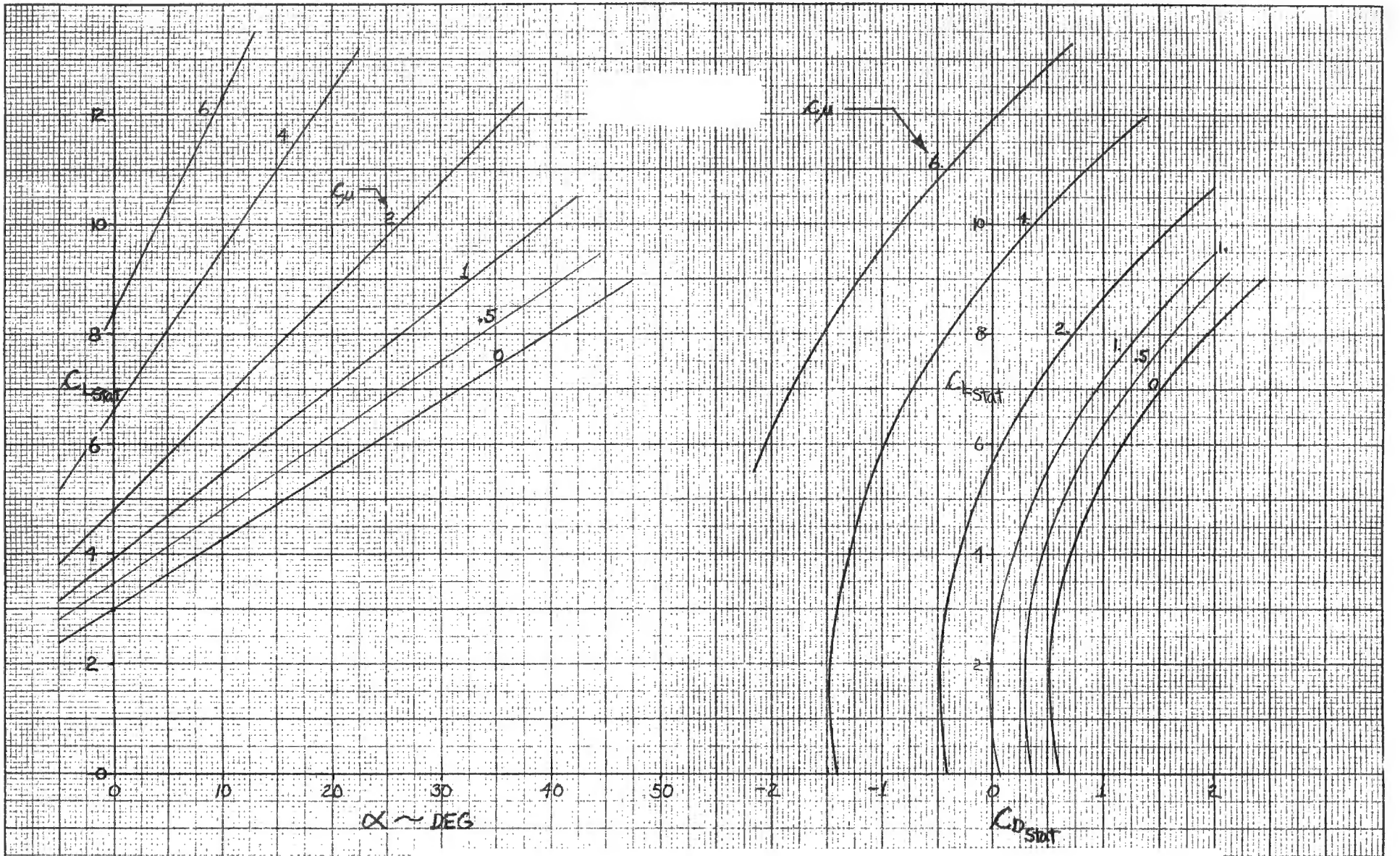

Figure E-1k. Untrimmed Drag Polar for AP7

K+E 10 X 10 TO THE CENTIMETER 46 1512
18 X 25 CM. MADE IN U.S.A.
KEUFFEL & ESSER CO.

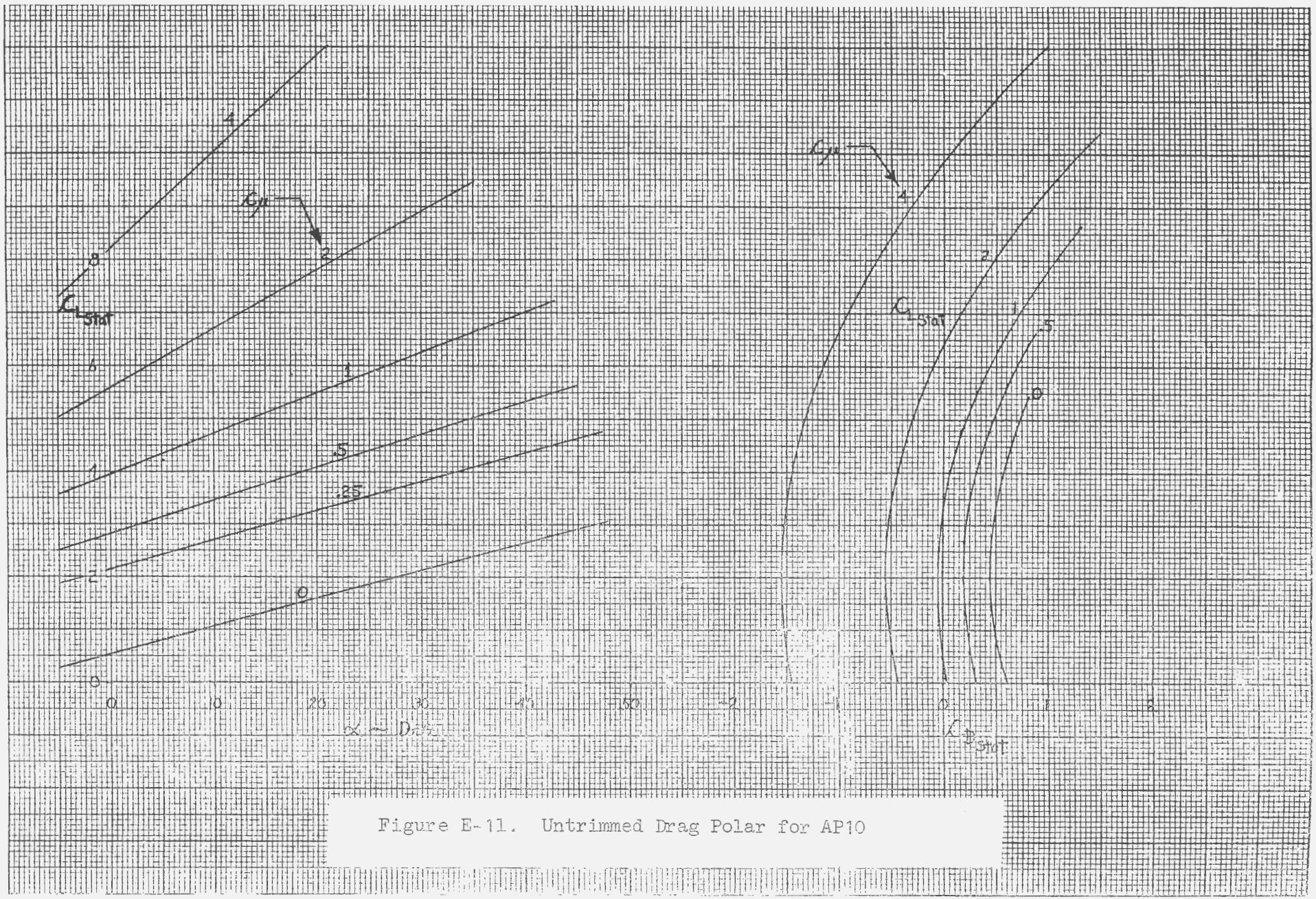

Figure E-11. Untrimmed Drag Polar for AP10

K+E 10 X 10 TO THE CENTIMETER 46 1512
18 X 25 CM. MADE IN U.S.A.
KEUFFEL & ESSER CO.

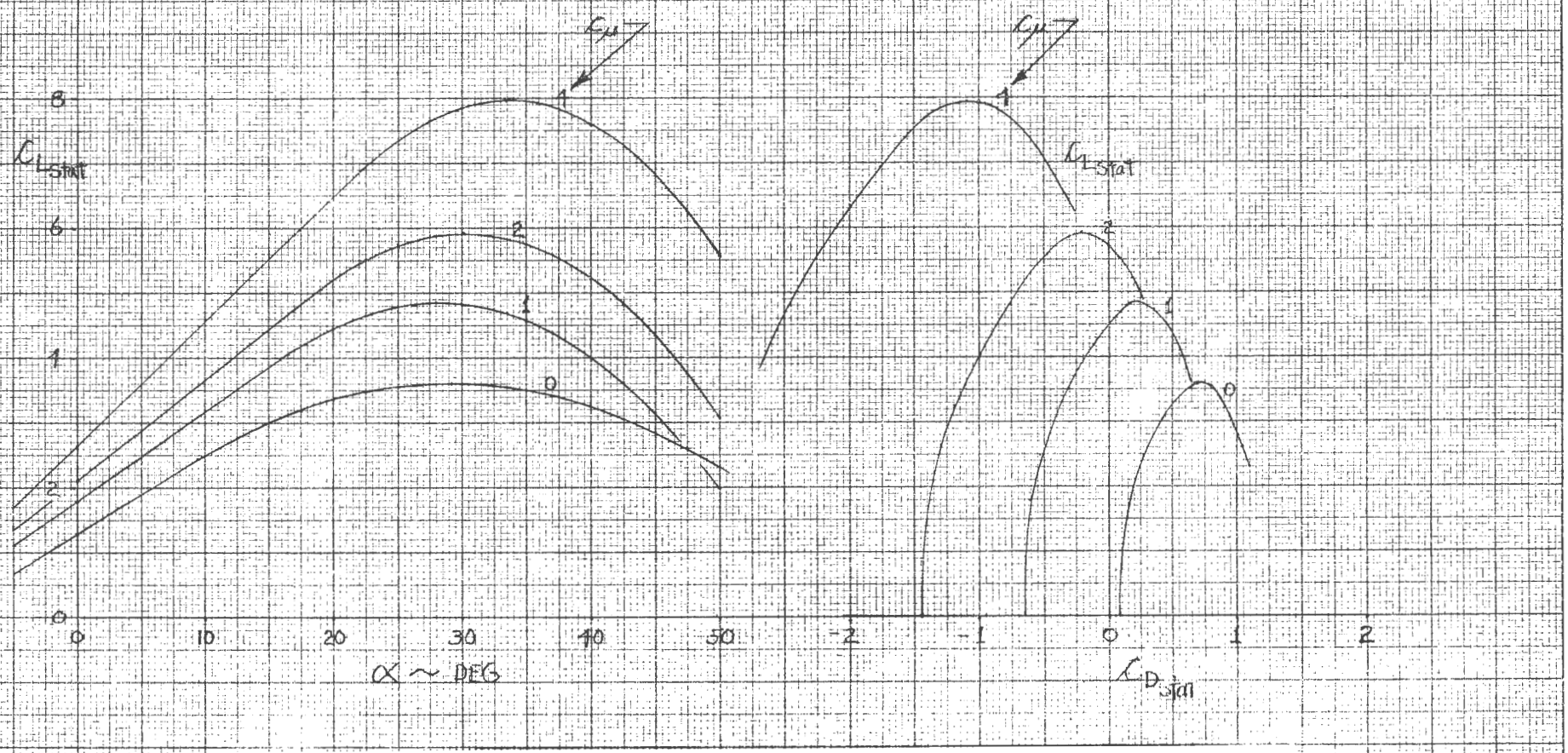

Figure E-1m. Untrimmed Drag Polar for BSL30 and AP30 (30 deg δ_f)

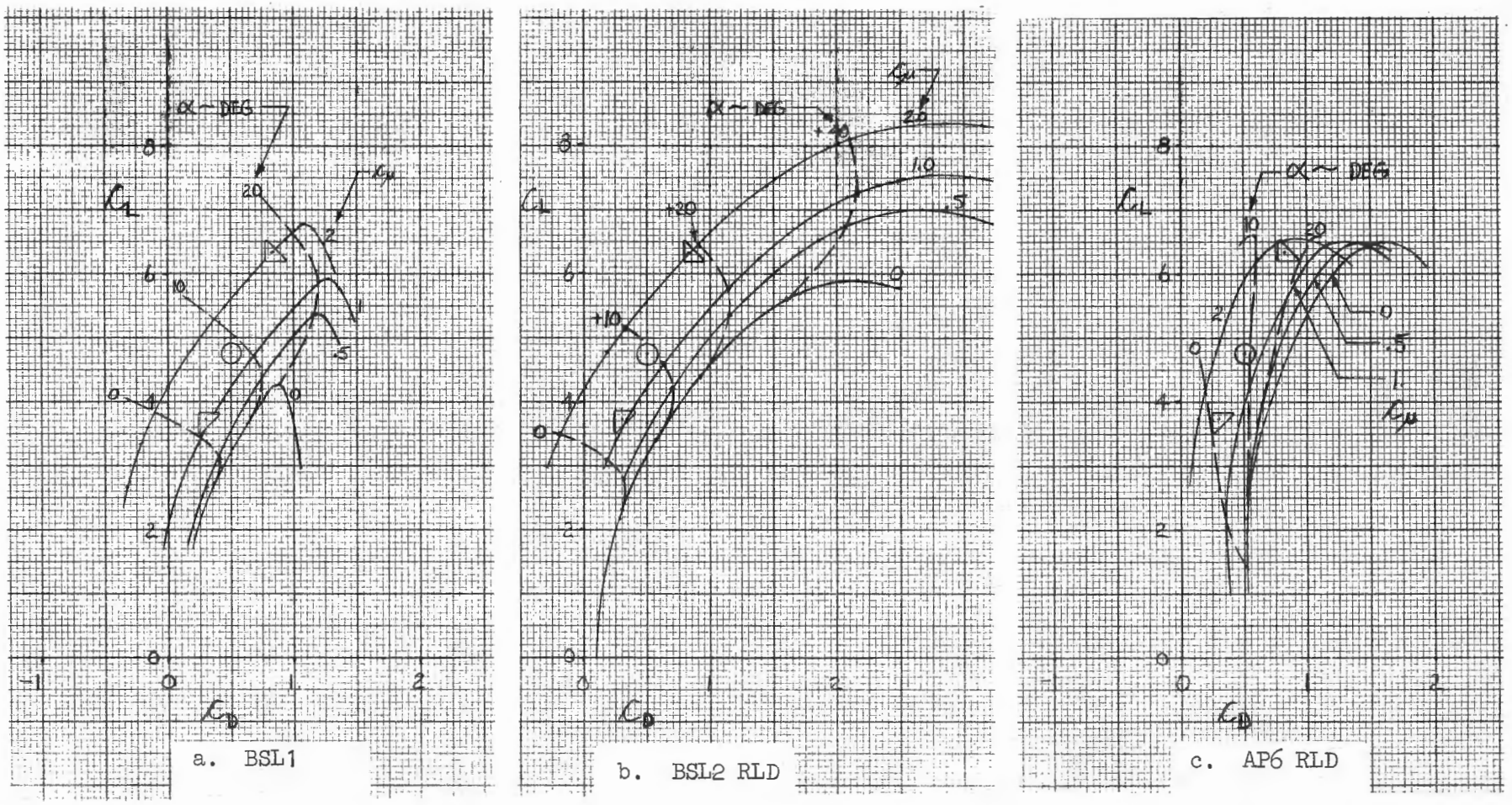

Figure E-2. Trim Drag Polars for Five Test Configurations

NOTE: The symbols ⊙, ▽ and △ are trim points for 75 kt/-6.0 deg γ, 85 kt/-4.6 deg γ, and 65 kt/-7.4 deg γ, respectively.

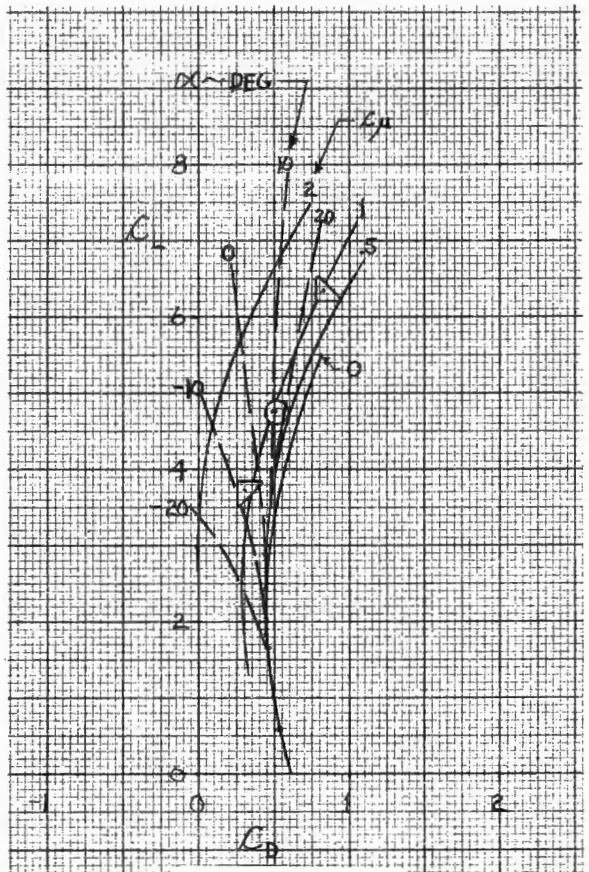

d. AP10

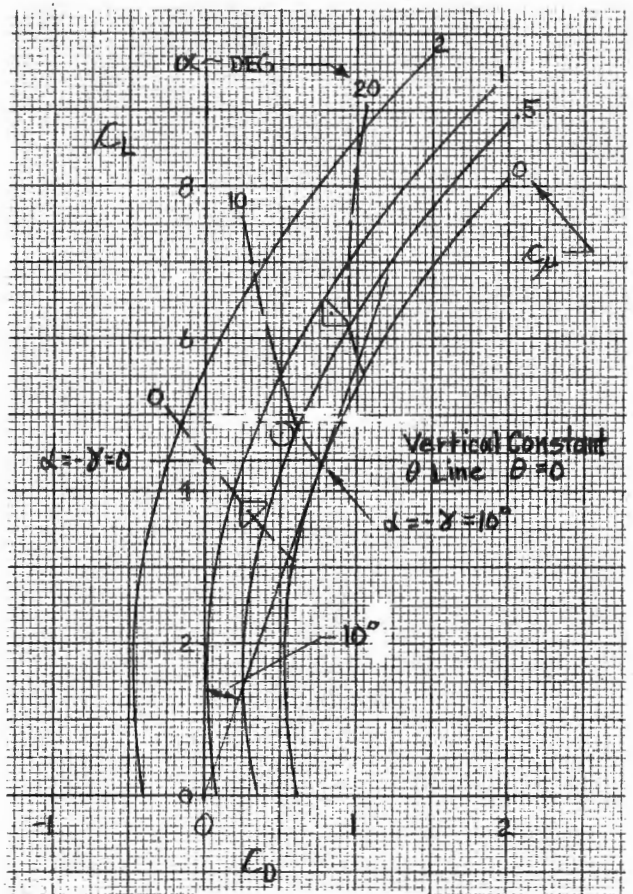

e. AP7

Figure E-2. Concluded

The trimmed C_L vs α curves are not shown because of the relatively small difference in the trimmed and untrimmed curves. The difference simply being the lift from the elevator. However, for the drag polar, in addition to the drag from the elevator, there is a large drag caused by ram effects. The result of this ram drag being a positive ΔC_D at various lift coefficients ($C_{D_{RAM}} \sim 1/V$).

B. PERFORMANCE CURVES

Flight path angle versus velocity for lines of constant power and pitch attitude are shown in Figure E-3a through m for all aircraft tested. This information is useful for comparing the relative amount of control cross-coupling. This is, how much airspeed change is experienced when using the power to change flight path and holding constant attitude. Or, how much flight path change is experienced when using attitude to change airspeed at constant power. Stall margin and the relative amounts of "up and down" capability are also readily obtained from these plots.

C. DYNAMICS

Dimensional stability derivatives and SAS on and off transfer functions for each test configuration are tabulated below for three approach flight conditions. This information is useful for ascertaining basic handling qualities data and conducting closed-loop analysis.

1. Longitudinal

a) Bare airframe dimensional stability derivatives are presented in Table E-1a through l. Complete definitions of the symbols used can be found in NASA CR-2144.*

b) SAS on and off transfer functions are presented in Table E-2a through l. Complete definitions of the symbols and notations used can be found in NASA CR-2144.* Note that the SAS on transfer functions include the engine dynamics ($1/\tau_2 = 0.667$).

*Heffley, Robert K., and Wayne F. Jewell, Aircraft Handling Qualities Data, NASA CR-2144, Dec. 1972.

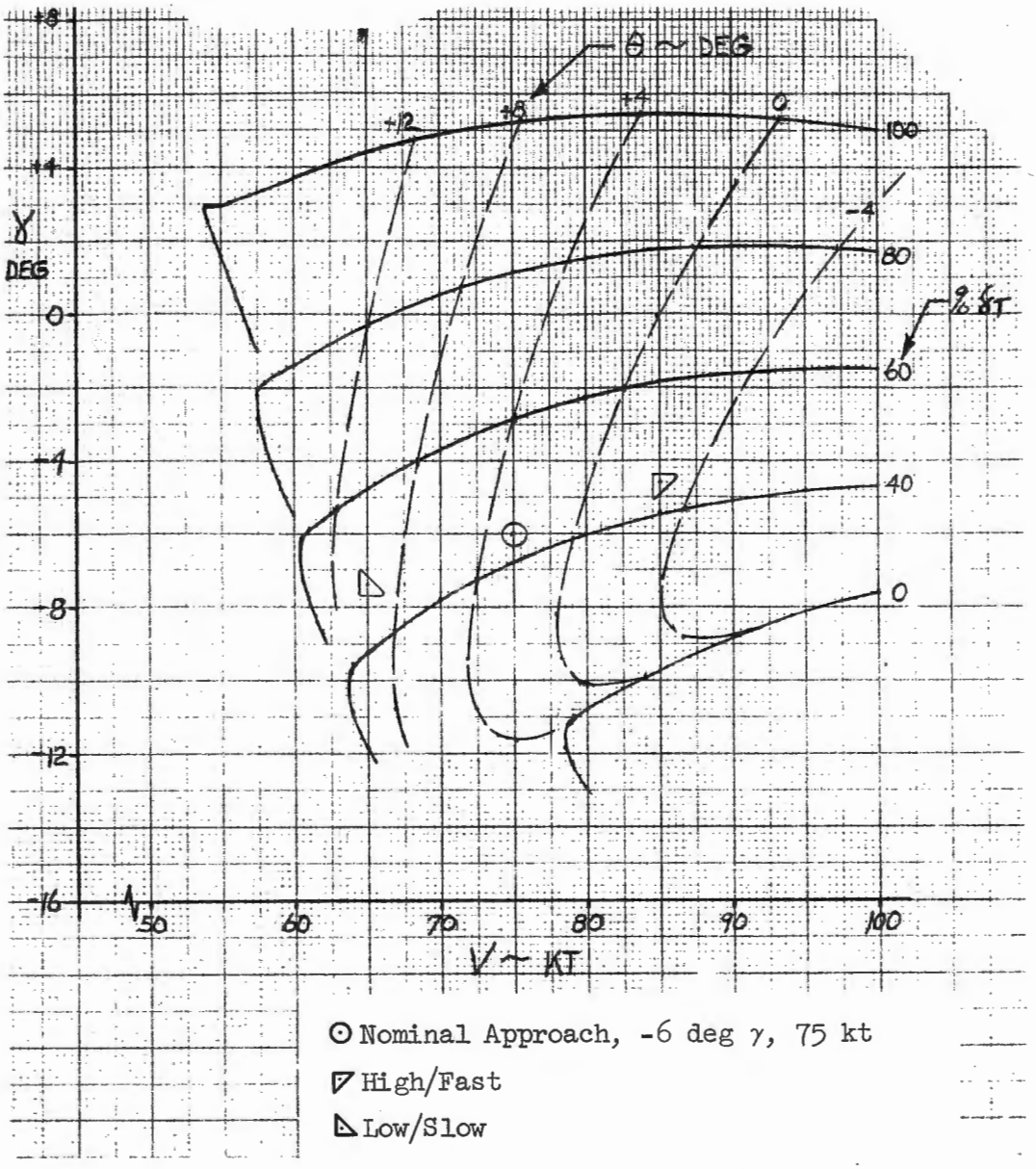

Figure E-3a. Performance Curve for BSL1

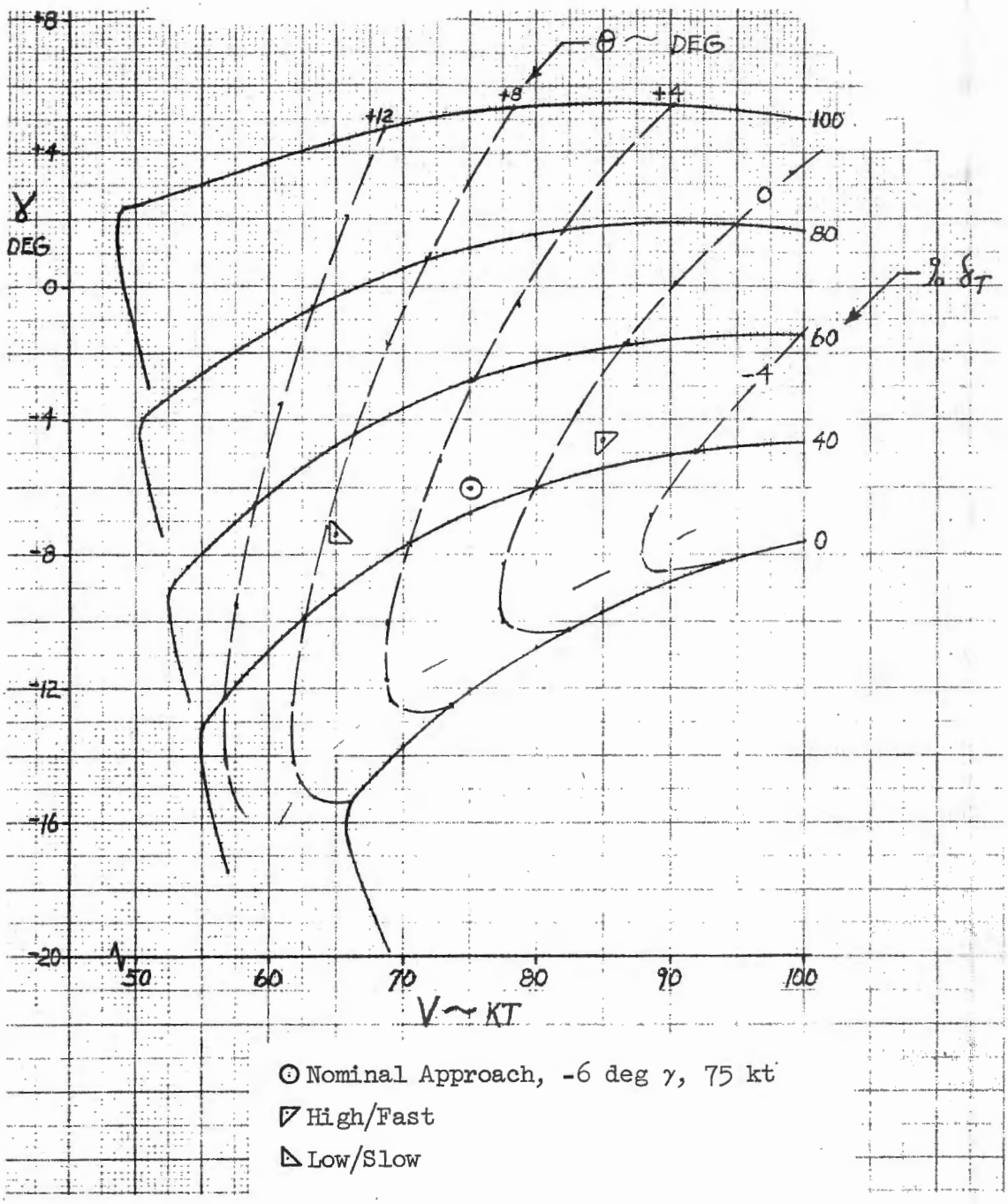

Figure E-3b. Performance Curve for BSL2

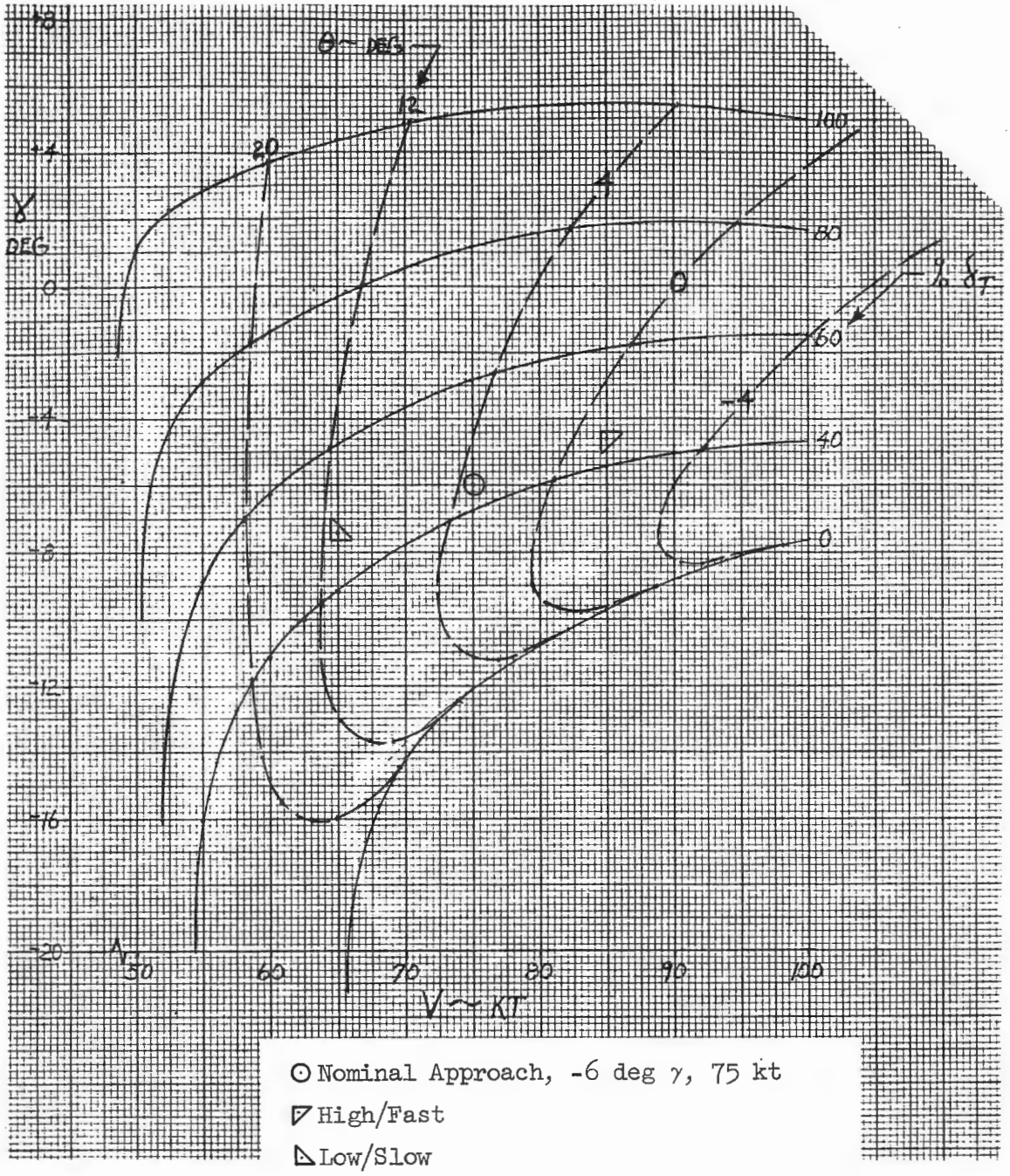

Figure E-3c. Performance Curve for BSL2 RLD

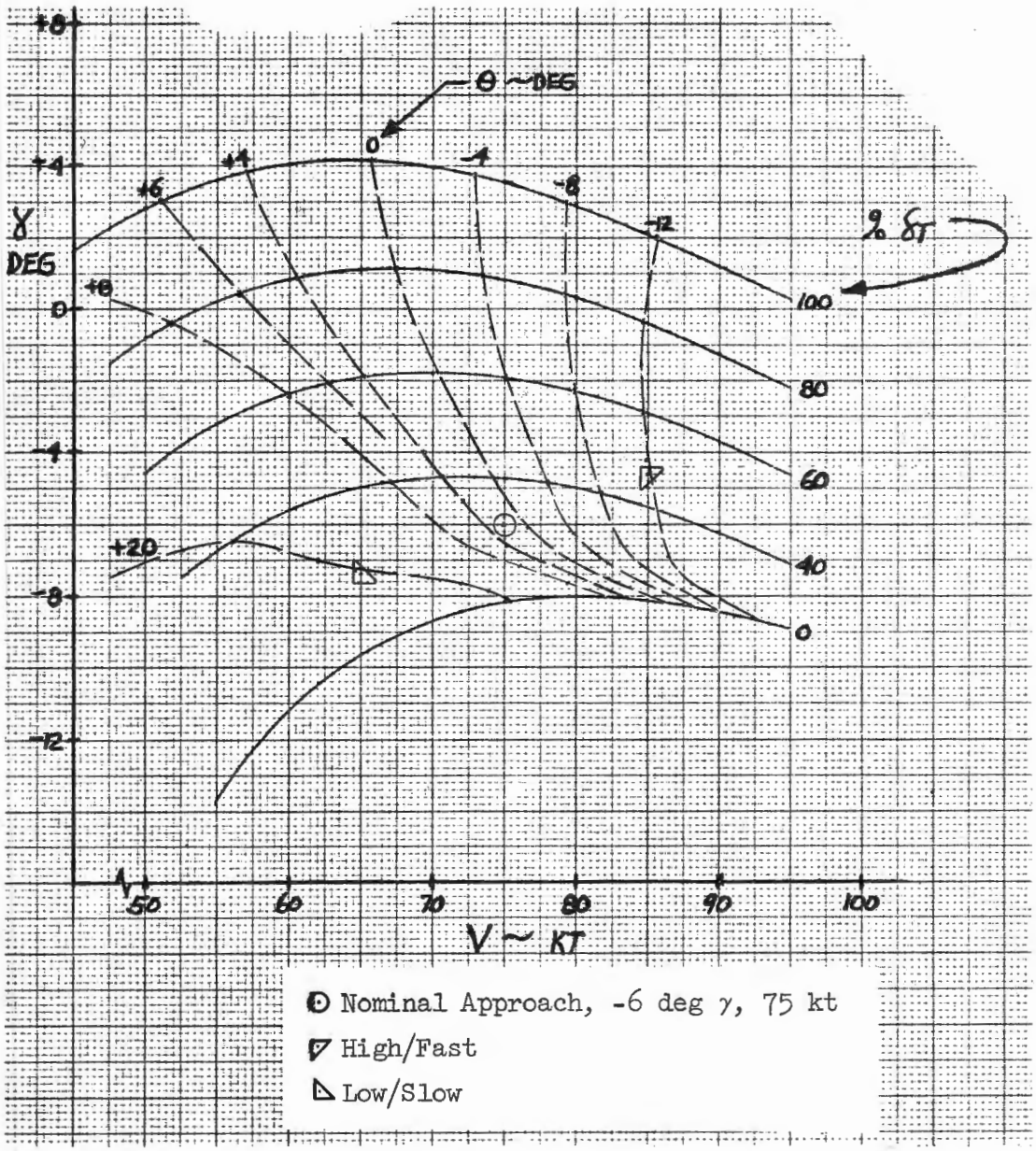

Figure E-3d. Performance Curve for AP1

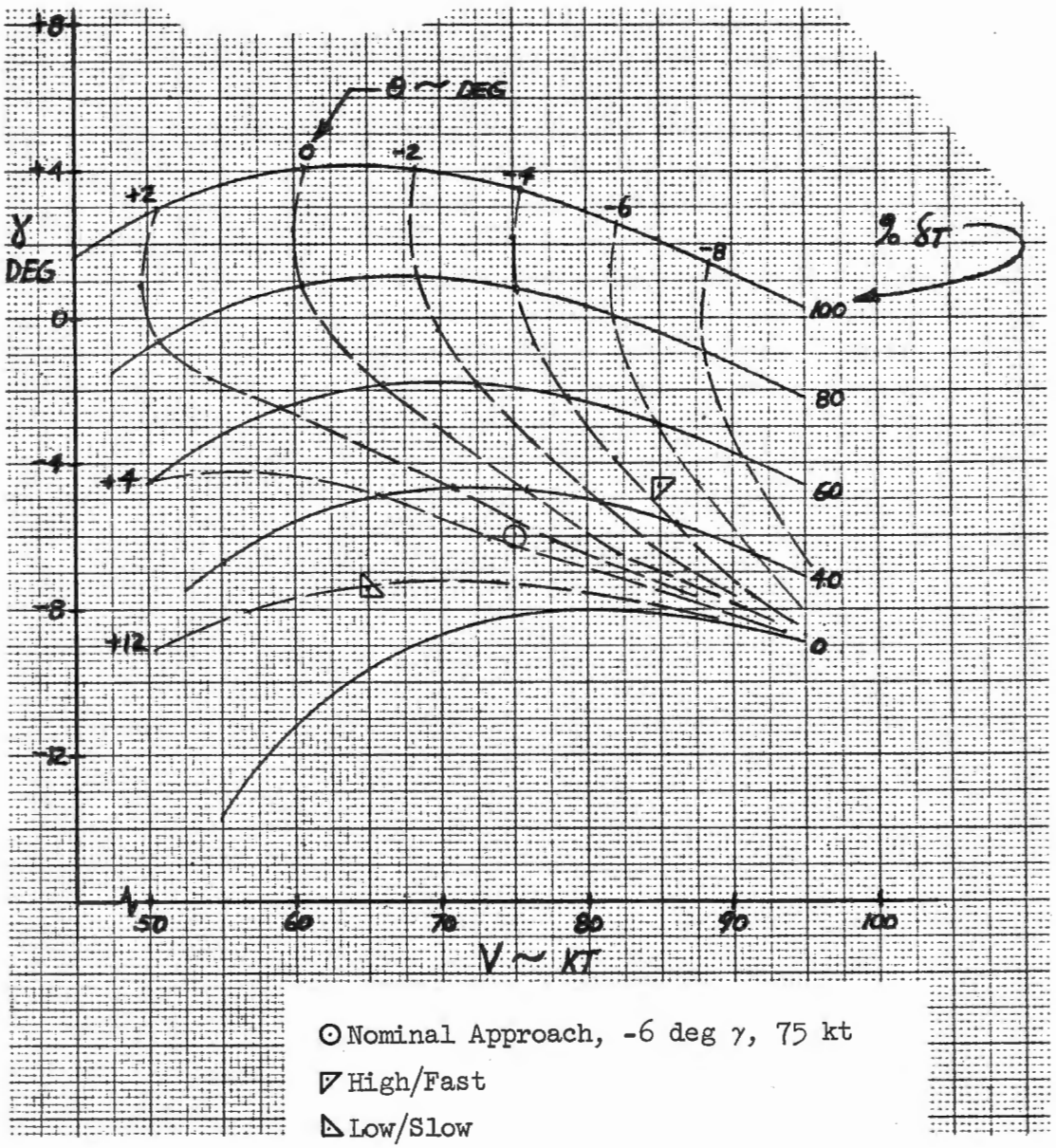

Figure E-3e. Performance Curve for AP2

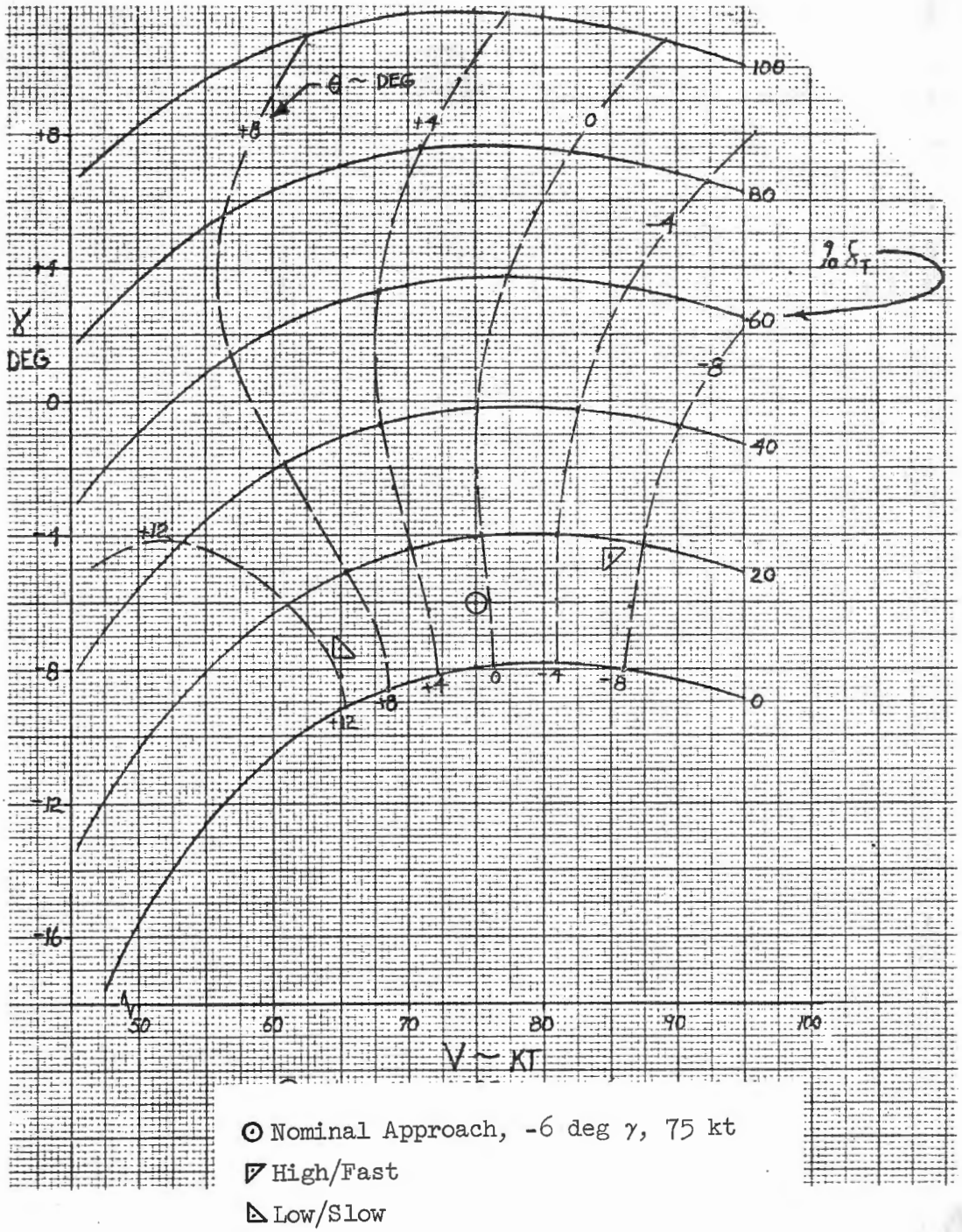

Figure E-3f. Performance Curve for AP3

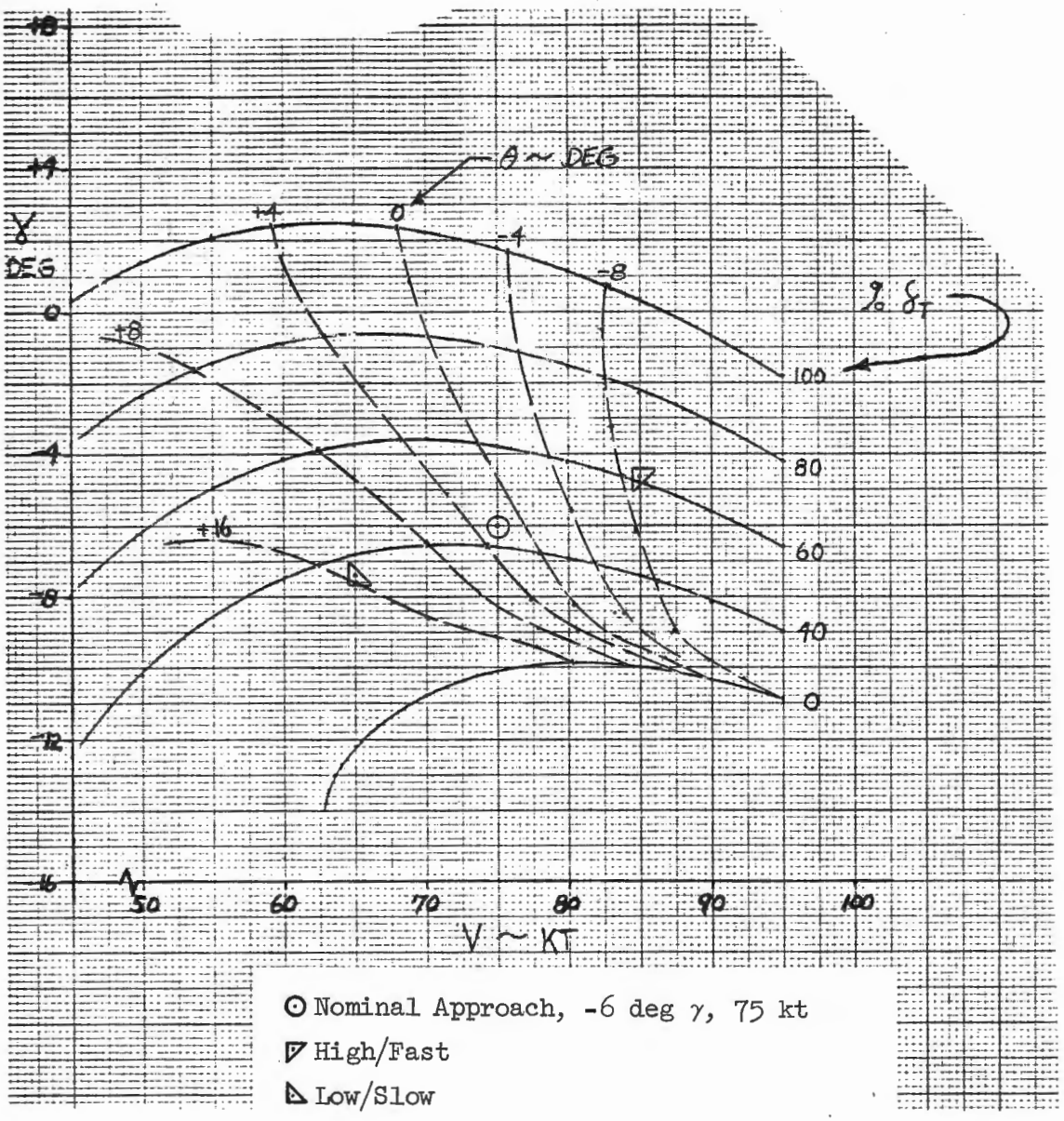

Figure E-3g. Performance Curve for AP5

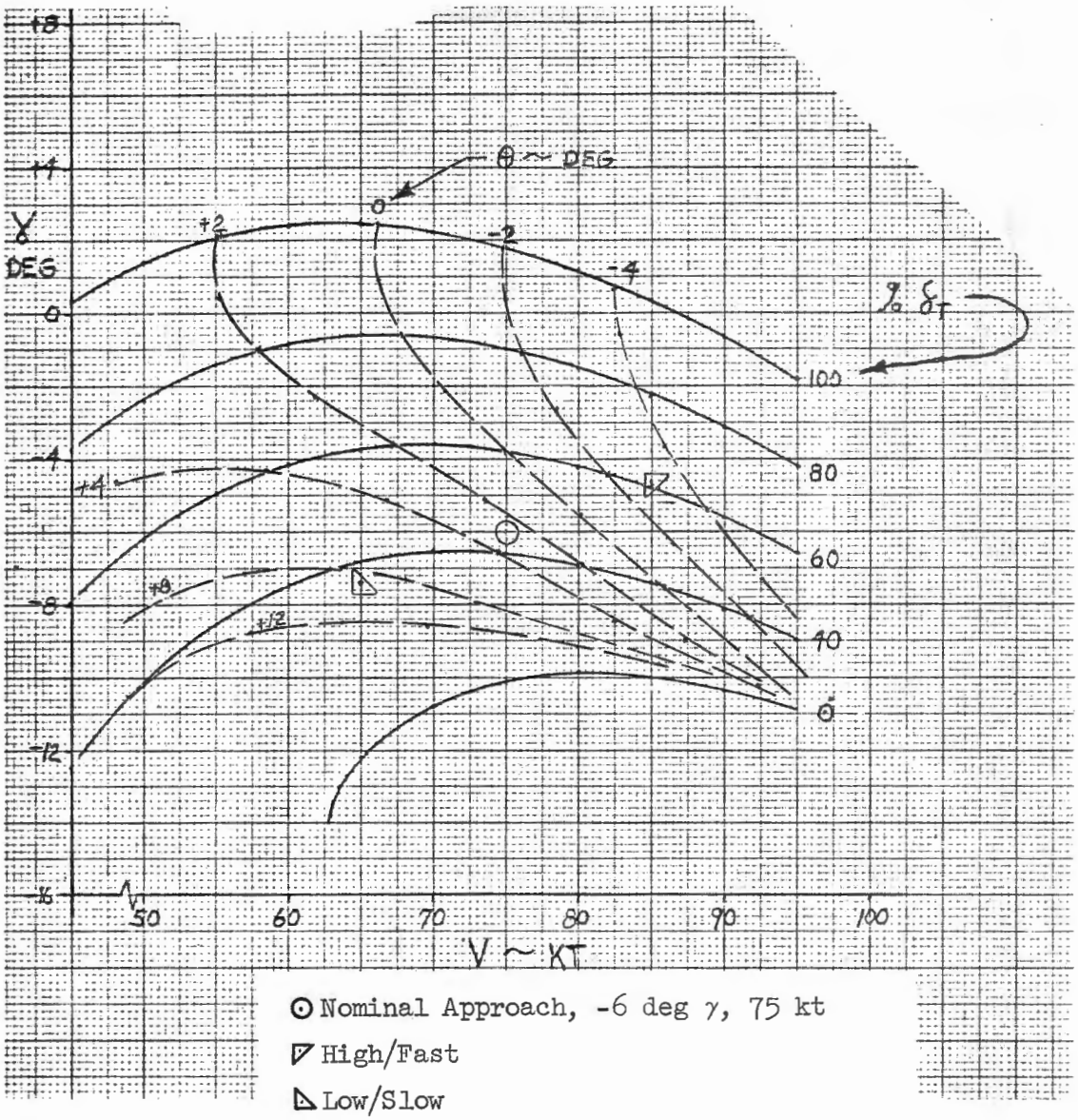

Figure E-3h. Performance Curve for AP6

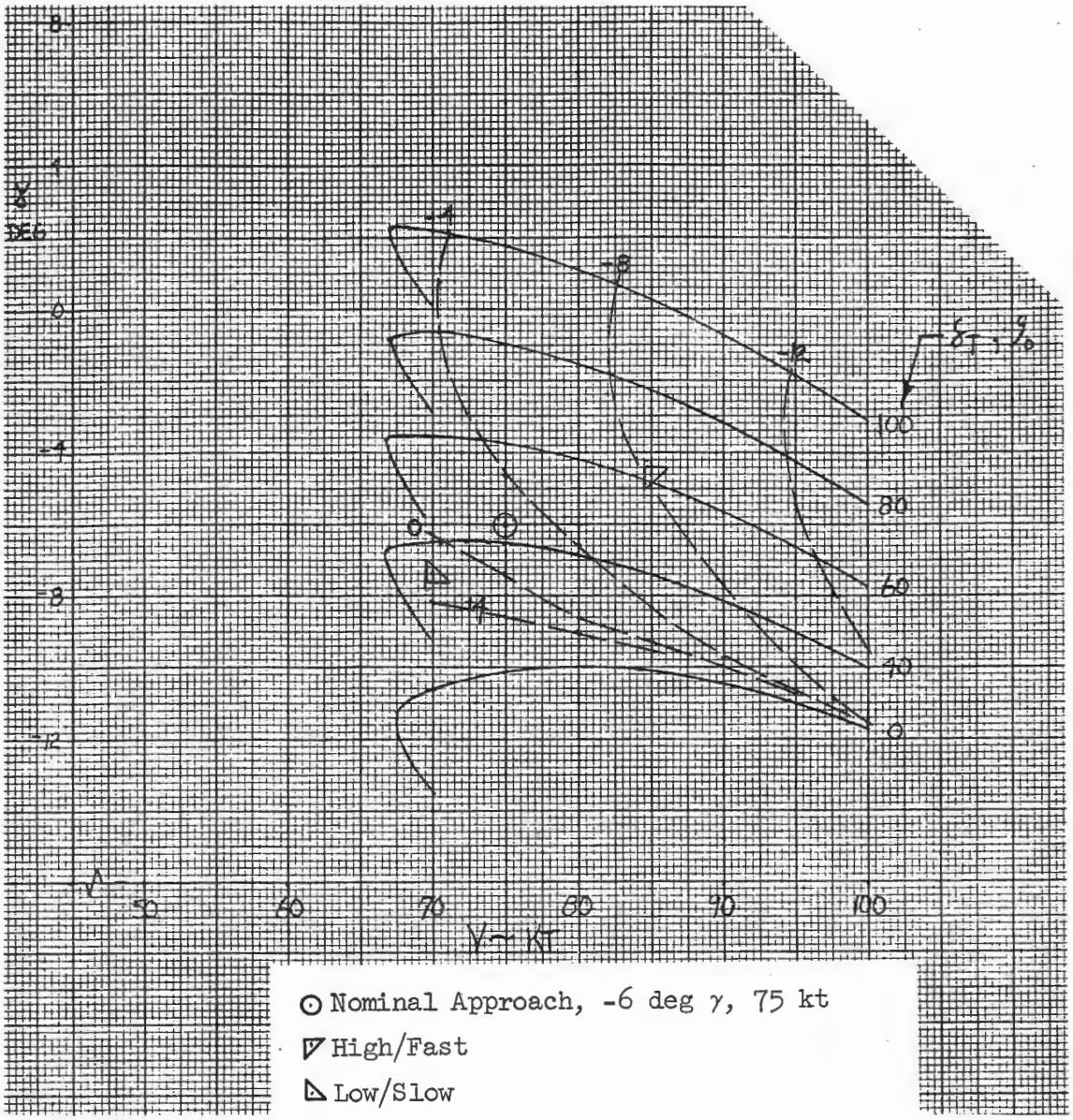

Figure E-3i. Performance Curve for AP6 SR

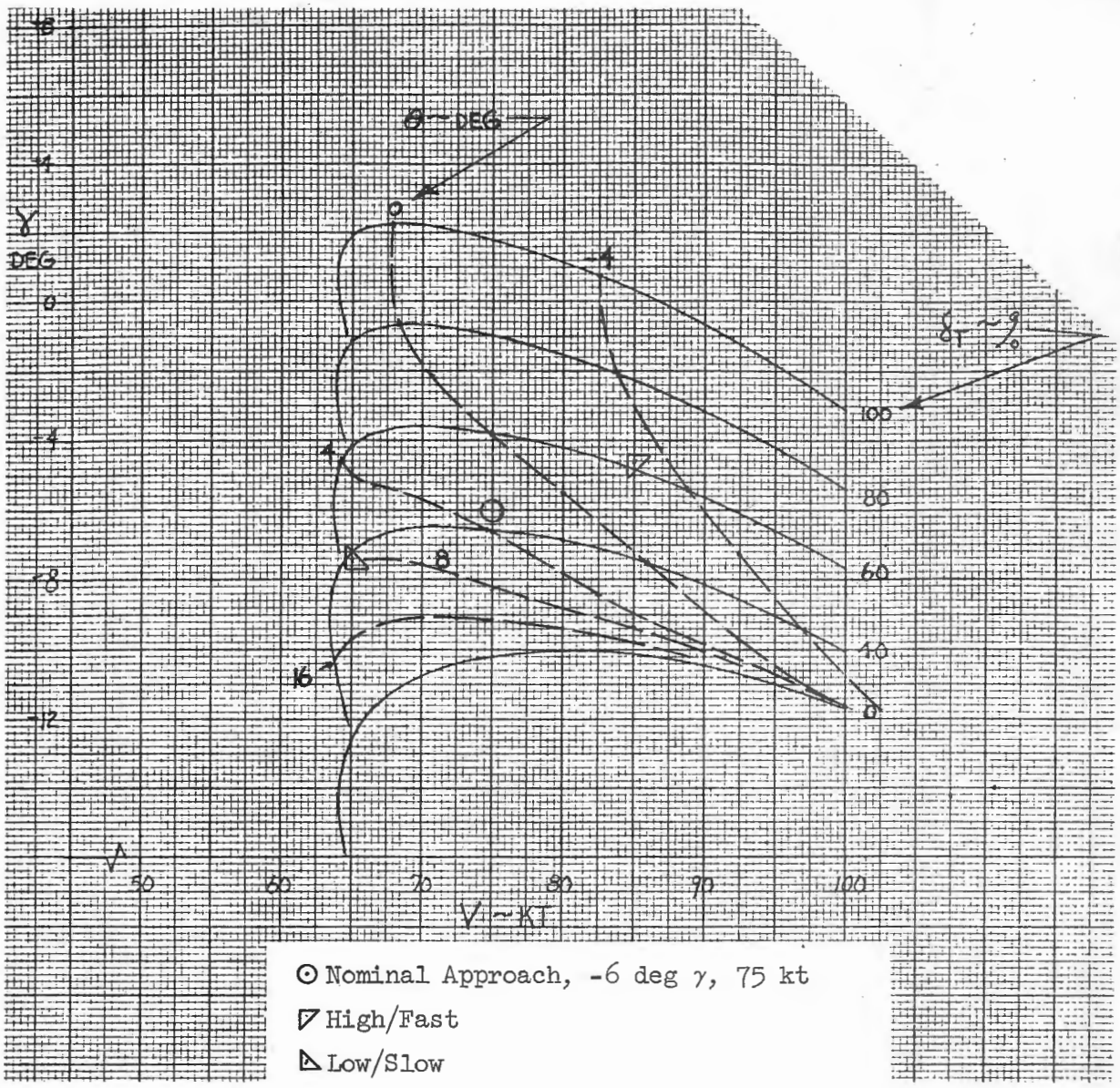

Figure E-3j. Performance Curve for AP6 RLD

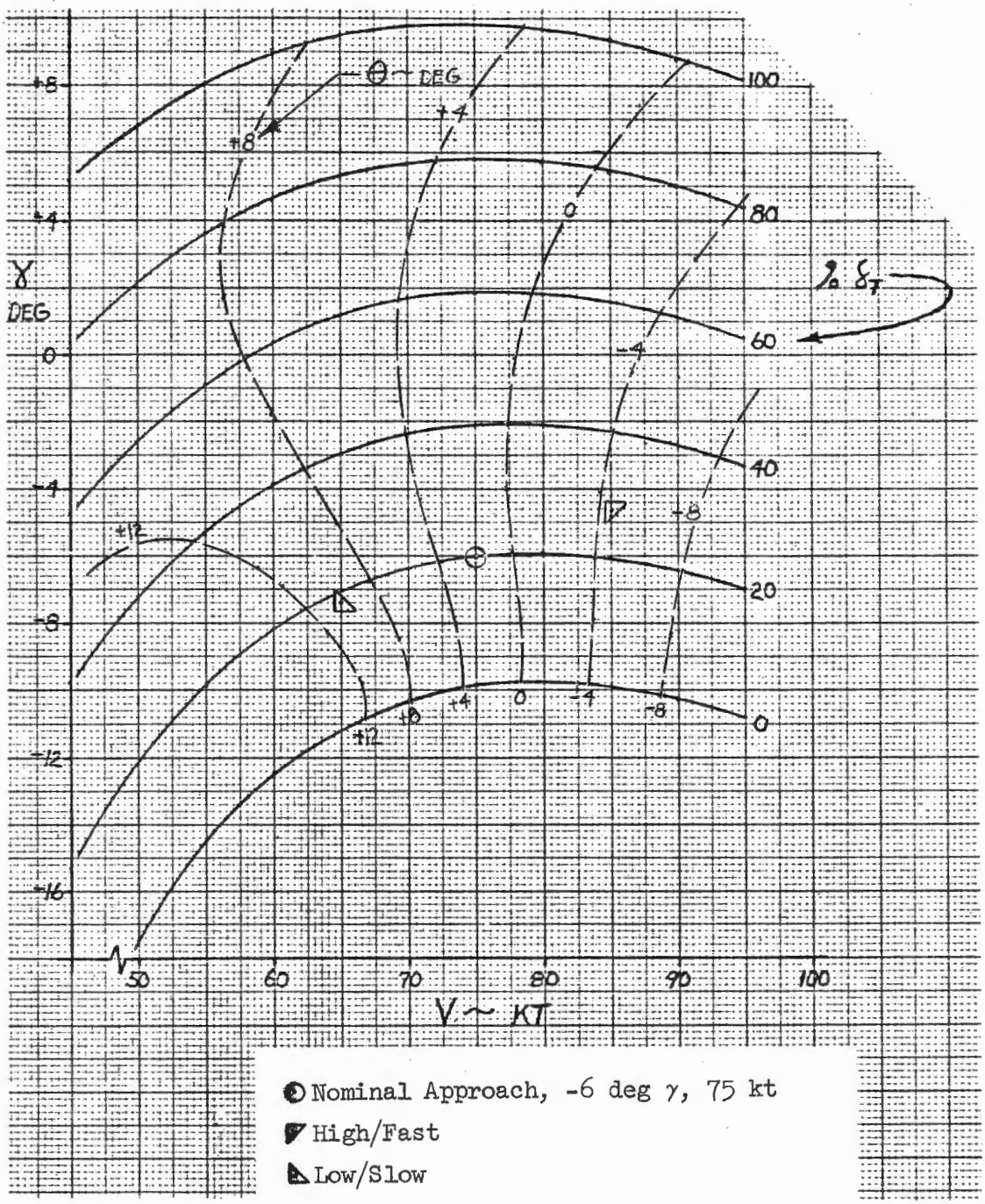

Figure E-3k. Performance Curve for AP7

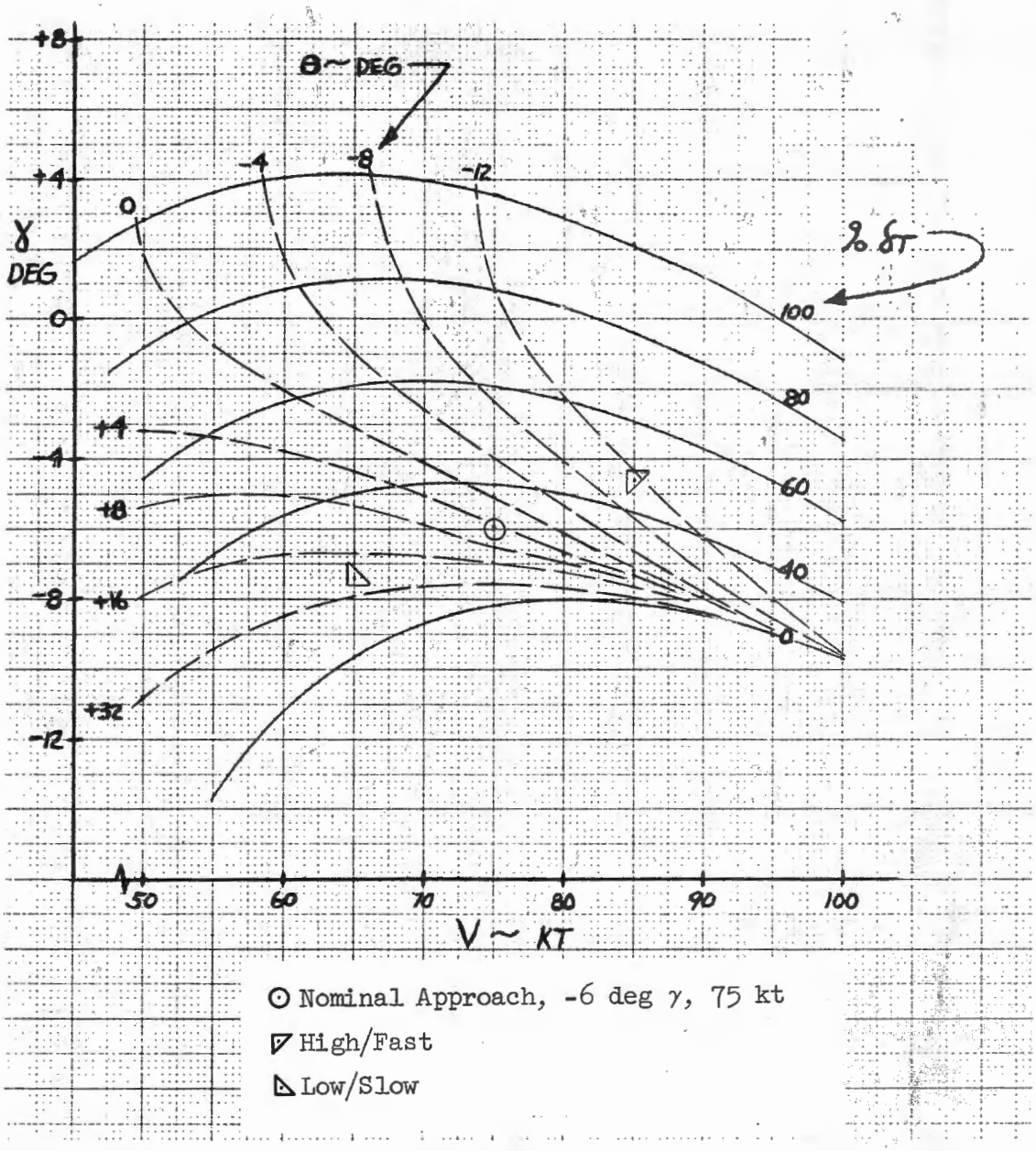

Figure E-31. Performance Curve for AP10

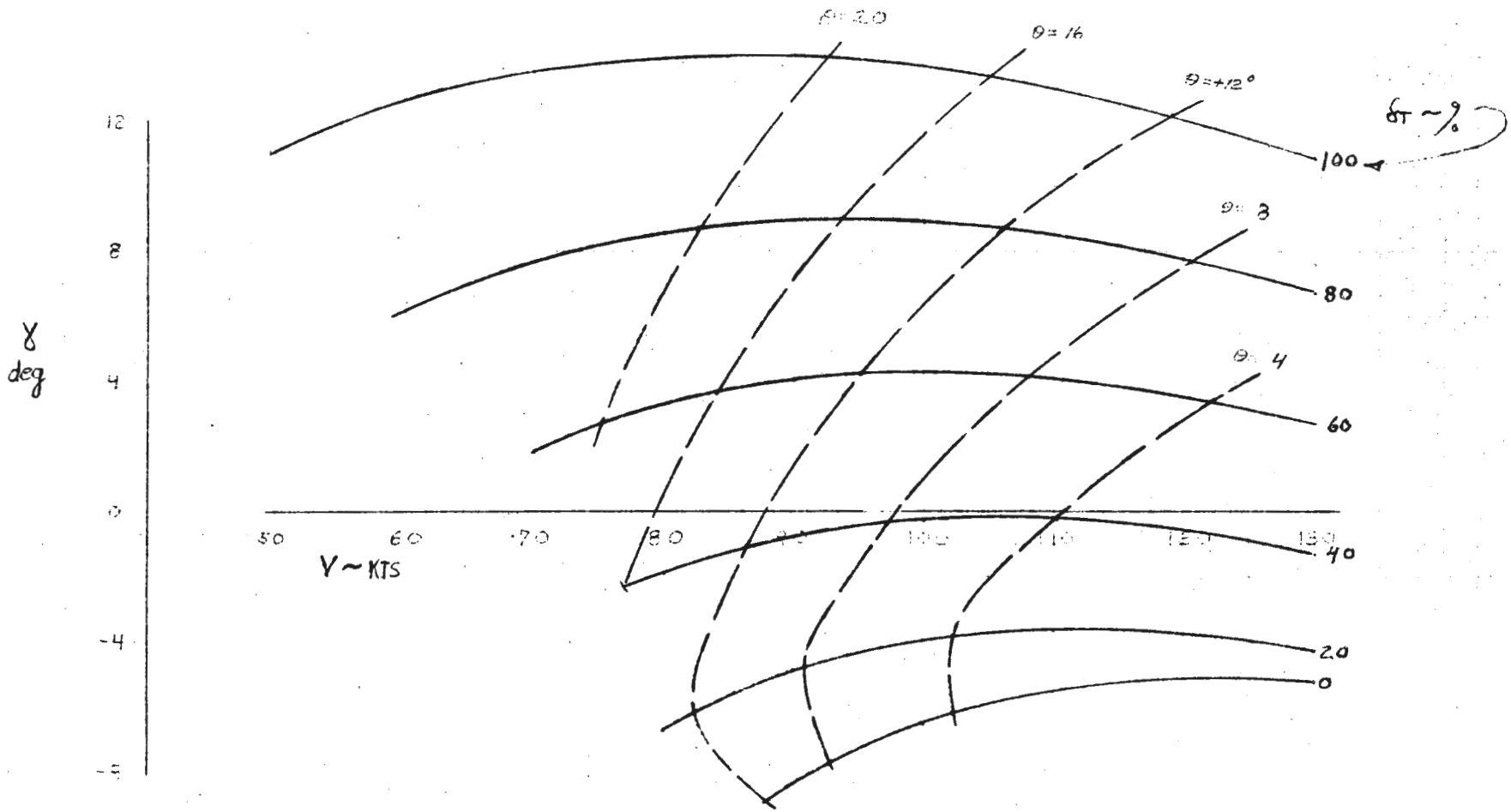

Figure E-3m. Performance Curve for BSL30 or AP30, 30 deg δ_f

TABLE E-1a

LONGITUDINAL STABILITY DERIVATIVES

Approach Configuration

Aircraft: BSL1

V_o (kt)	65	75	85
γ_o (deg)	-7.4	-6.0	-4.6
θ_o (deg)	9.70	2.67	-2.70
δ_{T_o} (%)	48.3	44.1	44.7
X_u^* (1/sec)	-.12990	-.1007	-.08167
Z_u^* (1/sec)	-.4575	-.421	-.3817
X_w (1/sec)	.10080	.09787	.09336
Z_w (1/sec)	-.4108	-.4266	-.4551
g/U_o (1/sec)	.293	.252	.224
$\tan^{-1}\left[\frac{-Z_{\delta_T}}{X_{\delta_T}}\right]$ (deg)	67.0	61.0	55.5
M_u^* (1/sec-ft)	.0002212	.000262	.0003528
M_w (1/sec-ft)	.0009134	.0014009	.0019533
$M_{\dot{w}}$ (1/ft)	-.0008847	-.0008847	-.0008847
M_q (1/sec)	-.5279	-.6091	-.6903
$Z_{\dot{w}}$ (1/1)	.02687	.02687	.02687
Z_q (ft/sec-rad)	2.71	3.13	3.55
M_{δ_e} (1/sec^2-rad)	-.5378	-.7020	-.8730
Z_{δ_e} (ft/sec^2-rad)	-2.785	-3.707	-4.762
X_{δ_T} (ft/sec^2-%)	.06002	.06757	.07227
Z_{δ_T} (ft/sec^2-%)	-.14119	-.12212	-.10509
T_{δ_T} (ft/sec^2-%)		.1395	

TABLE E-1b

LONGITUDINAL STABILITY DERIVATIVES

Approach Configuration

Aircraft: BSL2

V_o (kt)	65	75	85
γ_o (deg)	-7.4	-6.0	-4.6
θ_o (deg)	7.5	2.4	-1.2
δ_{T_o} (%)	48.1	44.1	44.8
X_u^* (1/sec)	-.1329	-.1009	-.08081
Z_u^* (1/sec)	-.4641	-.4212	-.3785
X_w (1/sec)	.04421	.04799	.04975
Z_w (1/sec)	-.5222	-.5554	-.6012
g/U_o (1/sec)	.293	.252	.224
$\tan^{-1}\left[\frac{-Z_{\delta_T}}{X_{\delta_T}}\right]$ (deg)	64.6	60.8	57.3
M_u^* (1/sec-ft)	.000260	.0002662	.0003227
M_w (1/sec-ft)	.001795	.002270	.002830
$M_{\dot{w}}$ (1/ft)	-.0008847	-.0008847	-.0008847
M_q (1/sec)	-.5279	-.6091	-.6903
$Z_{\dot{w}}$ (1/1)	.02687	.02687	.02687
Z_q (ft/sec-rad)	2.71	3.13	3.55
M_{δ_e} (1/sec^2-rad)	-.5362	-.7014	-.8802
Z_{δ_e} (ft/sec^2-rad)	-2.785	-3.707	-4.762
X_{δ_T} (ft/sec^2-%)	.06361	.06788	.07077
Z_{δ_T} (ft/sec^2-%)	-.1341	-.1213	-.1101

TABLE E-1c

LONGITUDINAL STABILITY DERIVATIVES

Approach Configuration

Aircraft: BSL2 RLD

V_o (kt)	65	75	85
γ_o (deg)	-7.4	-6.0	-4.6
θ_o (deg)	10.85	3.33	-1.08
δ_{T_o} (%)	48.4	44.1	44.8
X_u^* (1/sec)	-.13680	-.10101	-.08056
Z_u^* (1/sec)	-.4707	-.4213	-.3776
X_w (1/sec)	.12973	.08482	.06276
Z_w (1/sec)	-.3539	-.4602	-.5575
g/U_o (1/sec)	.293	.252	.224
$\tan^{-1}\left[\frac{-Z_{\delta_T}}{X_{\delta_T}}\right]$ (deg)	61.7	60.7	57.7
M_u^* (1/sec-ft)	.0003079	.0002641	.0003163
M_w (1/sec-ft)	.0004869	.0015855	.002534
$M_{\dot{w}}$ (1/ft)	-.0008847	-.0008847	-.0008847
M_q (1/sec)	-.5279	-.6091	-.6903
$Z_{\dot{w}}$ (1/1)	.02687	.02687	.02687
Z_q (ft/sec-rad)	2.71	3.13	3.55
M_{δ_e} (1/sec^2-rad)	-.5384	-.7036	-.8810
Z_{δ_e} (ft/sec^2-rad)	-2.785	-3.707	-4.762
X_{δ_T} (ft/sec^2-%)	.06777	.06799	.07037
Z_{δ_T} (ft/sec^2-%)	-.12599	-.12102	-.11142

TABLE E-1d

LONGITUDINAL STABILITY DERIVATIVES

Approach Configuration

Aircraft: AP1

V_o (kt)	65	75	85
γ_o (deg)	-7.4	-6.0	-4.6
θ_o (deg)	21.2	1.87	-11.9
δ_{T_o} (%)	23.1	30.6	46.8
X_u^* (1/sec)	-.06641	-.06898	-.07548
Z_u^* (1/sec)	-.4207	-.3879	-.3553
X_w (1/sec)	.2366	.2146	.1967
Z_w (1/sec)	-.2406	-.2601	-.3029
g/U_o (1/sec)	.293	.252	.224
$\tan^{-1}\left[\frac{-Z_{\delta_T}}{X_{\delta_T}}\right]$ (deg)	98.3	81.0	67.3
M_u^* (1/sec-ft)	-.0002612	-.0001454	.0002264
M_w (1/sec-ft)	-.001517	-.0003457	.0007516
$M_{\dot{w}}$ (1/ft)	-.0008847	-.0008847	-.0008847
M_q (1/sec)	-.5279	-.6091	-.6903
$Z_{\dot{w}}$ (1/1)	.02687	.02687	.02687
Z_q (ft/sec-rad)	2.71	3.13	3.55
M_{δ_e} (1/sec^2-rad)	-.5336	-.6998	-.8147
Z_{δ_e} (ft/sec^2-rad)	-2.785	-3.707	-4.762
X_{δ_T} (ft/sec^2-%)	-.05593	.03862	.05887
Z_{δ_T} (ft/sec^2-%)	-.3826	-.2437	-.1410

TABLE E-1e

LONGITUDINAL STABILITY DERIVATIVES

Approach Configuration

Aircraft: AP2

V_o (kt)	65	75	85
γ_o (deg)	-7.4	-6.0	-4.6
θ_o (deg)	12.4	3.0	-4.7
δ_{T_o} (%)	22.1	30.6	46.9
X_u^* (1/sec)	-.04478	-.04964	-.06058
Z_u^* (1/sec)	-.3440	-.2695	-.1974
X_w (1/sec)	.1848	.1768	.1709
Z_w (1/sec)	-.4367	-.4915	-.5719
g/U_o (1/sec)	.293	.252	.224
$\tan^{-1}\left[\frac{-Z_{\delta_T}}{X_{\delta_T}}\right]$ (deg)	100.6	90.2	84.6
M_u^* (1/sec-ft)	-.0006742	-.0006745	-.0006211
M_w (1/sec-ft)	-.0004882	.0006596	.001923
$M_{\dot{w}}$ (1/ft)	-.0008847	-.0008847	-.0008847
M_q (1/sec)	-.5279	-.6091	-.6903
$Z_{\dot{w}}$ (1/1)	.02687	.02687	.02687
Z_q (ft/sec-rad)	2.71	3.13	3.55
M_{δ_e} (1/sec^2-rad)	-.5388	-.7027	-.8624
Z_{δ_e} (ft/sec^2-rad)	-2.785	-3.707	-4.762
X_{δ_T} (ft/sec^2-%)	-.1105	-.001479	.03585
Z_{δ_T} (ft/sec^2-%)	-.5896	-.4886	-.3823
M_{δ_T}		.00142	

TABLE E-1f

LONGITUDINAL STABILITY DERIVATIVES

Approach Configuration

Aircraft: AP3

V_o (kt)	65	75	85
γ_o (deg)	-7.4	-6.0	-4.6
θ_o (deg)	11.02	.85	-6.7
δ_{T_o} (%)	9.04	9.99	17.6
X_u^* (1/sec)	-.07976	-.06402	-.05809
Z_u^* (1/sec)	-.5286	-.4683	-.4040
X_w (1/sec)	.1956	.1862	.1788
Z_w (1/sec)	-.3811	-.4163	-.4733
g/U_o (1/sec)	.293	.252	.224
$\tan^{-1}\left[\frac{-Z_{\delta_T}}{X_{\delta_T}}\right]$ (deg)	85.4	73.7	62.8
M_u^* (1/sec-ft)	-.000033	-.000024	-.0000134
M_w (1/sec-ft)	-.001343	-.0005369	.0002624
$M_{\dot{w}}$ (1/ft)	-.0008847	-.0008847	-.0008847
M_q (1/sec)	-.5279	-.6091	-.6903
$Z_{\dot{w}}$ (1/1)	.02687	.02687	.02687
Z_q (ft/sec-rad)	2.71	3.13	3.55
M_{δ_e} (1/sec^2-rad)	-.5384	-.6969	-.8503
Z_{δ_e} (ft/sec^2-rad)	-2.785	-3.707	-4.762
X_{δ_T} (ft/sec^2-%)	.02592	.06915	.09003
Z_{δ_T} (ft/sec^2-%)	-.3225	-.2368	-.1753

TABLE E-1g

LONGITUDINAL STABILITY DERIVATIVES

Approach Configuration

Aircraft: AP5

V_o (kt)	65	75	85
γ_o (deg)	-7.4	-6.0	-4.6
θ_o (deg)	15.4	1.99	-9.1
δ_{T_o} (%)	36.4	44.06	61.6
X_u^* (1/sec)	-.06661	-.07630	-.08634
Z_u^* (1/sec)	-.3488	-.3341	-.3102
X_w (1/sec)	.2190	.2003	.1830
Z_w (1/sec)	-.2885	-.3019	-.3439
g/U_o (1/sec)	.293	.252	.224
$\tan^{-1}\left[\frac{-Z_{\delta_T}}{X_{\delta_T}}\right]$ (deg)	91.9	82.5	71.6
M_u^* (1/sec-ft)	-.0004340	-.0002320	.0001388
M_w (1/sec-ft)	-.0008221	.000099	.001202
$M_{\dot{w}}$ (1/ft)	-.0008847	-.0008847	-.0008847
M_q (1/sec)	-.5279	-.6091	-.6903
$Z_{\dot{w}}$ (1/1)	.02687	.02687	.02687
Z_q (ft/sec-rad)	2.71	3.13	3.55
M_{δ_e} (1/sec^2-rad)	-.5384	-.7002	-.8350
Z_{δ_e} (ft/sec^2-rad)	-2.785	-3.707	-4.762
X_{δ_T} (ft/sec^2-%)	-.01138	.03259	.05312
Z_{δ_T} (ft/sec^2-%)	-.3512	-.2467	-.1596

TABLE E-1h

LONGITUDINAL STABILITY DERIVATIVES

Approach Configuration

Aircraft: AP6

V_o (kt)	65	75	85
γ_o (deg)	-7.4	-6.0	-4.6
θ_o (deg)	8.7	2.81	-3.05
δ_{T_o} (%)	36.1	44.1	61.7
X_u^* (1/sec)	-.03935	-.05080	-.06486
Z_u^* (1/sec)	-.2549	-.2002	-.1374
X_w (1/sec)	.1580	.1536	.1476
Z_w (1/sec)	-.5030	-.5468	-.6264
g/U_o (1/sec)	.293	.252	.224
$\tan^{-1}\left[\frac{-Z_{\delta_T}}{X_{\delta_T}}\right]$ (deg)	96.1	90.5	85.6
M_u^* (1/sec-ft)	-.00100	-.0008629	-.0007629
M_w (1/sec-ft)	.0004188	.001236	.002441
$M_{\dot{w}}$ (1/ft)	-.0008847	-.0008847	-.0008847
M_q (1/sec)	-.5279	-.6091	-.6903
$Z_{\dot{w}}$ (1/1)	.02687	.02687	.02687
Z_q (ft/sec-rad)	2.71	3.13	3.55
M_{δ_e} (1/sec^2-rad)	-.5372	-.7023	-.8712
Z_{δ_e} (ft/sec^2-rad)	-2.785	-3.707	-4.762
X_{δ_T} (ft/sec^2-%)	-.05288	-.004081	.0280
Z_{δ_T} (ft/sec^2-%)	-.4975	-.4388	-.3605

TABLE E-1i

LONGITUDINAL STABILITY DERIVATIVES

Approach Configuration

Aircraft: AP6 SR

V_o (kt)	70	75	85
γ_o (deg)	-7.4	-6.0	-4.6
θ_o (deg)	2.14	-2.4	-8.17
δ_{T_o} (%)	33.8	43.9	61.6
X_u^* (1/sec)	-.05524	-.05731	-.07002
Z_u^* (1/sec)	-.2814	-.2350	-.17884
X_w (1/sec)	.16238	.15406	.14790
Z_w (1/sec)	-.4919	-.5460	-.6262
g/U_o (1/sec)	.272	.252	.224
$\tan^{-1}\left[\frac{-Z_{\delta_T}}{X_{\delta_T}}\right]$ (deg)	92.9	89.2	83.8
M_u^* (1/sec-ft)	-.0008319	-.0008200	-.0006436
M_w (1/sec-ft)	.0007820	.0016082	.002853
$M_{\dot{w}}$ (1/ft)	-.0008847	-.0008847	-.0008847
M_q (1/sec)	-.5685	-.6091	-.6903
$Z_{\dot{w}}$ (1/1)	.02687	.02687	.02687
Z_q (ft/sec-rad)	2.93	3.13	3.55
M_{δ_e} (1/sec^2-rad)	-.6134	-.6860	-.8409
Z_{δ_e} (ft/sec^2-rad)	-3.230	-3.707	-4.762
X_{δ_T} (ft/sec^2-%)	-.02257	.005379	.03410
Z_{δ_T} (ft/sec^2-%)	-.4520	-.3904	-.3125

TABLE E-1j

LONGITUDINAL STABILITY DERIVATIVES

Approach Configuration

Aircraft: AP6 RLD

V_o (kt)	65	75	85
γ_o (deg)	-7.4	-6.0	-4.6
θ_o (deg)	7.76	2.81	-3.05
δ_{T_o} (%)	38.8	44.1	61.7
X_u^* (1/sec)	-.04193	-.05080	-.06486
Z_u^* (1/sec)	-.3788	-.2002	-.13744
X_w (1/sec)	.14844	.15358	.14766
Z_w (1/sec)	-.3376	-.5467	-.6263
g/U_o (1/sec)	.293	.252	.224
$\tan^{-1}\left[\frac{-Z_{\delta_T}}{X_{\delta_T}}\right]$ (deg)	99.2	90.5	85.6
M_u^* (1/sec-ft)	-.0007695	-.0008629	-.0007630
M_w (1/sec-ft)	.0002945	.0012356	.002440
$M_{\dot{w}}$ (1/ft)	-.0008847	-.0008847	-.0008847
M_q (1/sec)	-.5279	-.6091	-.6903
$Z_{\dot{w}}$ (1/1)	.02687	.02687	.02687
Z_q (ft/sec-rad)	2.71	3.13	3.55
M_{δ_e} (1/sec^2-rad)	-.5364	-.7023	-.8712
Z_{δ_e} (ft/sec^2-rad)	-2.785	-3.707	-4.762
X_{δ_T} (ft/sec^2-%)	-.04642	-.004081	.02800
Z_{δ_T} (ft/sec^2-%)	-.2868	-.4388	-.3605

TABLE E-1k

LONGITUDINAL STABILITY DERIVATIVES

Approach Configuration

Aircraft: AP7

V_o (kt)	65	75	85
γ_o (deg)	-7.4	-6.0	-4.6
θ_o (deg)	10.2	1.89	-4.6
δ_{T_o} (%)	18.3	19.95	27.8
X_u^* (1/sec)	-.08029	-.07193	-.06822
Z_u^* (1/sec)	-.4681	-.4253	-.3730
X_w (1/sec)	.1753	.1676	.1598
Z_w (1/sec)	-.4196	-.4503	-.5055
g/U_o (1/sec)	.293	.252	.224
$\tan^{-1}\left[\frac{-Z_{\delta_T}}{X_{\delta_T}}\right]$ (deg)	87.6	76.8	66.5
M_u^* (1/sec-ft)	-.0001302	-.000079	-.000044
M_w (1/sec-ft)	-.001040	-.0003112	.0004587
$M_{\dot{w}}$ (1/ft)	-.0008847	-.0008847	-.0008847
M_q (1/sec)	-.5279	-.6091	-.6903
$Z_{\dot{w}}$ (1/1)	.02687	.02687	.02687
Z_q (ft/sec-rad)	2.71	3.13	3.55
M_{δ_e} (1/sec^2-rad)	-.5381	-.6999	-.8629
Z_{δ_e} (ft/sec^2-rad)	-2.785	-3.707	-4.762
X_{δ_T} (ft/sec^2-%)	.01431	.05966	.08316
Z_{δ_T} (ft/sec^2-%)	-.3399	-.2552	-.1912

TABLE E-11

LONGITUDINAL STABILITY DERIVATIVES

Approach Configuration

Aircraft: AP10

V_o (kt)	65	75	85
γ_o (deg)	-7.4	-6.0	-4.6
θ_o (deg)	23.4	4.56	-11.5
δ_{T_o} (%)	23.4	30.7	46.8
X_u^* (1/sec)	-.03983	-.05028	-.06351
Z_u^* (1/sec)	-.3200	-.2732	-.2284
X_w (1/sec)	.2363	.2145	.19667
Z_w (1/sec)	-.2417	-.2604	-.3029
g/U_o (1/sec)	.293	.252	.224
$\tan^{-1}\left[\frac{-Z_{\delta_T}}{X_{\delta_T}}\right]$ (deg)	100.9	90.0	83.1
M_u^* (1/sec-ft)	-.0004227	-.0006248	-.0005580
M_w (1/sec-ft)	-.0015950	-.0004293	.0007414
$M_{\dot{w}}$ (1/ft)	-.0008847	-.0008847	-.0008847
M_q (1/sec)	-.5279	-.6091	-.6903
$Z_{\dot{w}}$ (1/1)	.02687	.02687	.02687
Z_q (ft/sec-rad)	2.71	3.13	3.55
M_{δ_e} (1/sec^2-rad)	-.5303	-.7065	-.8173
Z_{δ_e} (ft/sec^2-rad)	-2.785	-3.707	-4.762
X_{δ_T} (ft/sec^2-%)	-.11771	-.00017046	.04050
Z_{δ_T} (ft/sec^2-%)	-.6132	-.4800	-.3358

TABLE E-2a

LONGITUDINAL TRANSFER FUNCTIONS
(Approach Configuration)
Aircraft: BSL 1

TRIM CONDITION			
V_o (kt)	65	75	85
γ_o (deg)	-7.4	-6.0	-4.6
θ_o (deg)	9.70	2.67	-2.70
δ_{T_o} (%)	48.3	44.1	44.7
DENOMINATOR			
Δ	(-.109)(.93)[.54;.33]	(-.145)(1.09)[.50;.32]	(-.171)(1.26)[.46;.30]
BARE AIRFRAME PERTURBATION DYNAMICS			
$N^u_{\delta_e}$	-.29(.65)(-38.)	-.37(.73)(-36.)	-.46(.83)(-35.)
$N^w_{\delta_e}$	-2.9(22.)[.22;.37]	-3.8(25.)[.187;.33]	-4.9(27.)[.165;.29]
$N^\theta_{\delta_e}$	-.54[.87;.32]	-.70[.93;.30]	-.87(.23)(.34)
$N^d_{\delta_e}$	2.9(-.105)(-2.2)(3.6)	3.8(-.061)(-2.4)(3.9)	4.9(-.030)(-2.7)(4.3)
$N^h_{\delta_e}$	2.8(-.059)(-2.3)(3.7)	3.8(-.032)(-2.5)(4.0)	4.9(-.0113)(-2.7)(4.4)
$N^u_{\delta_T}$	.060(.93)[-.182;.35]	.068(1.08)[-.136;.38]	.072(1.25)[-.121;.40]
$N^w_{\delta_T}$	-.145(.85)[.47;.191]	-.125(1.16)[.40;.21]	-.108(1.67)[.32;.22]
$N^\theta_{\delta_T}$	-.000098(.39)(1.67)	-.00026(.39)(.84)	-.00047(.37)(.62)
$N^d_{\delta_T}$	.145(-.111)(.174)(.89)	.125(.158)(-.21)(1.12)	.108(.134)(-.34)(1.39)
$N^h_{\delta_T}$	.136(-.134)(.21)(.89)	.118(.185)(-.23)(1.12)	.102(.153)(-.37)(1.40)
$N^u_{\delta_e\delta_T}$	-.032(.186)	-.047(.27)	-.063(.34)
$N^d_{\delta_e\delta_T}$	-.077(.33)	-.087(.34)	-.091(.35)
$N^{u\,d}_{\delta_e\delta_T}$	-.172(-3.6)(4.8)	-.26(-3.4)(4.8)	-.35(-3.4)(4.9)
ATTITUDE LOOP CLOSED DYNAMICS			
Δ'	(.667)(1.872)(8.292)[.786;.191][.701;.511]	(.667)(2.0674)(8.305)[.734;.167][.637;.506]	(.667)(2.244)(8.343)[.710;.147][.570;.503]
$N^{u'}_{\delta_T}$	.0400(.0733)(1.870)(8.293)[.590;.483]	.0450(.0821)(2.041)(8.308)[.530;.519]	.0502(.0833)(2.199)(8.348)[.476;.552]
$N^{\theta'}_{\delta_T}$	-.0000656(.0)(.387)(1.674)(10.)	-.000174(.0)(.394)(.839)(10.)	-.000315(.0)(.366)(.618)(10.)
$N^d_{\delta_T}$	.0967(.190)(1.876)(8.297)[.747;.396]	.0837(.180)(2.119)(8.323)[.578;.384]	.0720(.164)(2.379)(8.380)[.344;.378]
STATIC PARAMETERS			
$\left[\frac{\partial\gamma}{\partial V}\right]_{\delta_T}$ (deg/kt)	.286	.172	.0878
$\left[\frac{\partial\gamma}{\partial V}\right]_{\theta}$ (deg/kt)	3.67	1.74	.981
$\left[\frac{\partial V}{\partial\theta}\right]_{\delta_T}$ (kt/deg)	-1.33	-1.66	-2.07
$\left[\frac{\partial V}{\partial\delta_T}\right]_{\theta}$ (kt/%)	.0646	.123	.197

TABLE E-2b

LONGITUDINAL TRANSFER FUNCTIONS
(Approach Configuration)

Aircraft: BSL 2

TRIM CONDITION

V_o (kt)	65	75	85
γ_o (deg)	-7.4	-6.0	-4.6
θ_o (deg)	7.5	2.4	-1.2
δ_{T_o} (%)	48.1	44.1	44.8

BARE AIRFRAME PERTURBATION DYNAMICS

Δ	(-.182)(1.109)[.538;.345]	(-.202)(1.264)[.508;.328]	(-.215)(1.440)[.477;.309]
$N^u_{\delta_e}$	14.30(.647)	18.0(.721)	21.6(.820)
$N^w_{\delta_e}$	-2.862(21.64)[.221;.370]	-3.810(24.55)[.187;.327]	-4.893(27.21)[.164;.290]
$N^\theta_{\delta_e}$	-.534(.193)(.489)	-.70(.149)(.538)	-.876(.119)(.599)
$N^{\dot\theta}_{\delta_e}$	2.862(-.103)(-2.548)(3.977)	3.810(-.060)(-2.886)(4.412)	4.893(-.030)(-3.227)(4.868)
$N^u_{\delta_T}$	.064(1.137)[-.083;.409]	.068(1.273)[-.079;.422]	.071(1.432)[-.082;.443]
$N^w_{\delta_T}$	-.138(.925)[.442;.207]	-.125(1.177)[.393;.209]	-.113(1.549)[.334;.209]
$N^\theta_{\delta_T}$	-.000154(.328)(2.088)	-.000268(.287)(1.509)	-.000417(.243)(1.259)
$N^{\dot\theta}_{\delta_T}$	.138(.189)(-.230)(1.025)	.125(.166)(-.328)(1.230)	.113(.139)(-.457)(1.478)
$N^{\theta\,u}_{\delta_e\delta_T}$	-.034(.454)	-.047(.499)	-.062(.559)
$N^{\theta\,\dot\theta}_{\delta_e\delta_T}$	-.073(.356)	-.086(.341)	-.097(.332)
$N^{u\,\dot\theta}_{\delta_e\delta_T}$	-.182(-4.059)(5.252)	-.259(-4.014)(5.379)	-.346(-4.079)(5.609)

ATTITUDE LOOP CLOSED DYNAMICS

Δ'	(.67)(2.0)(8.3)[.74;.16][.67;.58]	(.67)(2.19)(8.30)[.72;.14][.62;.56]	(.67)(2.4)(8.3)[.72;.13][.56;.55]
$N^{u'}_{\delta_T}$	.042(.10)(2.0)(8.3)[.54;.62]	.045(.099)(2.172)(8.307)[.504;.623]	.047(.095)(2.3)(8.3)[.46;.64]
$N^{\theta'}_{\delta_T}$	-.00010(0.0)(.33)(2.1)(10.)	-.000179(0.)(.287)(1.509)(10.0)	-.00028(0.0)(.24)(1.3)(10.)
$N^{\dot\theta'}_{\delta_T}$	.092(.19)(2.0)(8.3)[.62;.40]	.083(.181)(2.231)(8.320)[.450;.375]	.075(.16)(2.5)(8.3)[.22;.36]

STATIC PARAMETERS

$\left[\frac{\partial\gamma}{\partial V}\right]_{\delta_T}$ (deg/kt)	.283	.1719	.0872
$\left[\frac{\partial\gamma}{\partial V}\right]_{\theta}$ (deg/kt)	1.490	.949	.626
$\left[\frac{\partial V}{\partial \theta}\right]_{\delta_T}$ (kt/deg)	-1.90	-2.40	-2.96
$\left[\frac{\partial V}{\partial \delta_T}\right]_{\theta}$ (kt/%)	.181	.250	.330

TABLE E-2c

LONGITUDINAL TRANSFER FUNCTIONS
(Approach Configuration)
Aircraft: BSL 2 RLD

TRIM CONDITION			
V_o (kt)	65	75	85
γ_o (deg)	-7.4	-6.0	-4.6
θ_o (deg)	10.85	3.33	-1.08
δ_{T_o} (%)	48.4	44.1	44.8
DENOMINATOR			
Δ	(-.049)(.83)[.53;.33]	(-.158)(1.13)[.50;.32]	(-.20)(1.38)[.47;.31]
BARE AIRFRAME PERTURBATION DYNAMICS			
$N^u_{\delta_e}$	-.37(.65)(-25.)	-.32(.72)(-45.)	-.31(.82)(-65.)
$N^w_{\delta_e}$	-2.9(22.)[.22;.37]	-3.8(25.)[.188;.33]	-4.9(27.)[.164;.29]
$N^\theta_{\delta_e}$	-.54[.75;.34]	-.70(.29)(.29)	-.88(.135)(.54)
$N^{\dot{\theta}}_{\delta_e}$	2.9(-.107)(-1.92)(3.4)	3.8(-.061)(-2.5)(4.1)	4.9(-.030)(-3.1)(4.7)
$N^{\dot{h}}_{\delta_e}$	2.8(-.060)(-2.0)(3.4)	3.8(-.031)(-2.6)(4.1)	4.9(-.0111)(-3.1)(4.8)
$N^u_{\delta_T}$	.068(.82)[-.117;.31]	.068(1.13)[-.110;.39]	.070(1.38)[-.097;.43]
$N^w_{\delta_T}$	-.129(1.01)[.42;.22]	-.124(1.17)[.40;.21]	-.114(1.52)[.34;.21]
$N^\theta_{\delta_T}$	-.00021[.72;.53]	-.00026(.35)(1.0)	-.00041(.25)(1.14)
$N^{\dot{\theta}}_{\delta_T}$	.129(-.0046)(.117)(.91)	.124(.160)(-.24)(1.15)	.114(.138)(-.42)(1.43)
$N^{\dot{h}}_{\delta_T}$	.120(-.042)(.165)(.92)	.117(.186)(-.26)(1.15)	.108(.157)(-.44)(1.43)
$N^{\dot{\delta}_e u}_{\delta_T}$	-.036(.122)	-.048(.33)	-.062(.49)
$N^{\theta \dot{\delta}_e}_{\delta_T}$	-.069(.39)	-.086(.34)	-.098(.33)
$N^{u \dot{\delta}_e}_{\delta_T}$	-.194(-3.1)(4.3)	-.26(-3.6)(4.9)	-.34(-3.9)(5.4)
ATTITUDE LOOP CLOSED DYNAMICS			
Δ'	(.667)(1.811)(8.291)[.842;.227][.703;.459]	(.667)(2.1002)(8.299)[.733;.159][.637;.523]	(.667)(2.348)(8.321)[.720;.131][.570;.541]
$N^{u'}_{\delta_T}$	.04517(.0631)(1.779)(8.293)[.703;.433]	.0453(.0896)(2.0739)(8.302)[.526;.548]	.0469(.0923)(2.310)(8.326)[.460;.614]
$N^{\theta'}_{\delta_T}$	-.000139(.0)(10.)[.721;.530]	-.000176(.0)(.350)(.9998)(10.)	-.000270(.0)(.254)(1.144)(10.)
$N^{\dot{\theta}'}_{\delta_T}$	.0863(.183)(1.863)(8.306)[.756;.444]	.0829(.180)(2.152)(8.317)[.549;.384]	.0763(.162)(2.448)(8.348)[.270;.363]
STATIC PARAMETERS			
$\left[\frac{\partial \gamma}{\partial V}\right]_{\delta_T}$ (deg/kt)	.289	.173	.0858
$\left[\frac{\partial \gamma}{\partial V}\right]_{\theta}$ (deg/kt)	5.41	1.41	.719
$\left[\frac{\partial V}{\partial \theta}\right]_{\delta_T}$ (kt/deg)	-1.02	-1.84	-2.71
$\left[\frac{\partial V}{\partial \delta_T}\right]_{\theta}$ (kt/%)	.0427	.155	.282

TABLE E-2d

LONGITUDINAL TRANSFER FUNCTIONS
(Approach Configuration)

Aircraft: AP 1

TRIM CONDITION

V_o (kt)	65	75	85
γ_o (deg)	-7.4	-6.0	-4.6
θ_o (deg)	21.2	1.87	-11.9
δ_{T_o} (%)	23.1	30.6	46.8

BARE AIRFRAME PERTURBATION DYNAMICS

Δ	[.248;.257][.748;.544]	(.054)(.685)[.535;.300]	(-.073)(1.020)[.433;.302]
$N^u_{\delta_e}$	-.677(1.133)(-4.61)	-.818(1.545)(-4.30)	-.963(2.101)(-3.873)
$N^w_{\delta_e}$	-2.862(21.53)[.140;.349]	-3.810(24.50)[.146;.312]	-4.893(25.24)[.160;.281]
$N^{\dot{w}}_{\delta_e}$	-.531[.446;.344]	-.697[.520;.323]	-.810[.633;.311]
$N^{\dot{q}}_{\delta_e}$	2.862(-.052)(-1.439)(2.748)	3.810(.005)(-1.728)(3.156)	4.893(.043)(-2.007)(3.517)
$N^u_{\delta_T}$	-.056(1.879)[.621;.531]	.039(.167)(.630)(-1.198)	.059(1.029)[-.566;.336]
$N^w_{\delta_T}$	-.393(-.398)[.641;.394]	-.251(-.121)[.911;.394]	-.145(1.164)[.346;.179]
$N^{\dot{w}}_{\delta_T}$	.00183[.875;.336]	.000495[.668;.305]	-.000238[.861;.508]
$N^{\dot{q}}_{\delta_T}$	.393(-.015)[.616;.514]	.251(.031)(.263)(.554)	.145(.146)(-.154)(1.059)
$N^{\dot{w}u}_{\delta_e\delta_T}$	.0297(1.946)	-.0269(-1.141)	-.048(-.162)
$N^{\dot{w}\dot{q}}_{\delta_e\delta_T}$	-.214(.006)	-.176(.130)	-.116(.227)
$N^{u\dot{q}}_{\delta_e\delta_T}$	.160[.303;1.964]	-.147(-2.753)(4.117)	-.288(-2.296)(3.773)

ATTITUDE LOOP CLOSED DYNAMICS

Δ'	(.16)(.67)(.78)(1.4)(8.3)[.38;.34]	(.25)(.36)(.67)(1.81)(8.32)[.50;.33]	(.67)(2.0)(8.5)[.76;.21][.55;.41]
$N^{u'}_{\delta_T}$	-.037(.14)(.86)(8.3)[.98;1.6]	.026(.210)(.430)(-1.169)(1.816)(8.313)	.039(-.12)(2.0)(8.5)[.50;.32]
$N^{\theta'}_{\delta_T}$	.0012(0.0)(10.)[.88;.34]	.000330(0.)(10.0)[.668;.305]	-.00016(0.0)(10.0)[.86;.51]
$N^{\dot{\theta}'}_{\delta_T}$	.26(.0066)(.14)(1.0)(1.2)(8.3)	.167(.475)(1.753)(8.299)[.989;.163]	.097(.17)(2.0)(8.5)[.62;.32]

STATIC PARAMETERS

$\left[\frac{\partial\gamma}{\partial V}\right]_{\delta_T}$ (deg/kt)	.1469	-.0155	-.127
$\left[\frac{\partial\gamma}{\partial V}\right]_{\theta}$ (deg/kt)	-.0206	-.571	-2.30
$\left[\frac{\partial V}{\partial\theta}\right]_{\delta_T}$ (kt/deg)	-.581	-.773	-1.036
$\left[\frac{\partial V}{\partial\delta_T}\right]_{\theta}$ (kt/%)	-.544	-.250	-.0585

TABLE E-2e

LONGITUDINAL TRANSFER FUNCTIONS
(Approach Configuration)

Aircraft: AP 2

TRIM CONDITION			
V_o (kt)	65	75	85
γ_o (deg)	-7.4	-6.0	-4.6
θ_o (deg)	12.4	2.97	-4.7
δ_{T_o} (%)	22.1	30.6	46.9
BARE AIRFRAME PERTURBATION DYNAMICS			
Δ	(-.047)(.602)[.806;.352]	(-.142)(1.001)[.615;.341]	(-.186)(1.310)[.547;.316]
$N^u_{\delta_e}$	-.529(1.164)(-11.78)	-.673(1.598)(-10.24)	-.836(2.273)(-8.511)
$N^w_{\delta_e}$	-2.862(21.74)[.123;.314]	-3.810(24.60)[.141;.259]	-4.893(26.68)[.184;.208]
$N^\theta_{\delta_e}$	-.536[.845;.292]	-.699(.212)(.349)	-.858(.134)(.523)
$N^{\dot{\theta}}_{\delta_e}$	2.862(-.047)(-2.309)(3.597)	3.810(.007)(-2.714)(4.123)	4.893(.043)(-3.137)(-.671)
$N^u_{\delta_T}$	-.111(1.415)[.666;.507]	-.00148(.159)(.746)(60.32)	.036(-.110)(1.138)(-1.494)
$N^w_{\delta_T}$	-.606(-.419)[.647;.393]	-.502(-.279)[.718;.407]	-.393(-.213)[.764;.411]
$N^\theta_{\delta_T}$	.00289[.811;.326]	.00181[.437;.283]	.00129[-.323;.165]
$N^{\dot{\theta}}_{\delta_T}$	.606(-.047)[.658;.488]	.502(-.058)(.342)(.477)	.393(-.156)(.168)(.874)
$N^{\theta\, u}_{\delta_e \delta_T}$	.0593(1.486)	.00104(61.68)	-.0308(-1.307)
$N^{\theta\, \dot{\theta}}_{\delta_e \delta_T}$	-.333(-.018)	-.358(.049)	-.344(.079)
$N^{u\, \dot{\theta}}_{\delta_e \delta_T}$	.316[.305;1.959]	.0056[.028;24.51]	-.175(-4.724)(6.2-0)
ATTITUDE LOOP CLOSED DYNAMICS			
Δ'	(.67)(1.7)(8.3)[.81;.24][.97;.40]	(.67)(1.99)(8.31)[.74;.16][.75;.51]	(.67)(2.2)(8.4)[.73;.13][.62;.53]
$N^{u'}_{\delta_T}$	-.074(.15)(.75)(8.3)[.96;1.5]	-.0595(.216)(.386)(2.095)(8.202)	.024(-1.4)(2.2)(8.4)[.68;.26]
$N^{\theta'}_{\delta_T}$	.0019(0.0)(10.)[.81;.33]	.00120(0.)(10.0)[.437;.283]	.00086(0.0)(10.0)[-.32;.17]
$N^{\dot{\theta}'}_{\delta_T}$	.40(-.019)(.15)(.85)(1.4)(8.3)	.335(.058)(.164)(.507)(1.760)(8.273)	.26(.10)(2.0)(8.3)[.92;.25]
STATIC PARAMETERS			
$\left[\frac{\partial \gamma}{\partial V}\right]_{\delta_T}$ (deg/kt)	.1358	-.0192	-.127
$\left[\frac{\partial \gamma}{\partial V}\right]_{\theta}$ (deg/kt)	.0594	-.209	-.452
$\left[\frac{\partial V}{\partial \theta}\right]_{\delta_T}$ (kt/deg)	-1.64	-2.20	-2.76
$\left[\frac{\partial V}{\partial \delta_T}\right]_{\theta}$ (kt/%)	-1.14	-.731	-.392

TABLE E-2f

LONGITUDINAL TRANSFER FUNCTIONS
(Approach Configuration)

Aircraft: AP 3

TRIM CONDITION

V_o (kt)	65	75	85
γ_o (deg)	-7.4	-6.0	-4.6
θ_o (deg)	11.02	.85	-6.7
δ_{T_o} (%)	9.04	9.99	17.64
BARE AIRFRAME PERTURBATION DYNAMICS			
Δ	[.236;.251][.806;.609]	(.344)(.614)[.660;.196]	(-.038)(.999)[.643;.314]
$N^u_{\delta_e}$	-.560(1.109)(-9.933)	-.709(1.515)(-8.404)	-.875(2.152)(-6.856)
$N^w_{\delta_e}$	-2.862(21.73)[.140;.391]	-3.810(24.40)[.125;.342]	-4.893(26.31)[.121;.298]
$N^\theta_{\delta_e}$	-.536[.629;.371]	-.694[.717;.343]	-.846[.854;.321]
$N^{\dot{\alpha}}_{\delta_e}$	2.862(-.072)(-2.047)(3.394)	3.810(-.0167)(-2.381)(3.823)	4.893(.019)(-2.727)(4.273)
$N^u_{\delta_T}$	.026(-2.233)[.706;.533]	.0692(.387)(-.422)(.532)	.090(.965)[-.092;.085]
$N^w_{\delta_T}$	-.331(-.097)[.969;.350]	-.243(-.063)[.974;.407]	-.180(-.022)(.340)(.594)
$N^\theta_{\delta_T}$	.000496(.172)(.989)	.000365[.969;.348]	.000214(-.136)(.246)
$N^{\dot{\alpha}}_{\delta_T}$	.331(.083)[.755;.439]	.243(.068)[.987;.431]	.180(-.041)(.298)(.825)
$N^{\theta\,u}_{\delta_e\delta_T}$	-.014(-2.133)	-.048(-.234)	-.076(.130)
$N^{\theta\,\dot{\alpha}}_{\delta_e\delta_T}$	-.179(.122)	-.170(.200)	-.154(.265)
$N^{u\,\dot{\alpha}}_{\delta_e\delta_T}$	-.074(-5.125)(6.320)	-.263(-3.209)(4.570)	-.441(-3.057)(4.563)
ATTITUDE LOOP CLOSED DYNAMICS			
Δ'	(.15)(.67)(.78)(1.5)(8.3)[.50;.37]	(.19)(.47)(.67)(1.79)(8.33)[.63;.35]	(.67)(2.0)(8.4)[.84;.20][.71;.44]
$N^{u'}_{\delta_T}$	.017(.14)(.77)(1.5)(-2.2)(8.3)	.046(.158)(-.277)(.494)(1.797)(8.324)	.060(.10)(2.0)(8.4)[.71;.32]
$N^{\theta'}_{\delta_T}$	.00033(0.0)(.17)(.99)(10.)	.000244(0.)(10.0)[.969;.348]	.00014(0.0)(-.14)(.25)(10.)
$N^{\dot{\alpha}'}_{\delta_T}$	.22(.73)(1.5)(8.3)[.98;.14]	.162(.522)(1.715)(8.314)[.953;.194]	.12(.33)(1.9)(8.4)[.88;.26]
STATIC PARAMETERS			
$\left[\frac{\partial\gamma}{\partial V}\right]_{\delta_T}$ (deg/kt)	.205	.0492	-.0554
$\left[\frac{\partial\gamma}{\partial V}\right]_{\theta}$ (deg/kt)	-.650	-2.32	2.77
$\left[\frac{\partial V}{\partial\theta}\right]_{\delta_T}$ (kt/deg)	-.864	-1.147	-1.529
$\left[\frac{\partial V}{\partial\delta_T}\right]_{\theta}$ (kt/%)	-.238	-.0815	.0673

TABLE E-2g

LONGITUDINAL TRANSFER FUNCTIONS
(Approach Configuration)

Aircraft: AP 5

TRIM CONDITION			
V_o (kt)	65	75	85
γ_o (deg)	-7.4	-6.0	-4.6
θ_o (deg)	15.4	1.99	-9.1
δ_{T_o} (%)	36.4	44.06	61.6
BARE AIRFRAME PERTURBATION DYNAMICS			
Δ	[.677;.185][.889;.417]	(-.041)(.810)[.547;.312]	(-.114)(1.105)[.456;.296]
$N^u_{\delta_e}$	-.627(1.086)(-6.641)	-.763(1.393)(-6.098)	-.896(1.809)(-5.712)
$N^w_{\delta_e}$	-2.862(21.72)[.156;.318]	-3.810(24.51)[.171;.290]	-4.893(25.85)[.192;.263]
$N^{\dot{w}}_{\delta_e}$	-.536[.576;.313]	-.697[.638;.304]	-.831[.748;.300]
$N^{\dot{q}}_{\delta_e}$	2.862(-.035)(-1.703)(3.00)	3.810(.013)(-1.936)(3.364)	4.893(.049)(-2.219)(3.751)
$N^u_{\delta_T}$	-.011(7.165)[.824;.425]	.033(.071)(.751)(-1.345)	.053(1.096)[-.641;.380]
$N^w_{\delta_T}$	-.361(-.228)[.803;.386]	-.254(-.141)[.878;.397]	-.164(.931)[.490;.137]
$N^q_{\delta_T}$	.000933[.837;.347]	.000561[.429;.259]	-.0000604(.240)(3.955)
$N^{\dot{q}}_{\delta_T}$	.361(.002)[.814;.414]	.254(-.025)(.224)(.637)	.164(.155)(-.199)(1.056)
$N^q_{\delta_e}N^u_{\delta_T}$	.00610(7.331)	-.0227(-1.265)	-.0441(-.202)
$N^q_{\delta_e}N^{\dot{q}}_{\delta_T}$	-.196(.055)	-.179(.120)	-.136(.191)
$N^u_{\delta_e}N^{\dot{q}}_{\delta_T}$	.033[.092;6.502]	-.124(-3.396)(4.760)	-.260(-2.714)(4.208)
ATTITUDE LOOP CLOSED DYNAMICS			
Δ'	(.19)(.58)(.67)(1.6)(8.3)[.52;.31]	(.67)(1.88)(8.32)[.81;.26][.71;.35]	(.67)(2.1)(8.4)[.73;.19][.56;.44]
$N^{u'}_{\delta_T}$	-.0076(.17)(.63)(1.7)(6.8)(8.5)	.022(-1.307)(1.899)(8.309)[.984;.292]	.035(-.14)(2.1)(8.4)[.39;.33]
$N^{q'}_{\delta_T}$	.00062(0.0)(10.)[.84;.35]	.000374(0.)(10.0)[.429;.259]	-.000040(0.0)(.24)(3.9)(10.)
$N^{\dot{q}'}_{\delta_T}$	.24(.061)(.16)(.67)(1.5)(8.3)	.169(.418)(1.798)(8.294)[.994;.165]	.11(.16)(2.0)(8.4)[.62;.30]
STATIC PARAMETERS			
$\left[\frac{\partial\gamma}{\partial V}\right]_{\delta_T}$ (deg/kt)	.101	-.0385	-.145
$\left[\frac{\partial\gamma}{\partial\theta}\right]_{\theta}$ (deg/kt)	-.214	-.570	-1.96
$\left[\frac{\partial V}{\partial\theta}\right]_{\delta_T}$ (kt/deg)	-.890	-1.04	-1.28
$\left[\frac{\partial V}{\partial\delta_T}\right]_{\theta}$ (kt/%)	-.505	-.263	-.0704

TABLE E-2h

LONGITUDINAL TRANSFER FUNCTIONS
(Approach Configuration)
Aircraft: AP 6

TRIM CONDITION

V_o (kt)	65	75	85
γ_o (deg)	-7.4	-6.0	-4.6
θ_o (deg)	8.7	2.81	-3.05
δ_{T_o} (%)	36.1	44.1	61.7

BARE AIRFRAME PERTURBATION DYNAMICS

Δ	(-.169)(.883)[.652;.360]	(-.187)(1.118)[.606;.335]	(-.210)(1.40)[.560;.303]
$N^u_{\delta_e}$	-.452(1.101)(-17.16)	-.585(1.409)(-15.06)	-.723(1.861)(-13.41)
$N^w_{\delta_e}$	-2.862(21.67)[.136;.269]	-3.810(24.58)[.168;.223]	-4.893(26.9)[.23 ;.174]
$N^{\dot{\theta}}_{\delta_e}$	-.535(.149)(.412)	-.699(.119)(.503)	-.867(.101)(.624)
$N^{\dot{d}}_{\delta_e}$	2.862(-.032)(-2.563)(3.828)	3.810(.014)(-2.916)(4.318)	4.893(.049)(-3.341)(4.880)
$N^u_{\delta_T}$	-.053(.367)(.469)(1.835)	-.0041(.058)(.942)(17.26)	.028(-.195)(1.281)(-1.576)
$N^w_{\delta_T}$	-.511(-.349)[.690;.405]	-.451(-.282)[.716;.406]	-.371(-.214)[.772;.408]
$N^{\dot{\theta}}_{\delta_T}$	.00195[.544;.319]	.00164[.269;.258]	.00121(-.082)(-.149)
$N^{\dot{d}}_{\delta_T}$	.511(-.085)[.853;.418]	.451(-.102)(.250)(.613)	.371(.157)(-.204)(.931)
$N^{\dot{\theta}\,u}_{\delta_e\delta_T}$	.0283(2.080)	.00285(17.88)	-.0243(-1.329)
$N^{\dot{\theta}\,\dot{d}}_{\delta_e\delta_T}$	-.279(.013)	-.322(.049)	-.327(.075)
$N^{u\,\dot{d}}_{\delta_e\delta_T}$	.151[.145;4.122]	.016[.043;15.71]	-.137(-5.791)(7.314)

ATTITUDE LOOP CLOSED DYNAMICS

Δ'	(.67)(1.8)(8.3)[.73;.14][.81;.53]	(.67)(2.07)(8.30)[.73;.13][.72;.54]	(.67)(2.3)(8.3)[.76;.12][.61;.54]
$N^{u'}_{\delta_T}$	-.035(.18)(.50)(8.3)[.93;2.0]	-.003(2.347)(8.070)(17.32)[.942;.276]	.019(-1.5)(2.4)(8.3)[.52;.25]
$N^{\theta'}_{\delta_T}$	.0013(0.0)(10.)[.54;.32]	.00110(0.)(10.0)[.269;.258]	.00080(0.0)(-.082)(-.15)(10.0)
$N^{\dot{d}'}_{\delta_T}$	.34(.015)(.15)(.64)(1.6)(8.3)	.301(.061)(.172)(.445)(1.810)(8.272)	.25(.10)(2.1)(8.3)[.85;.24]

STATIC PARAMETERS

$\left[\frac{\partial\gamma}{\partial V}\right]_{\delta_T}$ (deg/kt)	.0927	-.0413	-.145
$\left[\frac{\partial\gamma}{\partial V}\right]_{\theta}$ (deg/kt)	-.0552	-.236	-.513
$\left[\frac{\partial V}{\partial\gamma}\right]_{\delta_T}$ (kt/deg)	-2.70	-3.06	-3.40
$\left[\frac{\partial V}{\partial\delta_T}\right]_{\theta}$ (kt/%)	-1.06	-.719	-.349

TABLE E-2i

LONGITUDINAL TRANSFER FUNCTIONS
(Approach Configuration)
Aircraft: AP 6 SR

TRIM CONDITION			
V_o (kt)	70	75	85
γ_o (deg)	-7.4	-6.0	-4.6
θ_o (deg)	2.14	-2.45	-8.17
δ_{T_o} (%)	33.8	43.9	61.6
DENOMINATOR			
Δ	(-.166)(.98)[.60;.35]	(-.20)(1.16)[.56;.34]	(-.22)(1.44)[.52;.31]
BARE AIRFRAME PERTURBATION DYNAMICS			
$N^u_{\delta_e}$	-.54(1.23)(-14.4)	-.59(1.42)(-14.6)	-.72(1.87)(-12.9)
$N^w_{\delta_e}$	-3.3(23.)[.158;.27]	-3.8(24.)[.167;.24]	-4.9(26.)[.22;.198]
$N^\theta_{\delta_e}$	-.61(.21)(.36)	-.68(.143)(.49)	-.84(.119)(.61)
$N^{\dot{d}}_{\delta_e}$	3.3(-.0096)(-2.6)(3.9)	3.8(.0143)(-2.9)(4.3)	4.9(.049)(-3.3)(4.8)
$N^{\dot{h}}_{\delta_e}$	3.3(.026)(-2.7)(4.0)	3.8(.041)(-2.9)(4.3)	4.9(.066)(-3.3)(4.8)
$N^u_{\delta_T}$	-.023(.171)(.75)(3.6)	.0054(-.000071)(1.03)(-11.2)	.034(-.34)(-.94)(1.35)
$N^w_{\delta_T}$	-.46(-.33)[.68;.41]	-.40(-.29)[.69;.41]	-.32(-.198)[.79;.41]
$N^\theta_{\delta_T}$	.00184[.43;.30]	.00154[.138;.24]	.0010(.032)(-.44)
$N^{\dot{d}}_{\delta_T}$	.46(-.082)[.95;.41]	.40(-.132)(.24)(.67)	.32(.158)(-.26)(1.0)
$N^{\dot{h}}_{\delta_T}$	.46(-.063)[.94;.42]	.40(-.124)(.26)(.65)	.32(.174)(-.26)(.99)
$N^{\theta\,u}_{\delta_e\delta_T}$	.0138(3.9)	-.0037(-11.2)	-.029(-.75)
$N^{\theta\,\dot{d}}_{\delta_e\delta_T}$	-.29(.042)	-.28(.060)	-.27(.089)
$N^{u\,\dot{d}}_{\delta_e\delta_T}$	.075[.102;6.2]	-.020(-12.9)(14.2)	-.167(-5.1)(6.6)
ATTITUDE LOOP CLOSED DYNAMICS			
Δ'	(.667)(1.921)(8.314)[.708;.155][.746;.524]	(.667)(2.073)(8.353)[.692;.136][.671;.543]	(.667)(2.320)(8.416)[.719;.128][.564;.545]
$N^{u'}_{\delta_T}$	-.0150(.210)(.40)(8.399)[.536;2.796]	.00359(2.289)(8.279)(-11.234)[.862;.268]	.0227(-.821)(2.373)(8.402)[.240;.245]
$N^{\theta'}_{\delta_T}$	.00123(.0)(10.)[.431;.299]	.00103(.0)(10.)[.138;.244]	.000663(.0)(.0325)(-.440)(10.)
$N^{\dot{d}'}_{\delta_T}$	.310(.051)(.153)(.553)(1.669)(8.278)	.267(.0844)(.164)(.407)(1.797)(8.319)	.214(.125)(2.042)(8.389)[.731;.235]
STATIC PARAMETERS			
$\left[\frac{\partial\gamma}{\partial V}\right]_{\delta_T}$ (deg/kt)	.0281	-.0420	-.146
$\left[\frac{\partial\gamma}{\partial V}\right]_{\theta}$ (deg/kt)	-.183	-.315	-.735
$\left[\frac{\partial V}{\partial\theta}\right]_{\delta_T}$ (kt/deg)	-2.16	-2.68	-2.96
$\left[\frac{\partial V}{\partial\delta_T}\right]_{\theta}$ (kt/%)	-.695	-.516	-.214

TABLE E-2j

LONGITUDINAL TRANSFER FUNCTIONS

(Approach Configuration)

Aircraft: AP 6 RLD

TRIM CONDITION			
V_o (kt)	65	75	85
γ_o (deg)	-7.4	-6.0	-4.6
θ_o (deg)	7.76	2.81	-3.05
δ_{T_o} (%)	38.8	44.1	61.7
DENOMINATOR			
Δ	(-.133)(.77)[.55;.34]	(-.187)(1.12)[.61;.34]	(-.21)(1.40)[.56;.30]
BARE AIRFRAME PERTURBATION DYNAMICS			
$N^u_{\delta_e}$	-.42(.69)(-19.2)	-.59(1.41)(-15.1)	-.72(1.86)(-13.4)
$N^w_{\delta_e}$	-2.9(22.)[.112;.33]	-3.8(25.)[.168;.22]	-4.9(27.)[.23;.174]
$N^\theta_{\delta_e}$	-.53[.73;.27]	-.70(.119)(.50)	-.87(.101)(.62)
$N^{\dot{u}}_{\delta_e}$	2.9(-.141)(-1.88)(3.3)	3.8(.0140)(-2.9)(4.3)	4.9(.049)(-3.3)(4.9)
$N^{\dot{w}}_{\delta_e}$	2.8(-.093)(-1.97)(3.3)	3.8(.040)(-3.0)(4.3)	4.9(.066)(-3.4)(4.9)
$N^u_{\delta_T}$	-.046(.23)[.95;.89]	-.0041(.058)(.94)(17.3)	.028(-.195)(1.28)(-1.58)
$N^w_{\delta_T}$	-.29(-.43)[.64;.41]	-.45(-.28)[.72;.41]	-.37(-.21)[.77;.41]
$N^\theta_{\delta_T}$	.00134[.44;.31]	.00164[.27;.26]	.00121(-.082)(-.149)
$N^{\dot{u}}_{\delta_T}$	.29(-.137)[.87;.42]	.45(-.102)(.25)(.61)	.37(.157)(-.20)(.93)
$N^{\dot{w}}_{\delta_T}$	.30(-.111)[.86;.43]	.45(-.091)(.27)(.60)	.37(.172)(-.20)(.92)
$N^{\theta\, u}_{\delta_e \delta_T}$	.025(1.32)	.0029(17.9)	-.024(-1.33)
$N^{\theta\, \dot{u}}_{\delta_e \delta_T}$	-.161(-.0176)	-.32(.049)	-.33(.075)
$N^{u\, \dot{u}}_{\delta_e \delta_T}$	.133[.168;3.5]	.0155[.043;15.7]	-.137(-5.8)(7.3)
ATTITUDE LOOP CLOSED DYNAMICS			
Δ'	(.667)(1.767)(8.299)[.666;.192][.796;.436]	(.667)(2.070)(8.304)[.734;.130][.718;.537]	(.667)(2.332)(8.345)[.763;.122][.614;.542]
$N^{u'}_{\delta_T}$	-.0309(.194)(.426)(8.322)[.901;1.652]	-.00272(2.347)(8.070)(17.318)[.942;.276]	.0187(-1.470)(2.399)(8.325)[.519;.247]
$N^{\theta'}_{\delta_T}$	.000890(.0)(10.)[.442;.307]	.001095(.0)(10.)[.269;.258]	.000804(.0)(-.0820)(-.149)(10.)
$N^{\dot{u}'}_{\delta_T}$	.196(-.02034)(.155)(.625)(1.579)(8.256)	.301(.0608)(.173)(.445)(1.810)(8.272)	.247(.101)(2.050)(8.317)[.848;.245]
STATIC PARAMETERS			
$\left[\frac{\partial\gamma}{\partial V}\right]_{\delta_T}$ (deg/kt)	.393	-.041	-.146
$\left[\frac{\partial\gamma}{\partial V}\right]_{\theta}$ (deg/kt)	.0748	-.237	-.527
$\left[\frac{\partial V}{\partial\theta}\right]_{\delta_T}$ (kt/deg)	-.500	-3.05	-3.38
$\left[\frac{\partial V}{\partial\delta_T}\right]_{\theta}$ (kt/%)	-.501	-.719	-.344

TABLE E-2k

LONGITUDINAL TRANSFER FUNCTIONS
(Approach Configuration)

Aircraft: AP 7

TRIM CONDITION			
V_o (kt)	65	75	85
γ_o (deg)	-7.4	-6.0	-4.6
$\bar{\theta}_o$ (deg)	10.2	1.89	-4.6
δ_{T_o} (%)	18.3	19.95	27.8
BARE AIRFRAME PERTURBATION DYNAMICS			
Δ	[.324;.208][.862;.583]	(.058)(.748)[.823;.275]	(-.061)(1.056)[.658;.315]
$N^u_{\delta_e}$	-.502(1.030)(-13.38)	-.639(1.325)(-11.73)	-.782(1.753)(-10.28)
$N^w_{\delta_e}$	-2.862(21.71)[.151;.369]	-3.810(24.50)[.143;.327]	-4.893(26.69)[.144;.287]
$N^{\bar{\theta}}_{\delta_e}$	-.536[.737;.345]	-.697[.819;.327]	-.859[.950;.312]
$N^{\dot{\theta}}_{\delta_e}$	2.862(-.065)(-2.203)(3.543)	3.810(-.014)(-2.516)(3.966)	4.893(.020)(-2.863)(4.428)
$N^u_{\delta_T}$	.014(-4.020)[.745;.537]	.060(.307)(-.512)(.655)	.083(1.019)[-.263;.107]
$N^w_{\delta_T}$	-.349(-.155)[.877;.374]	-.262(-.097)[.920;.409]	-.196(-.044)(.416)(.464)
$N^{\bar{\theta}}_{\delta_T}$	.000699(.198)(.648)	.000404[.880;.295]	.000286(-.171)(.214)
$N^{\dot{\theta}}_{\delta_T}$	.349(.033)[.767;.449]	.262(.021)[.977;.444]	.196(-.067)(.290)(.823)
$N^{\bar{\theta}\,u}_{\delta_e\delta_T}$	-.00766(-3.896)	-.0415(-.281)	-.0714(.144)
$N^{\bar{\theta}\,\dot{\theta}}_{\delta_e\delta_T}$	-.189(.100)	-.185(.171)	-.170(.230)
$N^{u\,\dot{\theta}}_{\delta_e\delta_T}$	-.041(-7.58)(8.78)	-.227(-3.714)(5.077)	-.407(-3.383)(4.899)
ATTITUDE LOOP CLOSED DYNAMICS			
Δ'	(.15)(.67)(.70)(1.6)(8.3)[.60;.35]	(.24)(.32)(.67)(1.84)(8.32)[.76;.36]	(.67)(2.1)(8.4)[.83;.19][.72;.47]
$N^{u'}_{\delta_T}$	.0095(.14)(.71)(1.6)(-4.0)(8.3)	.040(.163)(-.342)(.453)(1.864)(8.313)	.055(.099)(2.1)(8.4)[.65;.34]
$N^{\theta'}_{\delta_T}$	.00047(0.0)(.20)(.65)(10.)	.000323(0.)(10.0)[.880;.295]	.00019(0.0)(-.17)(.21)(10.0)
$N^{\dot{\theta}'}_{\delta_T}$	.23(.72)(1.5)(8.3)[.98;.13]	.175(.527)(1.730)(8.301)[.929;.178]	.13(.34)(1.9)(8.4)[.86;.24]
STATIC PARAMETERS			
$\left[\frac{\partial\gamma}{\partial V}\right]_{\delta_T}$ (deg/kt)	.184	.0409	-.0589
$\left[\frac{\partial\gamma}{\partial V}\right]_{\theta}$ (deg/kt)	-.557	-2.06	2.56
$\left[\frac{\partial V}{\partial\gamma}\right]_{\delta_T}$ (kt/deg)	-1.12	-1.38	-1.74
$\left[\frac{\partial V}{\partial\delta_T}\right]_{\theta}$ (kt/%)	-.278	-.0928	.0728

TABLE E-21

LONGITUDINAL TRANSFER FUNCTIONS
(Approach Configuration)
Aircraft: AP 10

TRIM CONDITION

V_o (kt)	65	75	85
γ_o (deg)	-7.4	-6.0	-4.6
θ_o (deg)	23.4	4.56	-11.5
δ_{T_o} (%)	23.4	30.7	46.8

DENOMINATOR

Δ	[.22;.22][.75;.55]	(-.0159)(.67)[.64;.30]	(-.123)(1.03)[.50;.30]

BARE AIRFRAME PERTURBATION DYNAMICS

$N^u_{\delta_e}$	-.68(1.13)(-4.6)	-.82(1.54)(-4.3)	-.96(2.1)(-3.9)
$N^w_{\delta_e}$	-2.9(21.)[.120;.30]	-3.8(25.)[.141;.26]	-4.9(25.)[.177;.22]
$N^\theta_{\delta_e}$	-.53[.48;.30]	-.70[.59;.27]	-.81[.74;.26]
$N^{\dot{u}}_{\delta_e}$	2.9(-.050)(-1.46)(2.7)	3.8(.0057)(-1.75)(3.2)	4.9(.043)(-2.0)(3.5)
$N^{\dot{w}}_{\delta_e}$	2.8(-.0096)(-1.50)(2.8)	3.8(.032)(-1.77)(3.2)	4.9(.060)(-2.0)(3.5)
$N^u_{\delta_T}$	-.118(1.50)[.62;.51]	-.106[1.0;.40]	.040(-.0036)(.93)(-1.47)
$N^w_{\delta_T}$	-.63(-.35)[.70;.36]	-.49(-.26)[.74;.40]	-.35(-.21)[.75;.42]
$N^\theta_{\delta_T}$	.0025(.20)(.44)	.00168[.59;.32]	.00114[.118;.23]
$N^d_{\delta_T}$	.63(-.031)[.62;.50]	.49(.00078)[.93;.41]	.35(-.073)(.177)(.79)
$N^{\dot{u}}_{\delta_T}$	.64(.0070)[.62;.50]	.49(.022)[.93;.41]	.34(-.069)(.191)(.79)
$N^{\delta u}_{\delta_e\delta_T}$	.062(1.53)	.076	-.033(-1.39)
$N^{\delta d}_{\delta_e\delta_T}$	-.34(-.020)	-.35(.050)	-.29(.090)
$N^{u d}_{\delta_e\delta_T}$	.34[.42;1.40]	.00065[.0133;51.]	-.198(-2.9)(4.4)

ATTITUDE LOOP CLOSED DYNAMICS

Δ'	(.151)(.667)(.808)(1.399)(8.328)[.391;.294]	(.667)(1.815)(8.298)[.571;.256][.986;.324]	(.667)(1.959)(8.479)[.664;.173][.644;.410]
$N^{u'}_{\delta_T}$	-.0785(.146)(.880)(8.340)[.980;1.416]	-.000114(.182)(.517)(1.848)(8.243)(620.93)	.0270(-1.435)(1.951)(8.471)[.862;.273]
$N^{\theta'}_{\delta_T}$	.00165(.0)(.203)(.441)(10.)	.00112(.0)(10.)[.591;.317]	.000771(.0)(10.)[.118;.234]
$N^{d'}_{\delta_T}$	.420(-.0205)(.146)(960)(1.217)(8.292)	.329(.0541)(.167)(.560)(1.716)(8.265)	.230(.111)(1.830)(8.448)[.978;.261]

STATIC PARAMETERS

$\left[\frac{\partial\gamma}{\partial V}\right]_{\delta_T}$ (deg/kt)	.144	-.0167	-.127
$\left[\frac{\partial\gamma}{\partial V}\right]_{\theta}$ (deg/kt)	.0640	-.178	-.381
$\left[\frac{\partial V}{\partial\gamma}\right]_{\delta_T}$ (kt/deg)	-.786	-1.11	-1.51
$\left[\frac{\partial V}{\partial\delta_T}\right]_{\theta}$ (kt/%)	-1.22	-.882	-.504

2. Lateral-Directional

The lateral-directional dynamics are independent of airplane, and do not drastically change with flight conditions, as do the longitudinal dynamics. Therefore only one set of dynamics are presented here; those for the nominal approach.

All derivatives and transfer functions are in the stability axis.

a. Flight Condition

$V_o = 75$ kt $\qquad \gamma_o = -6.0$ deg

$\alpha_o = 8.4$ deg $\qquad C_{\mu_o} = 1.39$

b. Primed Dimensional Derivatives

$Y_\beta = -9.452$	$L'_\beta = -.5755$	$N'_\beta = .2920$	
$L'_p = -.6488$	$N'_p = -.2654$	$L'_r = 1.1884$	$N'_r = -.10522$
$Y^*_{\delta_a} = 0.0$	$L'_{\delta_a} = .19737$	$N'_{\delta_a} = .016710$	
$Y^*_{\delta_{sp}} = 0.0$	$L'_{\delta_{sp}} = .7776$	$N'_{\delta_{sp}} = .06584$	
$Y^*_{\delta_r} = .02483$	$L'_{\delta_r} = .02276$	$N'_{\delta_r} = -.3091$	

c. SAS Off Dynamics

$$\Delta = (-.1038)(.825)[.0627;.860]$$

$$N^{\beta}_{\delta_a} = -.01671(.1223)(-5.57)$$

$$N^{p}_{\delta_a} = .1974(.0259)[.215;.591]$$

$$N^{r}_{\delta_a} = .01671(.612)(-.723)(-2.30)$$

$$N^{\varphi}_{\delta_a} = .1956[.254;.601]$$

$$N^{a_y}_{\delta_a} = .1579(.1223)(-5.57)$$

$$N^{\beta}_{\delta_{sp}} = -.0658(.1223)(-5.57)$$

$$N^{p}_{\delta_{sp}} = .778(.0259)[.215;.591]$$

$$N^{r}_{\delta_{sp}} = .0658(.612)(-.723)(-2.30)$$

$$N^{\varphi}_{\delta_{sp}} = .771[.254;.601]$$

$$N^{a_y}_{\delta_{sp}} = .622(.1223)(-5.57)$$

$$N^{\beta}_{\delta_r} = .0248(-.271)(1.038)(12.44)$$

$$N^{p}_{\delta_r} = .0228(.0250)(.468)(-17.08)$$

$$N^{r}_{\delta_r} = -.309(.876)[-.1961;.400]$$

$$N^{\varphi}_{\delta_r} = .0552(.499)(-6.91)$$

$$N^{a_y}_{\delta_r} = 3.14[-.774;.520][.912;.855]$$

d. SAS On Dynamics

Only the wheel numerators are shown below, since this is the only control required with a roll damper and turn coordination type stability augmentation system.

$$\Delta = (.0326)(.379)(4.98)(5.60)[.394;1.22]$$

$$N^{\beta}_{\delta_w} = 1.106(.207)(.795)(-4.11)$$

$$N^{p}_{\delta_w} = -12.15(.0260)(.366)[.419;1.21]$$

$$N^{r}_{\delta_w} = -1.029(.341)(1.55)[-.666;1.71]$$

$$N^{\varphi}_{\delta_w} = -12.04(.363)[.431;1.22]$$

$$N^{a_y}_{\delta_w} = 9.83(.167)(.448)[-.092;3.38]$$